University of Strathclyde

Strathclyde Institute of Pharmacy and Biomedical Sciences

‘Investigating the Influence of Aluminium Adjuvant on Antigen Presentation *In vitro* and T cell Responses *In vivo’*

by
Tirth Raj Ghimire

A thesis presented in fulfilment of the requirements
For the degree of Doctor of Philosophy

May 2012

AUTHOR'S DECLARATION

'This thesis is the result of the author's original research. It has been composed by the author and has not been previously submitted for examination which has led to the award of a degree.'

Signed:

Tirth Raj Ghimire

Date:

ACKNOWLEDGEMENTS

I would like to express my humble thanks to those who dedicated their precious help in accomplishing this thesis, with direct or indirect support and advice, leading to inspire to carry out it.

First of all, I am heartily grateful to Professor James Brewer, my mentor, without whose support my research would have crippled, for his outstanding knowledge of immunology, parasitology and vaccinology. Jim! My sincere thanks go to you for selecting me as your student for research and for your tolerance with my 'zero level brain of immunology' and for guiding me from the day I arrived at Glasgow. Thank you for teaching me science 'as an art of simple experiment with a rational approach' that gradually made me work independently in lab. You are, undoubtedly, a real Guru of my Immunology Life.

I would like to acknowledge Professor Paul Garside, my mentor, for his infinite supports during my PhD. Thank you for guiding my research, reviewing the thesis and teaching me 'tell people what you want to tell them, tell them what they expect to be told and tell them what you have told them'. Thank you Paul for accepting me as your student in lab!

I am thankful to Professor Craig Roberts and Professor Jim Alexander for being my PhD supervisors and for supporting me in academics in Strathclyde University. I am grateful to Dr. Trevor Bushell for his best help for the admission processes.

I am thankful to Lars-Inge Larsson, Professor of Cell Biology, Center for Advanced Bioimaging (CAB), Faculty of Life Sciences, University of Copenhagen, Denmark for his nice explanation regarding the impact of Cytochalasin D on the actin polymerisation.

I am not able to gear up my writing without acknowledging all the Centre for Biophotonics (CFB) and Garside Brewer Maffia (GBM) lab members. Firstly, I would like to thank Robert Benson (Bob) for teaching me everything and guiding me in the lab. Bob, I am really thankful to you for your kind support in poster presentation, designing experiments, lab presentation and importantly in energising me to reduce my 'Chicken Belly'. Thank you Pasquale, for the excited and up-to-date discussion on Italian politics and Hinduism and Hindu meditation. Thanks Owain for your teaching and advice in an understandable language which I could acquire. Thanks Sharon and Abbie for your help especially in the *in vivo* experiments and flow cytometry for the first time. Thanks Karen for making me a person adaptable in Glasgow. Thank you for each pal of your presence in my life especially in difficult situations. I know these words are not enough for acknowledging you. Thanks John, handsome man, for teaching me to prepare EαGFP and supporting me in lab. Thanks Neil, one of the cordial persons in my life, for sharing your knowledge regarding plasmacytoid dendritic cells (pDCs) and YAe assay. Thanks Andy for your kind support in flow cytometry and scientific discussion in lab. Thanks Ross for your nice words for me. The half-life of your smile can not be calculated. Agapitos, thank you for teaching me everything, even a minor aspect of immunology without any problems. Thank you Peter for supporting me in the labs and for being an invaluable source of offline news, movies, Glasgowegian culture and traditions. You are a multi-talented Scottish friend I have ever met in my life. Thanks to Tovah and Suleman for being friendly in lab by understanding my Nepanglish[a]. Thanks to Jonathan for your kind support in Confocal Imaging. I am sure you are able to scale the Everest and you will set up your name along Edmund Hillary and Tenzing Norgay. Thanks to Gianluca for your support in Glasgow cinema and pubs and discos and thanks for buying Chicken Pakora for me. Thanks to Marcella for being together in lab on weekends for the preparation of EαGFP and for teaching me some Italian language. Thanks to Bilal for the sharing your expertise of statistics with me.

[a]The term was given by Kamali, H.C. Nepanglish in 'A Standardizing Variety of English'. (http://neltachoutari.files.wordpress.com/2010/09/kamali-nepanglish.pdf) Accessed: 24 February 2012.

Thanks to Helen Arthur and Graham Tobasnick, for your help in joining Glasgow Biomedical Research Centre (GBRC). Thanks to all members of Central Research Facility (CRF) especially Colin Hughes, Douggie and Tony. Also thanks to Linda and Carol from Biological Procedures Unit (BPU) and Dave from Centre for Biophotonics, University of Strathclyde for their help in experiments.

Thanks to my colleagues Abhinav Sinha, Ganga Regmi, Kamal Kadel, Til Prasad Poudel, Shyam Adhikari, Hom Jyoti Adhikari, Khem Raj Adhikari, and Tek Raj Gurung for your constant support in my study. Thanks to Prakash Aryal, University of Highland and Islands, for encouraging me to get my access to Scotland and for supporting me in every problem in my life in Scotland.

I would also like to thank my family, especially my mum and dad for being extremely supportive throughout my nostalgic days and nights in Glasgow. Thank you for your kind suggestions to be 'an eagle eye' on study. Thanks to my brothers Raj Kumar and Hemu and my elder sister Bimala and her husband Jagannath and younger sister Nirmala and her husband Mukunda for their encouragement from my childhood. Safal and Oshil, I hope you will recognise your dad after the four-year return from Scotland. Thanks to Kanchhi (Sweta), for tolerating my lies about the visit to London due to thesis work.

Last but not the least, thanks go to Asmita, my better-half, for supporting me in every aspect of my life from the days we met. These words are not enough to acknowledge you regarding your support in thesis writing. Anyway, thanks for your patience Asu!

TABLE OF CONTENTS

Author's declaration……II
Acknowledgements……III
List of Figures……..X
List of Tables ……..XIII
Abstract……XIV
Abbreviations and Acronyms …….. XV

CHAPTER-1: INTRODUCTION..... 1
1.1 Vaccines 2
1.2 Vaccine technologies 3
1.2.1 Live attenuated vaccines..... 3
1.2.2 Killed or inactivated vaccines 5
1.2.3 Subunit vaccines..... 5
1.2.4 Recombinant vaccines..... 6
1.3 Key issues in vaccine development..... 6
1.4 Adjuvants 7
1.4.1 Clinically applicable adjuvants 8
1.4.2 Alum..... 9
1.4.3 Limitations of clinical adjuvants 13
1.4.4 Types of adjuvant 14
1.5 Adaptive Immune Responses..... 21
1.5.1 DCs and their development 22
1.5.2 DCs and their subsets 24
1.5.3 DCs and antigen uptake..... 27
1.5.4 Antigen processing..... 28
1.5.5 DC maturation 33
1.5.6 DC migration to the DLNs 34
1.5.7 T cell activation 35
1.5.8 Th polarisation..... 35
1.6 Effects of adjuvants on immune responses 39

1.6.1 DC activation 39
1.6.2 Inflammation 42
1.6.3 Antigen targeting 43
1.6.4 Depot hypothesis 44
1.7 How do Alum adjuvants work? 45
1.7.1 Alum-induced antigen targeting 46
1.8 Aims of the thesis 51
CHAPTER-2: MATERIALS AND METHODS 53
2.1 Materials, chemicals and antibodies 54
2.2 Animals 64
2.3 Antigens 64
2.3.1 Ovalbumin (OVA) 64
2.3.2 EαGFP 64
2.4 Adjuvants 65
2.5 Preparation of DCs from murine bone marrow 66
2.6 EαGFP/YAe system 66
2.7 Analysis of antigen uptake and presentation 69
2.8 Pulse chase assay to analyse kinetics of antigen presentation 69
2.9 Role of preadsorption of antigen in Alum uptake and presentation 70
2.10 Role of actin polymerisation in antigen uptake 72
2.11 Role of Na^+/H^+ pump in antigen uptake 72
2.12 Hybridoma assay 73
2.13 Analysis of antigen presentation using the DO11.GFP hybridoma 74
2.14 Costimulation asssay 74
2.15 Cell viability Assay 74
2.16 *In vivo* T cell tracking 75
2.17 Flow cytometry 77
2.18 ELISA 77
2.18.1 Sandwich ELISA 77
2.18.2 Luminex Assay for cytokines 78
2.19 Data Analysis 80

CHAPTER-3: EFFECT OF ALUM ADJUVANTS ON UPTAKE AND PRESENTATION OF ANTIGEN BY BMDC 81

3.1 Introduction 82

3.2 Impact of Alum on antigen uptake and presentation by BMDCs 83

3.3 Antigen dose response of Alum in antigen uptake and presentation 86

3.4 Dose response of Alum in antigen uptake and presentation 89

3.5 Role of Alum adjuvants in the kinetics of antigen uptake and presentation 92

3.5.1 Kinetics of antigen uptake and presentation in continuous presence of Alum and antigen 92

3.5.2 Kinetics of antigen uptake and presentation after a pulse chase assay…… 95

3.6 Role of Alum in MHC class II expression 99

3.7 Requirement for Actin polymerisation in Alum-mediated antigen internalisation by BMDCs 101

3.8 Impact of Na^+/H^+ on Alum-mediated antigen internalisation by BMDCs 104

3.9 Role of pre-adsorption of antigen in Alum-mediated antigen presentation 106

3.10 Analysis of antigen presentation using a T cell hybridoma 110

3.10.1 DO11.GFP hybridoma in antigen presentation assay 110

3.11 Discussion 114

CHAPTER-4: IMPACT OF ALUM ON THE ACTIVATION STATE OF BMDCs 119

4.1 Introduction 120

4.2 Impact of Alum on the expression of costimulatory molecules by DCs .. 121

4.2.1 Impact of Alum on CD86 costimulatory molecule expression by BMDCs 122

4.2.2 Impact of Alum on CD80 costimulatory molecule expression by BMDCs 124

4.2.3 Impact of Alum on CD40 costimulatory molecule expression by BMDCs 126

4.2.4 Impact of Alum on OX-40L (CD252) costimulatory molecule expression by BMDCs 128
4.3 Summary of the impact of Alum on the expression of costimulatory molecules by BMDC 130
4.4 Impact of Alum on the production of cytokines by BMDCs 132
4.4.1 Impact of Alum on IL-1β production by DCs 134
4.4.2 Impact of Alum on TNF-α production by DCs 137
4.4.3 Impact of Alum on IL-6 production by DCs 139
4.4.4 Impact of Alum on IL-10 production by DCs 141
4.4.5 Impact of Alum on IL-12p70 production by DCs 143
4.4.6 Impact of Alum on IL-13 production by DCs 145
4.4.7 Impact of Alum on IL-15 production by DCs 147
4.4.8 Impact of Alum on IL-33 production by DCs 147
4.5 Summary of influence of Alum on the production of cytokines by BMDCs 147
4.6 Impact of Alum on death of DCs 149
4.7 Discussion 152
CHAPTER-5: IMPACT OF ALUM ON CD4 T CELL RESPONSES *IN VIVO* 158
5.1 Introduction 159
5.2 Impact of Alum on magnitude and duration of the immune response 160
5.3 Impact of Alum on duration and magnitude of antigen-specific CD4 T cell expansion 164
5.4 Discussion 168
CHAPTER-6: CONCLUSIONS AND FUTURE STUDIES 171
6.1 Conclusions 172
6.2 Future studies 176
REFERENCES 181
APPENDIX-I 223
APPENDIX-II 224
APPENDIX-III 225

LIST OF FIGURES

CHAPTER-1

FIGURE 1.1: Poliomyelitis global annual reported cases and Pol3 (third dose of polio virus vaccine) coverage, 1980-2009..... 2

FIGURE 1.2: Chronology of adjuvant licensing in Europe (including UK) and the USA. 9

FIGURE 1.3: Schematic of surface of Aluminium hydroxide adjuvant…….28

FIGURE1.4: Development of DCs……..…….…..23

FIGURE 1.5: Current understanding of DC migration inside LN following immunisation……25

FIGURE 1.6: Steps involved in antigen processing and presentation by DC in the context of MHC Class II: peptide complexes……..……30

FIGURE 1.7: Mechanisms of antigen processing by DCs in the context of MHC class I pathway……...……..32

FIGURE 1.8: DC controls the initiation of adaptive immune responses *in vivo*.

FIGURE 1.9: TLR-signaling pathway……..……..40

FIGURE 1.10: Inflammatory pathway of Alum adjuvanticity……...50

CHAPTER-2

FIGURE 2.1: The Eα:YAe System. 68

FIGURE 2.2: Separation process of Alum from cells after antigen±Alum pulse period. 70

FIGURE 2.3: Study design for the assessment of impact of preadsorption of antigen in Alum on antigen presentation by BMDCs *in vitro*……..71

FIGURE 2.4: Hybridoma assay to study antigen presentation by DCs *in vitro*…… 73

FIGURE 2.5: Study design showing *in vivo* tracking of transgenic T cells. 76

CHAPTER-3

FIGURE 3.1: Application of the EαGFP/YAe system to reveal the impact of Alum adjuvants on antigen uptake and presentation by DCs. 84

FIGURE 3.2: EαGFP/YAe system can be used to study the impact of Alum on antigen uptake and presentation. 85

FIGURE 3.3: Alum efficiently targets DCs by enhancing both accumulation and presentation of antigen by DCs *in vitro*..... 87

FIGURE 3.4: Alum efficiently targets DCs by enhancing both accumulation and presentation of antigen by DCs *in vitro*..... 88
FIGURE 3.5: Alum efficiently targets DCs by enhancing antigen accumulating efficiency of DCs *in vitro.*..... 90
FIGURE 3.6: Alum efficiently targets DCs by enhancing antigen presenting efficiency of DCs *in vitro.*..... 91
FIGURE 3.7: Alum increases the rate and magnitude of antigen uptake by DCs. 93
FIGURE 3.8: Alum increases the rate and magnitude of antigen presentation by DCs. 94
FIGURE 3.9: Alum increases antigen uptake, reduces degradation and eventually sustains the antigen presenting efficiency of DCs *in vitro*..... 97
FIGURE 3.10: Alum adjuvants increase antigen uptake, reduce degradation and eventually sustain antigen presenting efficiency of DCs *in vitro*..... 98
FIGURE 3.11: Alum increases levels of MHC class II molecules in dose-dependent manner *in vitro.* 100
FIGURE 3.12: Alum induces BMDCs to take up majority of antigens via actin-dependent manner *in vitro.*..... 103
FIGURE 3.13: Alum induces BMDCs to take up small amounts of antigens via Na+/H+-dependent manner *in vitro.* 105
FIGURE 3.14: Pre-adsorption of antigen in Alum is not necessary to enhance the antigen presentation by DCs *in vitro.*..... 108
FIGURE 3.15: Pre-adsorption of antigen in Alum is not necessary to enhance the antigen presenting efficiency of DCs *in vitro*..... 109
FIGURE 3.16: Detecting antigen presentation using the DO11.GFP hybridoma. .. 112
FIGURE 3.17: Detecting antigen presentation using the DO11.GFP hybridoma. .. 113

CHAPTER-4

FIGURE 4.1: Alum increases the expression of CD86 molecules on the surface of DCs..... 123
FIGURE 4.2: Low dose of Alum increases the expression of CD80 molecules on the surface of DCs. 125
FIGURE 4.3: Alum has a broadly negative effect on CD40 expression by BMDC *in vitro.* 127

FIGURE 4.4: Alum has a biphasic effect on the expression of OX-40L by BMDCs *in vitro*. 129
FIGURE 4.5: Alum induces the production of IL-1β by DCs in time-dependent manner *in vitro*. 136
FIGURE 4.6: Alum induces the production of TNF-α by DCs in time-dependent manner *in vitro*. 138
FIGURE 4.7: Alum induces the production of IL-6 by DCs in time-dependent manner *in vitro*. 140
FIGURE 4.8: Alum reduces LPS-mediated IL-10 production by DCs *in vitro*..... 142
FIGURE 4.9: Alum reduces the LPS-mediated IL-12p70 production by DCs *in vitro*. 144
FIGURE 4.10: Alum reduces the LPS-mediated IL-13 production by DCs *in vitro*. 146
FIGURE 4.11: Gating strategy of apoptotic and necrotic bodies observed in BMDCs following incubation in 4% PFA. 150
FIGURE 4.12: Alum causes apoptosis of DCs *in vitro*. 151

CHAPTER-5

FIUGRE 5.1: Dot plots showing staining of total CD4 + and antigen-specific CD4+ T cells. 162
FIGURE 5.2: Alum enhances the recruitment of both total cells as well as total CD4+ and antigen-specific CD4+ T cells in DLNs. 163
FIUGRE 5.3: Alum immunisation enhances antigen-specific CD4+ T cell division *in vivo*. 166
FIGURE 5.4: Alum immunisation does not sustain antigen-specific CD4+ T cells expansion *in vivo*. 167

CHAPTER-6

FIGURE 6.1: Illustrative conclusion of mechanisms of Alum adjuvants *in vitro*... 175

LIST OF TABLES

CHAPTER-1

TABLE 1.1: Types of vaccines prepared by different techniques. 4
TABLE 1.2: A variety of new adjuvants, their innate immune receptors, ligand components and sources or origin in nature. 16
TABLE 1.3: Endogenous danger signals (DAMPs), their receptors and their immunological responses within the host body. 18
TABLE 1.4: Combined adjuvant formulations in vaccines currently in development by various vaccine companies. 20

CHAPTER-2

TABLE 2.1: Materials used in the experiments. 55
TABLE 2.2: Chemicals used in the experiments. 56
TABLE 2.3: Antibodies used in flow cytometry. 57
TABLE 2.4: Cell culture media used in the experiments. 58
TABLE 2.5: Buffers used in the experiments. 59
TABLE 2.6: Materials, chemicals and antibodies used in sandwich ELISA. 60
TABLE 2.7: Luminex antibodies, chemicals and reagents for 1-plex (IL-33 cytokine) ELISA. 61
TABLE 2.8: Luminex antibodies, chemicals and reagents for 6-Plex ELISA. 62
TABLE 2.9: Quality control ranges of cytokines. 63

TABLE-4

TABLE 4.1: Summary table of effects of Alum on DC costimulatory molecule expression. 131
TABLE 4.2: Summary table of effects of Alum on cytokine production by DCs... 148

ABSTRACT

Aluminium adjuvants (Alum) are the only widely approved adjuvants used in human vaccines, although their mechanism of action remains controversial. It is generally accepted that adjuvants mediate their effects on the adaptive immune system cells via innate antigen presenting cells (APCs), in particular dendritic cells (DCs). In this study the way in which Alum modulates several steps in DC functions that lead to T cell activation to underpin adjuvant function was investigated.

Using EαGFP/YAe, it was demonstrated that Alum increased the rate and magnitude of antigen internalisation in an actin-dependent manner by DCs *in vitro*. It was observed that Alum caused an initial reduction in presentation compared with soluble antigen, but eventually increased the magnitude and duration of antigen presentation that was associated with reduced protein degradation in DCs. Using costimulatory-independent-DO11.GFP hybridoma, it was shown that Alum enhanced presentation of antigens derived from protein as well as peptide. As well as having an antigen targeting effect on DCs, this adjuvant works by mechanism(s) other than simply antigen delivery as adsorption to Alum is dispensable for boosting their antigen presenting efficiency. Alum enhanced DC activation characterised by the enhanced expression of CD86, CD80 and OX-40ligand (L) and the production of interleukin (IL)-1β, tumour necrosis factor (TNF)-α and IL-6. In *in vivo* studies employing adoptive transfer of transgenic T cells and subcutaneous (s.c.) injection, Alum caused a sustained accumulation of cells leading to draining lymph node (DLN) shutdown.

In conclusion, it was shown that the dynamic alterations in phenotypic and functional changes underlie enhanced DC function in response to Alum. Due to increasing demand for novel adjuvants, a clearer understanding of the mechanisms that allow these important agents to affect adaptive immune responses will make a significant contribution to the rational design of future vaccines.

ABBREVIATIONS AND ACRONYMS

7-AAD	7-Aminoactinomycin D
°C	Degree Celsius
µ	micro
µg/mL	Microgram/millilitre
µM	Micromolar
AHFS	American Hospital Formulary Service
ANOVA	Analysis of Variance
APC	Antigen Presenting Cell
AS04	Adjuvant System 04
ATP	Adenosine Tri-phosphate
BCA	Bicinchoninic Acid
BCG	Bacillus Calmette-Guerin
BMDC	Bone Marrow-Derived Dendritic Cell
BMDM	Bone Marrow-Derived Macrophage
CARD	Caspase Activation and Recruitment Domain
CCR7	Chemokine Receptors 7
CDC	Centers for Disease Control and Prevention
cDC	Conventional DC
CFSE	Carboxyfluorescein Succinimidyl Ester
CIITA	MHC class II Transcription Activator
CLIP	Class II–Associated Invariant Chain Peptide
CLR	C-Type Lectin Receptor
CMI	Cell-Mediated Immunity
CpG ODN	Cytosine phosphate Guanine Oligodeoxynucleotide
CR	Complement Receptor
CTLA-4	Cytotoxic T Lymphocyte Antigen-4
DAI	DNA-Dependent Activator of IFN-Regulatory Factors
DAMP	Damage Associated Molecular Pattern
DC	Dendritic Cell
DC-SIGN	Dendritic Cell-Specific Intercellular Adhesion molecule-3-Grabbin Non-integrin
DDCs	Dermal Dendritic Cells
DEC	Decalectin
DLN	Draining Lymph Node
DMSO	Dimethyl Sulfoxide
DNA	Deoxyribonucleic Acid
DNAse	Deoxyribonuclease
DRiPs	Defective Ribosomal Products
dsRNA	Double-Stranded Ribonucleic Acid
DT	Diphtheria Toxoid
E	Epithelial
EDTA	Ethylenediaminetetraacetic Acid
eGFP	Enhanced Green Fluorescent Protein
EIPA	5-(N-Ethyl-N-isopropyl) Amiloride
ELC	Epstein-Barr virus-induced receptor Ligand Chemokine

ELISA	Enzyme Linked Immunoabsorbent Assay
ER	Endoplasmic Reticulum
et al.	and others
FACS	Fluorescence Activated Cell Sorting
FCA	Freund's Complete Adjuvant
FcR	Fc Receptor
FCS	Fetal Calf Serum
FcγRs	Fc gamma Receptors
FDC	Follicular Dendritic Cell
FITC	Fluorescein Isothiocyanate
Flt	Fms-like tyrosine kinase 3
FltL	Fms-like tyrosine kinase 3 ligand
g	Gravity, Gram
GFP	Green Fluorescent Protein
GITR	Glucocorticoid-induced Tumour Necrosis Factor Receptor
GMCSF	Granulocyte Macrophage Colony Stimulating Factor
GSK	GlaxoSmithKline
H-2	Histocompatability-2
HA	Haemagglutin
HBSS	Hank's Balanced Salt Solution
HEL	Hen Egg Lysozyme
HEV	High Endothelial Venule
Hib	*Haemophilus influenzae type* b
HIV/AIDS	Human Immunodeficiency Virus/Acquired Immunodeficiency Syndrome
HLA	Human Leukocyte Antigen
HMGB1	High Mobility Group Box 1
HPV	Human Papillomavirus
HSA	Human Serum Albumin
HSP	Heat Shock Protein
i.v.	Intravenous
ICOS	Inducible Costimulator
IFN-γ	Interferon-gamma
Ig	Immunoglobulin
Ii	Invariant chain
IL	Interleukin
IL-1R1	IL-1 receptor-like 1 molecule
IMDM	Iscove's Modified Dulbecco's Media
IPAF	Ice-Protease-Activating Factor
IPTG	Isopropyl-β-D-Thiogalactopyranoside
IRAK	Interleukin-1 Receptor-Associated Kinase
IRF	Interferon Regulatory Factor
iTregs	Induced T regulatory cells
L	Ligand
LAIV	Live Attenuated Influenza Vaccine
LC	Langerhans Cell
LGP2	Laboratory of Genetics and Physiology 2
LN	Lymph Node

LPS	Lipopolysaccharide
LSM	Laser Scanning Microscope
LY75	Lymphocyte Antigen 75
MALP-2	Macrophage Activating Lipopeptide of 2kDa molecular mass
MCV	Meningococcal Conjugate Vaccine
MDA5	Melanoma Differentiation Associated Gene 5
MDP	Muramyl Dipeptide
MES	2-{N-morpholino-4-ehtanesulphonic acid}
MFI	Mean/Median Fluorescence Intensity
MHCI	Major Histocompatability Class I
MHCII	Major Histocompatability Class II
MPL	Monophosphoryl lipid
MyD88	Myeloid Differentiation Primary Response Gene (88)
NA	Neuraminidase
NACHT	Neuronal Apoptosis Inhibitory Protein (NAIP), MHC class II Transcription Activator (CIITA), Incompability locus protein from *Podospora anserina* (HET-E), Telomerase-associated protein (TP1) family
NAIP	Neuronal Apoptosis Inhibitory Protein
NALP3	NACHT Domain-Leucine-Rich Repeat-, and Pyrin domain-containing Protein 3
NFAT	Nuclear Factor of activated T-cells
NF-kB	Nuclear Factor kappa-light-chain-enhancer of activated B cells
NLRP3	Nucleotide Oligomerisation Domain protein-like receptor family, pyrin domain containing 3
NLRs	Nucleotide Oligomerisation Domain Protein-like receptors
NOD	Nucleotide Oligomerisation Domain
nTregs	Naturally Occurring Tregs
OD	Optical Density
OxLDL	Oxidised low density lipoprotein
Pam2Cys	S-[2,3-bis(palmitoyloxy)propyl]cysteine
PAMPs	Pathogen Associated Molecular Patterns
PBMC	Peripheral Blood Mononuclear Cell
PBS	Phosphate Buffered Saline
PD-1	Programmed Death-1
pDC	Plasmacytoid DC
PDCA-1	Plasmacytoid Dendritic Cell Antigen-1
PerCP	Peridinin Chlorophyll
PFA	Paraformaldehyde
pH	*Potentia hydrogenii* (Latin)
Pol3	Third dose of polio virus vaccine
poly I:C	Polyinosinic:polycytidylic acid
PRRs	Pattern-Recognition Receptors
PVS	Perivenular Space
QS	*Quillaja saponaria*
R	Receptor
R-848	Resiquimod-848
RAGE	Receptor for Advanced Glycation End products

rBS-WC	Recombinant Cholera B subunit-Whole Cell
rcf	Relative Centrifugal Force
RER	Rough Endoplasmic Reticulum
rHBsAg	Recombinant Hepatitis B Surface Antigen
RIG-I	Retinoic Acid-Inducible Gene-I
RNA	Ribonucleic Acid
rpm	Revolutions Per Minute
RPMI	Roswell Park Memorial Institute
s.c.	Subcutaneous
S.E.M.	Standard error of the mean
S100	100% soluble in ammonium sulphate at neutral pH
SEM	Scanning Electron Microscope
SIGLEC	Sialic acid binding Immunglobulin-like Lectins
SLC	Secondary Lymphoid tissue Chemokine
SLO	Secondary Lymphoid Organ
ssRNA	Single-stranded Ribonucleic Acid
TAP	Transporter Associated with Antigen Processing
TB	Tuberculosis
TBK-1	Tank-Binding Kinase-1
TcR	T Cell Receptor
TEM	Transmission Electron Microscope
Tfh	T Follicular Helper
TGF-β	Transforming Growth Factor-beta
Th	T Helper
TIR	Toll/Interleukin 1 Receptor
TLR	Toll-Like Receptor
TNF-α	Tumour Necrosis Factor-alpha
TNF-β	Tumour Necrosis Factor-beta
TRAF	TNF Receptor-Associated Factor
TRIF	TIR-domain-containing adapter-Inducing Interferon-β
TT	Tetanus Toxoid
UDP	Uridine Diphosphate Glucose
UNICEF	United Nations Children's Fund
v/v	Volume per Volume
v/w	Volume per Weight
w/v	Weight per Volume
WHO	World Health Organisation
V-RG	Recombinant Rabies Vaccine
ZBP1	Z-DNA Binding Protein 1

CHAPTER-1: INTRODUCTION

1.1 Vaccines

Since the age of Edward Jenner, vaccines have revolutionised public health worldwide, successfully saving the lives of millions of people from infectious diseases. It has been about 30 years since the World Health Organisation (WHO) announced the complete control and eradication of smallpox, achieved through the widespread application of the smallpox vaccine [1]. With increasing vaccine coverage, the eradication of polio is also nearly complete [2,3]. This can be clearly observed in the globally decreased incidence of polio associated with increased immunisation coverage [2] **(FIGURE 1.1)**. In the same way, vaccine immunisation has reduced the incidence and mortality of many diseases such as diphtheria, *Haemophilus influenzae* type b (Hib) infection, hepatitis B viral infection, tetanus, measles, mumps, neonatal tetanus, pertussis, pneumococcal infection, rubella, and serogroup C meningococcal infection [2,4]. Therefore, vaccine discovery has been one of the greatest achievements and one of the most economic and safe interventions of biomedical science.

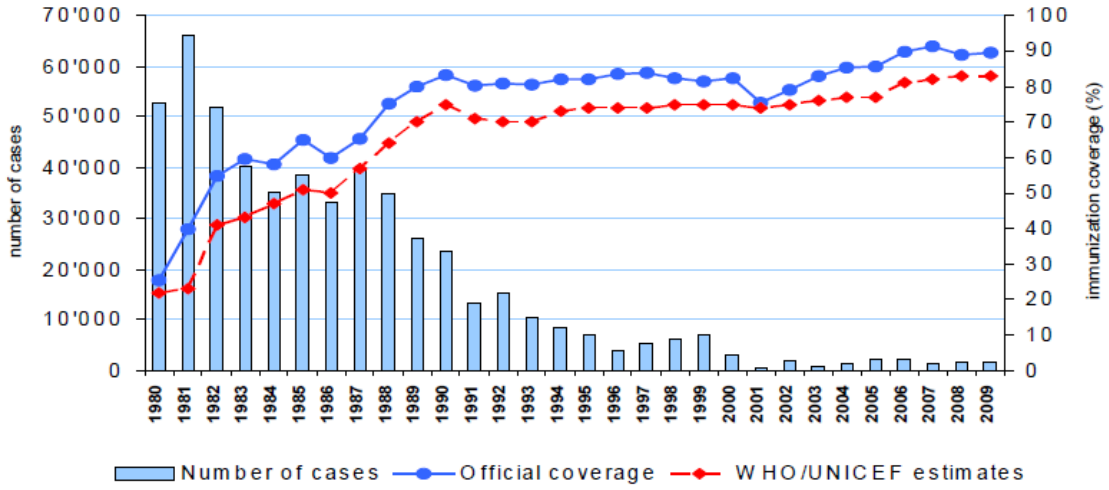

FIGURE 1.1: Poliomyelitis global annual reported cases and Pol3 (third dose of polio virus vaccine) coverage, 1980-2009.

The graph represents the data reported by the Member States to WHO, and WHO/United Nations Children's Fund (UNICEF). It shows decreasing polio cases around the world are associated with increased immunisation coverage with time (Adapted from: WHO vaccine-preventable diseases: monitoring system 2010 global summary [2]).

1.2 Vaccine technologies

The vaccines described above have been produced by a number of different technologies **(TABLE 1.1)**. These share the common goal of producing a version of the infectious agent or its antigens, in a form that is less infectious or pathogenic, but retains effective immunogenicity and ability to protect the host against subsequent exposure to infection.

1.2.1 Live attenuated vaccines

Live vaccines contain modified live microorganisms that replicate in the host, causing a mild infection and consequently stimulate the host immune response in a manner similar to the immune response stimulated by natural infection [5,6]. In these vaccines, the virulence of the organisms is reduced either via multiple passages in a nonhuman host such as embryonated eggs or tissue culture cells under suboptimal conditions of temperature or by chemical mutagenesis [6]. These modified organisms generate immune responses of high magnitude and long duration, thereby promoting cellular and humoral memory [5]. In addition, they are sufficient to induce protective immunity following a low number of immunisations [5,7,8]. The currently existing live vaccines are effective against polio (Sabin), mumps, measles, rubella, chickenpox, shingles, rotaviral infection, yellow fever, typhoid (oral ty21a) and tuberculosis (TB) (BCG, Bacillus Calmette–Guerin) **(TABLE 1.1)**. However, there are several limitations of live vaccines, firstly they are able to replicate in the host and can revert to the virulent wild-type strain [9]. In addition, they are able to induce disease in immunocompromised patients and patients undergoing immunosuppressive therapy [7,8].

TABLE 1.1: Types of vaccines prepared by different techniques.

Types of vaccines	Examples of vaccines used for different diseases
Live attenuated vaccines	MMR (Measles, Mumps, Rubella) vaccine, Yellow Fever, Vaccinia (Smallpox) and Rotavirus Vaccine, Live Attenuated Influenza Vaccine (LAIV), Varicella zoster vaccine, Polio vaccine (Oral, Sabin), Typhoid vaccine (oral, ty21a) and BCG (Bacillus Calmette-Guerin) vaccine.
Inactivated vaccines	Polio (Salk), Hepatitis A, Influenza, Cholera (Recombinant Cholera B subunit-Whole Cell, WC-rBS) and Plague Vaccine.
Toxoid subunit vaccines	Diphtheria Toxoid (DT) and Tetanus Toxoid (TT).
Polysaccharide subunit vaccines	Pneumococcal, Meningococcal and Typhoid (Vi capsular) Vaccines.
Conjugate subunit vaccines	Hib (Polysaccharide linked to the TT or DT), Meningococcal Conjugate Vaccine (MCV) 4 (Polysaccharide linked to the DT), and Pneumococcal (Polysaccharide linked to the DT or *H. influenzae*) Vaccines.
Recombinant subunit vaccines	Hepatitis B, Human Papillomavirus (HPV) and Recombinant Rabies Vaccine (V-RG).

1.2.2 Killed or inactivated vaccines

Killed or inactivated vaccines contain whole organisms that are inactivated by heating and or treating with chemicals such as formaldehyde, glutaraldehyde or phenol to prevent *in vivo* growth, but retain most of their epitopes and factors associated with immunogenicity [5,10]. Polio (Salk) and hepatitis A are standard inactivated vaccines [9] **(TABLE 1.1)**. Following immunisation with killed vaccines, there is neither risk of persistent infection nor reversion to a virulent form [7,8]. These vaccines induce potent humoral immunity characterised by long-lasting antibody production because most of the epitopes and virulence factors are preserved after inactivation [3].

Though killed vaccines have excellent safety in immunodeficient patients, they have been associated with adverse side effects. For example, use of the whole cell killed pertussis vaccine has been associated with inflammation at the injection site and fever-associated seizures called febrile convulsions [11,12]. Furthermore, killed vaccines are poor inducers of cellular immune responses [5]. In addition, a fairly large number of microorganisms and multiple vaccine doses are required to maintain detectable antibody levels [7-9].

1.2.3 Subunit vaccines

Subunit vaccines contain purified antigens or extracts of whole organisms. Subunit vaccines are composed of toxoids, subcellular fragments or surface antigens [13,14]. DT derived from *Corynebacterium diphtheriae* and TT derived from *Clostridium tetani* are examples of toxoid vaccines, where the bacterial toxin was isolated biochemically and then the enzyme activity, and associated pathogenicity were removed by chemical inactivation [14]. Similarly, purified carbohydrate antigens from *Pneumococcus* were used in the first polysaccharide vaccine. However, due to the T cell independent nature of carbohydrate antigens, this vaccine could not generate a T cell response and failed to work in infants [15]. This problem was overcome by conjugating polysaccharide antigens to proteins, in particular toxoid vaccines **(TABLE 1.1)**. This technique gave safe and effective conjugate

vaccines against Hib, *Streptococcus pneumoniae* and *Neisseria meningitidis* serogroup A, C, Y, W-135 [16,17]. Subunit vaccines can be safely given to immunosuppressed people [5] and one of the main factors driving technology development towards subunit vaccines is their unrivalled safety profile. However, a major limitation of these vaccines is their lack of strong immunogenicity and the requirement for multiple doses for protection [9].

1.2.4 Recombinant vaccines

The inability to cultivate certain pathogens in bulk, for example hepatitis viruses, has been a major limitation to the mass production of vaccine antigens. However, these antigens can be produced using recombinant DNA approaches to isolate antigen coding genes and express these in heterologous expression systems. For example, recombinant viral vaccines such as recombinant hepatitis B surface antigen (rHBsAg) and HPV vaccines are produced by inserting genes encoding the virus surface protein into a yeast expression vector. The modified yeast cell grows and produces refined HBsAg or HPV capsid protein [18,19]. One important viral recombinant vaccine is V-RG (Recombinant Rabies Vaccine) that is prepared by insertion of the rabies glycoprotein gene into live vaccinia virus [20,21]. Although these approaches have allowed the bulk production of antigens hard to grow, they suffer equally as subunit vaccines from a lack of immunogenicity.

1.3 Key issues in vaccine development

With increased understanding of pathogen biology, molecular biology, biochemistry and biotechnology, vaccine development has progressed from trial and error based empirical vaccine studies towards more rational and reductionist approaches [22]. Nevertheless, these techniques have had limited success in developing effective vaccines against emerging diseases like Human Immunodeficiency Virus/Acquired Immunodeficiency Syndrome (HIV/AIDS) and re-emerging diseases like TB and malaria [23].

One important limitation of vaccine development is the incomplete understanding of the components required to form an ideal vaccine. An ideal vaccine would be safe in humans and animals and would induce immune response of high antigen specificity, high magnitude and long duration. Therefore, these vaccines would induce the generation of a large number of memory cells capable of quick and precise recognition of the specific epitope of an antigen and re-stimulation upon consequent antigen exposure within the body [24,25]. This would secure the induction of long-lasting protective cellular and humoral immune responses. Unfortunately, in many diseases, our knowledge of what the protective response looks like is incomplete. In addition, we do not know completely how to induce these responses safely, appropriately, and precisely [26].

One of the major obstacles to continued progress in vaccine development has been the reduced immunogenicity of refined subunit or recombinant protein vaccines compared with live vaccines. This may be due a number of factors, such as rapid clearance from the body, poor recognition by the immune system and failure to adequately stimulate appropriate immune cells [27]. Therefore, while appropriate and safe antigen discovery has been the main target of vaccinology in recent years, the discovery of the substances that increase the immunogenicity of the antigens is also gaining equal importance. These substances are called adjuvants.

1.4 Adjuvants

The term ‘adjuvant’ is derived from the Latin verb *adjuvare* which means to help. In 1926, Ramon coined this term for substances such as bread crumbs, agar, tapioca, starch oil, lecithin or saponin which, when used in combination with specific antigens, produced a higher level of immunity than that produced by the antigen alone [28]. Janeway in 1989 called adjuvants ‘the immunologists’ dirty little secret’; ‘dirty’ because the purified vaccine antigens recognised by T and B-lymphocytes were contaminated with the undefined components of adjuvants, for example heat killed mycobacteria, and ‘secret’ because their mode of action remained a mystery [29].

Using adjuvants in vaccines has several advantages. The limitations of refined vaccines can be overcome by formulating a vaccine with adjuvants. The formulation of a vaccine with an adjuvant may reduce the antigen dose and number of immunisations required to establish protective immune responses [9]. Adjuvants can also affect the initiation, strength and duration of immune responses. In addition, they may induce immune responses in immunologically immature children, immunocompromised individuals and immunologically less responsive, aged people [30-32].

1.4.1 Clinically applicable adjuvants

Despite a great deal of interest in developing novel adjuvants, there are currently few adjuvants approved for use in human health. In the United States, Alum and AS04 (adjuvant system 04) are the only licensed adjuvants and these plus virosomes and MF59 and AS03 (oil-in-water emulsion) are licensed in the European Union [33-36] (**FIGURE 1.2)**. Among these adjuvants, Alum is a dominant adjuvant used in vaccines since 1920s in the USA and the Europe. This mineral adjuvant is used in different vaccines such as those against hepatitis A, hepatitis B, polio virus, HPV, rabies virus, tick-borne encephalitis virus, *Bacillus anthracis, Clostridium botulinum, Clostridium tetani, Corynebacterium diphtheriae, Bordetella pertussis,* Hib, *Pneumococcus* spp, and foot-and-mouth disease virus [37,38]. AS04 is a combination of two adjuvants, MPL and Alum (Aluminium hydroxide in Cervarix or Gardasil used to prevent cervical cancer caused by human papillomavirus (HPV) and Aluminium phosphate in Fendrix used to prevent hepatitis B virus infection) [39-41]. Two GSK products, Fendrix and Cevarix, were licensed in the Europe in 2005 and 2007 respectively. Gardasil, a vaccine developed by Merck and Co, Inc, was first approved by the US Food and Drug Administration (FDA) in 2006, whereas Cervarix was first approved in 2009. MF59 (FLUAD®) is a squalene-based oil-in-water emulsion developed by Novartis and is used in influenza vaccines. AS03 (Prepandrix), licensed in 2008, is an oil-in-water emulsion developed by GSK and is used against pandemic influenza caused by H1N1 strain. Virosomes (Inflexal, developed by Crucell), licensed in 1997, are liposomes, tiny spherical vesicles that consist of synthetic and natural phospholipid molecules. They are trivalent seasonal

influenza vaccines that contain virosomes, and the influenza surface proteins like haemagglutin (HA) and neuraminidase (NA) [34,42,43].

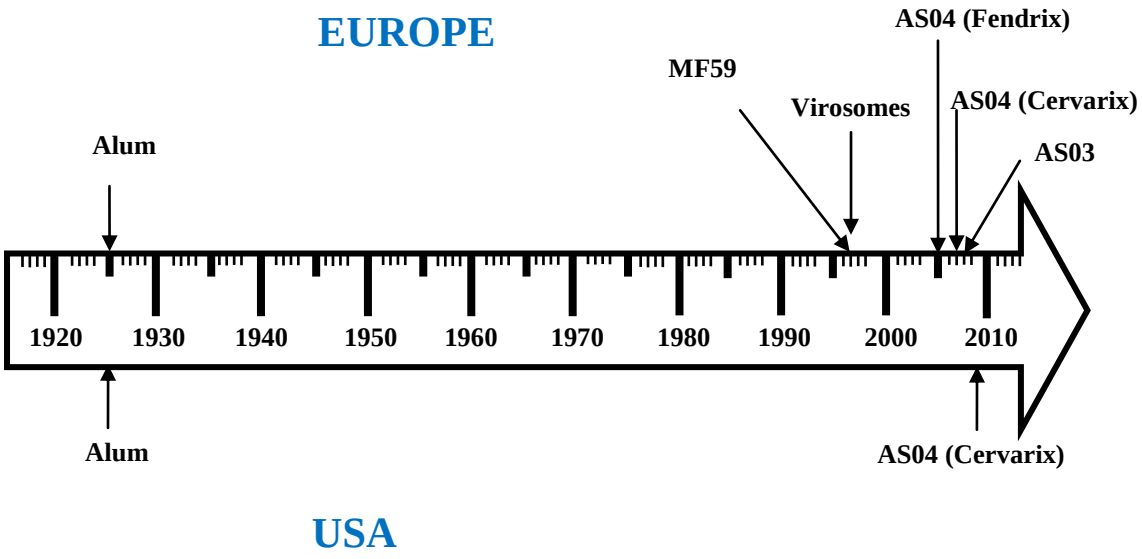

FIGURE 1.2: Chronology of adjuvant licensing in Europe (including UK) and the USA.

This diagram is derived from various publications [34,42,43].

1.4.2 Alum

1.4.2.1 Range of Aluminium compounds used in vaccines

Alum is by far, the oldest adjuvant in the history of human vaccination. This adjuvant was first used by Alexander T. Glenny who prepared potassium Aluminium sulphate or Alum [$KAl(SO_4)_2$]-adjuvanted vaccines by co-precipitation with DT dissolved in carbonate buffer [44-46]. Due to the problems in manufacturing reproducibility [47], the technique of Alum precipitation has been substituted by the adsorption of vaccines onto preformed Aluminium hydroxide or alhydrogel (chemically crystalline Aluminium oxyhydroxide) and Aluminium phosphate or

adju-phos gels (chemically amorphous Aluminium hydroxyphosphate) [48,49]. Literatures are found regarding the wide application of other forms of Aluminium compounds [50] such as Aluminium silicate [51], Algammulin (gamma inulin plus Aluminium hydroxide) [52], cesium Alum [53], Imject Alum (Aluminium hydroxide plus magnesium hydroxide) [54,55] have also played a significant space in the vaccinology benchsides. All of these Aluminium compounds are called 'Alum' in the literature, although this type of chemical definition is incorrect [56].

1.4.2.2 Properties of Aluminium compounds

The solubility of Aluminium hydroxide, $Al(OH)_3$ is extremely low in water, but it increases in acidic or alkaline media [57]. The molecular formula of this mineral seems to have an Aluminium atom (with +3 positive charges) at the centre with three hydroxyl (OH^-) groups attached to it. However, Stanley Hem's group at Purdue University carried out detailed studies of this compound used in vaccine preparation. Using X-ray crystallography and infrared spectroscopy, this group has studied a boehmite-like pattern of Aluminium hydroxide called Aluminium oxyhydroxide AlO(OH) rather than the usual chemical formula, $Al(OH)_3$ in adjuvant preparations [49,58]. The surface of this adjuvant comprises metallic hydroxyl groups coordinated to Aluminium **(FIGURE 1.3)**. These hydroxyl (OH) groups can accept a proton to produce a positive site or can donate a proton to produce a negative site at the surface [57]. Therefore, the surface charge depends on the pH of the adjuvant formulations. Aluminium hydroxide has an approximately 11.4 point-of-zero-charge (PZC) at which this compound carries no charge within it or in its surface. Therefore, at physiological pH (pH=7.4), this mineral consists of a positive surface charge. The PZC of Aluminium hydroxide adjuvant can be decreased to an acidic value by treating this adjuvant with phosphate anions [59].

While studying the structure of Alum, the Hem group has shown a fibrous primary particle of size 4.5x2.2x10 nm for Aluminium oxyhydroxide [58]. These particles form a loose and irregular aggregate of 1–10μm size [57] that is significant for phagocytosis by APC [60]. In addition, the very small primary particles of this

adjuvant has a high surface area (surface area=500m^2/g) [58,61] that may enhance strong protein antigen adsorption [50].

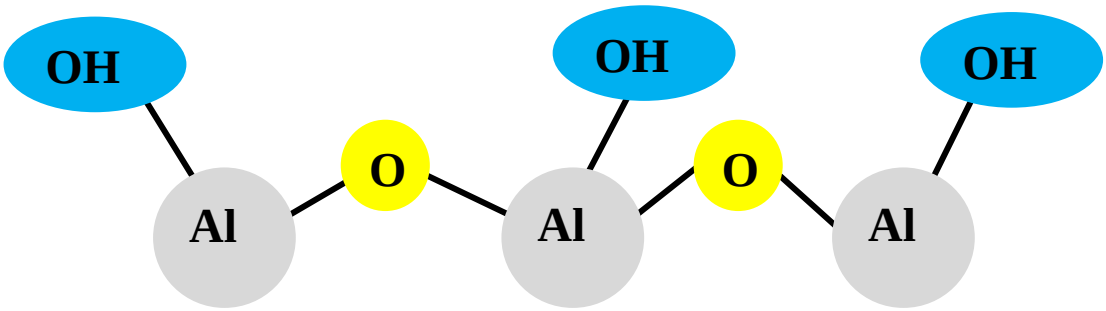

FIGURE 1.3: Schematic of surface of Aluminium hydroxide adjuvant.

This diagram is adapted from [57].

1.4.2.3 Adsorption properties of Aluminium adjuvants

The general guideline for adsorption of many protein antigens in both Aluminium hydroxide and Aluminium phosphate is optimum in the pH interval between the PZC and isoelectric point (IEP). In this interval, the adjuvant and the antigen will have opposite electrical charges that increase electrostatic attraction and adsorption [62]. Therefore, at physiological pH, Aluminium hydroxide can efficiently bind with an antigen with an acidic IEP and Aluminium phosphate can efficiently bind with an antigen with an alkaline IEP [63]. This is quite important in binding or adsorbing the proteins with an acid IEP via electrostatic attraction between the positively charged Aluminium hydroxide and the negatively charged proteins [59]. In this context, the proteins or peptides which have higher IEP may show efficient binding with this mineral adjuvant. Another adsorption mechanism involves ‘ligand exchange’ between positively charged Aluminium hydroxide and negatively charged proteins containing $(PO4)^{3-}$ groups [59,62,64]. Ligand exchange may occur when an electrostatic repulsive force is present [57]. However, this

mechanism may also reduce adsorption by electrostatic attraction if anions [for example, $(PO4)^{3-}$ ions from buffer] with affinity for ligand exchange with OH^- on the surface of Aluminium hydroxide [65]. This is because of the lack of available OH^- groups for ligand exchange as the higher concentration of $PO4^{3-}$ groups from buffer treatment already binds with the higher numbers of surface OH^- groups available for other binding options between proteins and Aluminium adjuvants that may occur via hydrophilic-hydrophobic interaction, van der Waal's force and hydrogen bonds [50].

1.4.2.4 Effects of temperature on Aluminium adjuvants

Aluminium adjuvants are irreversibly damaged by freezing and subsequently thawing. The freezing also results in the loss of the protein adsorption capacity [63]. In the same way, autoclaving causes a slight reduction in pH, viscosity, surface area of protein and increase in crystallinity and finally reduction in the adsorption capacity of Aluminium hydroxide. The protein adsorption capacity also decreases following autoclaving Aluminium phosphate adjuvants though their amorphous structure does not change [66].

1.4.2.5 Dose of Aluminium compounds in vaccines

In experimental vaccinology, different labs use various ranges of Aluminium compounds. In the preclinical phase of vaccine development, the dose is empirically determined, but there are no accepted limits of Aluminium for veterinary vaccines. In human vaccines, the European limit is 1.25mg elemental Aluminium per dose [67], whereas the US limit as guided by the FDA is 0.85mg elemental Aluminium per dose if determined by assay or 1.14mg if determined by calculation on the basis of the amount of Aluminium compound added or 1.25mg determined by assay provided that this amount is safe and effective [67], http://www.accessdata.fda.gov/scripts/cdrh/cfdocs/cfcfr/CFRSearch.cfm?fr=610.15, accessed on 23 May 2012).

1.4.2.6 Side-effects of immunisation with Aluminium compounds

In recent years, researchers have reported various adverse effects of Aluminium adjuvants such as 'macrophagic myofascitis' [68-70] and 'muscle granuloma' following intramuscular immunisation [71] and Aluminium hydroxide granuloma of the subcutaneous tissue following immunisation [72,73]. These effects are almost similar [74] and are characterised by dermatologic reactions such as granulomas, erythema, cutaneous nodules, angioedema and myalgias and fatigue with increased IL-1 and IL-6 secretion [75,76]. Aluminum-containing vaccines like Hepatitis B vaccines (Engerix-B) and Anthrax vaccines (BioThrax) produce post-licensure adverse effects such as idiopathic thrombocytopenia, anaphylaxis and or other generalised hypersensitivity reactions, facial palsy, Guillain-Barre syndrome, visual disturbances, asthma and arthritis (http://www.fda.gov/OHRMS/DOCKETS/98fr/05n-0040-bkg0001.pdf, accessed on 23 May 2012)(http://us.gsk.com/products/assets/us_engerixb.pdf, accessed on 23 May 2012). Recently, Tomlejenovic and Shaw (2011) [77] has reviewed the neurodevelopmental toxicity comprising long-term brain inflammation and serious health consequences due to Aluminium compounds in cats, rabbits, mice and humans.

In spite of few reports of adverse reactions, these adjuvants are not pyrogenic or carcinogenic or teratogenic [50]. They even reduce the reactogenicity of some microbial adjuvants such as lipopolysachharide (LPS) [60]. In addition to their excellent safety records, other factors such as ease of preparation, stability and immunomodulatory effects have created them to be a dominant adjuvant in the vaccine industry [63,75,78,79]. Therefore, in the absence of development of new safe adjuvants, Aluminium adjuvants will continue for many years.

1.4.3 Limitations of clinical adjuvants

Currently available vaccines confer immunity primarily through a humoral response, characterised by antibody production [80]. While the recently available clinical adjuvants have been effectively applied in many of these vaccines, they have broadly failed to initiate protective responses against protein and peptide vaccines

against HIV, *Mycobacterium* and *Plasmodium*. Though the humoral response can be sufficient in preventing infection by HIV [81,82] and can affect certain stages of infection by *Plasmodium* [83], cell-mediated immunity (CMI) is entirely or partially required to clear these intracellular organisms [84]. In this context, the current clinical adjuvants fail to induce protective CMI. For example, Alum has been shown to generate and enhance T helper (Th) 2 type responses characterised by the production of cytokines such as interleukin (IL)-4 and IL-5 and B cell responses characterised by the immunoglobulins (Ig) gamma1 (IgG1) and epsilon (IgE) production [85,86]. Alum, therefore, is not able to stimulate CMI responses such as interferon gamma (IFN-γ) production and B cell IgG2a production [87,88]. Similarly, virosomes and the oil emulsions (AS03 and MF59) are primarily strong antibody producing adjuvants [36,89-93]. In contrast to these adjuvants, AS04 adjuvant containing MPL and Alum is well-known for its efficacy to increase the magnitude and persistence of antibody production and the generation of CMI [94]. This suggests that the addition of MPL to Alum adjuvants converts them from Th2- into Th1- inducing adjuvants. Therefore, regulating Th1 immunity through the formulations of TLR-based adjuvants may have significant contribution in the rational vaccine design against intracellular pathogens [95].

1.4.4 Types of adjuvant

The classification of vaccine adjuvants is complex due to the enormous diversity of compounds and the range of functions they perform. Vaccine adjuvants have been variously classified on the basis of their particulate nature [96], origin or sources [27] and mechanism of action [32,97]. Vaccine adjuvants can be classified as delivery vehicles and/or immunostimulatory substances [98].

Delivery vehicles include mineral salts (Alum), oil emulsion (water-in-oil emulsion like FCA and oil-in-water emulsion like MF59), liposomes, microparticles, virosomes and immunostimulatory complexes. These agents are thought to target formulated antigens to antigen presenting cells (APCs) in the secondary lymphoid organs (SLOs) and/or slowly release antigen from the site of immunisation [31,32].

Immunostimulatory substances are thought to directly activate aspects of the innate and/or adaptive immune responses. These include pathogen associated molecular patterns (PAMPs) and damage associated molecular patterns (DAMPs). PAMPs include LPS, and derivatives such as monophosphoryl lipid A (MPL A), Mannans, single-stranded (ss) or double stranded (ds) deoxyribonucleic acid (DNA), ss or ds ribonucleic acid, muramyl dipeptide (MDP) and Cytosine phosphate Guanine Oligodeoxynucleotide (CpG ODN). These molecules are recognised by pattern-recognition receptors (PRRs) such as toll-like receptors (TLRs) and Nucleotide Oligomerisation Domain protein-like receptors (NLRs) and retinoic acid-inducible gene-I (RIG-I)-like receptors (RLRs). Therefore, PAMPs target their specific receptors directly resulting in enhanced adjuvanticity. That is why several microbial adjuvants such as tripalmitoyl cysteine (Pam3Cys), macrophage activating lipopeptide of 2kDa molecular mass (MALP-2), S-[2,3-bis(palmitoyloxy)propyl]cysteine (Pam2Cys), polyinosinic:polycytidylic acid (poly I:C), BCG, FCA, MPL A, flagellin, imiquimod, resiquimod-848 (R-848), CpG ODN and haemozoins have been currently developed and are under vaccine clinical trials [95,99,100] **(TABLE 1.2)**.

TABLE 1.2: A variety of new adjuvants, their innate immune receptors, ligand components and sources or origin in nature.

Adjuvants isolated from different sources consist of agonists that bind the innate immune receptors of APCs and induce or enhance innate and adaptive immune responses. IPAF: Ice protease-activating factor, NALP5: NACHT [Neuronal Apoptosis Inhibitory Protein (NAIP), MHC class II Transcription Activator (CIITA), Incompability locus protein from *Podospora anserina* (HET-E), Telomerase-associated protein (TP1) family] Domain-Leucine-Rich Repeat-, and PYD (Pyrin domain)-containing Protein 5.

Adjuvants	**Innate Immune Receptors**	**Ligand Components**	**References**
Pam3Cys	TLR1 + TLR2	Lipoprotein	[101]
MALP-2 Pam2Cys	TLR2 + TLR6	Diacyl lipopeptide	[102-104]
BCG, FCA	TLR2 NOD2 (NLR)	Peptidoglycans Muramyl dipeptide	[105-107]
Poly I:C	TLR3 MDA5 (RLR)	ds RNA	[108-110]
BCG MPL A	TLR4	LPS	[102,107]
Flagellin	TLR5 IPAF NALP5	Flagellin	[111-113]
Imiquimod, Resiquimod-848 (R-848)	TLR7, TLR8	ssRNA	[114]
CpG ODN Haemozoins	TLR9	Unmethylated CpG Haemozoin	[115,116]

On the other hand, DAMPs include uric acid, HSPs, DNA, RNA, nucleotides, and adenosine triphosphate (ATP) [117]. DAMPs are recognised by DAMP receptors (DAMPR) as well as by some PRRs. Though many DAMPs can trigger adjuvant properties via DAMPRs or PRRs **(TABLE 1.3)**, very few of them, such as HSPs, have been directly used in vaccine design. For example, HSPs are recognised by DAMPRs (CD91) leading to enhanced antigen internalisation [118,119] and has been used to deliver antigens in cancer vaccine development [120].

TABLE 1.3: Endogenous danger signals (DAMPs), their receptors and their immunological responses within the host body.

The binding of danger signals released through tissue damage with their receptors lead to immunological effects such as phagocytosis, APC activation and migration to DLNs, cytokine production, inflammation and ultimately T cell activation.

Endogenous Danger Signal (DAMPs)	DAMP Receptors	Effects as Adjuvants	References
Heat shock proteins (HSP60, HSP70, HSP90, glycoprotein (GP) 96, calreticulin)	CD91, TLR4, TLR4/TLR2, lectin-type oxidised low-density lipoprotein receptor 1 (LOX-1)	Phagocytosis, DC maturation, Ag presentation, IL-1β, IL-6, IL-12 and TNF-α *production* and humoral and cellular immunity, cytotoxic responses and tumour immunity.	[121-125]
Uric acid crystals	TLR2, TLR4, NLRP3	DC migration and Secretion of proinflammatory cytokines.	[126]
ssRNA	TLR3, TLR7, TLR8	Secretion of proinflammatory cytokines.	[127]
DNA	TLR9, retinoic acid-inducible gene-I (RIG-1), DNA-dependent activator of IFN-regulatory factors (DAI)	Secretion of proinflammatory cytokines and IFN-γ.	[55,127,128]
Nucleotides	$P2Y_{1,2,4,6,11}$, $P2X_{4,7}$	Recruitment of immature DCs by chemotaxis.	[129,130]
Sugar metabolites (Uridine Diphosphate Glucose, UDP)	$P2Y_6$	IL-8 (CXCL8) production in monocytes and in human mature DCs.	[129,130]
S100 calgranulin proteins (A8, A9,A12) (100% soluble in ammonium sulphate at neutral pH)	Receptor for Advanced Glycation End products (RAGE)	Monocyte chemoattractant, leukocyte transmigration and inflammation.	[131]
High mobility group box 1 (HMGB1, Chromatin-associated protein)	TLR2, TLR4, RAGE	DC maturation, T cell activation and Th1 polarisation.	[132,133] [134]
Adenosine Tri-phosphate (ATP)	$P2X_7$, P2Y, P2(?)	Mycobacteria clearance, acidification of phagosomes, phagosome-lysosome fusion, production of nitric oxide (NO) and reactive Oxygen intermediates	[135,136]
Heparin sulfate (Proteoglycans)	TLR2, TLR4, NLRP3	NLRP3 stimulation, IL-1β secretion, DCs maturation and T cell priming	[137]

Adjuvant formulations often contain combinations of delivery systems with immunostimulators. For example heat killed mycobacteria with water-in-oil emulsion in FCA and the recently licensed adjuvant AS04 containing Alum with MPL A [138]. This approach has many advantages, for example the delivery system allows physical linkage of the vaccine components, which has been shown to be important for decreasing the dose of immunostimulator and antigen required as well as often reduces adverse effects associated with free immunostimulator [139]. In this context, liposomes and microparticles seem to be an excellent example because these adjuvants can be used to entrap immunostimulatory antigens such as bacterial and viral components and both adjuvants and antigens can be targeted to the same cell for the efficient immune responses [140]. This strategy is particularly important for mucosal vaccination where vaccine antigens are subjected to low pH, enzymatic degradation, rapid transit and poor absorption [140]. The strategy of using more than one adjuvant is currently being considered in many clinical trials of HIV, malaria, TB and cancer vaccines to achieve mixed immune responses [95]. For example, different adjuvant systems currently devised by GlaxoSmithKline (GSK) Biologicals, Dynavax, Intercell, Novartis and Chiron contain more than one adjuvant with the aim of achieving advantages of mixed adjuvant responses [34,141] **(TABLE 1.4)**.

TABLE 1.4: Combined adjuvant formulations in vaccines currently in development by various vaccine companies.

Different combined adjuvant formulations are under development (Adapted from [34,141]. MTP-PE: Muramyl tripeptide phosphatidylethanolamine, IC: Inosine Cytosine, ISS: Immunostimulatory DNA sequence.

Adjuvant Name	**Formulations**	**Stage of Development**	**Current vaccine target**	**Company**
AS01	Liposome+ MPL+ QS21	II	TB HIV	GSK
AS01	Liposome+ MPL+ QS21	III	Malaria	GSK
AS02	MPL+O/W emulsion+QS21	II	Malaria, TB	GSK
AS03	O/W emulsion+ α tocopherol	Licensed	Pandemic flu	GSK
AS04	MPL+Alum	III	Herpes Simplex Virus	GSK
AS15	Liposome+ MPL+ QS21+CpG	III	Lung cancer melanoma	GSK
IC31	Peptide+ oligonucleotides	I	TB	Intercell
RC-529	Synthetic MPL+Alum	II	HBV	Dynavax
ISS	Oligonucleotide+Alum	II	HBV	Dynavax
MF59 +MTP-PE	Lipidated MDP+ O/W emulsion	I	HIV, Flu	Chiron Novartis

1.5 Adaptive Immune Responses

Historically, adjuvant development has largely been empirical. For rational vaccine development, we need to understand the basic immunology underlying the induction of immune responses. Understanding this process in more detail will define where existing adjuvants affect this process, how they can be rationally improved or combined and reveal new targets for adjuvant development. Vertebrates are constantly at risk of pathogen invasion and consequently have developed innate and adaptive immune mechanisms to prevent establishment and fight infection [142]. The innate immune response is able to recognise a range of invading microbes via a series of germline encoded receptors [142]. The innate immune system is characterised by immediate responses, preformed cells and effectors and the lack of memory [143]. In contrast to innate response, the adaptive response is characterised by the delayed activation of effectors, the ability to increase specificity for foreign antigens and immunological memory [143,144]. Importantly, the adaptive immune system provides immunological memory that vaccines exploit; generating antigen-specific memory capable of combating future pathogens very quickly and specifically [26,143,145].

It is becoming increasingly clear that these two systems do not work in isolation, and particularly relevant to adjuvant design is the increasing evidence supporting the ability of the innate immune system to shape the ensuing adaptive response. The innate immune system comprises various APCs such as macrophages, DCs and B cells. Among them, DCs are the professional APCs which can process the antigens and present them to the naïve T cell to generate adaptive immunity [146]. Therefore, they act as a bridge between innate and adaptive immunity [147]. These characteristic features of DCs strongly suggest they are a major target of adjuvant effects [148-150]. Consequently, understanding how DCs are affected by adjuvants and how these effects impact on the development of T cell responses and the generation of adaptive immunity is a key aim in vaccine immunology.

1.5.1 DCs and their development

DCs are found in many different organs and tissues, including skin and internal organs, circulatory systems and afferent lymphatic vessels [149]. Most of these DCs originate from haematopoietic stem cells of the bone marrow [151,152] **(FIGURE 1.4)**. Haematopoietic stem cells have the capacity to divide into common myeloid precursor or common lymphoid precursor cells. Both of these precursors can develop into distinct subsets of DCs. Conventional DCs (cDCs) can be developed from bone marrow precursors during *in vitro* culture in the presence of granulocyte macrophage colony stimulating factor GMCSF [153] whereas; plasmacytoid DCs (pDCs) can be developed in the presence of flt3ligand (Flt3L) [154]. This evidence came from the study conducted in 1993 by Inaba and colleagues who demonstrated that mouse BM myeloid precursors had a capacity to produce macrophages, granulocytes, and DCs in the presence of GMCSF [153]. Clinically, human DCs can be differentiated from peripheral blood monocytes in the presence of GMCSF and IL-4 *in vitro* [155].

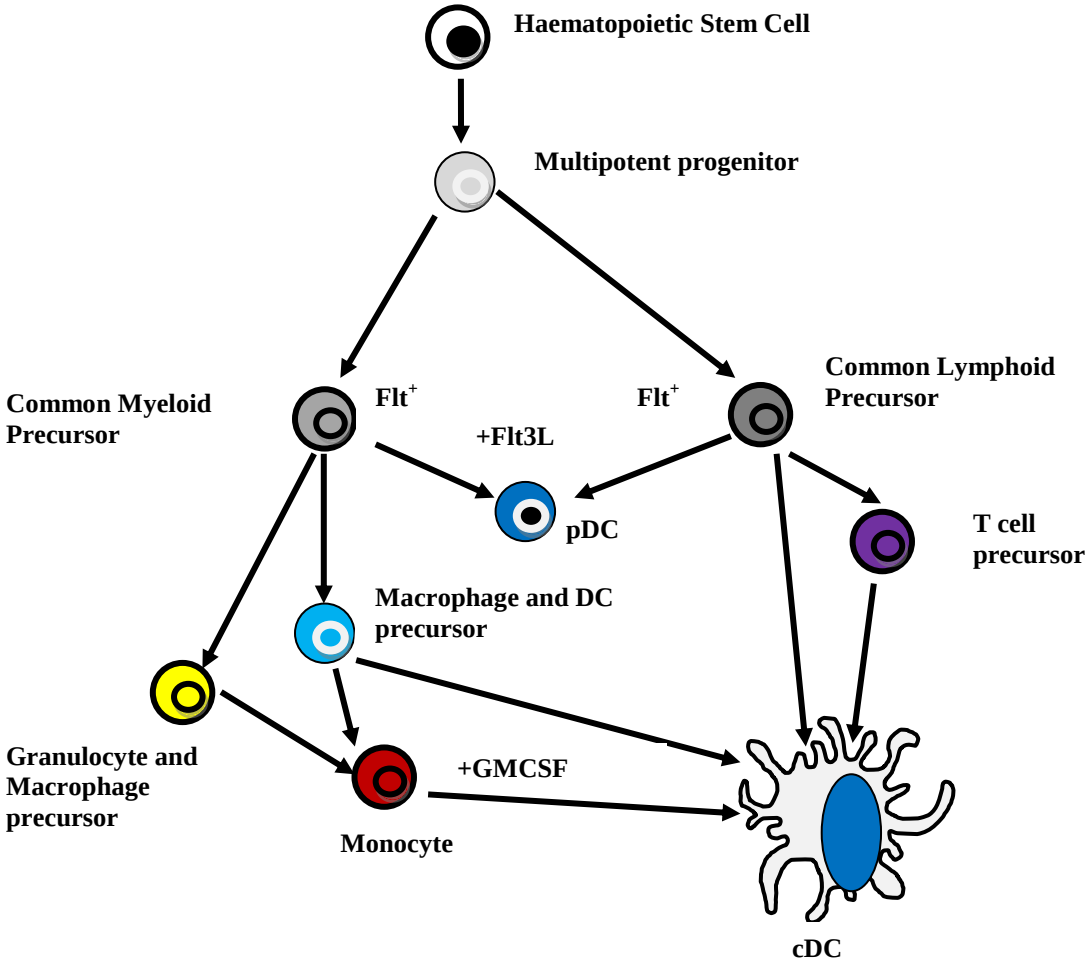

FIGURE 1.4: Development of DCs.

Different DCs can develop from common myeloid progenitor cells (CMPs) or common lymphoid progenitor cells (CLPs) derived from haematopoietic stem cell. CLP and CMP both are Flt+ cells and can give rise to conventional DCs or plasmacytoid DCs depending on the cytokines. cDC: conventional dendritic cell, pDC: plasmacytoid dendritic cell, GMCSF: granulocyte macrophage colony stimulating factor, Flt3L: Fms-like tyrosine kinase 3 ligand (Adapted from [154]).

1.5.2 DCs and their subsets

DCs can be distinguished by specific surface and intracellular phenotypic markers, immunological roles and anatomical distribution [156,157]. There are principally two subsets of DCs [158]. Firstly, type-1 interferon-producing pDCs are found in spleen, BM, thymus and LNs in mice [159,160]. pDCs are spherical and non-dendritic in immature state and they change into the dendritic form following exposure to inflammatory stimuli such as viruses and other microbial infections [161,162]. They highly express plasmacytoid dendritic cell antigen-1 (PDCA-1) and sialic acid binding immunoglobulin-like lectin H (SIGLEC-H) and moderately express major histocompatability class II (MHCII), CD11c and B220 [158]. Mature pDCs also acquire the properties of antigen processing and antigen presentation and activate naïve T cells and memory T cells [162,163]. These cells are also associated with viral immunity and autoimmune diseases [146,164,165].

Secondly, cDCs are found all over the body such as in blood, primary and SLOs and skin. On the basis of cell surface marker expression of CD11c and MHCII in combination with CD4, CD8α, CD11b, and CD205, different cDCs subsets have now been defined in mouse lymphoid organs [158]. Among these subsets, the lymphoid $CD4^{-}CD8\alpha^{high}$ subsets are found in T cell areas of LNs **(FIGURE 1.5)** or spleen. They highly express CD8α, CD11c, CD205 and MHCII and do not express CD11b and CD4. These subsets of DCs have been reported primarily to cross present and activate CD8 T cells [166,167]. In addition, these subsets take part in the induction of CD4+ T cell responses following direct presentation of antigens derived from viruses, bacteria and parasites to the CD4+ T cells [168-171]. These subsets of DCs are important in producing IL-12 *in vivo* following microbial stimulation [172] and during *in vivo* infection [173]. However, recent *in vivo* data support that these DCs can induce protective Th1 responses in an IL-12-independent manner, but CD70-dependent manner [174] indicating the significance of costimulatory molecules in type of immune responses.

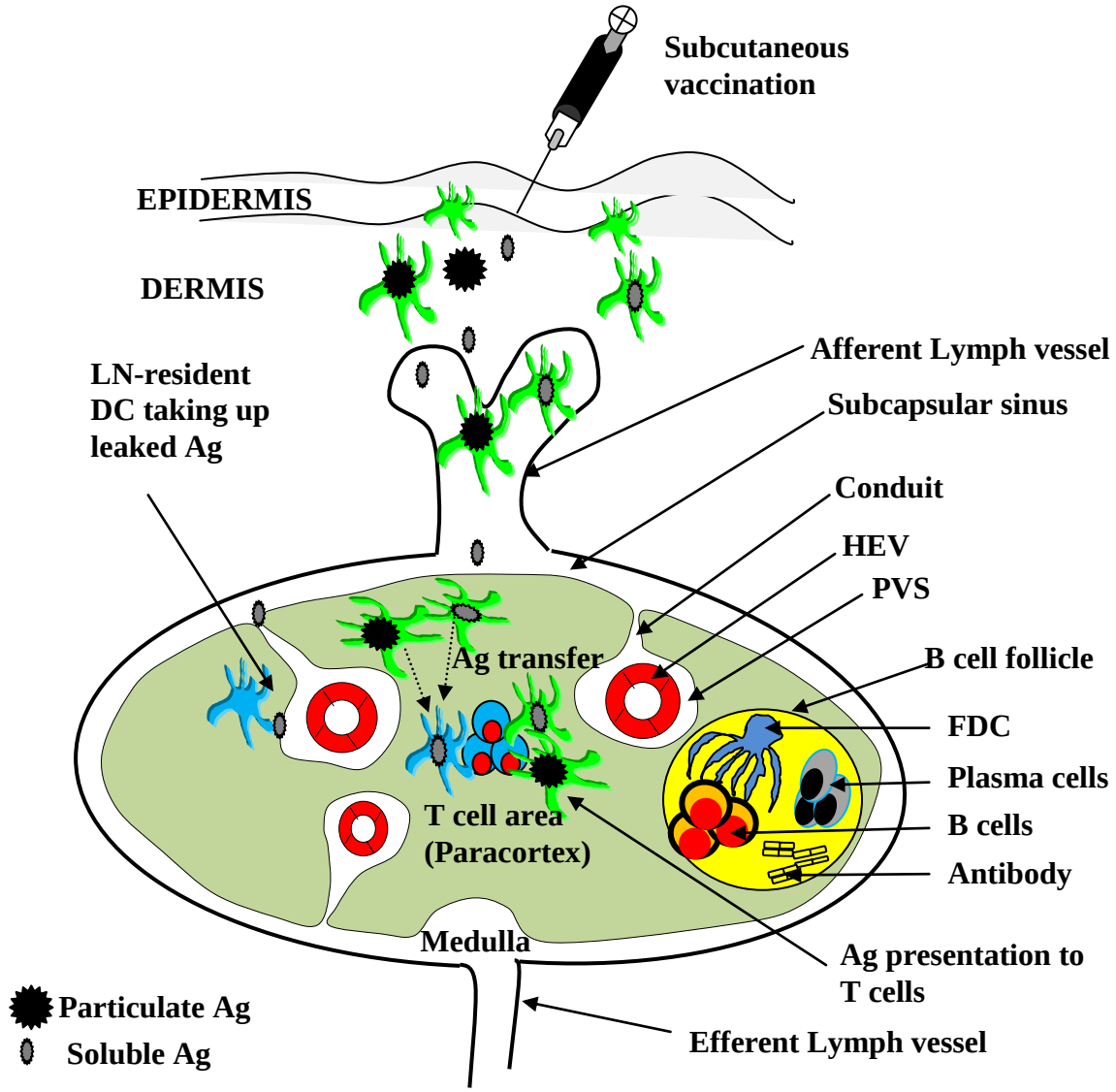

FIGURE 1.5: Current understanding of DC migration inside LN following immunisation.

Immature DCs take up soluble or particulate Ags in the subcutaneous areas and migrate towards the paracortex of the DLN where DCs present Ag to antigen-specific T cells and may also transfer Ag to the resident APCs. Soluble antigen can reach the DLNs without help of DCs. Soluble Ags move via the LN conduit network and can be taken up by resident DCs. DCs are thought to stick dendrites between the fibroblastic reticular cells that line the conduits to sample soluble antigens. Class switched, high affinity humoral responses require B cell antigen presentation, where B cells acquire antigen from follicular Dendritic Cell (FDC). The acquisition of antigen by FDC can be greatly enhanced in the presence of complement or antigen-specific antibodies. HEV: High Endothelial Venule, PVS: Perivenular Space, DLN: draining lymph node **(See text for explanation)**.

cDCs with myeloid lineage can be found in the marginal zone between white pulp and red pulp of spleen and in LNs [175]. They have two different subsets: $CD4^-$ $CD8\alpha^-$ expressing high levels of MHCII without any expression of CD8α and CD4 molecules and $CD4^+CD8\alpha^-$ expressing CD205 and high levels MHCII and CD11b and CD4 moderately in the absence of CD8α expression [175]. Both subsets migrate to the T cell areas of SLOs upon stimulation [176] and both take part in T cell responses *in vitro* and *in vivo* [177,178]. These subsets of DCs take part in taking up pathogens by phagocytosis or their antigens by endocytosis and presenting them to CD4+ T cells in p:MHCII-dependent pathway [177]. However, no single data support the defined role of these subsets of DCs in polarising T helper cells into Th1 or Th2 subsets. Studies suggest that these APCs induce either Th1 or Th2 responses depending on different factors such as the inflammatory adjuvants and the internalisation, processing and presentation of antigens [177].

Langerhans cells (LCs) ($CD4^-CD8\alpha^{low}$) are myeloid in origin and are characterised by the high expression of Langerin, CD205, CD11c, MHCII, CD86, CD80 and CD40 [158,179]. LCs are one of the important subsets of DCs restricted mainly to the skin and draining lymph nodes (DLNs) **(FIGURE 1.5)**. This is because they act as sentinels in the pathogen invading sites like skin surface where they capture antigens [179,180]. These subsets are fundamental examples of migratory DCs that can migrate to DLNs steadily even in the absence of inflammatory stimuli because of their Langerin receptors [179,181,182].

In addition to Langerhans cells, Dermal DCs (DDCs) are also important in the context of subcutaneous (s.c.) immunisation. This is because DDCs migrate into the DLNs from the injection site and present p:MHCII complexes to the activated CD4 T cells that play a role in delayed-type of hypersensitivity [183]. There are two types of DDCs. Firstly, Langerin positive DDCs are characterised by the expression of Langerin, MHCII, CD103 and CD45 and the low expression of CD11b and the lack of expression of CD8α [184-186]. Secondly, Langerin negative DDCs are characterised by the expression of MHCII, CD11c and DEC-205 and the lack of expression of Langerin and CD24α [187].

1.5.3 DCs and antigen uptake

As mentioned above, DCs are central to the induction of adaptive immunity through their unique ability to activate naïve T cells [149]. To initiate an adaptive immune response, a number of signals are required in naïve T cells. Among these signals, signal 1 is the cognate signal provided by p:MHC complexes expressed on APCs [188]. To provide this signal from an exogenous antigen, DCs internalise protein antigens, process them into peptides, load these onto MHC molecules and export these complexes onto the APC surface [189,190].

Once an antigen is introduced into the body, DCs start their crucial role of antigen uptake. DCs are 'voracious eaters' during their lifetime, feeding on antigens from their immature to mature age [191,192]. They constitutively take up large quantities of fluid antigens by macropinocytosis. Macropinocytosis is a process in which cells undergo membrane ruffling producing large and irregular vesicles (1–3µm) [193]. They also take up particulate antigens, such as dying or apoptotic cells, microorganisms [191] and vaccine antigens adsorbed to particulate adjuvants [194,195], by phagocytosis. This involves triggering of cell surface receptors that drive actin polymerisation and active internalisation of particles [196]. DCs can also efficiently take up very smaller antigens (less than 200nm) by different modes of pinocytosis such as clathrin or caveolin-mediated endocytosis [195,197].

The processes of internalisation described above are either dependent on, or are made significantly more efficient, through receptor mediated recognition. Receptors known to be involved in recognition of microbes, vaccines and adjuvants include, complement receptors (CRs), Fc gamma receptors (FcγRs) and c type lectin receptors (CLRs) [191]. Among these receptors, CLRs such as decalectin (DEC205, LY75, CD205, Lymphocyte antigen 75), Mannose receptor (CD206), Langerin (CLEC4K, CD207) and DC-SIGN (DC-specific intercellular adhesion molecule-3-grabbin non-integrin, CD209) recognise carbohydrate structures [198,199]. Antigen internalisation by CLRs or other receptors enhance antigen presenting efficiency of DCs but, independent uptake of antigen by these receptors without any TLR ligation

may induce antigen-specific tolerance [198,199]. The basic function of TLRs is sensing pathogens and subsequently providing maturation stimuli to DCs, but TLR2 and TLR4 are the important molecules involved both in maturation as well as antigen internalisation. TLR2 has been shown to target the lipid ligand (such as lipoprotein) to DCs with subsequent antigen internalisation resulting in cytotoxic as well as Th2 responses [104,200]. TLR4 recognises LPS, initiating redeployment of actin cytoskeleton to enhance antigen internalisation following stimulation of DCs within 30 to 60minutes *in vitro* [201]. Therefore, vaccines which consist of LPS or LPS derivatives such as MPL in AS04 adjuvant may be taken up by resident APCs such as monocytes and DCs and directly activated [202].

1.5.4 Antigen processing

T cells play a central role in CMI and are activated in response to specific vaccine-derived, peptide epitopes bound to MHC class II and class I molecules displayed on the surface of APCs [203-205]. Therefore, proteins in native states require denaturation and processing inside cells before they are presented to T cells. Interestingly, DCs possess highly controlled antigen processing functions utilising intracellular lysosomal protease systems or cytosolic proteasomal systems that are optimised for the generation of peptides with MHCII or MHC I binding capacity, respectively [189-191].

1.5.4.1 MHC Class II pathway

Once an antigen **(FIGURE 1.6A)** is internalised, it travels though the endocytic pathway which consists of increasingly lytic and acidic compartments: early endosome or phagosome (pH 6.5–6.0) **(FIGURE 1.6B)**, late endosomes or endolysosomes (pH 6.0–5.0) **(FIGURE 1.6C–D)** and lysosomes (pH <4.5) [191,206] **(FIGURE 1.6E)**. These features of endocytic vacuoles are designed to digest and kill invading pathogens, however in APC such as DC, these compartments also favour the progressive generation of antigenic peptides of about 13–18 residues [189,203,207]. In parallel, in the nucleus **(FIGURE 1.6F)**, the polymorphic MHCII genes are transcribed [208] and subsequently translated in the rough endoplasmic

reticulum (RER) **(FIGURE 1.6G)**. Here, the nascent MHCII-complex, which consists of the MHC Class II molecules with invariant chain (Ii), is formed [206]. Ii promotes correct assembly of heterodimers, prevents the binding of other peptides or partly folded proteins and targets delivery of the MHCII-complexes [209] from the RER via the Golgi complex and trans-Golgi network [210,211] **(FIGURE 1.6H)** to either a low pH compartment directly **(FIGURE 1.6B)** or via the plasma membrane [212,213] **(FIGURE 1.6I)** or directly to a high pH compartment [214-217] **(FIGURE 1.6E)**. During migration of MHC class II:Ii complex in the intracellular compartments, the Ii chain is successively degraded by acid proteases such as cathepsin S, leaving a short fragment of this chain called CLIP (Class II–associated invariant chain peptide) [218,219] **(FIGURE 1.6D)**. CLIP physically occupies the peptide binding groove and prevents any premature binding of peptide [209,218]. Another MHC-like molecule, human leukocyte antigen HLA-DM (H-2M in mice) **(FIGURE 1.6D,E)** helps in catalysing the formation of MHC class II:CLIP complexes and the subsequent release of the CLIP fragment from these complexes [220,221]. This molecule also assists in binding of antigenic peptides of about 13–18 amino acid residues in the groove [222,223] **(FIGURE 1.6E)**. Finally, this molecule helps to export p:MHCII molecules to the surface of DCs [191,224] **(FIGURE 1.6J,K)**.

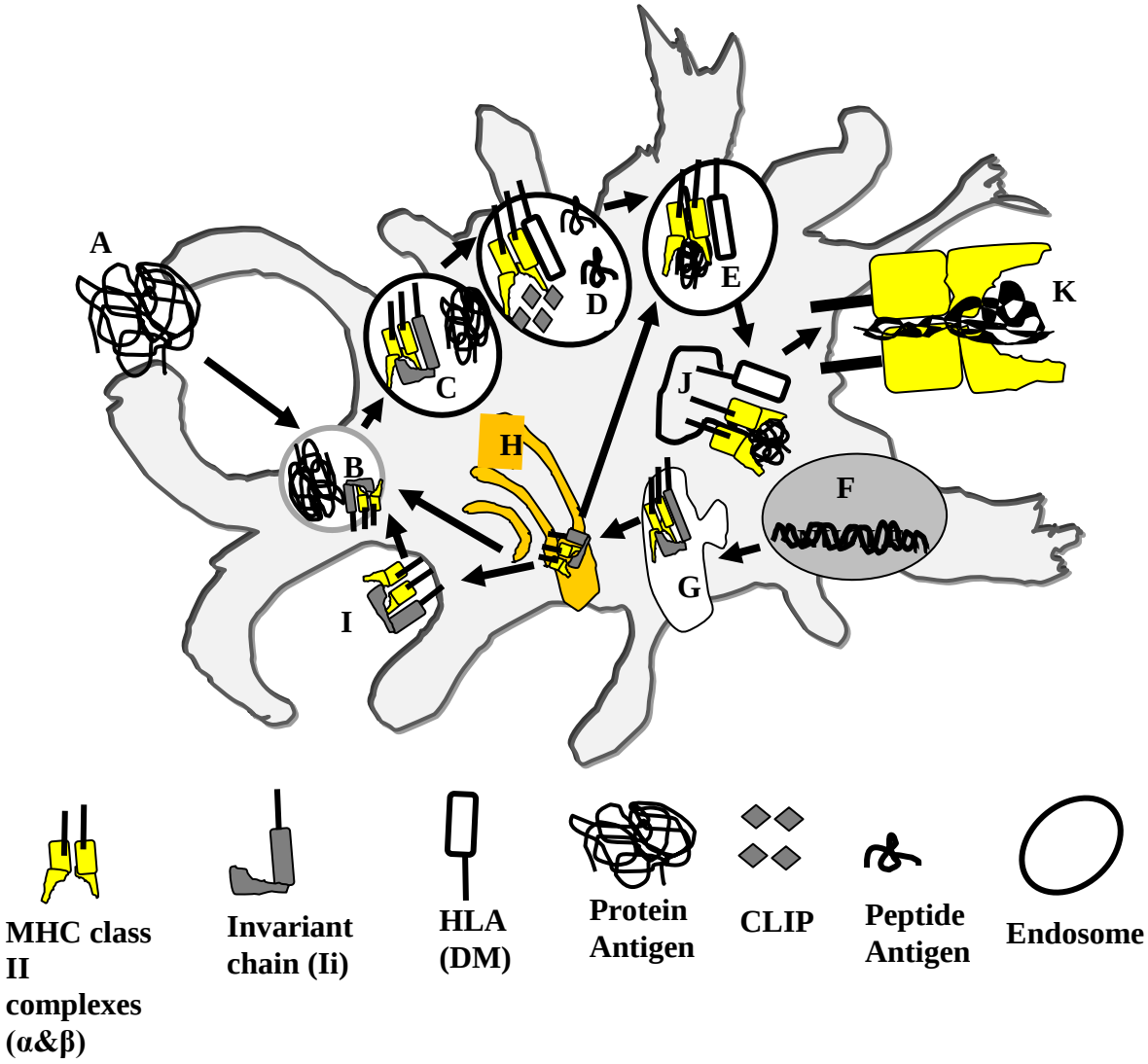

FIGURE 1.6: Steps involved in antigen processing and presentation by DC in the context of MHC Class II: peptide complexes.

Protein antigens are internalised in the phagosomes and are successively processed in the endocytic compartments with the help of different proteases. **A**: Protein antigens being internalised by DC, **B**: Early endosome with protein antigens+MHCII molecules with Ii, **C** and **D**: successively acidic endosomes, **E**: Lysosome, **F**: Nucleus, **G**: RER, **H**: Golgi complexes, **I**: MHCII+Ii complexes exported in plasma membrane, **J**: p:MHCII in an exocytic vacuole and **K**: p:MHCII exported on cell surface.

1.5.4.2 MHC Class I pathway

DCs can also efficiently process endogenous antigens derived from the viruses or proteins synthesized in the cytosol [225] or defective ribosomal products (DRiPs) with prematurely terminated polypeptides and misfolded proteins [226]. In these contexts, the proteasome **(FIGURE 1.7A)** plays significant roles for MHC class I processing. The proteasome is a complex cytosolic protease that contains a total of 28 units with each 7 α chain subunits in the upper and lower portion and 2 rows of 7 β chain subunits in between the α chains [227]. The proteasome degrades proteins favouring the production of oligopeptides with the correct length and structure for binding to the MHC class I peptide binding groove [228].

In parallel, the newly synthesised MHC class I α chain in the ER binds to a chaperone protein, calnexin, which becomes dissociated following binding of α chain with β2-microglobulin **(FIGURE 1.7B)**. The resulting MHC class Iα:β molecules bind to calreticulin, tapasin, two subunits of the transporter associated with antigen processing (TAP) and a thiol-oxidoreductase enzyme called Erp57 [229] **(FIGURE 1.7C)**. Calreticulin acts as a chaperone molecule. Erp57 helps to break and reform the disulfide bond in the MHC class I-α_2 domains during peptide loading [229-231]. TAP helps to transport short peptides from the cytosol into the lumen of the RER [232]. To enhance the speed of peptide loading onto MHC class I molecule, tapasin stabilises TAP [227,233]. The entered peptide is of short amino acids (about 8–13) because it interacts in the MHC class I groove which is closed at both ends **(FIGURE 1.7D)**. Following binding, the peptide-loaded MHC class I molecules move from the RER to the cell surface **(FIGURE 1.7H)** *via* Golgi complex **(FIGURE 1.7E,F,G)**.

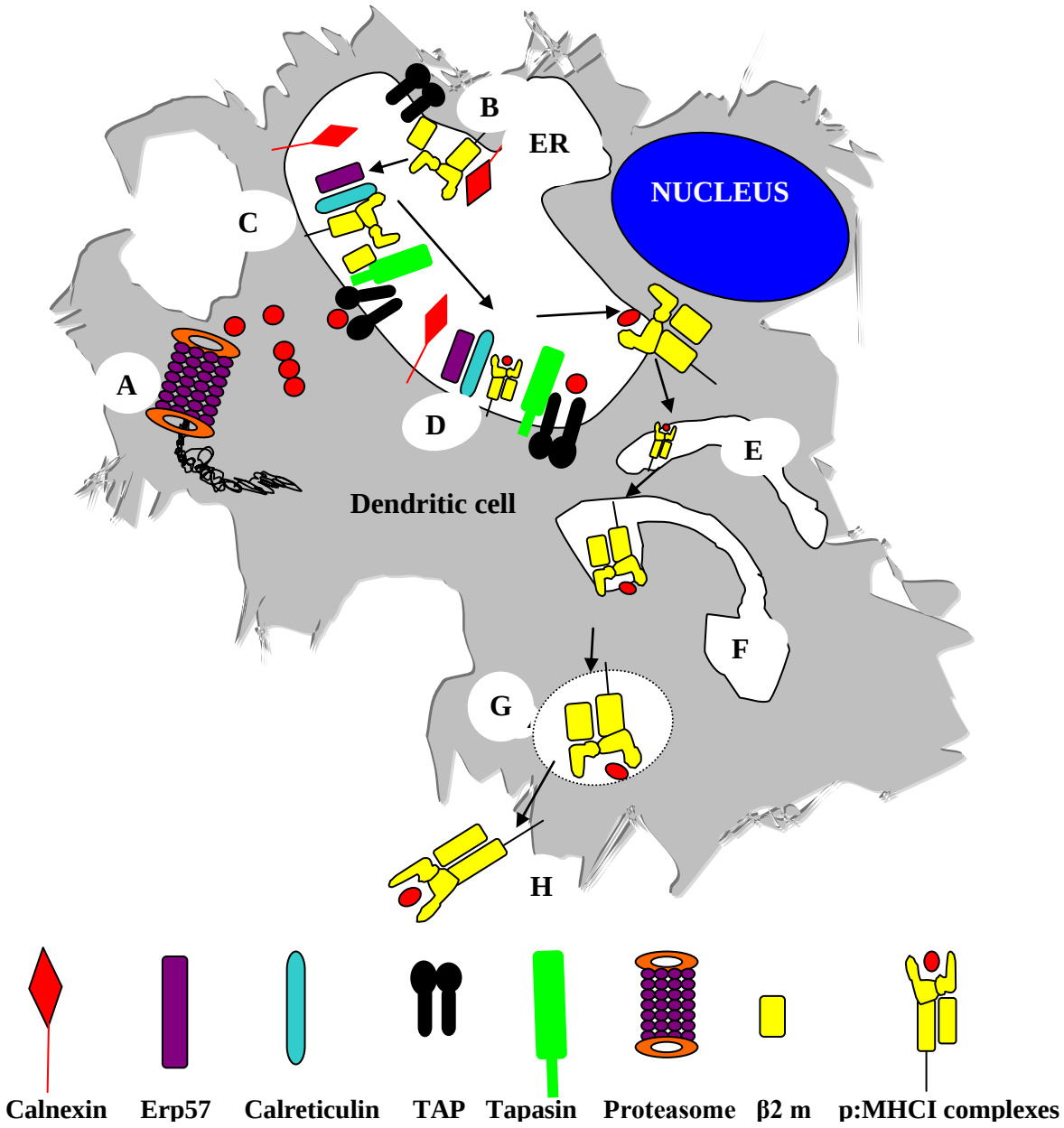

FIGURE 1.7: Mechanisms of antigen processing by DCs in the context of MHC class I pathway.

This pathway is guided by proteasome which prepares a specific peptide antigen to be bound in MHCI molecule. **A**: proteasome, **B**: ER showing MHC α:β formation, **C**:MHC α:β:chaperone complex, **D**: peptide loading process, **E–F**: Golgi complexes, **G**: exocytic vacuole, **H**: exported p:MHCI complexes on cell surface.

1.5.4.3 Cross presentation

Apart from MHC Class II and Class I pathway, DCs can process exogenous protein antigens and load them onto MHC I molecules by a mechanism called cross presentation [234-237]. Studies have suggested that the endocytosed extracellular antigens are translocated by different mechanisms into the cytosol, where they are degraded into antigenic peptides by the proteasome and are bound to the MHC Class I molecule [238]. Cross presentation is important to allow Class I-restricted antigen presentation on professional APCs to drive naïve CD8 T cell activation. This is particularly important for generating CD8 T cell effector responses against intracellular pathogens that do not directly infect DCs or for clearing tumours that are not derived from DCs [234,239-241].

1.5.5 DC maturation

DC maturation involves changes in both location and phenotype of DC, turning them from cells specialised in surveillance into potent activators of naïve T cells. DCs undergo maturation processes when they get signals such as TLR ligands, necrosis, inflammatory soluble factors (cytokines), T cell ligands (such as CD40 ligands) and disruption of homotypic contacts between immature DCs [191,242]. DC maturation is particularly relevant to the study of adjuvant mechanisms, because only mature DCs are able to induce T cell clonal expansion and prime immune responses [243]. DC maturation is characterised by the appearance of dendritic processes, diminished antigen internalisation efficiency and the increased expression of MHC class II molecules, costimulatory molecules (B7-1/CD80, and B7-2/CD86) and chemokine receptors (CCR7) [244-246]. Among these molecules, MHC class II molecules take part in antigen presentation, costimulatory molecules take part in T cell activation and the CCR7 chemokine receptor is involved in migration of cells to the DLNs.

1.5.6 DC migration to the DLNs

DCs continuously migrate to SLOs from the periphery bearing fragments of apoptotic cells [246]. These cells are non-activated, and may be important in the maintenance of self-tolerance [241,247]. Following activation signals, DCs migrate into DLNs at a high rate [151] **(FIGURE 1.5)**. In this context, increased CCR7 expression on DC plays a central role in initiating migration [248]. This is because the peripheral lymphatic endothelial cells and lymph node (LN) stroma cells constitutively express the CCR7 ligands, CCL19 (Epstein-Barr virus-induced receptor ligand chemokine, ELC) and CCL21 (secondary lymphoid tissue chemokine, SLC). Activated DCs are therefore attracted to migrate towards the thymus dependent area of DLNs *via* afferent lymphatic vessels from skin [151,244,245,248]. When DCs with p:MHCII complexes reach the T cell areas, they start to present antigen and initiate adaptive immune response [249,250] **(FIGURE 1.5)**.

DC migration from periphery to DLNs is important in the context of vaccines containing particulate forms of antigen as these are unable to pass directly to the LN and require internalisation and movement within migrating cells. Particulate antigens are unable to pass through thin tubes, called conduits that link the floor of subcapsular sinus with the perivenular space surrounding the high endothelial venule [251-253]. These conduits radiate out from the HEVs toward the LN capsule [251-253] **(FIGURE 1.5)**. In these contexts, the peripheral DCs migrate to the DLN where they directly activate T cells or transfer their antigens to the DLN-resident DCs and activate them [177,250]. However, soluble antigens derived from microbial debris or subunit vaccines are not required to be internalised by peripheral DCs because they can easily pass through the conduits and can be internalised by LN-resident DCs [183] **(FIGURE 1.5)**. This situation is also important if Aluminium salts containing vaccines work by releasing antigens at the injection site due to displacement by citrate anions [62] or fibrinogen [254]. Therefore, antigen released from Alum would be carried from the peripheral site into the subcapsular sinus and conduit network via afferent lymph vessels within 15 to 30 minutes of injection as shown for soluble

antigens *in vivo* [183]. Consequently, the resident DCs acquire antigen either by sticking dendrites between the fibroblasts or simply by taking up small amounts of antigen that leak out of the conduits [255] **(FIGURE 1.5)**. Finally, these conduit-derived antigens are presented by the resident DCs in the context of p:MHCII complexes even as early as 30 minutes following s.c. injection [183,256].

1.5.7 T cell activation

Antigen binding alone is insufficient to activate T cells, because the signal derived from TcR (Signal 1) alone leads to a state of paralysis called anergy, a condition that makes them unresponsive to a subsequent exposure to antigen [257-260]. Therefore, another signal, called signal 2 is necessary for the development of functional T cells. This signal is provided by DCs in the form of costimulation. For example, the costimulatory molecules CD80 and or CD86 on DCs interact with CD28 molecules expressed on T cells to provide signals crucial for antigen-specific T cell growth, activation, expansion and survival [260,261]. Other costimulatory molecules like CD40 and CD70 also play a significant role in adaptive immune response [262]. For example, the ligation of CD40 molecules on DCs has been shown to increase MHC class II molecules, CD80, CD86, CD70 and CD54 molecules inducing the antigen presenting and costimulatory efficiency of DCs [263,264]. Recently, CD70, through its interaction with the CD27 molecule expressed on T cells, has also been described to have T cell costimulatory activity. This interaction seems to be more important than CD80/86-CD28 interaction in the survival of antigen-activated CD8 T cells in non-lymphoid tissues [265].

Following activation, naïve CD4 T cells can differentiate into a diverse range of T cell subsets following activation with distinct phenotypes and functions in immunology [266-269]**.**

1.5.8 Th polarisation

Th polarisation is an important step in ensuring that the emerging immune response has appropriate effector functions to combat specific types of pathogen.

Therefore, Th cells undergo polarisation into different subsets such as Th1, Th2, Th17, T regulatory (Treg) and T follicular helper (Tfh) cells [270-272] **(FIGURE 1.8)**. Among these subsets, Th1, Th2, Th17 and Tfh are associated with immunity; whereas Tregs are associated with antigen-specific tolerance.

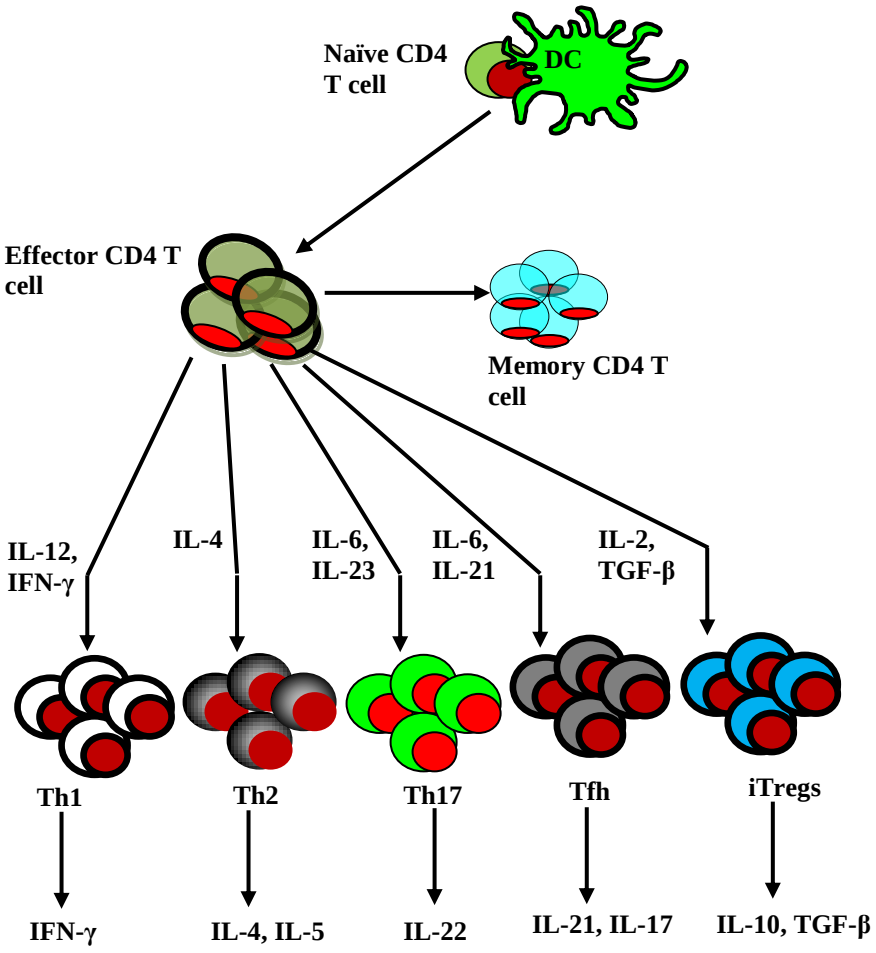

FIGURE 1.8: DC controls the initiation of adaptive immune responses *in vivo*. DC presents p:MHCII complexes to naïve CD4 T cell resulting in the development of effector CD4 T cells via Ag-specific expansion. Some of the effector CD4 T cells develop into memory CD4 T cells, whereas others undergo polarisation into different subsets depending on the signals derived from cytokines **(See text for explanation)**.

1.5.8.1 Th1 cells

Th1 cells predominantly produce proinflammatory cytokines like IFN-γ, TNF-α and TNF-β. Their induction is favoured by IL-12, IL-18, IL-27 and IFN-γ [266] **(FIGURE 1.8)**. The role of Th1 cells in CMI has been well characterised

during infection of mice with *Leishmania major*. An infection with *Leishmania major* is lethal to genetically susceptible mouse strains such as BALB/c, which correlates with the development of an inappropriate IL-4/Th2 response [273,274]. In contrast, C57BL/6 mice are resistant to the infection and produce IFN-γ-mediated Th1 responses to clear the infection [273,274]. Th1 cells and IFN-γ production seem to be crucial in the protection of the hosts from other intracellular pathogens such as *Listeria monocytogenes* [275], and *Mycobacterium avium* [276]. Th1 responses are also involved in elimination of tumour cells [277,278]. In addition, IFN-γ and Th1 cells are involved in underlying tissue damage and inducing inflammatory bowel diseases [279] and autoimmune diseases such as rheumatoid arthritis [280].

1.5.8.2 Th2 cells

Th2 cells predominantly produce IL-4, IL-5, IL-10 and IL-13 [267,268]. They are induced by IL-4 [266] **(FIGURE 1.8)**. Helminth infections are ideal examples of Th2-cell inducers in both humans as well as experimental models because they are associated with high-level tissue eosinophilia, mucosal mastocytosis and IgE switching [281-283]. These responses are involved in resisting extracellular helminths; for example, type 2 cytokines act on mucosal mast cells to expel *Trichuris muris* [284] and goblet cells to resist *Nippostrongylus brasiliensis* [285].

1.5.8.3 Th17 cells

Recently, another important subset of Th cell subset, Th17 has been well established. Th17 cells produce IL-17, IL-21, and IL-22. They are induced by IL-6/TNF-β, IL-21/TNF-β and IL-23 [266] **(FIGURE 1.8)**. In mouse models, Th17 responses are associated with resistance to *Klebsiella* that infects the lung [286], and intravenous (i.v.) infection of mice with *Candida albicans* [246]. IL-17, the key Th17 cytokine, has been associated with autoimmune diseases such as multiple sclerosis (MS), rheumatoid arthritis (RA) and psoriasis [287,288].

1.5.8.4 Tregs

Immunologists have also described CD4 T cells called T regulatory cells (Tregs) which can be divided into naturally occurring Tregs (nTregs) and inducible Tregs (iTregs). nTregs develop in the thymus and constitutively express high levels of IL-2Rα chain (CD25), cytotoxic T lymphocyte Antigen 4 (CTLA-4) and glucocorticoid-induced tumour necrosis factor receptor (GITR) [266]. iTregs are differentiated from naïve T cells following ligation of TcR and environmental antigens bound to MHC molecules by DCs in SLOs [289]. The induced Tregs (iTregs) produce large amounts of IL-10 and transforming growth factor (TGF)-β and play role in tolerance [272,290,291] **(FIGURE 1.8)**.

1.5.8.5 Tfh cells

While Th1 and Th2 cells have been described to support B cell responses and antibody production [292], recently, T follicular helper (Tfh) cells have been suggested as a distinct T cell subset with the ability to migrate to B cell follicles to provide help to B cells [293]. Tfh cells produce IL-21, which has B cell stimulatory and differentiation functions [294]. Tfh cells also express CXCR5 and various costimulatory molecules such as inducible T cell costimulatory (ICOS), CD40 ligand (CD40L), OX-40 and programmed death 1 (PD-1) that are signature molecules for follicular localisation and B cell help [293,295-298]. Therefore, Tfh may be associated with germinal centre formation, B cell activation, long-lived memory B and plasma cell production and antibody secretion [299,300]. In this way, targeting the generation of sustained Tfh response may be important in the optimum antibody production in response to vaccines in future.

1.6 Effects of adjuvants on immune responses

It is generally accepted that vaccine adjuvants impact on adaptive immune responses via direct or indirect effects on APCs such as DCs [148-150,301]. Direct activation of DCs has been well defined for PAMPs at a molecular level using mice or cells with deficiencies in the TLR/MyD88 signalling pathway. The ability of non-microbial adjuvants to induce inflammation *in vivo* has also suggested that indirect activation of DC in response to this inflammation may also play a significant role in the activity of these adjuvants.

1.6.1 DC activation

PAMPs robustly activate DCs because these molecules recognise and bind their respective receptors called PRRs like TLRs, NLRs, and RLRs and induce the expression of MHCII and costimulatory molecules and the production of cytokines [302-305]. These cytokines act as adjuvants *in vitro* and *in vivo* [86,155,306,307].

TLR1 is present on the plasma membrane of cDCs and macrophages. TLR2 is expressed on the plasma membrane of cDCs, macrophages and lymphocytes [100,142,308]. TLR4 is expressed on the plasma membrane of cDCs and macrophages and non-immune cells like fibroblasts and epithelial cells [100,142,308-310]. TLR5 is expressed on the surface of monocytes, mDCs, Langerhans cells, T cells and natural killer cells [100,308,311-315] **(FIGURE 1.9)**. Recognition of PAMPs via TLR1-triacyl lipopeptide [316], via TLR2–glycolipids/lipopeptides/lipoproteins/lipoteichoic acid/ HSP70/zymosan [102,105-107,317-319] and via TLR5–flagellin [320,321] signaling results in the activation of cells via Myeloid differentiation primary response gene (MyD88)-Interleukin-1 receptor-associated kinase (IRAK)-4–TNF receptor-associated factor (TRAF)-6–nuclear factor kappa-light-chain-enhancer of activated B cells (NF-kB) pathway which induces the production of inflammatory cytokines [100,322]. Recognition of PAMPs such as LPS via TLR4 results in the activation of cells via either MyD88–IRAK-4–TRAF-6–NF-kB pathway or Toll/interleukin-1 receptor-domain-containing

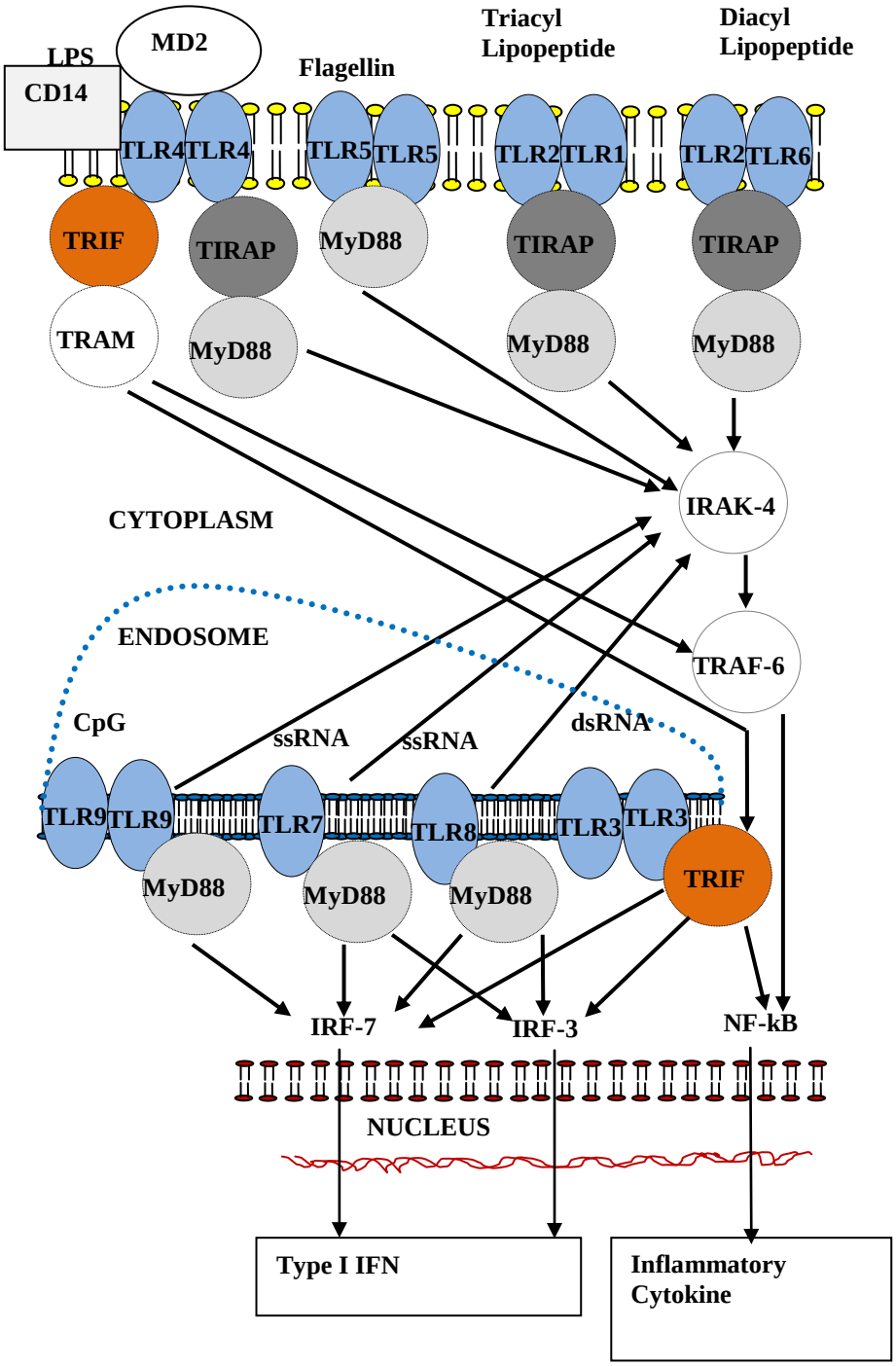

FIGURE 1.9: TLR-signaling pathway.

TLR-signalling involving PAMP recognition by cell surface and intracellular TLRs resulting in various cytokines secretion [100,142,308,323,324] **(See text for description)**.

adapter-inducing interferon-β (TRIF)–TRAF-6–NF-kB to produce inflammatory cytokines or TRIF–TANK-binding kinase (TBK)-1– interferon regulatory factor (IRF)-3 or TRIF–TBK1–IRF-7 pathway to produce type I IFN cytokines [100,322] **(FIGURE 1.8)**.

TLR3 is expressed within the endosomal compartment of cDCs and macrophages and is present on the surface membrane of non-immune cells like epithelial cells [142]. TLR7/8 are restricted on the intracellular vesicles such as the ER, endosomes, lysosomes and endolysosomes DCs, monocytes, macrophages, lymphocytes, Langerhans cells and NK cells [100,314,325,326]. TLR9 is localised on the endo-lysosomal compartments in human B cells and pDC [308] **(FIGURE 1.9)**. TLR3-dsRNA signaling occurs through the TRIF-dependent manner and produces both type I IFN via IRF-3 or IRF-7 and inflammatory cytokines via NF-kB pathway [109,327]. The recognition via TLR7-ssRNA signaling [328] occurs via MyD88-depending pathway and produces proinflammatory cytokines through IRAK-4 or TRAF3 pathway and type I IFN via IRF-3 or IRF-7 pathway. TLR8-ssRNA signaling [308] occurs via IRAK-4–NF-kB pathway to produce proinflammatory cytokines and IRF-7 pathway to produce type I IFN cytokines. TLR9-CpG/haemozoins [116,327,329] results in the activation of IRAK-4–NF-kB signaling to produce inflammatory cytokines and MyD88 signaling to produce Type I IFN via IRF-7 as well as TBK1–IRF-3 pathway.

RLRs are the cytoplasmic sensors that can sense ssRNA or dsRNA or dsDNA molecules derived from viruses that trigger anti-viral signaling pathways and produce type I IFN [308,324,330]. The RLR family has three members; RIG-I, MDA5 and laboratory of genetics and physiology 2 (LGP2). Firstly, the RIG-I recognises the various viruses such as paramyxoviruses, influenza A virus and Japanese encephalitis virus. Secondly, the MDA5 recognises poly I:C and RNA of picornaviruses [308] **(TABLE 1.2)**. Thirdly, immune responses resulting via LGP2 signaling may be both positive as well as negative. The recognition of poly I:C and vesicular stomatitis virus via LGP2 results in an enhanced type I IFN, but the

recognition of encephalomyocarditis virus via LGP2 results in the reduction of this cytokine [331].

In the same way, NLR, one of the cytoplasmic PRRs, recognises the microbial peptidoglycan [332,333]. The NLR subfamily has been variously classified such as NALP groups containing NALP1 to NALP14 in humans and NALP1 to NALP6 and NALP9, NALP10, NALP12 and NALP14 in mice, IPAF (ICE-protease-activating factor)/NAIP (Neuronal Apoptosis Inhibitory Protein) groups containing IPAF and NAIP in both humans as well as mice and NOD groups containing NOD1 to NOD5 and CIITA (MHC class II transcription activator) in both humans as well as mice [334]. These immune receptors are characterized by the presence of an amino terminal PYD, caspase activation and recruitment domain (CARD) or baculovirus inhibitory repeat domain followed by a nucleotide-binding domain, and LRRs at the C-terminus [334-336]. Interestingly, most of these molecules have been identified as capable of forming inflammasomes that control the activity of the proinflammatory caspase-1 and consequently produce inflammatory cytokines such as IL-1β and IL-18 [334-336]. Notably, inflammasomes have been a subject of interest of many researchers around the world, especially due to their association in recognition of danger signals.

In addition to microbial adjuvants, mineral adjuvants have been demonstrated to induce DC activation. For example, Alum has been reported to induce the expression of MHC class II and costimulatory molecules on the surface of the DCs [337-339]. However the molecular mechanism behind this observation has not been elucidated.

1.6.2 Inflammation

The use of adjuvants in vaccination is usually associated with some degree of injection site inflammation, and this process is considered an essential part of adjuvant function [340]. This is consistent with the ‘Danger Theory’ of immune activation as proposed by Polly Matzinger in 1994 [341]. According to this theory,

initiation of the immune response is not dependent on microbial recognition, but rather on the ability of pathogens or other agents such as adjuvants to cause tissue damage. The danger signals released from damaged tissues then have the capacity to drive inflammation and initiate an adaptive immune response [341]. Interestingly, necrotic cells themselves act as adjuvants [342,343] and may play a role in the activity of both microbial adjuvants like FCA, and non microbial adjuvants like Aluminium adjuvants [55]. More recently danger signals or DAMPs released from stressed and dying cells have been identified **(TABLE 1.3)**. These feature obligate intracellular materials such as proteins (calreticulin, HSPs and HMGB1), lipid moieties (phosphatidylserine), nucleic acids (polynucleotides and oligonucleotides) and urate and ATP and their degradation products [117,121-124,126,127,131-137,344-346]. These DAMPs are crucial for innate immunity such as in microbial clearance and necrotic/apoptotic cell removal. In addition, they trigger and enhance adaptive immunity such as antigen internalisation, antigen presentation, APC maturation accompanied by costimulatory and cytokine expression, T cell activation, T cell polarisation and efficient cellular and humoral immune response induction. Therefore, DAMPs released by adjuvants or inflammatory responses have crucial significance in vaccine design [117,342,343]. Interestingly, as described in previous section, some of the DAMPs can be implicated in the mechanisms of adjuvant action by targeting their receptors in innate cells such as DCs.

1.6.3 Antigen targeting

An important mechanism by which adjuvants increase the availability of a vaccine is by targeting antigen to cells of the immune system. This can happen by modifying antigens to make them particulate, either by forming multimolecular aggregates as in case of Alum [57,96] or encapsulation as in case of microparticles, liposomes and virus like particles [347], or by directly targeting antigen to receptors on the surface of APC (for example, anti-DEC205) [348,349]. In the case of particulate antigen targeting, the size of the particle has been shown to be important. Researchers have experimentally proved the qualitative significance of immune response triggered by different size of the adjuvants. For example, antigen prepared

in particles with mean sizes of greater than 200nm are targeted for phagocytosis by Bone Marrow-derived Macrophages (BMDMs) and produce quantitatively more efficient presentation than pinocytosis of similar dose of antigen prepared in smaller particles (<200nm) indicating the exploitation of size of adjuvants in targeting APCs [350]. Encapsulation of antigenic proteins, peptides, DNA and RNA inside particles, such as polymer microparticles, liposomes and Virus-like particles, can also protect these antigens from immediate degradation with the sustained and controlled antigen release over a period of time [351-354].

Antigen targeting depends not only on the size of the modified antigens, but also on the receptors present on the APCs. Vaccine adjuvants also target several types of receptors such as CLRs (DC-SIGN or CD209, Langerin or CD207 and MR or CD206). These CLRs bind and internalise many microbes, for example, HIV-1 efficiently binds and target DC-SIGN, Langerin [355] and MR [356] resulting viral internalisation by APCs [357]. When the HIV gag protein antigen is delivered via an antibody to DEC-205 receptor, cross-presentation becomes 100-fold more efficient than non-targeted antigen [358,359] suggesting the potential role of antigen targeting in enhancing vaccine efficacy.

Antigen targeting also influences the antigen processing pathways in APCs. This is because targeted particulate antigens are taken up via phagocytosis and are more likely cross-presented than soluble antigens [360,361]. Possible advantages of particulate delivery are that antigen and adjuvant are delivered to the same cell to enhance immune responses [347,362]. One of the important antigen targeting adjuvants is liposome. This adjuvant effectively targets antigenic peptides or DNA to professional APC to enhance their efficiency of humoral and cytotoxic responses *in vivo* [363-366].

1.6.4 Depot hypothesis

The depot hypothesis is the earliest proposed mechanism for adjuvant action, hypothesised by Glenny, Buttle and Stevens in 1931 while working on DT-

precipitated in Alum. They excised a portion of skin containing the site of injection from guinea pigs 3 days after administration of Alum-precipitated DT or soluble DT. They then homogenised the skin and injected the emulsion into naïve guinea-pigs. The Alum-precipitated DT-recipients were successfully immunised whereas, the DT-recipients (controls) groups were not, as measured by anti-toxin titers. This experiment led them to generate a hypothesis that the slow elimination of Alum-precipitated antigens from the injection site resulted in the associated enhanced antibody production they observed [45]. Consequently, it gave an idea that the rate of absorption and elimination of antigens may depend on the strength of interaction between antigen and adjuvant. Therefore, strong adsorption to an adjuvant may ensure a high localised concentration of antigen for a period of time [367-369], that may be sufficient to allow antigen uptake and activation of DCs [370]. Therefore, several authors have suggested that depot is crucial for enhancing adaptive immune responses, although precisely how this happens is unclear. Glenny suggested that the slow release of small amounts of antigen over a long period of time may stimulate both primary and secondary stimulation from a single injection, generating enhanced antibody titers [44,45]. White and colleagues suggest that depot causes persisting inflammation that stimulates immune cells within the regional lymphatic glands, and partly in the production of a local granuloma, which also contains antibody-producing plasma cells [369]. Although depot effects are most commonly studied with Alum and emulsion adjuvants [371-379] particulate adjuvants such as liposomes and microparticles may form transient as well as long-term depots as part of their mechanisms for enhanced and sustained adaptive immune responses [96,380].

1.7 How do Alum adjuvants work?

As highlighted in the **FIGURE 1.2**, Alum adjuvants have been in continuous use in human vaccines for over 80 years. Despite this, the mechanism(s) of action of this adjuvant have remained unclear. A number of Alum-induced effects have been observed with Alum that may result in improved immunogenicity of vaccines,

however in many cases these effects are only partially described or lack clear causal association with adjuvant function. These are described below.

1.7.1 Alum-induced antigen targeting

Very few studies have been conducted to quantify the antigen uptake by APC in the presence of Alum *in vitro*. Mannhalter and colleagues in 1985 measured antigen uptake by human monocytes derived from peripheral blood mononuclear cells (PBMCs) using radioactively labelled TT antigens. They reported increased antigen-specific T cell expansion following incubation of monocytes with TT adsorbed to Alum compared with soluble antigens [381]. Similarly, Morefield and colleagues in 2005 observed the quantitatively higher uptake by BMDCs of antigen adsorbed to Alum compared with soluble antigens [194]. Recently, Flach and colleagues investigated interactions between Alum crystals and DCs using atomic force microscopy [53]. The authors suggested that Alum binds lipids in the DC plasma membrane *in vitro*. Subsequently, lipid sorting occurs, resulting in enhanced antigen delivery to the cell without Alum internalisation. They also showed that Alum-stimulated DCs mediate strong binding to CD4 T cells for the enhanced T cell responses *in vivo* [53].

To date, two *in vivo* experiments have shown the MHC class I-restricted cytotoxic T response elicited by Alum adjuvants. First, in 1992, Dillon and colleagues reported the induction of long-lasting protective cytotoxic T cell response in mice primed and boosted with a recombinant influenza protein vaccine formulated in Alum adjuvants [382]. Then, in 2009, McKee and colleagues found CD8 and CD4 T cell activation by Alum was independent of macrophages, mast cells and eosinophils [383]. These experiments suggest that Alum adjuvants may have the potential to direct processing of antigens into MHCI pathway for the activation of CD8 cells and cytotoxic induction. Interestingly, Alum has been shown to destabilise and damage the lysosome following actin-dependent phagocytosis in APC [328]. Therefore, if Alum damages lysosomal membrane, the lysosomal antigens may be

released into the cytosol allowing cross presentation of exogenous antigens via the MHC class I pathway.

All these studies have analysed the role of Alum adjuvants in antigen presentation by APCs indirectly via a readout of T cell activation. These studies do not directly provide crucial steps in antigen uptake, its processing and its presentation in the context of MHC molecules on the surface of the APCs. Furthermore these studies have not addressed the issues of duration, and magnitude of Alum-mediated antigen internalisation and presentation. Only assessing the p:MHCII complexes on the surface of DCs give the information about the role of Alum in enhancing the antigen presenting efficiency of DCs.

1.7.1.1 Direct activation of DC by Alum

Several studies have suggested that Aluminium-containing compounds have direct effects on DC activation as measured by expression of MHC class II and costimulatory molecules. Ulanova *et al.* reported IL-4-dependent increased MHC class II and CD86, CD83, IL-1α, IL-1β, TNF, IL-4 and IL-6 in human peripheral PBMC which later on acquired a dendritic cell morphology [339]. Another study [384] reported the IL-4-independent MHC class II and costimulatory molecule upregulation and CD83 expression on human PBMCs. In contrast, Sun and colleagues did not observe any significant increases in MHCII or costimulatory molecules expression on murine BMDCs in the presence of Alum [384]. Sokolovska and colleagues in 2007 reported the enhanced CD4 T cell activation, with increased CD86 and CD80 expression following Aluminium hydroxide treatment. They did not see any effect on CD40 and CD275 expression on BMDCs [338]. They also highlighted the involvement of Alum in Th2-mediated immune responses with the induction of IL-4, inflammatory responses with the induction of IL-1β, IL-18 and TNF and both proinflammatory and anti-inflammatory responses with the induction of IL-6. Seubert and colleagues observed the enhanced CD86, MHCII, CD71, CD83 and CCR7 molecules and decreased CD80 and CD1a molecules on DCs derived from the CD14 positive monocytes. They also observed the enhanced CCL2, CCL3,

CCL4, CXCL8, MHCII, CD86, CD71, CD54 and decreased CD14 molecules accompanied by the increased granularity of the monocytes derived from human PBMCs [337]. These results suggest that Alum adjuvants act on monocytes and macrophages and enhance monocyte differentiation toward DCs. These DCs are equipped with several surface molecules such as chemokine receptors and costimulatory molecules that enhance their migration from peripheral to DLNs for the sufficient encounter with T cells. Importantly, if Alum directly induces cytokine production and costimulation by DC, it becomes impossible to disentangle these effects from other observed changes in antigen presenting function using T cells as an indirect readout.

1.7.1.2 Alum-mediated inflammation

Since the discovery of Alum adjuvants, lots of reports have been published on their inflammatory effects at the injection site. Nodule or granuloma formation following Alum injection has been reported in several experiments conducted in the early 1930s [45,367,368], in the 1950s [369,375], in the 1970s [385] and in recent years [386]. The experiment conducted by White in 1955 provided the first histological characterisation of the Alum granuloma that contained necrotic polymorphonuclear leukocytes and DT-fed macrophages [369]. The transient local environment created in the Alum-injected site recruits immune cells such as neutrophils, macrophages, monocytes and DCs [376,387]. Following their recruitment, these cells take part in immunological duties such as antigen uptake, antigen processing, antigen presentation and inflammatory cytokine production [54].

A key question remains regarding how Aluminium adjuvants (as well as other non-microbial adjuvants) are recognised by the host immune system. Recently, Aluminium adjuvants have been described as an inducer of a cytosolic recognition system, NLRP3 or NALP3 inflammasome [328,388-390]. The inflammasome activates inflammatory caspases, mainly caspase-1, which catalyse the proteolytic activation of proinflammatory cytokines such as IL-1β, IL-18 and possibly IL-33 into their mature forms [334]. IL-18 induces IFN-γ production in TcR-independent

manner from IL-12-primed naïve T cells to promote the differentiation of Th1 cells [391-393]. IL-18 is also related to the induction of IL-4 and IL-13 secretion from CD4 T cells and B cell isotype switching to IgE [394,395]. Similarly, IL-1β is a strong proinflammatory cytokine that can induce CD28-independent T cell activation [396]. It is a pleiotropic cytokine and has adjuvant activity in its own right [381,397]. IL-1β is also associated with the recruitment and activation of inflammatory monocytes and DCs and their migration to the DLNs [54].

There are controversies in the literature about the role of NALP3 in Alum adjuvanticity. In one study, antigen-specific IgG1 and IL-5 production was reduced following immunisation of NLRP3-deficient mice with OVA adsorbed to Alum (Imject Alum) or human serum albumin (HSA) adsorbed to Alum [390] indicating Alum adjuvanticity through NLRP3-dependent pathway. This study also showed a reduced innate immune response in the context of reduced airway eosinophilia in absence of NALP3 signalling indicating its significant contribution in adjuvanticity [390]. Similarly Kool and colleagues found a reduction in IgE and increase in IgG2c and no effect on IgG1 antibody specific to OVA in response to immunisation with OVA adsorbed to Alum (Imject Alum) in NALP3-deficient mice [388]. They observed a reduced antigen-reactive T cells in LN and a reduced infiltration of eosinophil, neutrophil and monocytes and a reduced DC activation and IL-1β production [388]. In contrast to these studies, Franchi and Nunez found no effect on immune response in the context of IgA, IgM, IgG or IgG subclasses in the absence of NALP3 signalling after immunisation of NALP3-deficient mice with HSA adsorbed to Alum (Aluminium hydroxide) [112]. Likewise McKee and colleagues, using DT or Alum (Alhydrogel), proved that the absence of caspase-1 or NLRP3 was not associated with altered CD4 or CD8 T cell responses, antigen-specific IgG1 and Th2 induction [383]. The difference in the results in these labs may be associated with the different cells studies, different formulations of Alum, contamination with TLR agonists or incomplete characterisation of the Alum induced immune response [398].

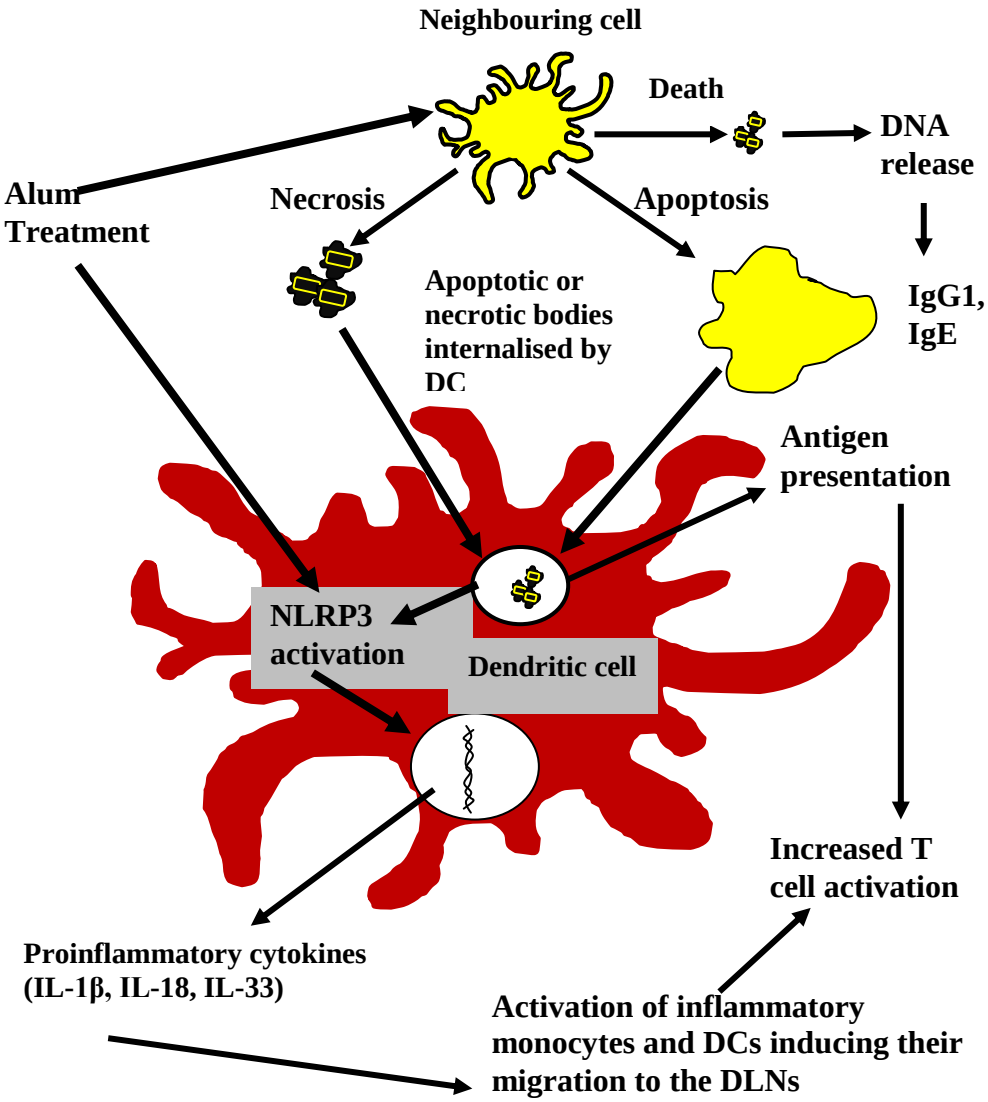

FIGURE 1.10: Inflammatory pathway of Alum adjuvanticity.

Inflammatory role (hypothetical) of Alum mediated immune response that consists of transient inflammatory effects with the induction of NLRP3 molecules and subsequent proinflammatory molecules release, DNA release following resident cell death, enhanced antigen presentation following apoptotic and necrotic cell death.

As previously described, Alum may damage the lysosomal membrane of APC [328]. When the lysosomal membrane becomes destabilised, lysosomal contents, such as cathepsin B and antigens, are released into the cytosol. Currently

there are two key predicted outcomes of this process on the resulting immune response. Firstly, as mentioned above, antigens may become available for presentation via the class I pathway and subsequent activation of CD8 T cells [191]. Secondly, the release of cathepsin B into the cytosol results in the activation of inflammasome, subsequent secretion of proinflammatory cytokines [328] and finally necrosis-like cell death [399]. Alum has been suggested to directly mediate these effects on APCs [54,388] or may also mediate the death of tissue resident cells which in turn release DAMP molecules, such as DNA which in turn activate DC and are associated with IgE isotype switching and IgG1 production [55] **(FIGURE 1.10)**.

In the context of DAMPs, the alarmin IL-33 may play a significant role in Alum-mediated immune response [400]. IL-33 can be released by either apoptotic or necrotic cells. The caspases, caspase-3, caspase-7 and calpain are involved in cleaving pro-IL-33 cytokine during apoptosis although in this form IL-33 does not appear to have any biological significance [401,402]. However, biologically active IL-33 is released in a caspase-1, caspase-8 and calpain-independent manner by necrotic cells rather than active secretion [403,404]. Therefore, a significant contribution to the effects of Alum adjuvants may be necrosis-mediated induction of inflammatory responses via elaboration of active IL-33, although this remains to be fully elucidated.

1.8 Aims of the thesis

The lack of detailed knowledge regarding the mechanisms of action of adjuvants is one of the major barriers in developing new vaccines, particularly those directed against diseases caused by intracellular pathogens. Understanding how adjuvants work will allow the rational design of improved adjuvants. In the current experiments, Alum (Aluminium hydroxide) has been used as a model adjuvant to analyse how it influences the important features of DCs such as antigen uptake, antigen processing, antigen presentation, costimulation and cytokine production that ultimately allow the induction of antigen-specific T cell responses. Understanding the mechanism of Alum adjuvant in determining the magnitude and duration of these

factors will make a significant contribution to the rational design of effective, safe and new adjuvants in the future. In summary, in this thesis, experiments have been conducted to find out the answers to the following questions:

1. **Questions related to Signal 1**

    a. How does Alum affect antigen uptake by BMDCs?

    b. How does Alum affect antigen presentation by BMDCs?

    c. How does Alum affect the magnitude and duration of antigen uptake and presentation by BMDCs?

    d. How does Alum affect the presentation of antigens derived from proteins and peptides?

2. **Question related to Signal 2**

    a. How does Alum affect the expression of the various costimulatory molecules on BMDCs?

3. **Question related to Signal 3**

    a. How does Alum affect the production of various costimulatory molecules by BMDCs?

4. **Question related to T cell responses**

    a. How does Alum affect the duration and magnitude of antigen-specific T cell responses?

CHAPTER-2: MATERIALS AND METHODS

2.1 Materials, chemicals and antibodies

Details of all materials, chemicals, buffers, cell culture media and antibodies (Abs) for flow cytometry, immunocytochemistry and Enzyme-Linked Immunoabsorbent Assays (ELISA) used in this project have been listed in tables **(TABLE 2.1 – TABLE 2.9)**.

TABLE 2.1: Materials used in the experiments.

Materials	Company/Provider
6-well cell culture cluster (sterile)	Corning Incorporated, US
Amicon Ultra centrifugal filters	Millipore, UK
BD 30 G1 precision Glide R Needle	Becton, Dickinson and Company (BD) Biosceinces, UK
BD Flacon Cell strainer (40µm Nylon)	BD Biosciences, UK
BD Plastipak-5mL	BD Biosciences, UK
Cell scrapers Costarr®	Corning Incorporated, US
Deoxi-Gel Endotoxin Removing Column	Thermo Fisher Scientific, UK
HisPur™ Cobalt Spin Columns	Thermo Fisher Scientific, UK
Polystyrene Round Bottom Tube (5mL)	BD Biosciences, UK
Sterile filter Minisart (0.20µm)	Sartorius Stedim Biotech, Germany
Syringe-5/10mL	BD Biosciences, UK

TABLE 2.2: Chemicals used in the experiments.

Chemicals	**Company/Provider**
2-{N-morpholino-4-ehtanesulphonic acid}(MES)	Sigma Aldrich, UK
7-Aminoactinomycin D (7-AAD)	BD Biosciences, UK
Agar	Sigma Aldrich, UK
Alum	Brenntag Biosector, Denmark
Ampicillin	Sigma Aldrich, UK
Annexin-V	Miltenyi Biotec, US
Annexin-V binding buffer	Miltenyi Biotec, US
Benzamidine hexachloride	Sigma Aldrich, UK
Blocking Reagent	Molecular probes, UK
Carboxyfluorescein Succinimidyl Ester (CFSE)	Invitrogen, UK
Cytochalasin D	Sigma, UK
Deoxycholate	Sigma, UK
Deoxyribonuclease (DNase)	Roche Diagnostics GmbH
Dimethyl Sulfoxide (DMSO) $(CH_3)_2SO$	Invitrogen, UK
Ethylenediaminetetraacetic Acid (EDTA)	Sigma, UK
Fetal Calf Serum (FCS)	Invitrogen, UK
G418	Sigma Aldrich, UK
Hank's Balanced Salt Solution (HBSS)	Invitrogen, UK
Hen Egg Lysozyme (HEL)	NALGENE, US
Histopaque	Sigma, UK
Hydrogen Peroxide (H_2O_2)	Sigma Aldrich, UK
Imidazole ($C_3H_4N_2$)	VWR International Ltd, UK
Iscove's Modified Dulbecco's complete Media (IMDM)	Invitrogen, UK
Isopropyl-β-D-thiogalactopyranoside (IPTG)	Melford, UK
L-Glutamine, 200mM (X100)	Invitrogen, UK
Lipopolysaccharide (LPS)	Sigma, UK
Lysis Buffer	eBioscience, UK
Lysogeny broth (LB)	Sigma Aldrich, UK
Mouse serum	Biosera, UK
Paraformaldehyde (PFA)	Sigma Aldrich, UK
Penicillin-Streptomycin, Bioreagent	Sigma Aldrich, UK
Phosphate Buffered Saline (PBS)	Invitrogen, UK
Roswell Park Memorial Institute Media (RPMI)	Sigma, UK
Saponin, from Quillaja Bark	Sigma Aldrich, UK
Sodium azide (NaN_3)	Sigma Aldrich, UK
TritonX100	Sigma Aldrich, UK
Trypan blue solution [0.4%(v/v)]	Sigma Aldrich, UK

TABLE 2.3: Antibodies used in flow cytometry.

Antibody and clone	**Isotype**	**Company**
CD40 (1C-10)	Rat IgG2a,k	eBioscience
CD80 (16-10A1)	Hamster IgG2a	BD pharmingen
CD11c (HL3)	Hamster IgG1, λ2	BD Pharmingen
CD11c (N418)	Hamster IgG (eBio299Arm)	eBioscience
CD4 (GK1.5)	Rat IgG2b, k	eBioscience
DO11.10TCR (KJ1.26)	Mouse IgG2a, k	eBioscience
MHCII APC (I-A/I-E) (M5/114.15.2)	bioRat IgG2b,k	Biolegend
CD80 (16-10A1)	Hamster IgG2, κ	BD Pharmingen
CD4 (GK1.5)	Rat IgG2b, k	eBioscience
CD69 (H12F3)	Hamster IgG1, λ3	BD Pharmingen
CD86 (GL1)	Mouse IgG1, κ	BD Pharmingen
DO11.10 TCR (KJ1.26)	Mouse IgG2a	eBioscience
Eα52–68 (eBioYAe)	IgG2b bio (A-1)	eBioscience Southern Biotech
Streptavidin APC	-	eBioscience
Streptavidin PerCP	-	BD Bioscience

TABLE 2.4: Cell culture media used in the experiments.

Culture Media	**Components**
T cell media	RPMI-500mL
	FCS-10% (v/v)
	Penicillin-100U/mL
	Streptomycin-100µg/mL
	L-Glutamate-2mM
E.coli growing media	LB agar-25gm in 1000mL deionised water
	Ampicillin-100µg/mL
Hybridoma growing media	RPMI-500mL
	FCS-10% (v/v)
	Penicillin-100U/mL
	Streptomycin-100µg/mL
	L-Glutamate-2mM
	G418-1mg/mL
x63 growing media	IMDM-500mL
	FCS-10% (v/v)
	Penicillin-100U/mL
	Streptomycin-100µg/mL
	L-Glutamate-2mM
	G418-1mg/mL
DC media (complete DC media)	RPMI-500mL
	GMCSF-10% (v/v)
	FCS-10% (v/v)
	Penicillin-100U/mL
	Streptomycin-100µg/mL
	L-Glutamate-100µg/mL (2mM)

TABLE 2.5: Buffers used in the experiments.

Buffers	**Components**
Lysis Buffer: NPI-10 (pH: 8.0)	$NaH_2PO_4.H_2O$: 3.45g (50mM)
	NaCl: 8.77 g (300mM)
	Imidazole: 0.34g (10mM)
	Deionised water: 500mL
Wash Buffer: NPI-20 (pH: 8.0)	$NaH_2PO_4.H_2O$: 3.45g (50mM)
	NaCl: 8.77g (300mM)
	Imidazole: 0.68g (20mM)
	Deionised water: 500mL
Elution Buffer: NPI-250 (pH:8.0)	$NaH_2PO_4.H_2O$: 3.45g (50mM)
	NaCl: 8.77g (300mM)
	Imidazole: 8.77g (250mM)
	Deionised water: 500mL
PBS (1X): pH-7.4 (1,000mL)	NaCl: 8.00g
	KCl: 0.20g
	$Na_2HPO_4.2H_2O$: 1.44g
	KH_2PO_4: 0.24g
	Deionised water: 1000mL
FACS (Fluorescence Activated Cell Sorting) Buffer	PBS: 500mL
	FCS (2%) (v/v)
	Azide (0.1%) (w/v)
ELISA washing buffer	PBS: 10mM
	Tween 20: 0.05% (v/v)
Fixing buffer (4%PFA)	PFA: 4% made in PBS (w/v)
Fc receptor blocking buffer	Supernatant of 2.4G2 hybridoma + Mouse serum:10% (v/v)+ NaN_3:0.01% (w/v)

TABLE 2.6: Materials, chemicals and antibodies used in sandwich ELISA[b].

Materials, chemicals and antibodies	Dilutions
Capture Ab: purified anti-mouse IL-10 (clone: JES5-16E3)	1/1,000 (12µL in 12mL coating buffer).
Standard: Recombinant mouse IL-10 (1µg/mL)	½ serial dilution.
Detection Ab: Biotin-conjugate anti-mouse IL-10 (clone: JES5-2A5)	1/1,000 (12µL in 12mL coating buffer).
Enzyme: Avidin-HRP	1/250 (48µL in 12mL coating buffer).
Working Solution: 5X Assay Diluent	1XAssay Diluent (10mL in 40mL of DI water).
Substrate:1XTMB solution	Working concentration (no dilution).
ELISA Coating Buffer Powder	1 packet of ELISA Coating Buffer Powder in 1L of deionised (DI) water.

[b] Mouse Interleukin-10 (IL-10) ELISA Ready-SET-Go!® All reagents from eBioscience, UK.

TABLE 2.7: Luminex antibodies, chemicals and reagents for 1-plex (IL-33 cytokine) ELISA[c].

Materials, chemicals and antibodies	**Catalogue (Millipore)**
Mouse Cytokine/Chemokine Panel III Standard	MXM8074
Mouse Cytokine/Chemokine Panel III Quality Controls 1&2	MXM6074
Mouse Cytokine Panel III Detection Antibodies	MXM1074
Streptavidin-Phycoerythrin	L-SAPE9
Assay Buffer	L-MAB
96-Well plates with sealers	MAG-PLATE
10X Wash Buffer	L-WB
IL-33	MIL33-MAG

[c] All reagents were purchased from Millipore, UK.

TABLE 2.8: Luminex antibodies, chemicals and reagents for 6-Plex ELISA[d].

Materials, chemicals and antibodies	**Catalogue (Millipore)**
Mouse Cytokine Standard	MXM8070
Mouse Cytokine Standard	MXM8070-2
Mouse Cytokine Quality Controls	MXM6070
Mouse Cytokine Quality Controls	MXM6070-2
Mouse Cytokine Detection Antibodies	MXM1070-2
Streptavidin-Phycoerythrin	L-SAPE4
Assay Buffer	L-AB
10X Wash Buffer	L-WB
IL-1β	MIL1B-MAG
IL-6	MCYIL6-MAG
IL-12(p70)	MIL12P70-MAG
IL-13	MIL13-MAG
IL-15	MIL15-MAG
TNF-α	MCYTNFA-MAG

[d] All reagents were purchased from Millipore, UK.

TABLE 2.9: Quality control ranges of cytokines.
The table shows the average standard values of control 1 and control 2 set up while analysing cytokine concentration by the multiplex experiment[e].

Cytokine	Quality Control Level	Expected Range
IL-1β	Control 1	93–193pg/mL
	Control 2	503–1045pg/mL
IL-6	Control 1	106–220pg/mL
	Control 2	554–1150pg/mL
IL-12(p70)	Control 1	93–194pg/mL
	Control 2	475–987pg/mL
IL-13	Control 1	126–378pg/mL
	Control 2	585–1755pg/mL
IL-15	Control 1	86–179pg/mL
	Control 2	468–971pg/mL
TNF-α	Control 1	103–214pg/mL
	Control 2	493–1024pg/mL
IL-33	Control 1	1254–2605pg/mL
	Control 2	6321–13129pg/mL

[e] The information was provided by Millipore catalogues.

2.2 Animals

BALB/c (H-$2^{d/d}$) mice, between 6–12 weeks old, were either bred in the Biological Procedures Unit, University of Strathclyde or purchased from Harlan, UK. C57BL/6 (H-$2^{b/b}$) mice were purchased from Harlan, UK. DO11.10 BALB/c (H-$2^{d/d}$) mice were bred in the Biological Procedures Unit, University of Strathclyde and in the Central Research Facility, University of Glasgow. The DO11.10 BALB/c (H-$2^{d/d}$) mice, expressing the DO11.10 TcR transgenic (tg) mice specific for epitope derived from chicken Ovalbumin (OVA) peptide 323–339 bound to I-A^{d}–restricted MHC class II [405] were used as CD4 T cell donors [406]. Similarly, six- to eight-week-old C57BL/6 (H-$2^{b/b}$) and BALB/c (H-$2^{d/d}$) mice were used for the DC culture experiments. All the procedures were performed according to the UK Home Office regulations.

2.3 Antigens

2.3.1 Ovalbumin (OVA)

Chromatographically pure egg white Ovalbumin (OVA) was purchased from Worthington Biochemical Corporation, US and OVA peptide (residues 323–339) was bought from Cambridge Biosciences, UK.

2.3.2 EαGFP

EαGFP is a chimaeric fluorescent protein antigen [407] produced from a genetic fusion of Eα peptide to green fluorescent protein (GFP) [408]. Eα peptide (amino acid residues 52–68) is the immunodominant epitope derived from I-E^{d} alpha chain and presented by I-A^{b}–restricted MHC class II molecules [216,409,410].

EαGFP antigen was prepared in the lab according to the method described previously [407]. EαGFP was cloned into a pTrcHis expression vector, downstream to a strong T7-RNA polymerase-specific T7 promoter. T7-RNA is produced

following IPTG (Isopropyl β-D-1-thiogalactopyranoside) addition in the bacterial culture that consequently results in the production of EαGFP [411]. A starter culture was prepared by taking a single colony of *Escherichia coli* pTrcHis Eα-GFP, DH5α in 20mL sterile LB media **(TABLE 2.4)** containing 100µg/mL Ampicillin and incubated in a vigorous shaker [200 revolutions per minute (rpm), 37°C for 6hours]. The starter culture was transferred to a 2 litre-flask containing LB and Ampicillin (100µg/mL) and was shaken vigorously (200 rpm, 37°C for 6hours) and subsequently checked for the optical density $(OD)_{660}$ against LB medium. IPTG (1mM) was added in the culture medium followed by shaking (200 rpm, 37°C for 6hours). Following IPTG induction, culture was checked for optimum growth of bacteria. The cultures were split in centrifuge flasks (250ml) and centrifuged in a Beckman Optima (3,500xg, 30minutes at 4°C). The supernatants were discarded and pellets were frozen (-18°C) and thawed (x3) for optimal lysis. The pellet was resuspended in 10mL NPI-10 buffer (10mM imidazole), bacterial lysis buffer **(TABLE 2.5)** with the addition of 1mg/mL HEL, a pinch of DNAse and a pinch of benzamidine hexachloride for optimal bacterial lysis. The pellet was centrifuged (7000xg, 1hour, 4°C) and green supernatant was collected. The supernatant was passed through a HisPur Cobalt Spin Columns followed by washing first with NPI-10 buffer (10mM imidazole) and then with NPI-20 buffer (20mM imidazole) **(TABLE 2.5)** to maximise the inhibition of the binding of nontagged contaminating proteins resulting in greater purity. Then, all bound proteins in the column were eluted out using NPI-250 (250mM imidazole) **(TABLE 2.5)**. Then, proteins were washed in PBS (3150xg, 4°C, 20minutes) in an Amicon Centrifugal Filter (Amicon Ultra-15) to replace NPI buffer with PBS. Endotoxin contents of protein were removed by using 1% sodium deoxycholate in Deoxi-Gel Endotoxin Removing Column and sterilised by passing proteins through a 0.2µm syringe filter. The eluted EαGFP was quantified by spectrophotometer (NanoDrop 1000 3.7.0) and was ready for use.

2.4 Adjuvants

ALHYDROGEL^{R} (Alum) was used as a model adjuvant in the experiment. This adjuvant consists of 3% Aluminium hydroxide. Different concentrations of

Alum were mixed with pre-determined concentrations of OVA or OVApeptide323–339 or EαGFP and incubated at room temperature for 20minutes to allow adsorption. A sample of the mixture of antigen and Alum was centrifuged (14,000xg, 10minutes) and the supernatant in triplicate was checked for unbound protein according to the bicinchoninic acid (BCA) protein assay as described previously [412,413]. The amount of adsorbed proteins or peptides was determined by subtracting the amount found in the supernatant from the total amount.

LPS (*Escherichia coli* O111.B4) was also used as a control adjuvant in DC activation and cytokine production assays. DCs were treated with 1µg/mL LPS as a standard positive control in these assays.

2.5 Preparation of DCs from murine bone marrow

DCs were generated from bone marrow of C57BL/6 or BALB/c mice in complete DC media **(TABLE 2.4)**, as described previously [152]. The femurs and tibias were collected in ice-cold PBS. The bone marrow was flushed out with 2mL of media in a syringe with a 30G precision Glide R needle in a 60mm tissue culture plate. The cells were passed through the 40 µm cell strainer with the help of a serological pipette. Bone marrow cells were collected in a 50mL centrifuge tube and washed twice (400xg, 5minutes, 4°C) with complete DC media. The cells were counted by haemocytometer. A total of $2x10^6$ cells were cultured in a six-well plate in 2mL total volume per well. At day 3 and 6, cells were fed with each 2mL/well fresh complete DC media. DC development was examined on a microscope (0.2 Nikon TMS Japan) at each day. Day 7 DCs were used in most of the experiments unless otherwise stated.

2.6 EαGFP/YAe system

In this study, EαGFP/YAe system was used to address the impact of Alum and particulates on antigen uptake and antigen presentation by BMDCs [183,216,409,410] **(FIGURE 2.1)**. This system allows assessment of antigen

uptake/degradation and, in combination with the YAe antibody antigen presentation *in situ* [183,216,409,410]. When this antigen is internalised by DCs, EαGFP is degraded and the Eα peptide is presented by I-A^b MHC class II molecules on the cell surface. These p:MHCII complexes can be detected by staining the cells with YAe antibody because this antibody can efficiently bind the complex of Eα(52–68) with I-A^bMHCII [216,409,410]. Therefore, the YAe antibody sees what T cell receptor sees **(FIGURE 2.1)**. The system is important in the study of antigen internalisation and presentation because we can evaluate the number of GFP positive cells and level of GFP in these cells (cells with intact native antigens) as well as number of YAe positive cells and level of antigen presentation.

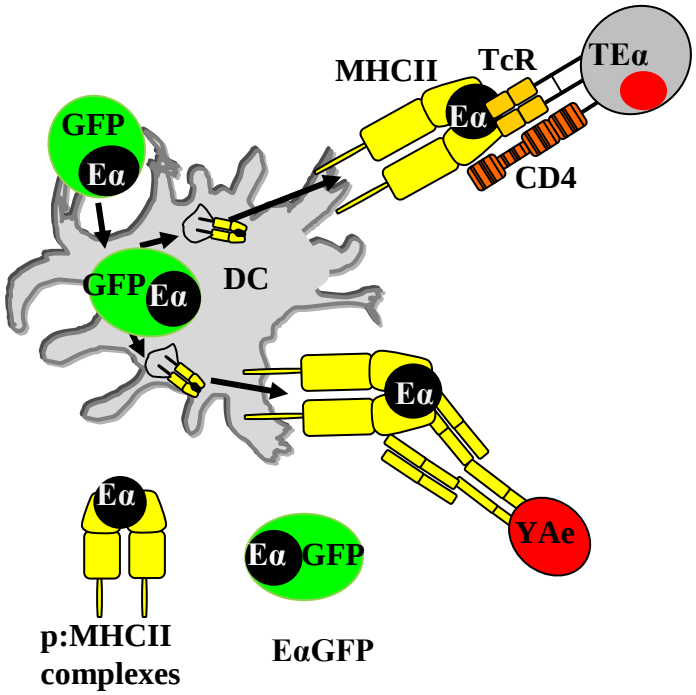

FIGURE 2.1: The Eα:YAe System.

The Eα:YAe System was originally described by Rudensky and colleagues [216,409,410]. The YAe antibody sees what the TcR sees. This antibody binds Eα(52–68):MHCII complexes presented by APCs such as DCs. GFP signal represents the antigen accumulating cells whereas YAe positive signal represents expression of the surface p:MHCII complexes. Currently, the EαGFP/YAe system has been used to elucidate the roles of Alum in antigen uptake and presentation.

2.7 Analysis of antigen uptake and presentation

To assess the role of Alum in antigen uptake and presentation, BMDCs were incubated with different concentrations of EαGFP or EαGFP adsorbed to different concentrations of Alum in a six well plate containing $2x10^6$ cells/5mL media in each well. Control wells contained media only. After 24hours incubation, cells were analysed by flow cytometry.

2.8 Pulse chase assay to analyse kinetics of antigen presentation

To assess the role of Alum in the kinetics of uptake, degradation and antigen presentation, a pulse chase assay was performed. BMDCs ($3x10^6$/mL) were pulsed with EαGFP (100.0µg/mL) or, EαGFP (100.0µg/mL) adsorbed to Alum (100.0µg/mL) for 1hour. Some of the cells were incubated in media and this was used as a blank control. Cells were harvested, washed in HBSS buffer (400xg, 5minutes, 4°C) and BMDCs were separated from Alum using sterile histopaque (400xg, 25minutes, 20°C) followed by washing twice in HBSS buffer (400xg, 5minutes, 4°C) **(FIGURE 2.2)**. BMDCs ($1.5x10^6$ cells/5mL) were resuspended in each well of a six well plate containing cDC media and incubated for different chase periods (0hour, 24hours, 48hours and 72hours). After each chase period, cells were analysed by flow cytometry.

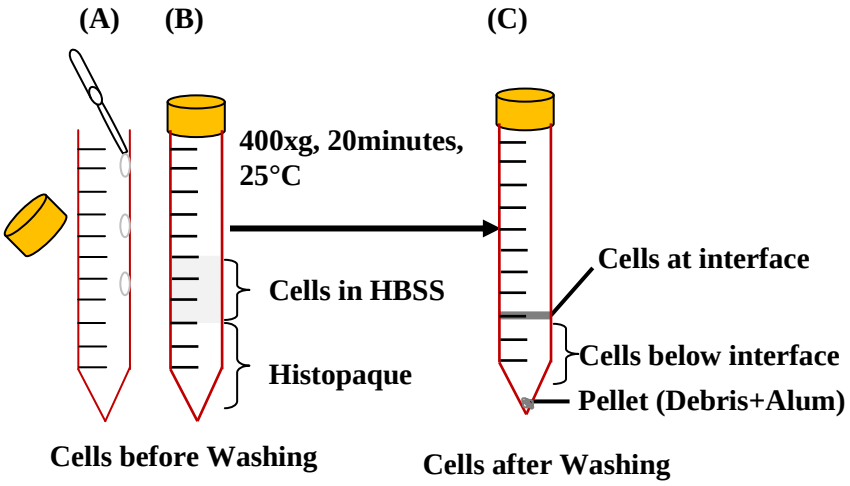

FIGURE 2.2: Separation process of Alum from cells after antigen±Alum pulse period.

(A) Cells are carefully layered on top of a cushion of histopaque. **(B)** Centrifuge tube containing histopaque in lower level and HBSS media with cells. Cells were washed (400xg, 20minutes, 25°C). **(C)** Most of the cells were found at interface between upper media and lower media. Some of the cells were observed just below interface layer. Pellet contained debris and Alum. The cells found in interface layer and below interface were carefully collected by a pipette and washed (400xg, 5minutes, 4°C) in HBSS to incubate for different chase periods.

2.9 Role of preadsorption of antigen in Alum uptake and presentation

To assess the role and mechanisms of pre-adsorption of antigen in Alum uptake and presentation, a pulse chase assay was used **(FIGURE 2.3)**. BMDCs ($3x10^6$) were pulsed with EαGFP (100.0µg/mL), EαGFP (100.0µg/mL) adsorbed to Alum (100.0µg/mL) or Alum (100.0µg/mL) only for 1hour. Some of the cells were incubated in media to provide blank controls. These cells were washed in HBSS buffer (400xg, 5minutes, 4°C) followed by washing first in sterile histopaque (400xg, 25minutes, 20°C) then twice in HBSS buffer (400xg, 5minutes, 4°C) **(FIGURE 2.2, 2.3)**. Cells treated with either EαGFP or Alum alone were incubated in Alum and

EαGFP respectively for 1hour. All cells were again washed in sterile histopaque followed by washing twice in HBSS buffer (400xg, 5minutes, 4°C). Cells ($1.5x10^6$ cells/5mL) were resuspended in each well of a six well plate containing cDC media and incubated for different chase periods. After the indicated chase period, cells were analysed by flow cytometry.

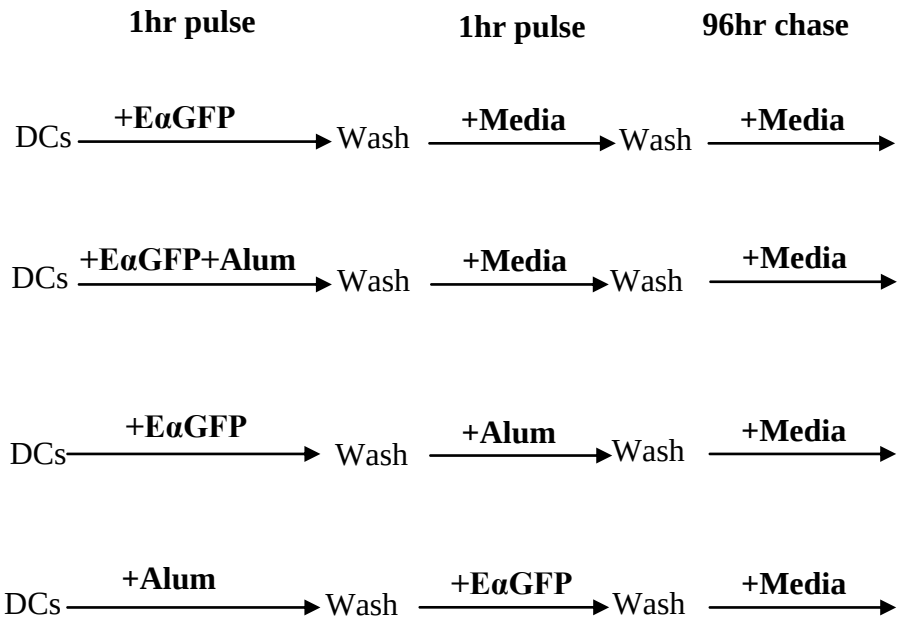

FIGURE 2.3: Study design for the assessment of impact of preadsorption of antigen in Alum on antigen presentation by BMDCs *in vitro*.

DCs were pulsed with EαGFP or Alum or EαGFP adsorbed to Alum for 1hour. Then cells were washed and again pulsed for 1hour with different sequence of EαGFP or Alum or media. Cells were washed and incubated in media for 96hours and then analysed by flow cytometry.

2.10 Role of actin polymerisation in antigen uptake

To study the mechanism of antigen uptake, Cytochalasin D was used. This drug disrupts the actin polymerisation and inhibits the actin-dependent antigen internalisation by APCs [414,415]. The stock solution of Cytochalasin D (Mass: 1mg, formula weight: 507.62g/mol) was reconstituted in 500µl DMSO to prepare final concentration of 2mg/mL. The stock solution was aliquoted and stored at -20°C until use. DC media of each DC culture well plate were replaced with RPMI containing Penicillin (100U/mL), Streptamycin (100µg/mL) and Glutamate (2mM). FCS was not included in this media to prevent the constitutive uptake of antigens by DCs. BMDCs ($2x10^6$/5mL) were incubated with different concentrations of Cytochalasin D (0, 10, 20, 30µg/mL) in each well of a six-well plate for 2hours. Then, cells were treated with EαGFP (100µg/mL) or EαGFP (100µg/mL) adsorbed to Alum (100µg/mL) in each well of a six-well plate for 2hours as this duration is ample for antigen internalisation by DCs. Controls included treating cells with EαGFP or EαGFP adsorbed to Alum. The level of GFP in the cells was analysed by flow cytometry.

2.11 Role of Na^+/H^+ pump in antigen uptake

To study the mechanism of antigen uptake, 5-(N-Ethyl-N-isopropyl) amiloride (EIPA) was used. This drug strongly inhibits Na^+/H^+ exchange and inhibits fluid phase uptake of antigen by APCs [416,417]. The stock solution of EIPA (Mass: 25mg, formula weight: 299.76g/mol) was reconstituted in 1,111µL DMSO to prepare final concentration of 75mM (22.5µg/mL). The stock solution was aliquoted and stored at -20°C until use. DC media of each DC culture well plate were replaced with RPMI containing Penicillin (100U/mL), Streptamycin (100µg/mL) and 100µg/mL Glutamate (2mM). FCS was not included in this media to prevent the constitutive uptake of antigens by DCs. BMDCs ($2x10^6$/5mL) were incubated with different concentrations of EIPA (0, 25, 50, 100µM) in each well of a six-well plate for 2hours. Then, cells were treated with EαGFP (100µg/mL) or EαGFP (100µg/mL) adsorbed to Alum (100µg/mL) in each well of a six-well plate for 2hours as this

duration is ample for the antigen internalisation by DCs. Some of the controls were made by treating cells with EαGFP or EαGFP adsorbed to Alum. The level of GFP in the cells were analysed by flow cytometry.

2.12 Hybridoma assay

To study antigen presentation, DO11.GFP hybridoma was used **(FIGURE 2.4)**. This hybridoma was kindly gifted by David M Underhill (Department of Immunology, University of Washington, Seattle, US). This cell line recognises aa 323–339 of OVA presented by I-A^dMHCII in a costimulator-independent fashion [384]. The DO11.GFP hybridoma has been modified by the introduction of a plasmid reporting nuclear factor of activated T cells (pNFATeGFP). This construct consists of a promoter with the NFAT binding site linked to the IL-2 promoter. This promoter is activated by the binding of NFAT to an NFAT binding site that drives enhanced GFP (eGFP) expression [418] **(FIGURE 2.4)**. The GFP-expressing DO11.GFP hybridoma was selected by incubating this cell line in the presence of G418 (Geneticin, 1mg/mL) in hybridoma growing media **(TABLE 2.4)** for 2-5days.

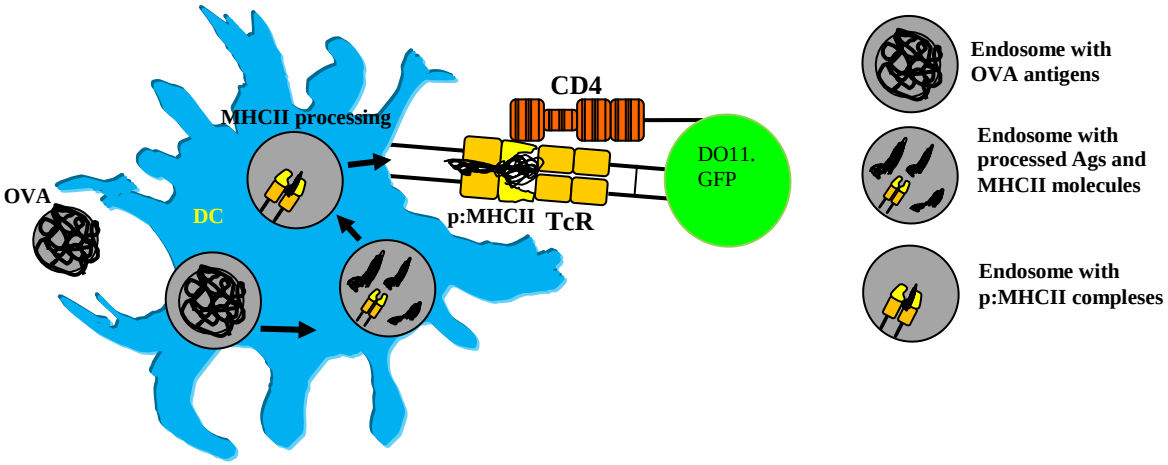

FIGURE 2.4: Hybridoma assay to study antigen presentation by DCs *in vitro*.

When DC takes up antigen such as OVA (Ovalbumin), it processes into the OVApeptide323–339 and presents this peptide bound in MHC class II molecules (p:MHCII) to the T cell receptor (TcR) of T cell such as DO11.GFP hybridoma. The encounter of p:MHCII with TcR and CD4 results in enhanced GFP expression from this hybridoma.

2.13 Analysis of antigen presentation using the DO11.GFP hybridoma

To analyse the impact of Alum on antigen presentation, DCs ($1x10^6$cells) were treated with different concentrations of OVA or OVApeptide323–339 and OVA or OVApeptide323–339 adsorbed to different concentrations of Alum in a six-well plate for 6hours. These cells were then incubated with the hybridoma ($1x10^6$cells) overnight (about 20hours). Then, cells were collected, washed and stained for flow cytometry.

2.14 Costimulation asssay

To evaluate the costimulatory molecules expressed on DC following Alum treatment, DCs ($2x10^6$/5mL) were incubated with different concentrations of Alum (0.1, 1.0, 10.0, 100.0, 1,000.0µg/mL) in a six-well plate for different periods. Some of the wells were incubated with LPS (1.0µg/mL) as a positive control and in media as a negative control. The cells were stained with different costimulatory and activation markers of DC and analysed by flow cytometry.

2.15 Cell viability Assay

To analyse the impact of Alum the viability of DCs, BMDCs ($2x10^6$/5mL) were incubated in different concentrations of Alum (0.1, 1.0, 10.0, 100.0, 1,000.0 µg/mL) and in media for 24hours. Cells were collected and washed (400xg, 5minutes, 4°C) with FACS buffer. Some cells were treated with 200µL 4% (w/v) PFA **(TABLE 2.5)** for control experiments. They were incubated first in Fc block (2.4G2 hybridoma supernatant) **(TABLE 2.5)** to block non-specific binding of Fc-receptors on the cell surface. Then, cells were incubated with fluorescently labelled anti-CD11c antibody (1:100 dilution) for 30minutes. Cells were washed in FACS buffer (400xg, 5minutes, 4°C) followed by washing twice in 2mL of 1XBinding Buffer (400xg, 5minutes, 4°C). Cells were resuspended in 200µL of 1XBinding

Buffer. In each tube, 4µL of Annexin-V fluorescein isothiocyanate (FITC) was added and incubated in the dark at room temperature. Cells were washed twice in 2mL of 1XBinding Buffer (400xg, 5minutes, 4°C). Cells were resuspended in 200µL of 1XBinding Buffer followed by adding 4µL of 7-AAD solution. Both Annexin-V FITC and 7-AAD were added either differently or in the same tubes in some of the controls containing fixed cells with 2% (w/v) PFA. The cells were analysed by flow cytometry within 30minutes. Apoptotic cells were analysed in the FITC positive channel, and necrotic cells were analysed in the Peridinin Chlorophyll (PerCP) positive channel.

2.16 *In vivo* T cell tracking

LNs were extracted from DO11.10 mice and single cell suspensions prepared in cRPMI **(FIGURE 2.5)**. The cells were resuspended in HBSS ($5x10^7$ cells in 1mL cells) and then fluorescently labelled by incubating with CFSE (0.5µL CFSE in 1mL HBSS) for 5minutes and then washed and resuspended in cRPMI. About 25% of the cells were antigen-specific CD4+ T cells (positive for CD4 and KJ). A total of $3x10^6$ cells in 200µL were injected via the tail vein of BALB/c mice at day -1. On the next day (day 0), mice were divided into three groups; PBS, OVA and Alum adjuvanted OVA recipients. Mice were injected subcutaneously in the nape of the mice with 100µL of PBS, 100µL of OVA (final concentration: 1mg/mL) and 100µL of OVA (1mg/mL) adsorbed to Alum (final concentration: 1% (w/v) Alum). At day 1, day 5 and day 10, after immunisation LNs (brachial and axillary) were extracted from the BALB/c mice and processed for staining. The cells from LNs were stained with anti-CD4 antibody that recognises CD4 coreceptor and a clonotypic antibody, DO11.10TCR or KJ1.26 that recognises TcR that recognises OVApeptide323–339 **(TABLE 2.3)** and analysed by FACS.

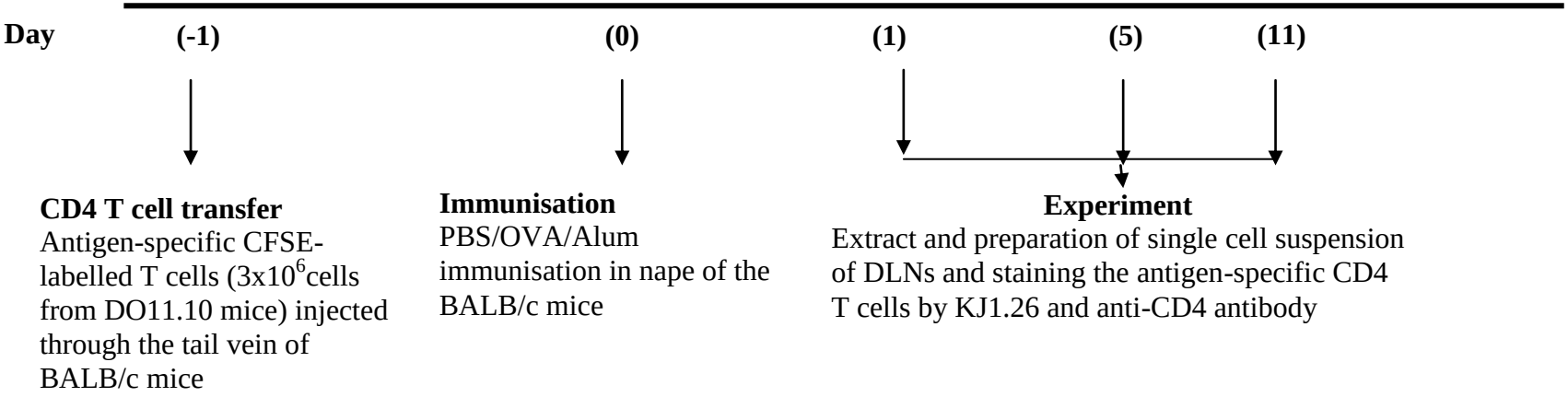

FIGURE 2.5: Study design showing *in vivo* tracking of transgenic T cells.

Antigen-specific CD4 T cells from DO.11.10 mice were transferred into the BALB/c mice through tail vein at day (-1). In the next day, antigen or antigen adsorbed to Alum were immunised in the nape of the BALB/c mice. In day 1, day 5, day 11, BALB/c mice were culled and single cell suspensions were prepared from LNs. Cells were stained with anti-CD4 and DO11.10 TCR KJ1.26 antibody and analysed by flow cytometry.

2.17 Flow cytometry

Cells were collected in 5mL FACS tubes and washed (400xg, 5minutes, 4°C) in FACS buffer [5% (v/v) FCS +0.1% (w/v) sodium azide] and incubated with either purified anti-mouse CD16/CD32 (1 in 100 dilution) or 100µL Fc block (2.4G2 hybridoma supernatant) **(TABLE 2.5)** for 30minutes to prevent non-specific binding via Fc receptors **(TABLE 2.5)**. Then, cells were stained with fluorophore-labelled antibody **(TABLE 2.3)** and incubated for 30minutes. Cells were washed with FACS buffer twice (400xg, 5minutes, 4°C) and analysed on a FACS Caliber (BD Biosciences). A total of 50,000 events were collected based on forward and side scatter unless otherwise stated. The results of flow cytometry were analysed by FlowJo software (FlowJo 8.7.1, Stanford University 1995-96). The level of GFP, YAe, MHCII and costimulatory molecules present on CD11c positive cells was analysed by both mean fluorescence intensity (MFI) and percentages.

2.18 ELISA

2.18.1 Sandwich ELISA

To assess the concentration of IL-10 in supernatants obtained from DCs incubated in different concentration of Alum, a sandwich ELISA was used. All the materials and antibodies used in this assay have been listed in **TABLE 2.6**. First of all, Corning Costar 9018 ELISA plates were coated with 100µL/well of capture antibody (purified anti-mouse IL-10) in 12mL coating buffer. The plate was sealed and incubated overnight at 4˚C. Plates were washed with ELISA wash buffer (0.05% Tween-20 and PBS, 5X), and non-specific protein binding was blocked by incubation with blocking buffer (200µL per well, 10% (v/v) FCS in PBS, room temperature, 1hr). The plates were washed with ELISA Wash Buffer (x5) **(TABLE 2.6)**. Using Assay diluents, the standards were diluted as 4,000, 2,000, 1,000, 500, 250, 125, 62.5, 31.25 and 0pg/mL with their final volumes 100µL in each well. Then, the DC supernatant (100µL) obtained from cell culture was added in each well. The plate was sealed and incubated at room temperature for 2hours. The plate

was washed (x5) and 100µL detection antibody **(TABLE 2.6)** was added in each well. The plate was sealed and incubated at room temperature for 1hour. Plate was washed (x5). In each well, 100µL of horse-radish-peroxidase (HRP)-conjugated Streptavidin-Avidin was added followed by incubation of plate at room temperature for 30minutes. Plate was washed (x14) following soaking of wells in Wash Buffer for 1–2minutes. In each well, 100µL of Substrate Solution **(TABLE 2.6)** was added followed by incubation at room temperature for 15minutes. The reaction was terminated by the addition of 10% (v/v) H_2SO_4 and the absorption was determined at OD_{450} using an ELISA plate reader (Molecular Devices).

2.18.2 Luminex Assay for cytokines

Luminex consists of internally colour-coded microspheres with two fluorescent dyes via which several coloured bead sets can be created. Each of the bead is coated with a specific capture antibody that captures an analyte (cytokine or protein) from a DC supernatant. Then, a biotinylated detection antibody is treated followed by incubation with a fluorescent reporter molecule, Streptavidin-Phycoerythrin (PE) conjugate to complete the reaction on the surface of each microsphere. Then, a first laser is passed via microsphere resulting in excitation of internal dyes and indication of microsphere set. The second laser excites PE resulting in recognition of fluorescent dye on the reporter molecule. Based on this reporter molecule, each individual microsphere and the concentration of different cytokines are assessed with a high-speed digital-signal processor.

For the Luminex assay, the protocol provided by Millipore Corporation was used (Milliplex® MAP Kit, Mouse Cytokine/Chemokine Magnetic Bead Panel, MCYTOMAG-70K, 96-Well Plate Assay) to analyse IL-1β, IL-12p70, TNF-α, IL-13, IL-15 and IL-6 (6-plex) in the supernatants obtained from DC culture with different doses of Alum at different incubation periods. In the same way, to analyse the amounts of IL-33 (1-plex), another protocol was used (Milliplex R MAP Kit, Mouse Cytokine/Chemokine Magnetic Bead Panel III, MCYP3MAG-74K, 96-Well Plate Assay). Therefore, two different plates were used to analyse the cytokine level

in these assays. Details of all materials, chemicals, buffers, antibodies and quality control ranges used in Luminex assay have been listed in **TABLE 2.7** to **TABLE 2.9**.

2.18.2.1 Preparation of reagents

Each antibody vial was vortexed for 1minute and 60µL of each antibody vial was diluted in final volume of 3.0mL Assay Buffer. Quality Control 1 and Quality Control 2 were reconstituted in 250µL deionised water. 60mL of 10X Wash Buffer **(TABLE 2.7)** was diluted in 540mL deionised water to prepare Wash Buffer. Mouse cytokine standard was reconstituted with 250µL deionised water to give a 10,000pg/mL (6-plex) or 100,000pg/mL (1-plex) concentration of standard for all analytes. Standards were prepared by serial dilution to 10,000, 2,000, 400, 80, 16, 3.2, 0pg/mL concentrations for 6-plex or 100,000pg/mL, 20,000, 4,000, 800, 160, 32 and 0pg/mL concentrations for 1-plex ELISA. Before putting the standard in polypropylene microfuge tube, the vial was kept at room temperature for 5-10minutes and processed for standard controls.

2.18.2.2 Immunoassay procedure

In each well of the plate, 200µL Wash Buffer **(TABLE 2.7)** was added. The plate was sealed and shaken for 10minutes at room temperature followed by subsequent removing. Then, 25µL of each Standard or Control was added into the previously pre-coated magnetic wells followed by putting 25µL of cDC media to the background, standard and control wells. Then, 25µL of Assay Buffer **(TABLE 2.7)** was added to the sample wells followed by addition of 25µL DC supernatant into each sample wells and then 25µL beads into the entire well. The plate was sealed with a plate sealer and wrapped with Aluminium foil followed by incubation with agitation for 2hours at room temperature. The plate was put above magnet for 1minute to allow complete settling of magnetic beads. The contents of the well were gently decanted followed by washing with 200µL of Wash Buffer **(TABLE 2.7)**. This process was repeated three times following shaking for 30minutes and then reattaching to magnet for 1minute and then subsequent washing the contents gently.

Then, 25µL detection antibodies were added into each well followed by incubation with agitation on a plate shaker for 1hour at room temperature. 25µL Streptavidin-Phycoerythrin was added to each well containing the 25µL of detection antibodies and incubated with agitation on a plate shaker for 30minutes at room temperature. The contents were removed and washed the plate twice with 200µL of Wash Buffer and putting over a magnet to allow complete settling of magnetic beads on the bottom of wells. Finally, 150µL of Sheath Fluid (containing sodium chloride, sodium phosphate and an antimicrobial component) was added to each well as a delivery medium of the sample to the laser component of the analyser. The plate was analysed by MAGPIX® with xPONENT software (Luminex Corporation, Build: 4.1.308.0). The median fluorescent intensity[f] data and curve-fitting methods **(APPENDIX-II)** were used to assess cytokine concentration.

2.19 Data Analysis

Data were analysed using Statistical software packages (GraphPad Prism version 5.00 for Windows, GraphPad Software, San Diego California, USA). Results were expressed as mean±S.E.M. unless otherwise stated. In the data with one independent variable, Tukey Post Test (One Way ANOVA) was used to test significance between any two different treatment groups unless otherwise stated. Similarly, in the data having more than one independent variable such as in the dose response and the kinetics experiments, Bonferroni Post Test (Two Way ANOVA) was used to test the significance between any two different treatment groups either at specific dose or at specific time. A P-value of <0.05 was considered as significant. The letter 'n' was denoted for the number of replicates in all *in vitro* experiments; whereas it was denoted for the number of mice in each treatment group *in vivo* experiments.

[f]Median fluorescence intensity is the total fluorescent emission accumulated in a particular bead characterised by a specific antigen-antibody reaction among various reaction within the microsphere.

CHAPTER-3: EFFECT OF ALUM ADJUVANTS ON UPTAKE AND PRESENTATION OF ANTIGEN BY BMDC

3.1 Introduction

The recognition of p:MHCII complexes by CD4 T cells is the foremost step in initiating an adaptive immune response. To allow recognition of these complexes, APCs such as DCs perform a sequence of events including antigen uptake, antigen processing, loading of processed antigen onto MHC class II molecules and finally presenting these molecules on the DC surface. Antigen presentation by DCs has been poorly understood in the context of Alum adjuvants. This is because most of the studies conducted to date have assessed antigen presenting efficiency of APCs using T cells as an indirect readout. Therefore, in this chapter, the impact of Alum on antigen uptake and presenting efficiency of DCs has been investigated by directly measuring the amounts of presented antigens in the context of MHC molecules on cell surface. To address this, the EαGFP/YAe system was applied in which EαGFP was used as a model antigen. EαGFP is a green fluorescent protein antigen which contains the GFP coupled to Eα, an antigenic peptide. When APCs such as DCs, internalise this antigen, they become fluorescent. As the antigen is processed inside the cell, the cell loses this associated fluorescent signal. During processing, the peptide, Eα, is free to associate with intracellular MHCII molecules for subsequent presentation on the cell surface. These p:MHCII complexes can then be detected by staining the cells with YAe antibody because this antibody can efficiently bind with the Eα-I:A^bMHCII complex [216,409,410]. The YAe system is important in the study of antigen internalisation and presentation because we can evaluate the magnitude and dynamics of GFP acquisition and loss, as well as the number of APCs and their level of antigen presentation.

3.2 Impact of Alum on antigen uptake and presentation by BMDCs

To investigate the impact of Alum on antigen uptake and presentation by BMDCs, first the suitability of the EαGFP/YAe system was determined. BMDCs were incubated with EαGFP, Alum-adsorbed EαGFP or in the presence of media or Alum alone for 24hours. Then, the level of GFP and YAe staining within the CD11c positive population was analysed **(FIGURE 3.1A,B)**. Detection of GFP or YAe staining was dependent on the presence of EαGFP, incubating BMDC with Alum alone did not produce any increase in either of these parameters compared with control cultures **(FIGURE 3.2B,C)**. Adsorption of EαGFP to Alum produced a significant increase in antigen uptake and presentation ($P<0.0001$), with about a 5-fold higher MFI of GFP and a 2-fold higher MFI of YAe compared with cells incubated in EαGFP alone. Similar results were obtained by analysing the proportion of GFP or YAe positive cells **(FIGURE 3.2C)**. The results suggest that EαGFP/YAe system is appropriate for the *in vitro* study of antigen uptake and presentation by DCs following Alum treatment.

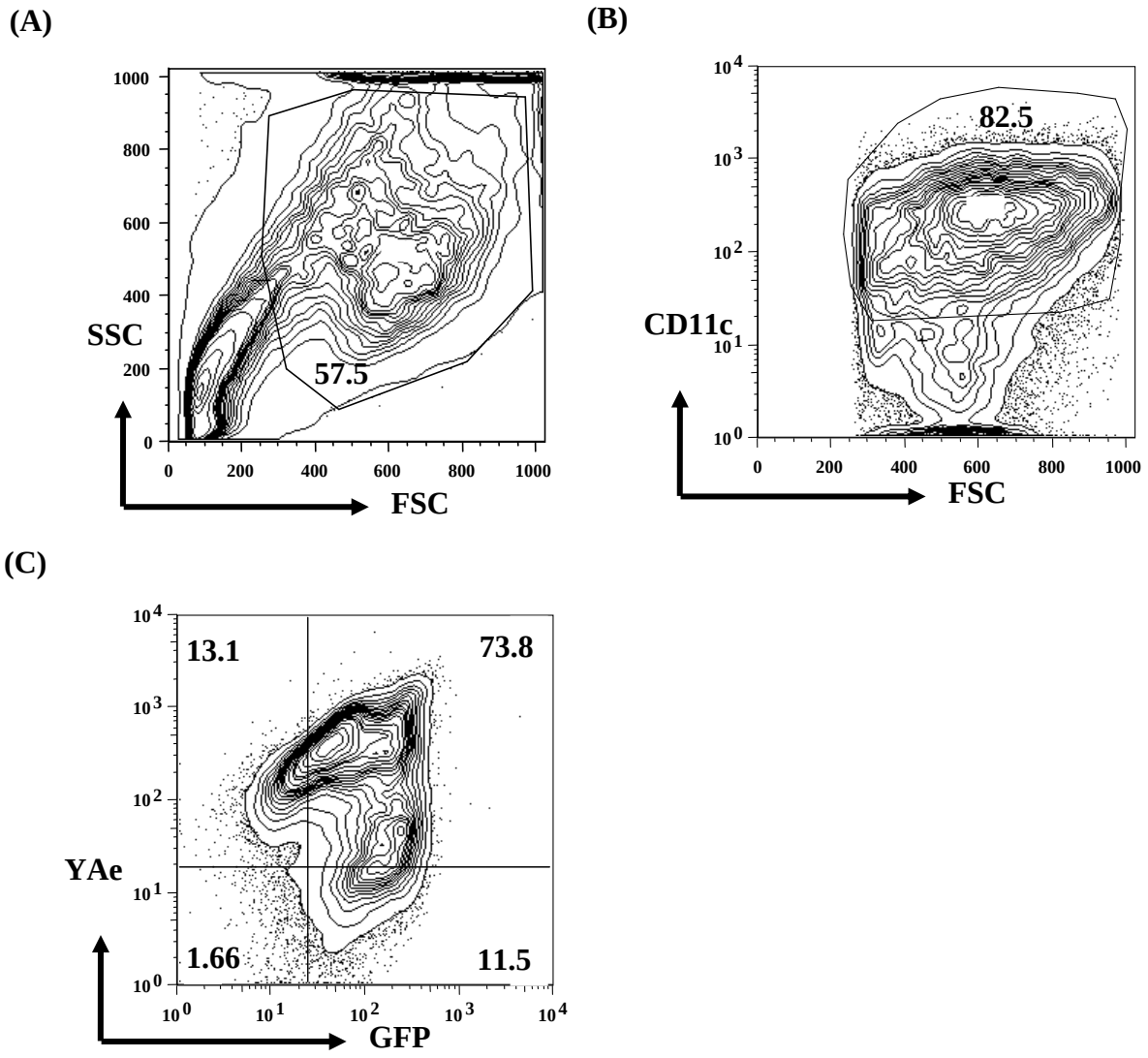

FIGURE 3.1: Application of the EαGFP/YAe system to reveal the impact of Alum adjuvants on antigen uptake and presentation by DCs.

BMDCs ($2x10^6$/5mL) obtained from C57BL/6 mice were incubated in media, Alum (100µg/mL), EαGFP (100µg/mL) and EαGFP adsorbed to Alum (100µg/mL) for 24hours. **(A)** A total of 50,000 cells were analysed on the basis of FSC (forward scatter) and SSC (side scatter). **(B)** DCs were identified by CD11c expression. **(C)** Analysis of GFP and YAe levels was performed on CD11c positive populations.

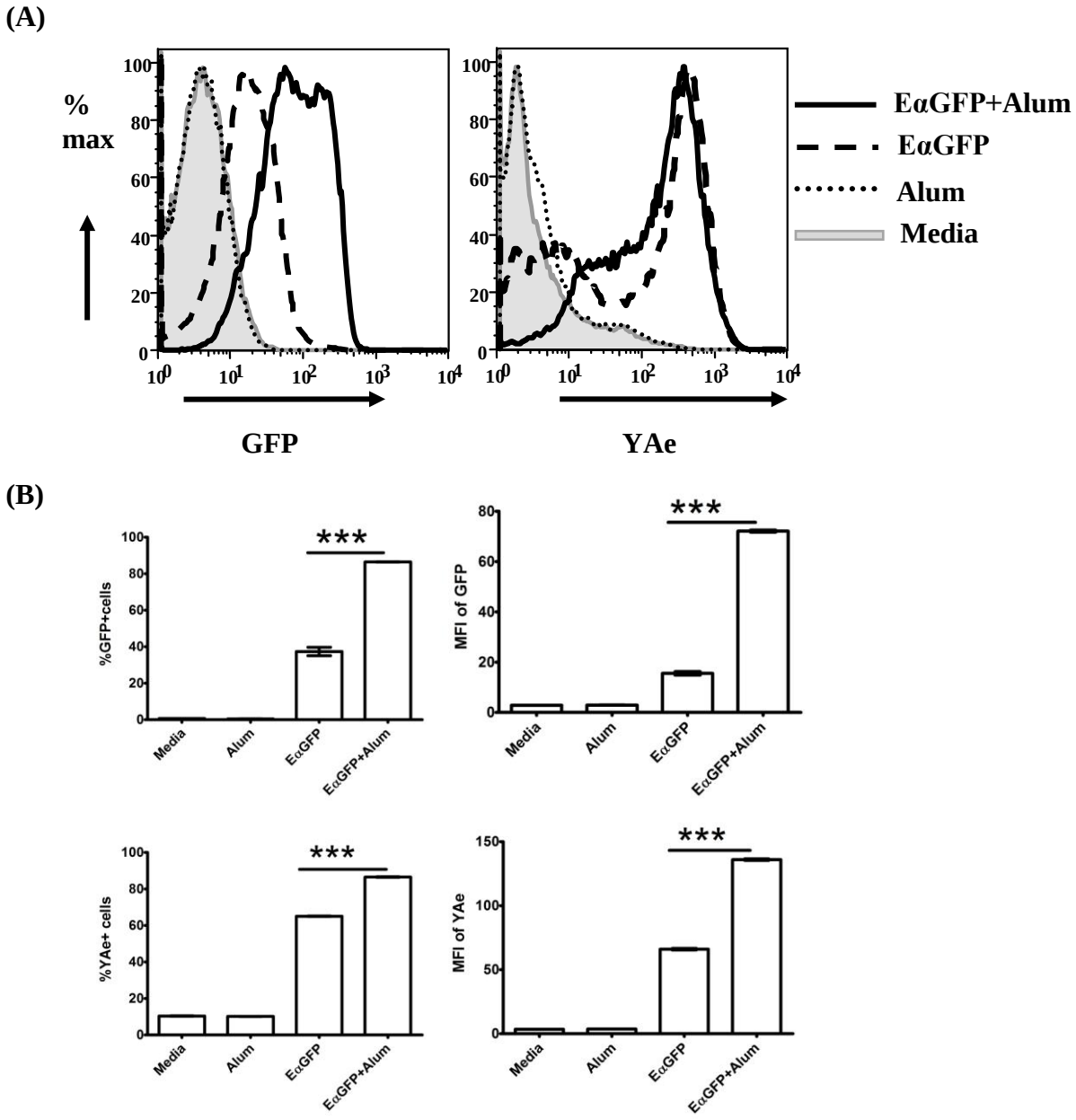

FIGURE 3.2: EαGFP/YAe system can be used to study the impact of Alum on antigen uptake and presentation.

The data obtained in **FIGURE 3.1** were expressed in bar graphs. **(A)** The overlay histograms represent the levels of GFP (left) and YAe (right) detected in DCs following different treatments as indicated in legends. **(B)** Bar charts show the % of GFP (upper left) and MFI of GFP (upper right) and the % of YAe (lower left) and MFI of YAe (lower right) in different treatment groups. Tukey post tests were used to compare the mean±S.E.M. (n=3) between EαGFP and EαGFP+Alum. ***, P<0.0001.

3.3 Antigen dose response of Alum in antigen uptake and presentation

In the previous experiment, the enhancing role of Alum on antigen internalisation and presentation by DCs at a single antigen dose was analysed. In this experiment, the effect of Alum on antigen accumulating and presenting efficiency of DCs over a range of antigen doses was examined. Interestingly, adsorption of EαGFP to Alum significantly enhanced antigen uptake and presentation compared with soluble antigen over a range (1–100µg/ml) of antigen doses tested ($P<0.001$) **(FIGURE 3.3, 3.4A,B)**. Comparing the antigen dose response curves demonstrated that, Alum could induce similar antigen uptake by BMDCs at a 100-fold lower dose compared with soluble antigen **(FIGURE 3.4A)**. Similarly, equivalent levels of YAe expression were observed on cells incubated with 1µg/mL EαGFP/Alum compared with 10µg/mL EαGFP alone suggesting that Alum causes a 10-fold increase in antigen presenting efficiency of DCs *in vitro* **(FIGURE 3.4B)**. The increased GFP accumulation and antigen presentation in the context of Eα:MHCII complexes by DCs even at low dose of antigen (1µg/mL) formulated in Alum adjuvant suggests that Alum acts as an antigen delivery vehicle *in vitro*.

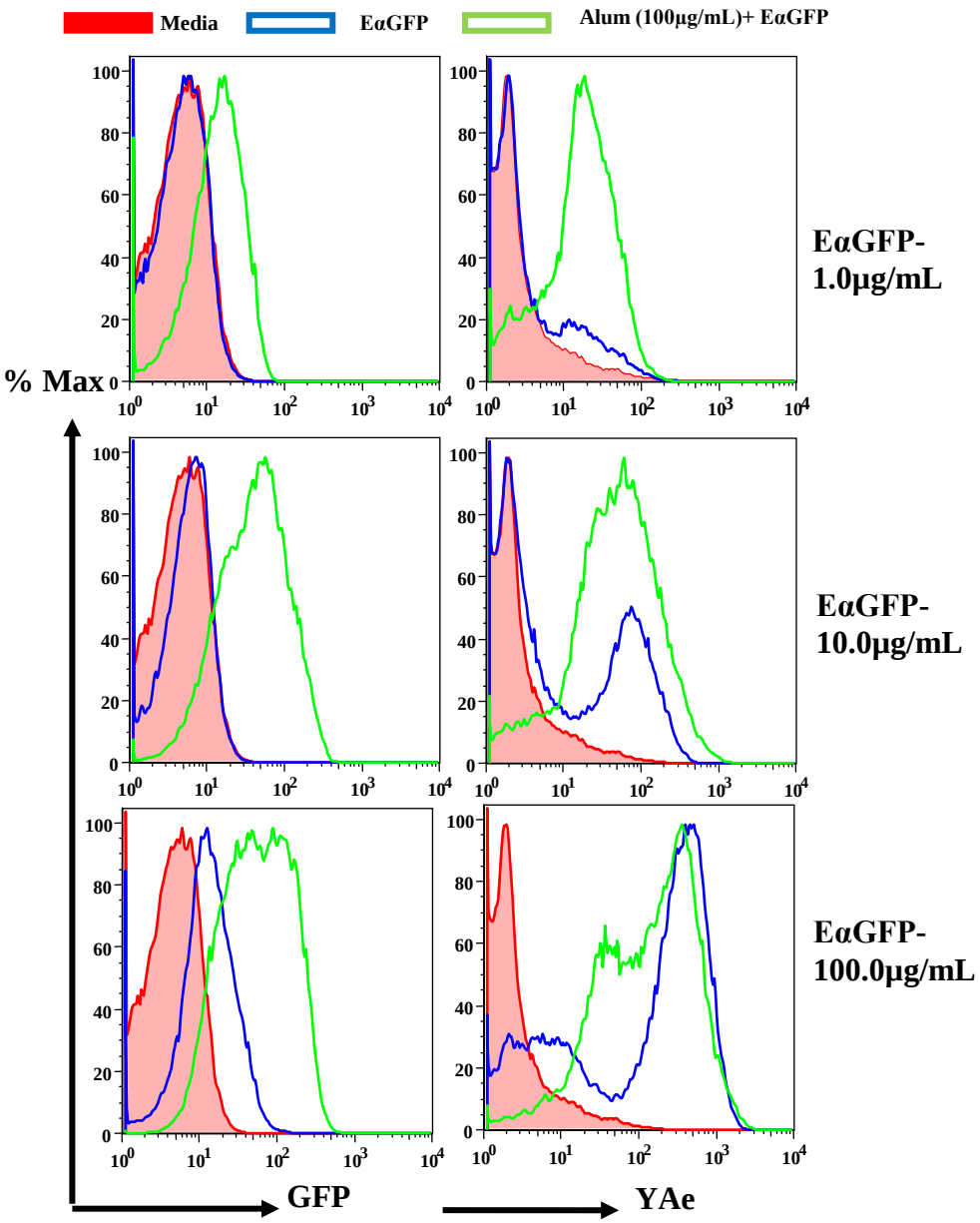

FIGURE 3.3: Alum efficiently targets DCs by enhancing both accumulation and presentation of antigen by DCs *in vitro*.

BMDCs ($2x10^6$/5mL) obtained from C57BL/6 mice were incubated with EαGFP (1.0, 10.0, 100.0µg/mL) and EαGFP adsorbed to Alum (100.0µg/mL) for 24hours. Cells were stained with anti-CD11c and YAe antibody and were analysed by flow cytometry. Above histograms show the GFP or YAe populations gated from CD11c positive cells.

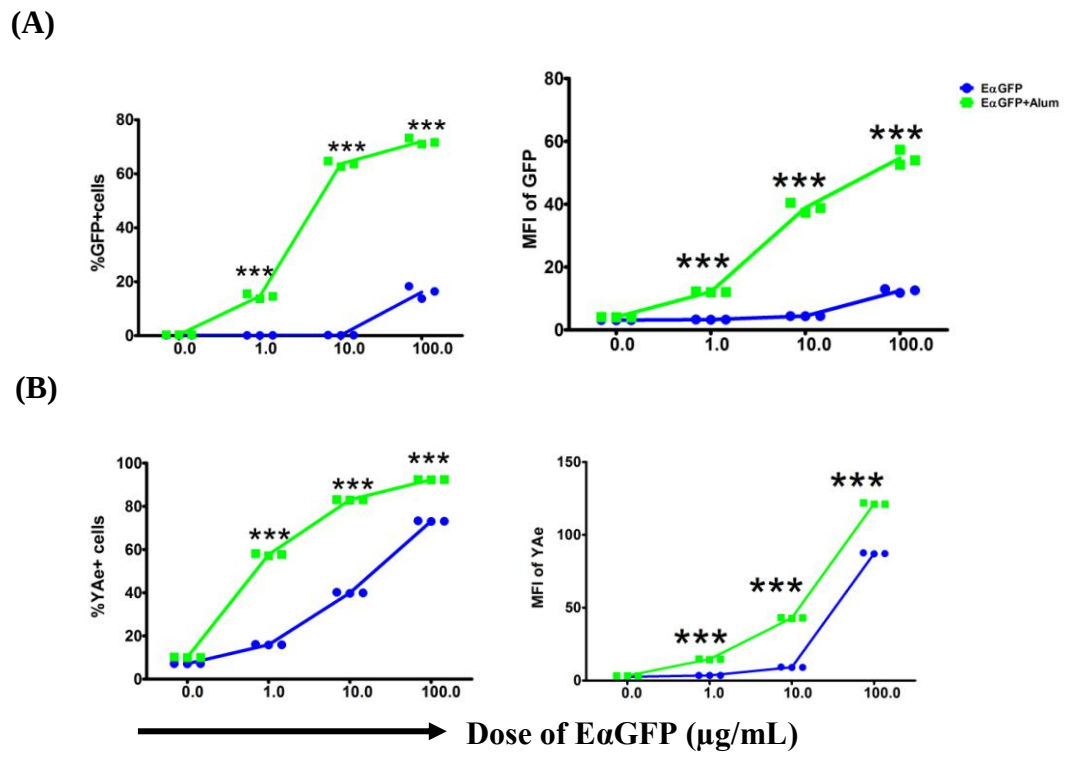

FIGURE 3.4: Alum efficiently targets DCs by enhancing both accumulation and presentation of antigen by DCs *in vitro*.

Above histograms show the level of GFP and or YAe positive cells within CD11c positive population as analysed in **FIGURE 3.3**. The line graphs were made by the scatter dot plots and joining the mean values. The line graphs show the proportion of GFP positive cells or MFI GFP **(A)** or the proportion of YAe positive cells or MFI of YAe **(B)**. Bonferronni post tests (Two Way ANOVA) were used to compare the mean±S.E.M. (n=3) between EαGFP or EαGFP+Alum-treated groups at specific dose of EαGFP. ***, P<0.001.

3.4 Dose response of Alum in antigen uptake and presentation

In the previous section, a positive effect of Alum in enhancing antigen uptake and presenting efficiency of DCs was found even at low dose of available antigen. Next, an attempt was made to analyse the role of different concentrations of Alum on antigen uptake and presenting efficiency of DCs. Morphologically, Alum (Aluminium hydroxide) is a particulate adjuvant because it consists of fibrous primary particles of size 4.5x2.2x10nm that form loose, irregular aggregates of 1–10µm [58], [57]. Therefore, following antigen adsorption in these aggregates, they are more likely targeted by DCs in particulate manner than soluble antigens [60,194]. Therefore, if Alum is a good antigen targeting adjuvant, it should target antigens even at lower doses.

To address this issue, BMDCs were incubated with different concentrations of Alum (0.1, 1, 10, 100, 1000µg/mL)-adjuvanted EαGFP (with constant concentration of EαGFP=100µg/mL) for 24hours. Interestingly, doses of Alum between 0.1 and 10µg/mL produced a small, though significant increase in antigen uptake compared with soluble antigen **(FIGURE 3.5A,B)**. This was reflected in a corresponding significant increase in presentation of the pEα:MHCII complexes emphasising the targeting impact of Alum to BMDCs *in vitro*. Higher doses of Alum (100 and 1000µg/mL) produced much greater increase in GFP signal in BMDCs, however the impact on antigen presentation was more modest, with decreased presentation being observed between 100 and 1000µg/mL Alum **(FIGURE 3.6A,B)**. The difference in antigen presence and presentation in BMDC implied that the presence of Alum may affect the rate of antigen degradation. Therefore, to address the impact of Alum on antigen degradation, in the next step, kinetic analysis of GFP and YAe signals following antigen uptake *in vitro* was performed.

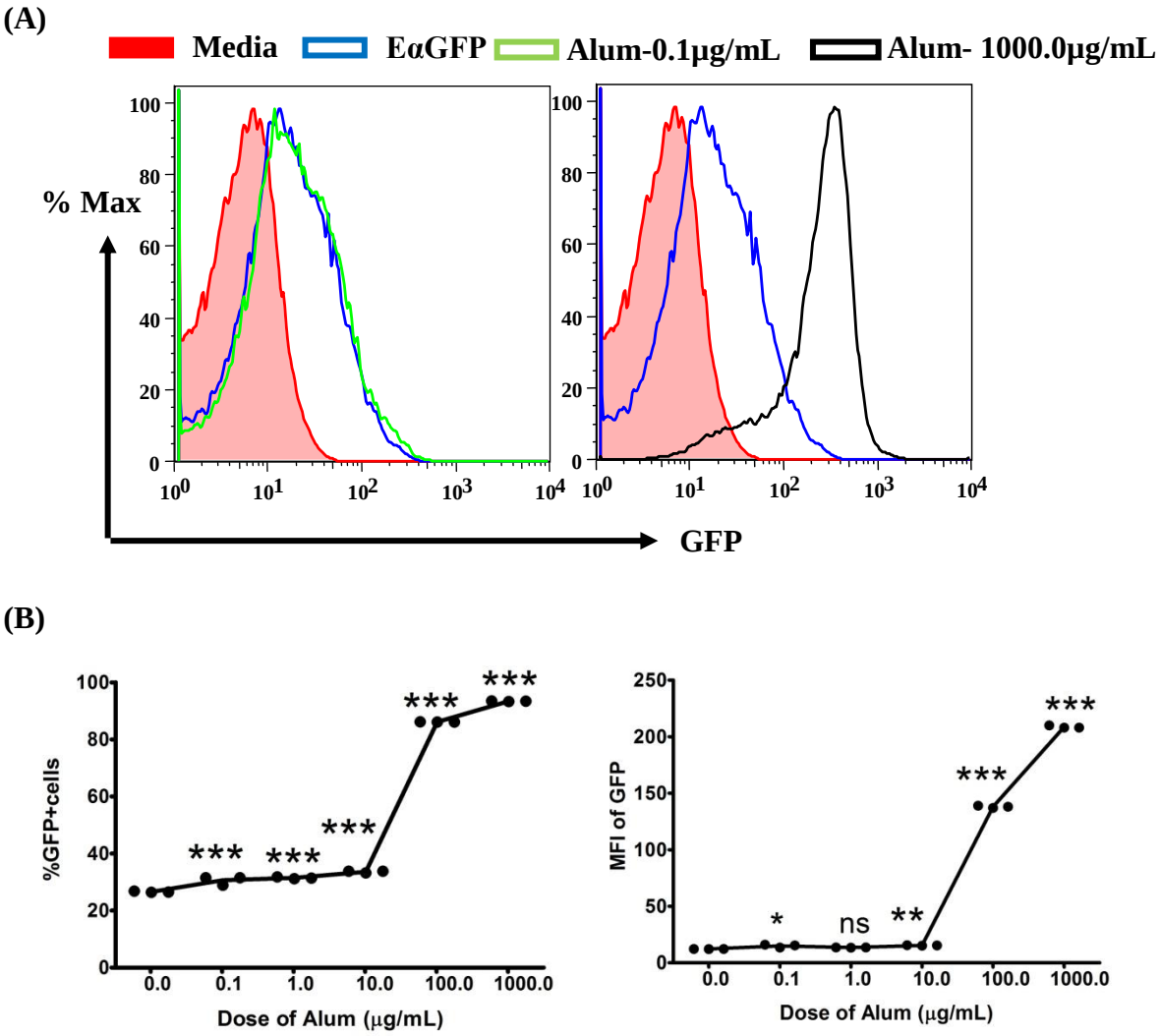

FIGURE 3.5: Alum efficiently targets DCs by enhancing antigen accumulating efficiency of DCs *in vitro*.

BMDCs ($2x10^6$/5mL) obtained from C57BL/6 mice were incubated with EαGFP (100µg/mL) and EαGFP adsorbed to Alum (0.1, 1.0, 10.0, 100.0, 1000.0µg/mL) for 24hours. Cells were stained with anti-CD11c and YAe antibody and analysed by flow cytometry. (A) Overlay histograms show % maximum of GFP in different treatment groups. (B) The lower line graphs were made by the scatter dot plots and joining the mean values. The line graphs show the % of GFP+ cells (left) or MFI of GFP (right) at different Alum concentration. Tukey post test (One Way ANOVA) was used to compare the level (mean±S.E.M., n=3) of GFP between control (Alum; 0.0µg/mL or EαGFP (100µg/mL)-treated group and increasing concentrations of Alum. ***: P<0.0001, **: P<0.001, *: P<0.01, ns=not significant.

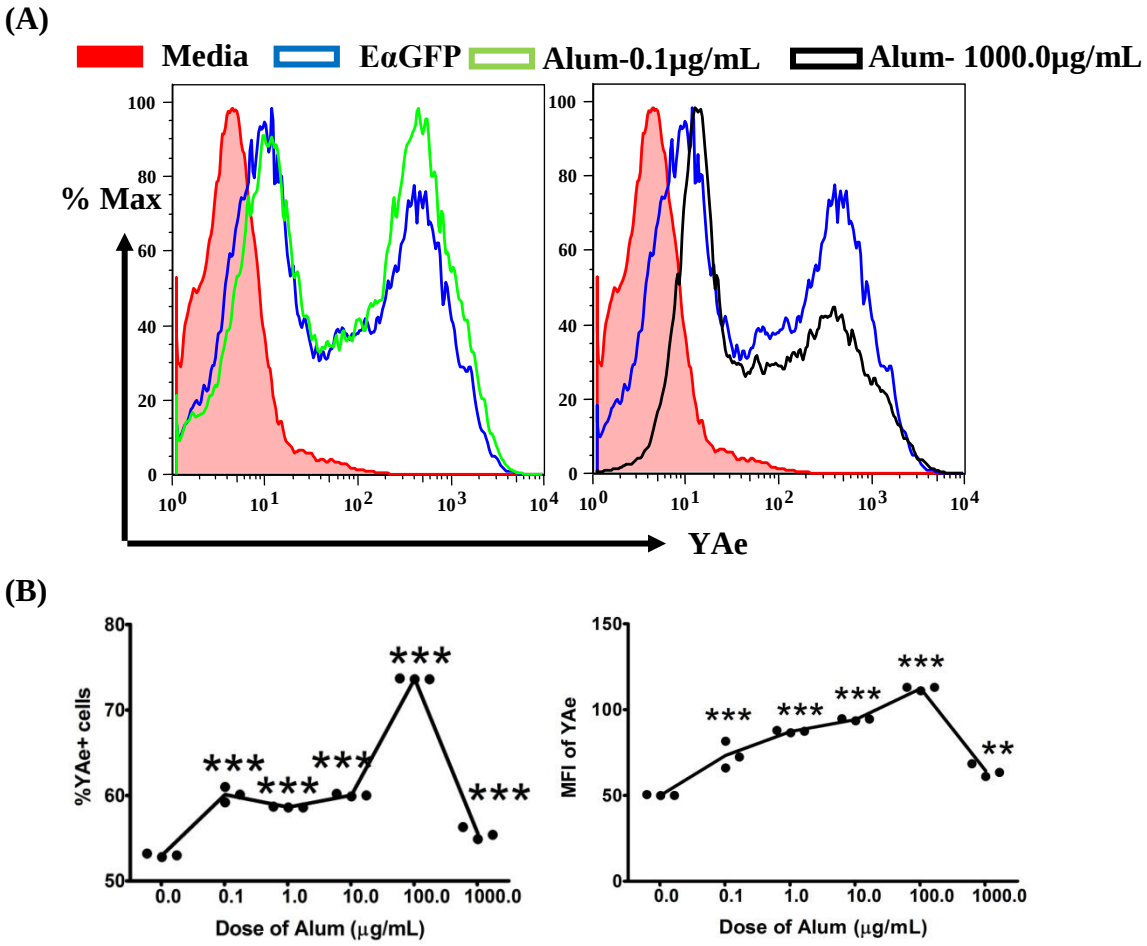

FIGURE 3.6: Alum efficiently targets DCs by enhancing antigen presenting efficiency of DCs *in vitro*.

BMDCs ($2x10^6$/5mL) obtained from C57BL/6 mice were incubated with EαGFP (100 µg/mL) and EαGFP adsorbed to Alum (0.1, 1.0, 10.0, 100.0, 1000.0µg/mL) for 24hours. Cells were stained with anti-CD11c and YAe antibody and analysed by flow cytometry. (A) Overlay histograms showing % maximum of cells positive for YAe. (B) The lower line graphs were made by the scatter dot plots and joining the mean values. The line graphs show the % of YAe-positive cells (left) or MFI of YAe (right) at different Alum concentration. Tukey post test (One Way ANOVA) was used to compare the level (mean±S.E.M., n=3) of YAe between control (Alum; 0.0µg/mL or EαGFP (100µg/mL)-treated group and increasing concentrations of Alum. ***: P<0.0001, **: P<0.001.

3.5 Role of Alum adjuvants in the kinetics of antigen uptake and presentation

3.5.1 Kinetics of antigen uptake and presentation in continuous presence of Alum and antigen

To understand the role of Alum on the kinetics of antigen uptake and presentation by DCs, I incubated cells with soluble antigen alone or antigen adsorbed to Alum for different periods of time. Without washing antigens/adjuvants, GFP **(FIGURE 3.7A)** and YAe staining **(FIGURE 3.8A)** were analysed after each incubation period. In the absence of adjuvant, the level of antigen accumulation by DCs becomes maximum at 12hours, however, the values are not significant ($P>0.05$) compared with that of cells incubated for 1hour, for the % parameter and ($P>0.05$) for the MFI parameter indicating antigen uptake becomes almost saturated within 1hour of antigen uptake *in vitro* **(FIGURE 3.7B)**.

On the other hand, Alum increased the rate and magnitude of antigen internalisation by BMDCs within 15minutes of antigen treatment **(FIGURE 3.7A,B)**. The level of GFP accumulation decreased by 3 fold at 3hours and became almost constant until 48hours. Similar results were obtained when DCs were incubated for 96hours **(APPENDIX-I)** indicating the impact of Alum on enhanced rate and magnitude of uptake of antigen. I observed a different pattern of YAe expression by the cells in this experiment **(FIGURE 3.8A,B)**. Following Alum treatment, from 1hour to 3hours, the numbers of Eα:MHCII complexes as well as the proportion of cells expressing the Eα:MHCII complexes increased by 3 fold **(FIGURE 3.8B)**. Consequently, compared with soluble antigen-treated cells, Alum enhanced the expression of the Eα:MHCII complexes from 6hours to 48hours incubation periods. Similar results were obtained when DCs were incubated for 96hours **(APPENDIX-I)** indicating the impact of Alum on enhanced rate and magnitude of presentation of antigen. Overall, the data suggests that Alum may slow down antigen degradation and sustain antigen presentation by DCs. Therefore, to address these issues, the pulse chase studies were performed.

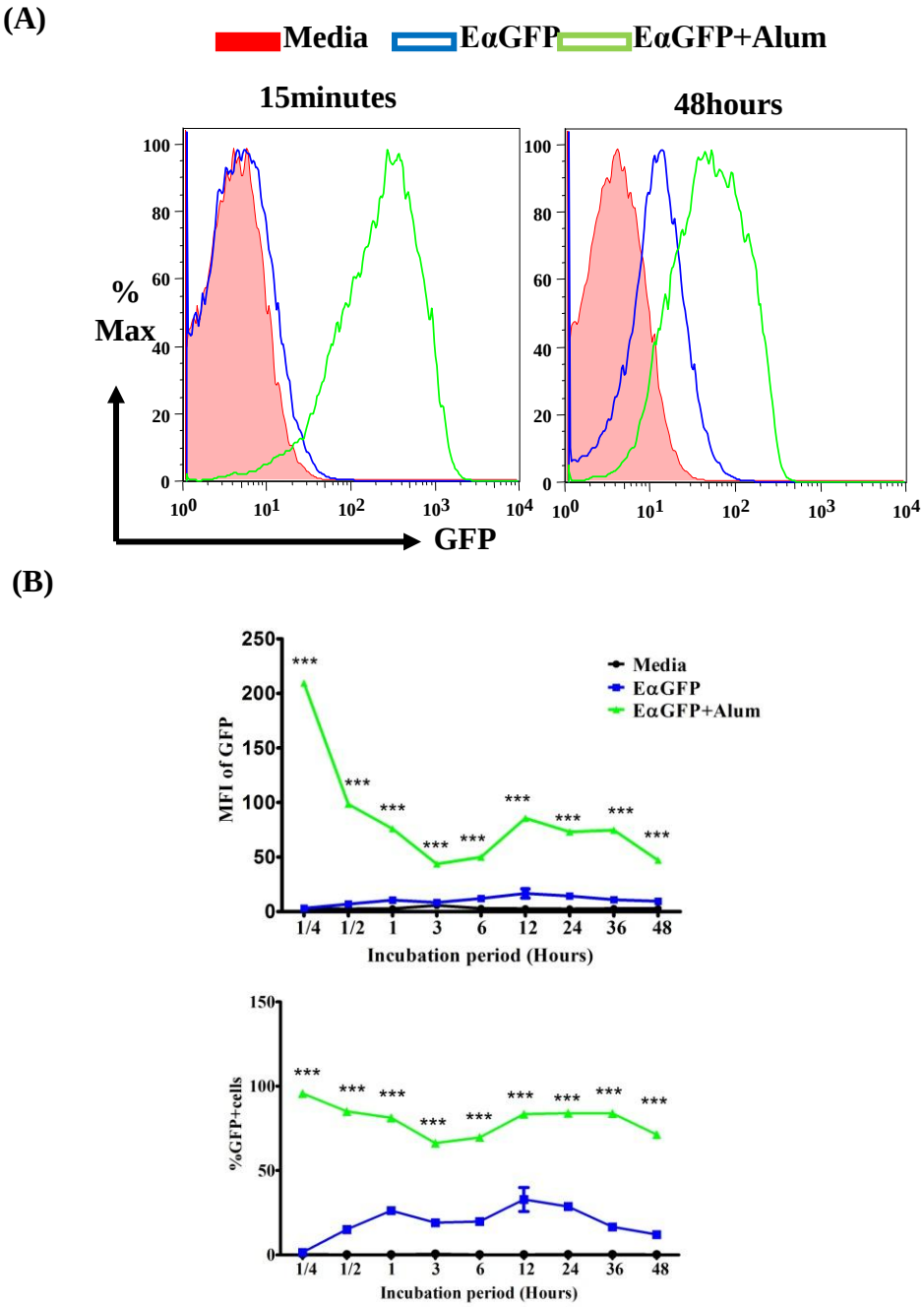

FIGURE 3.7: Alum increases the rate and magnitude of antigen uptake by DCs.

BMDCs ($2x10^6$/5mL) obtained from C57BL/6 mice were incubated in media, EαGFP (100µg/mL) and EαGFP adsorbed to Alum (100µg/mL) for different periods. Cells were stained with anti-CD11c and YAe antibody and analysed for GFP by flow cytometry. **(A)** Overlay histograms in different treatment groups at different incubation periods. **(B)** Line graphs showing kinetics of antigen uptake by BMDCs at different treatment groups. Bonferronni post tests (Two Way ANOVA) were used by comparing mean±S.E.M. (n=3) to analyse the significance between EαGFP or EαGFP+Alum groups at specific time points. Data have been presented as the mean±S.E.M. of three independent experiments. ***: P<0.001.

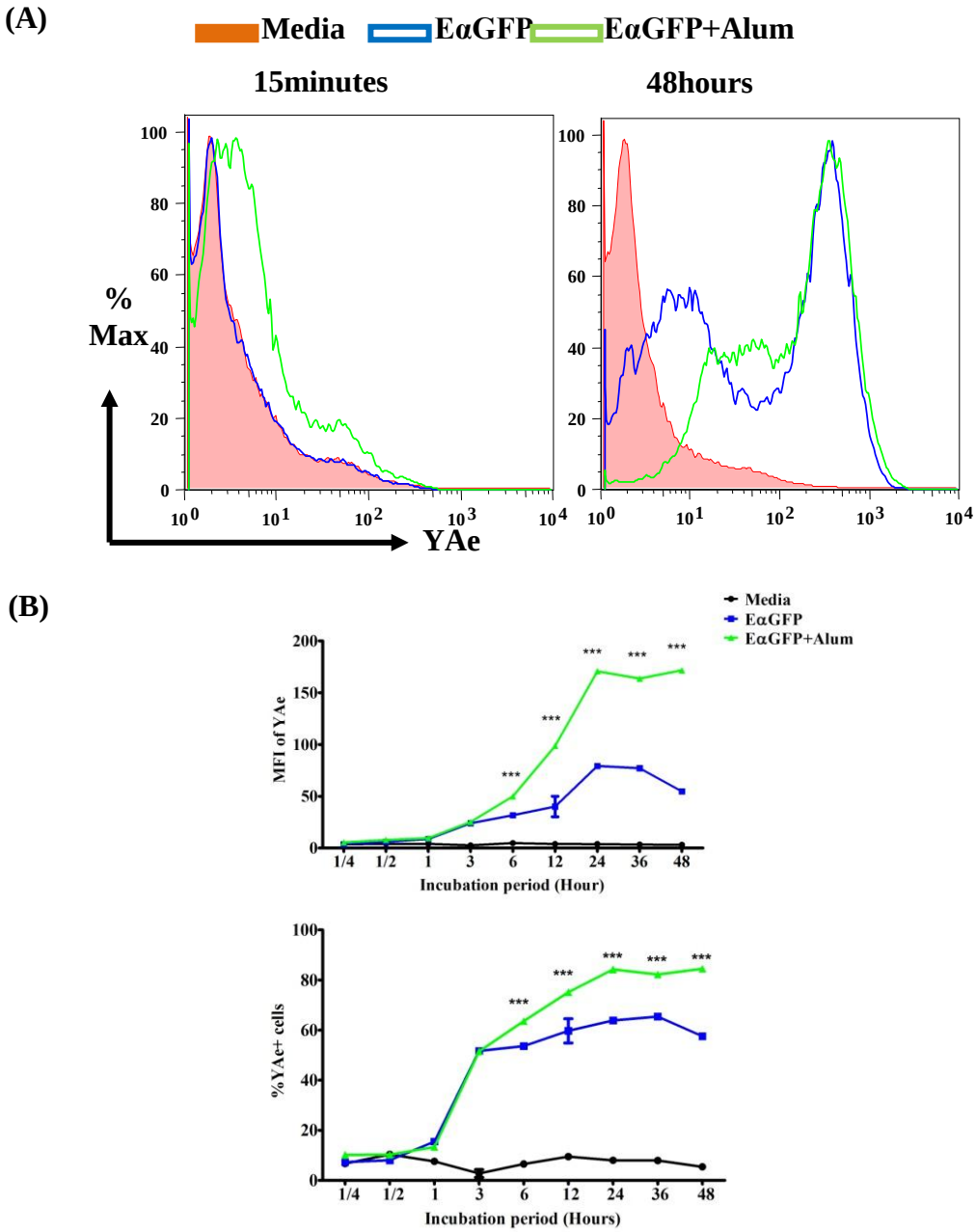

FIGURE 3.8: Alum increases the rate and magnitude of antigen presentation by DCs.

BMDCs ($2x10^6$/5mL) obtained from C57BL/6 mice were incubated in media, EαGFP (100µg/mL) and EαGFP adsorbed to Alum (100µg/mL) for different periods. Cells were stained with anti-CD11c and YAe antibody and were analysed for YAe by flow cytometry. **(A)** Overlay histograms showing the % maximum of cells positive for YAe at different incubation periods. **(B)** The line graphs showing the kinetics of % of YAe-expressing cells (lower) or MFI of YAe (upper) in different treatment groups. Bonferronni post tests (Two Way ANOVA) were used to analyse the significance between EαGFP or EαGFP+Alum groups at specific period by comparing mean±S.E.M. (n=3). Data have been presented as the mean±S.E.M. of three independent experiments. ***: P<0.001.

3.5.2 Kinetics of antigen uptake and presentation after a pulse chase assay

To understand the impact of Alum on antigen internalisation, degradation and presentation by BMDCs, a pulse chase experiment was conducted. From the previous experiment, it appeared that antigen uptake by DCs *in vitro* was maximal within 1hour **(FIGURE 3.7B)**. Therefore, DCs were exposed to EαGFP or EαGFP adsorbed to Alum for a 1hour 'pulse', then separated from antigen and Alum and 'chased' for various periods of time.

Notably, a greater proportion of cells were GFP positive ($P<0.001$) and had a greater GFP signal ($P<0.001$), as determined by assessment of mean fluorescence intensity **(Results Not Shown)**, following treatment with EαGFP adsorbed to Alum compared with exposure to EαGFP at each chase period tested. Following exposure to soluble antigen, both the GFP signal and proportion of cells that were GFP positive returned to background levels within 24hours **(FIGURE 3.9, 3.10A)**. While there was also rapid decay in GFP in cells exposed to antigen formulated in Alum, the residual GFP signal was sustained up to 72hours ($P<0.0001$) following exposure, suggesting intact antigen is degraded more slowly and persists for longer in the presence of Alum.

This would suggest that Alum would also affect the rate of antigen presentation by BMDC. In keeping with this observation, formulation of antigen with Alum decreased the fraction of YAe-positive BMDC immediately after a 1hour pulse (0hour; $P<0.01$) **(FIGURE 3.9, 3.10B)**, which then gradually increased to an equal level as induced by EαGFP treatment at 24hours ($P>0.05$). At later time points, Alum significantly enhanced antigen presentation at 48hours ($P<0.001$) which was sustained up to 72hours ($P<0.001$). Similar trends were observed while analysing the data on the basis of MFI of the YAe **(Results Not Shown)**.

The data were also analysed on the basis of cells positive for both GFP and YAe **(FIGURE 3.9, 3.10C)**. In contrast to EαGFP-treated cells which have no GFP+YAe+ cells within 24hours, EαGFP adsorbed to Alum-treated cells have about

6% GFP+YAe+ cells by 72hours. This suggests two possibilities: firstly it takes a long time (more than 72hours) to completely break down the high volumes of antigen taken up by the APCs following Alum treatment or secondly, it takes a long time to completely break down the antigens because Alum may slow down antigen processing. In the same way, in contrast to EαGFP-treated cells which have undetectable levels of GFP within 24hours, the EαGFP adsorbed to Alum-treated cells have about 16% of cells positive for intact antigen by 72hours. In summary, data from these pulse chase experiments suggest that Alum decreases the rate of antigen degradation resulting in prolonged antigen presentation by BMDCs.

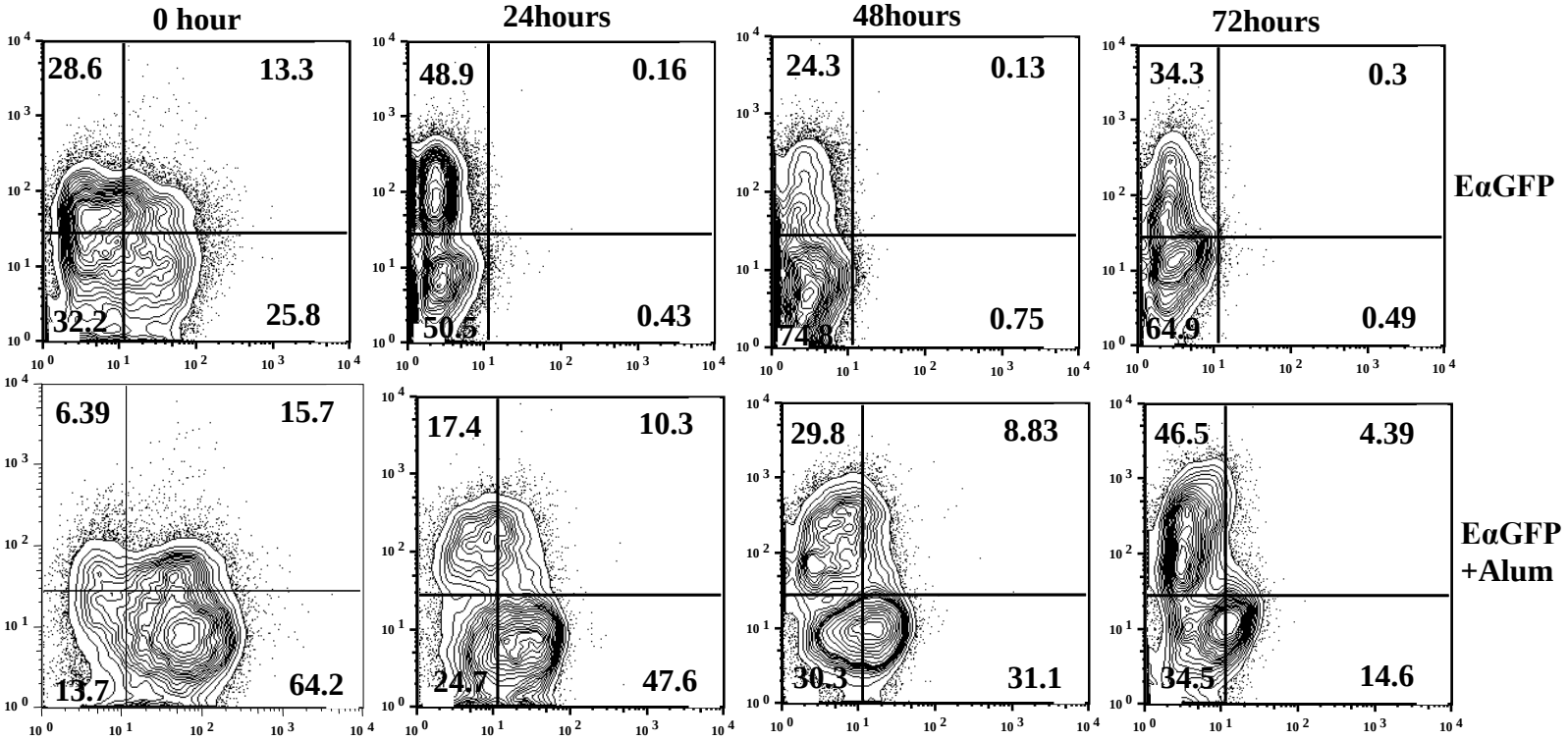

FIGURE 3.9: Alum increased antigen uptake, reduced degradation and eventually sustained the antigen presenting efficiency of DCs *in vitro*.

BMDCs ($3x10^6$/5mL) obtained from C57BL/6 mice were pulsed with EαGFP (100µg/mL) or EαGFP adsorbed to Alum (100.0µg/mL) for 1hour. They were washed in histopaque and incubated for different chase periods (0, 24, 48, 72hours). Cells were stained with anti-CD11c and YAe antibody and analysed by flow cytometry. CD11c+ cells were gated on the basis of isotype control and then from these populations GFP+and or YAe+ populations were analysed.

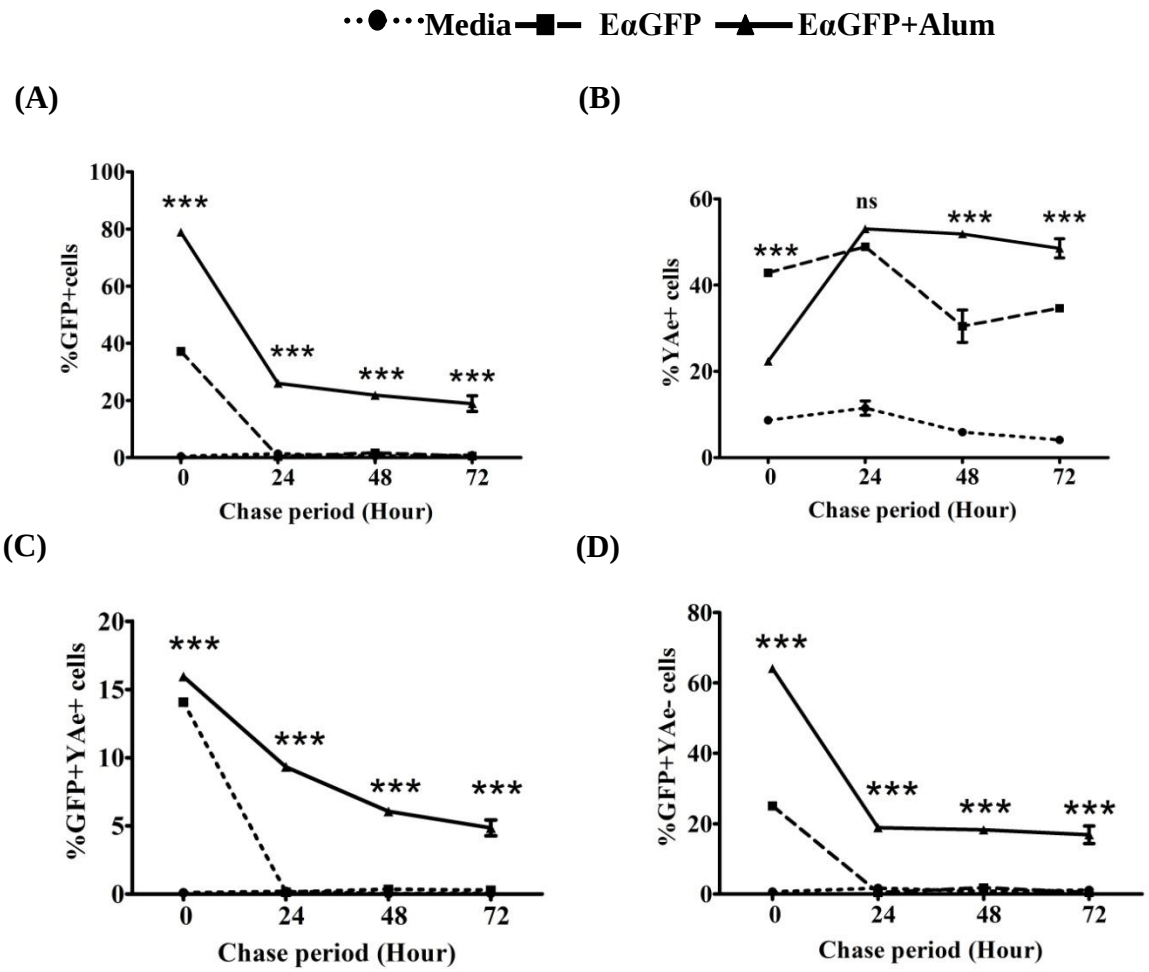

FIGURE 3.10: Alum adjuvants increase antigen uptake, reduce degradation and eventually sustain antigen presenting efficiency of DCs *in vitro*.

Data obtained in **FIGURE 3.9** were expressed as line graphs. The line graphs show the proportion of GFP positive cells **(A)** or the proportion of YAe positive cells **(B)** and proportion of cells positive for both GFP and YAe **(C)** or proportion of cells positive for GFP and negative for YAe **(D)**. Bonferronni post tests (Two Way ANOVA) were used to evaluate the probabilities by comparing the mean±S.E.M. (n=4) between EαGFP- or EαGFP+Alum-treated groups at specific chase periods. ***:P<0.001, ns=not significant.

3.6 Role of Alum in MHC class II expression

In the above experiment, the positive impact of Alum on antigen uptake and presentation was observed. While Alum may act to make processed peptides available for longer, presumably to mediate increased antigen presentation would require increased cell surface MHCII expression. Therefore, levels of MHC class II expression on BMDCs were analysed by incubation with different concentrations of Alum (**FIGURE 3.11)**. Notably, following Alum treatment an increase in MHC class II expression was observed, although these values were lower than in the cells treated with LPS **(FIGURE 3.11B)**. The expression of MHC class II molecules was dependent on the dose of Alum used, with both the highest proportion of the cells positive for MHC class II molecules and the highest expression of MHC class II molecules in the cells treated with 100µg/mL of Alum. BMDCs treated with 1000µg/mL had lower MHC class II expression than the cells treated with 100µg/mL Alum, but higher than other doses used in the experiment indicating Alum at high doses sustains MHC class II expression on the surface of DCs. A similar dose response was seen for YAe expression in the previous experiment (**FIGURE 3.6B)**, suggesting a link between increased antigen presentation and increased availability of MHC class II molecules following Alum treatment *in vitro*.

(A)

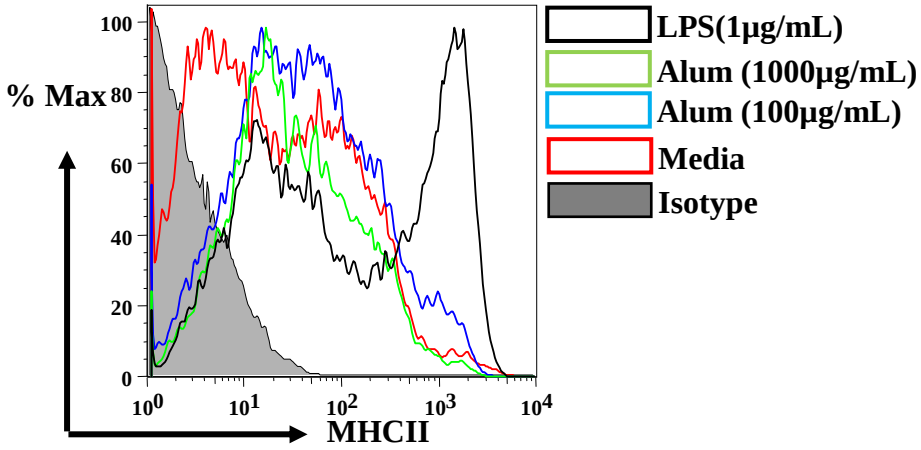

(B)

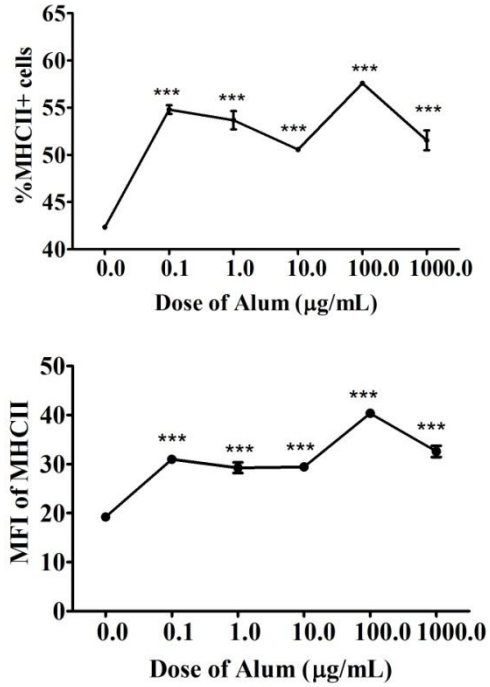

FIGURE 3.11: Alum increases levels of MHC class II molecules in dose-dependent manner *in vitro*.

BMDCs ($2x10^6$/5mL) obtained from C57BL/6 mice were incubated with media, or with different doses of Alum (0.1, 1.0, 10.0, 100.0, 1000.0µg/mL) and LPS (not shown) for 24hours. Cells were stained with anti-CD11c, anti-mouse MHC Class II antibody and analysed by flow cytometry. **(A)** Overlay histograms showing % maximum of cells positive for MHCII at different doses of Alum. **(B)** The line graph shows the proportion of MHC class II positive cells (upper) and MFI of MHC class II molecules (lower) at different doses of Alum. Tukey post-tests (One Way ANOVA) was used to compare the mean±S.E.M. (n=3) between untreated (incubated in media) and cells treated with various concentrations of Alum. ***, $P<0.0001$.

3.7 Requirement for Actin polymerisation in Alum-mediated antigen internalisation by BMDCs

In the previous experiments, an inductive effect of Alum on antigen internalisation by BMDCs was observed. This could be due to a quantitative effect of Alum on EαGFP uptake or Alum inducing a fundamentally different mechanism of EαGFP internalisation. It has been previously demonstrated that BMDCs take up soluble antigens via macropinocytosis and particulate antigens via phagocytosis [191]. The routes and mechanisms of antigen internalisation by APCs are known to influence the efficiency of antigen processing and presentation of antigens [419]**.**

Therefore, in this experiment, Cytochalasin D was used. This drug inhibits actin subunit addition to the fast-growing or 'barbed' end of actin filaments resulting from the breakage of actin [420] and inhibits the rate of Filamentous (F)-actin polymerisation [421-423]. This drug therefore blocks actin-dependent endocytosis such as phagocytosis and macropinocytosis resulting in reduced antigen uptake and presentation [196,414]. In addition, it has also been shown to block antigen uptake via caveolae [424].

Firstly, trypan blue was used to determine the viability of cells following Cytochalasin D treatment. Cytochalasin D at 10µg/mL caused not more than 5% cell death of total cells, whereas a concentration of 20–30µg/mL resulted in the death of 30–60% of total cells. Therefore, 10µg/mL trypan blue was used as a standard concentration of this drug as an inhibitor of antigen internalisation without affecting death of DCs. Secondly; this drug was used to investigate the effects on antigen internalisation. Blocking actin polymerisation using Cytochalasin D significantly reduced antigen internalisation by BMDC **(FIGURE 3.12A,B)**. An approximately a 7-fold decrease in MFI of GFP ($P<0.001$) and a 2-fold decrease in the proportion of GFP-accumulating cells ($P<0.001$) at 10µg/mL Cytochalasin D concentration was clearly observed. In this study, following Cytochalasin D treatment, there was 16% reduction in the level of antigen accumulation in DCs incubated in soluble antigen. By contrast, there was an 86% reduction in the level of antigen accumulation in DCs incubated in antigens adsorbed to Alum indicating a greater inhibitory effect of

Cytochalasin D on Alum-treated DCs. The data also suggest that Alum induces BMDCs to take up the majority of antigens via actin-dependent pathway; however, Alum induces BMDCs to internalise some amounts of antigen (about 14%) via other unknown pathways *in vitro*. In addition, the reduction in soluble antigen internalisation following Cytochalasin D suggests that macropinocytosis is also an actin-dependent fluid uptake mechanism [425] that can be inhibited by Cytochalasin D treatment [426].

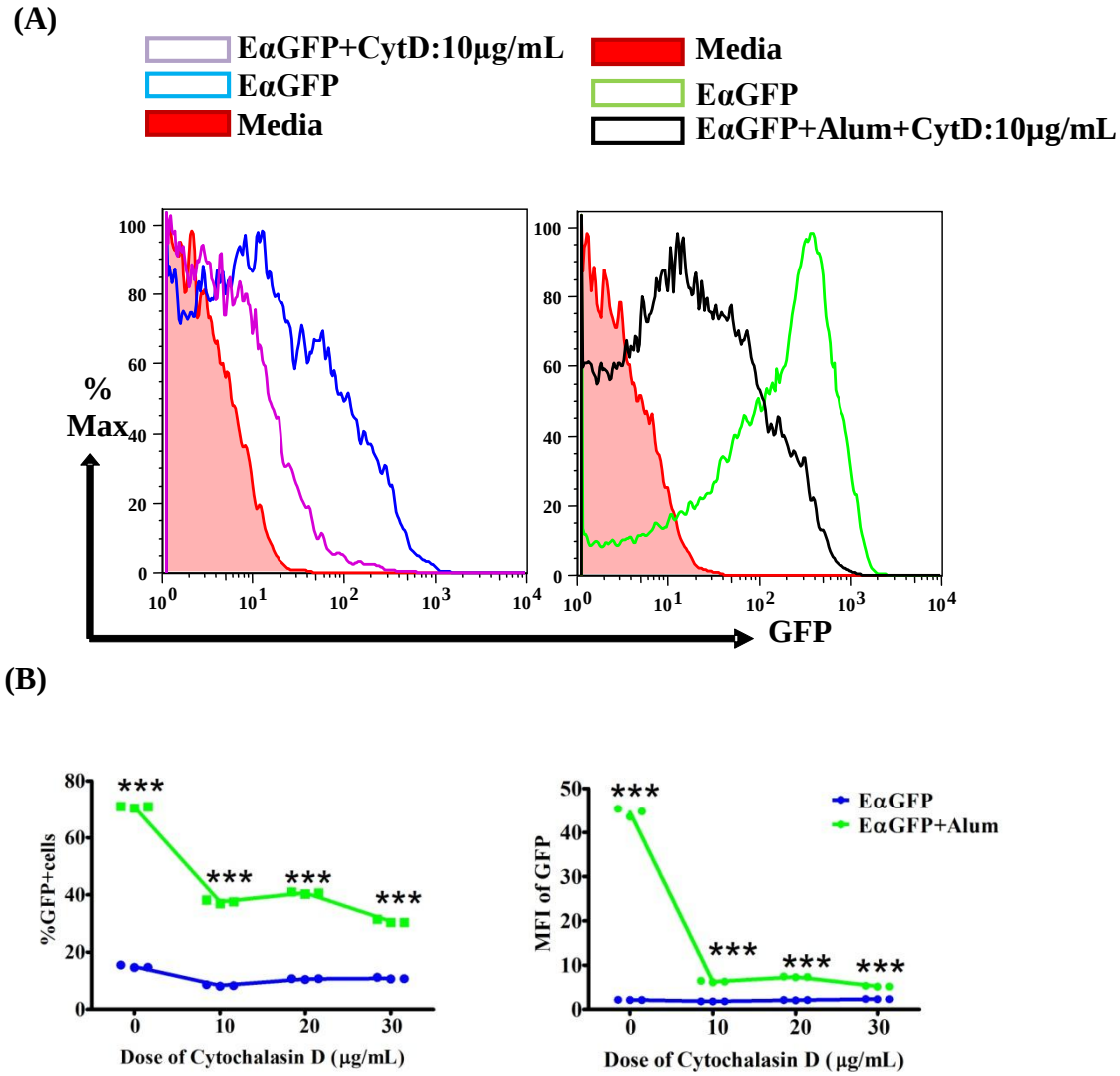

FIGURE 3.12: Alum induces BMDCs to take up majority of antigens via actin-dependent manner *in vitro*.

BMDCs ($2x10^6$/5mL) obtained from C57BL/6 mice were pre-treated with Cytochalasin D (0, 10, 20, 30µg/mL) for 2hours. Then, they were incubated in media, EαGFP (100µg/mL) or EαGFP adsorbed to Alum (100.0µg/mL) for 2hours. Cells were stained with anti-CD11c antibody and analysed by flow cytometry. **(A)** Overlay histograms showing the % maximum of cells positive for GFP in different treatment groups. **(B)** The line graphs were made by the scatter dot plots and joining the mean values. They show the % of GFP+ cells (left) or the MFI of GFP (right) at different Cytochalasin D doses in different treatment groups. Bonferroni post tests (Two Way ANOVA) were used to compare the mean±S.E.M. (n=3) of EαGFP-treated samples and EαGFP+Alum-treated samples at specific concentration. ***, P<0.001.

3.8 Impact of Na^+/H^+ on Alum-mediated antigen internalisation by BMDCs

To investigate the role of macropinocytosis in antigen internalisation in the presence and absence of Alum and EIPA was used [416,417,427]. These agents inhibit Na^+/H^+ channels enhancing acidification in the immediate vicinity of lamellipodia, blocking the cytoskeleton rearrangements required for macropinocytosis [417,428,429]. In contrast to phagocytosis, which requires the engagement of specific receptors, macropinocytosis is constitutive and allows immature DCs to take up large amounts of soluble antigens rapidly and non-specifically [430].

Using a trypan blue exclusion assay, the effects of different concentrations of EIPA were tested on the viability of cells. At a concentration of 25µM, about 5% cells died, but from 50–75µM, cell death ranged from 40–80% of total cells. Therefore, I took 25µM as a standard EIPA concentration in this experiment. Addition of EIPA at a 25µM concentration reduced both GFP positive cells (55% reduction) as well as MFI of GFP accumulation (29.5% reduction) by cells incubated in soluble antigens **(FIGURE 3.13)**. By contrast, addition of this inhibitor at each dose reduced the very low proportion of cells (6% reduction) with highly reduced the GFP accumulation (=38% reduction in MFI) following incubation in soluble antigens adsorbed to Alum. The data indicate that EIPA has little effect on GFP accumulation without any impact on the proportion of cells incubated in Alum compared with cells incubated in soluble antigens. The data suggest that Alum has a minor impact on antigen accumulating efficiency of DCs via macropinocytosis depending on Na^+/H^+ channels. By contrast, Alum induces the majority of antigen accumulation in a Na^+/H^+-independent manner or macropinocytosis-independent manner by BMDCs.

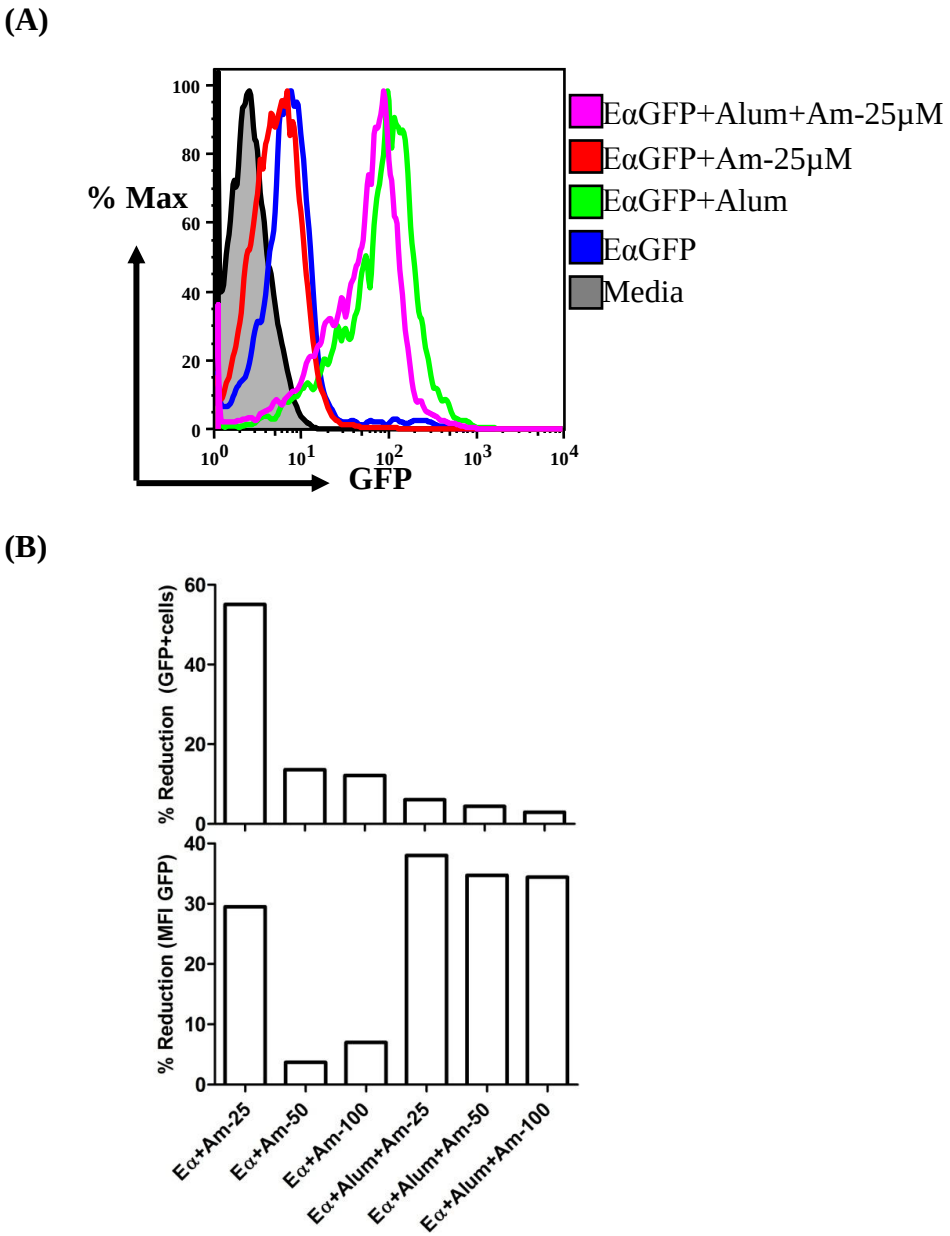

FIGURE 3.13: Alum induces BMDCs to take up small amounts of antigens via Na+/H+-dependent manner *in vitro*.

BMDCs ($2x10^6$/5mL) obtained from C57BL/6 mice were pre-treated with EIPA (25, 50, 100μM) for 2hours. Then, they were incubated in media, EαGFP (100μg/mL) or EαGFP adsorbed to Alum (100.0μg/mL) for 2hours. Cells were stained with anti-CD11cPE antibody and analysed by flow cytometry. (A) Overlay histograms showing the % maximum of cells positive for GFP in different treatment groups. (B) The bar graphs showing the reduction in % of GFP+ cells (upper) or the reduction in MFI of GFP (lower) in different treatment groups (n=1). Eα-EαGFP, Am-25, Am-50, Am-100 means concentrations of Amiloride in μM.

3.9 Role of pre-adsorption of antigen in Alum-mediated antigen presentation

From the previous studies, the positive impact of Alum on uptake of antigen by DCs was observed, the phenomenon of which predominantly occurs through an actin-dependent manner *in vitro*. The most likely explanation for this effect is that Alum adsorbed antigen is internalised more efficiently because it is particulate, which would be critically dependent on physical association between antigen and adjuvant. Therefore, an attempt was made to find out whether adsorption of antigen to Alum is necessary for enhanced antigen uptake and presentation by DCs. The role of Alum adsorption in antibody titers has been previously studied by using different types of antigens that are non-adsorbed to Aluminium compounds [431]. Their experiments highlighted that pre-adsorption is not necessary in the production of antibody titers *in vivo* [431]. However, the role of preadsorption of proteins in antigen presentation has not been elucidated, therefore, the pulse chase technique described above was used to examine the role of Alum/antigen association in the mechanisms of antigen presentation.

To analyse this, DCs were incubated with EαGFP or Alum for 1hour, washed and incubated with Alum or EαGFP respectively for 1hour, and washed and chased for 96hours. Positive controls were made by pulsing DCs with EαGFP or EαGFP adsorbed to Alum for 1hour **(FIGURE 3.14)**.

Surprisingly, the data clearly indicates that preadsorption of antigen to Alum is not required to enhance the antigen presenting efficiency of DCs **(FIGURE 3.14, 3.15)**. When cells were treated sequentially with Alum or EαGFP, levels of antigen presentation were at least equivalent to those observed with Alum adsorbed EαGFP, and these levels were significantly greater ($P<0.0001$) than seen with soluble antigen. Interestingly, the sequence of antigen/adjuvant exposure did not affect this response **(FIGURE 3.15)**.

Similarly, compared with soluble antigen-pulsed DCs, the percentage of GFP+YAe+ cells was a 7-fold higher in Alum-pulsed DCs ($P<0.0001$), a 2-fold

higher in soluble antigen-pulsed DCs followed by Alum-pulsed DCs ($P<0.0001$) and a 4-fold higher in Alum-pulsed DCs followed by soluble antigen-pulsed DCs ($P<0.005$) **(FIGURE 3.15)**. The data also suggest that there are still some unprocessed antigens in the cells treated with Alum-nonadsorbed group indicating the possibility of increasing more presentation in time-dependent manner.

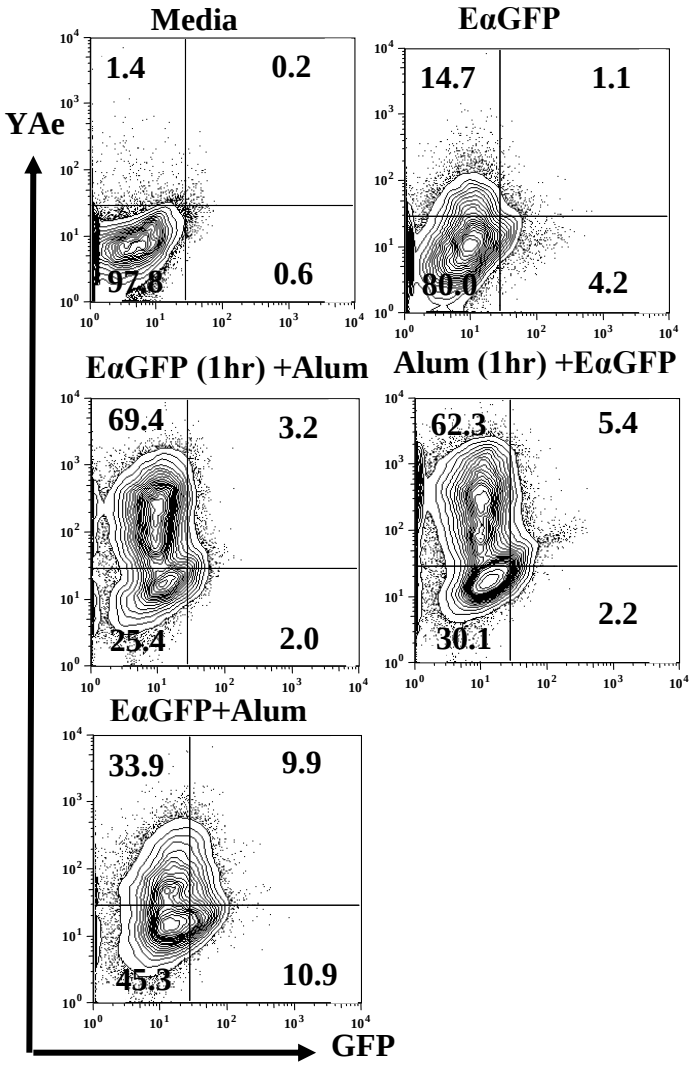

FIGURE 3.14: Pre-adsorption of antigen in Alum is not necessary to enhance the antigen presentation by DCs *in vitro*.

BMDCs ($3x10^6$/5mL) obtained from C57BL/6 mice were pulsed with EαGFP (100µg/mL) followed by pulse with Alum (100.0µg/mL) or EαGFP (100.0µg/mL) followed by Alum (100.0µg/mL) for 1hour and then incubated for 96hours. Positive controls were made by stimulating DCs with EαGFP (100.0µg/mL) or EαGFP adsorbed to Alum (100.0µg/mL) for 1hour, followed by 96hours incubation. Then, DCs were stained with anti-CD11c and YAe antibody and analysed by flow cytometry. The histograms show the proportion of GFP and or YAe positive cells in CD11c+ populations.

(A)

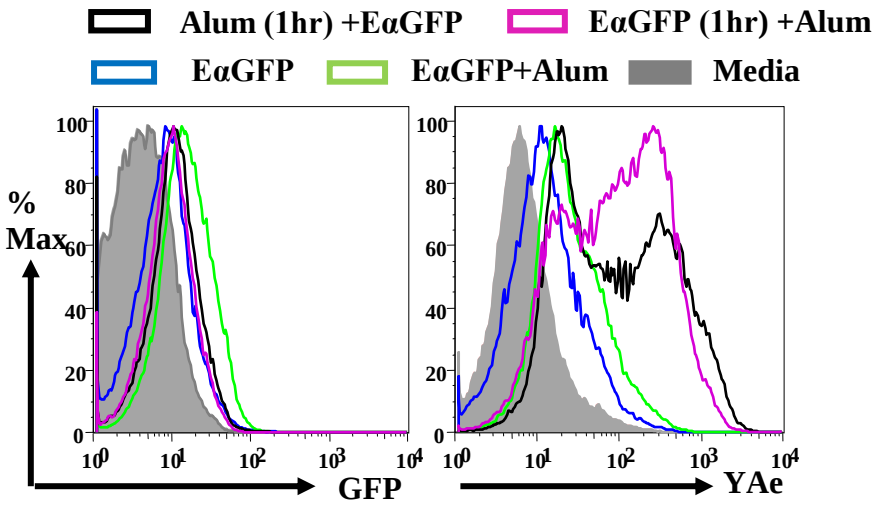

(B)

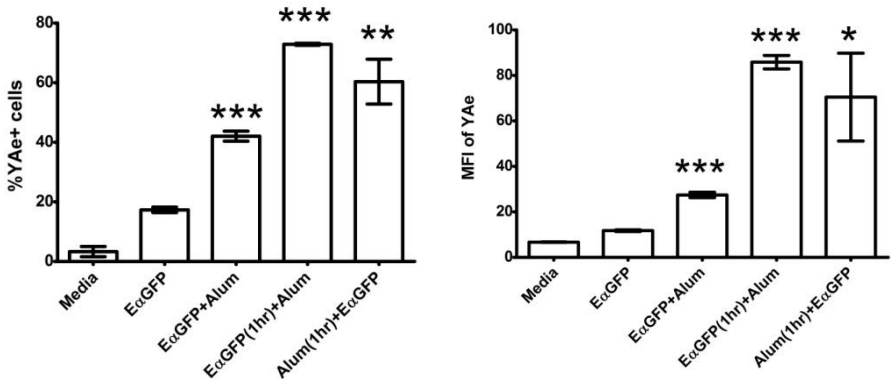

FIGURE 3.15: Pre-adsorption of antigen in Alum is not necessary to enhance the antigen presenting efficiency of DCs *in vitro*.

The data obtained in **FIGURE 3.14** were expressed in overlay histograms **(A)** and bar charts **(B)**. **(A)** Overlay histograms showing the % of GFP (left) and % of YAe (right) populations within CD11c populations in different treatment groups. **(B)** The bar charts show the MFI and % of CD11c populations positive for YAe in different treatment groups (n=3). To compute the probability values, the two-tailed‘t’ Test was used by comparing the mean±S.E.M. between EαGFP-treated group and other treatment groups. ***: P<0.0001, **:P<0.001, *P<0.01.

3.10 Analysis of antigen presentation using a T cell hybridoma

In the previous experiments, an enhancing role of Alum was observed on antigen uptake and presentation by DCs. To confirm these findings, a T cell hybridoma reporter system was employed to address the issue of antigen presentation *in vitro*. In this assay, the DO11.GFP hybridoma that recognises the OVA peptide (aa 323–339) in the context of I-A^d was used. Antigen recognition was finally reported by NFAT-driven, GFP expression [418].

3.10.1 DO11.GFP hybridoma in antigen presentation assay

To determine the suitability of the DO11.GFP hybridoma to investigate the impact of Alum on antigen presentation, BMDCs were first treated with OVA, Alum-adsorbed OVA or in the presence of media followed by co-culture with the hybridoma for 24hours. Antigen-specific T cells were identified by CD4 and the clonotypic antibody, KJ1.26, and the level of GFP expression analysed **(FIGURE 3.16)**. Incubation of the DO11.GFP hybridoma with OVA treated BMDC resulted in GFP expression which increased following co-culture with Alum/OVA-treated DCs ($P<0.01$). The results suggest that DO11.GFP hybdridoma are appropriate for the *in vitro* study of antigen presentation by DCs following Alum treatment.

The enhanced activation of the hybridoma confirms that Alum impacts on antigen presentation as described previously using the YAe assay. The studies above also suggested that Alum may impact on both the processing of antigens as well as the expression of MHC class II molecules. Therefore the OVApeptide323–339 was used to investigate the role of Alum in antigen presentation independently of processing. This peptide can directly bind MHC class II molecules internally and on the surface of BMDC as it does not require further processing [432]. Remarkably, the data demonstrate that Alum adjuvants can efficiently enhance presentation of peptide antigens ($P<0.0001$) **(FIGURE 3.17)**. This suggests that Alum can enhance antigen presentation with or without requirement for processing of antigens. In the latter

case, increasing surface expression of MHC class II molecules by Alum may be the default mechanisms of enhanced antigen presentation *in vitro*.

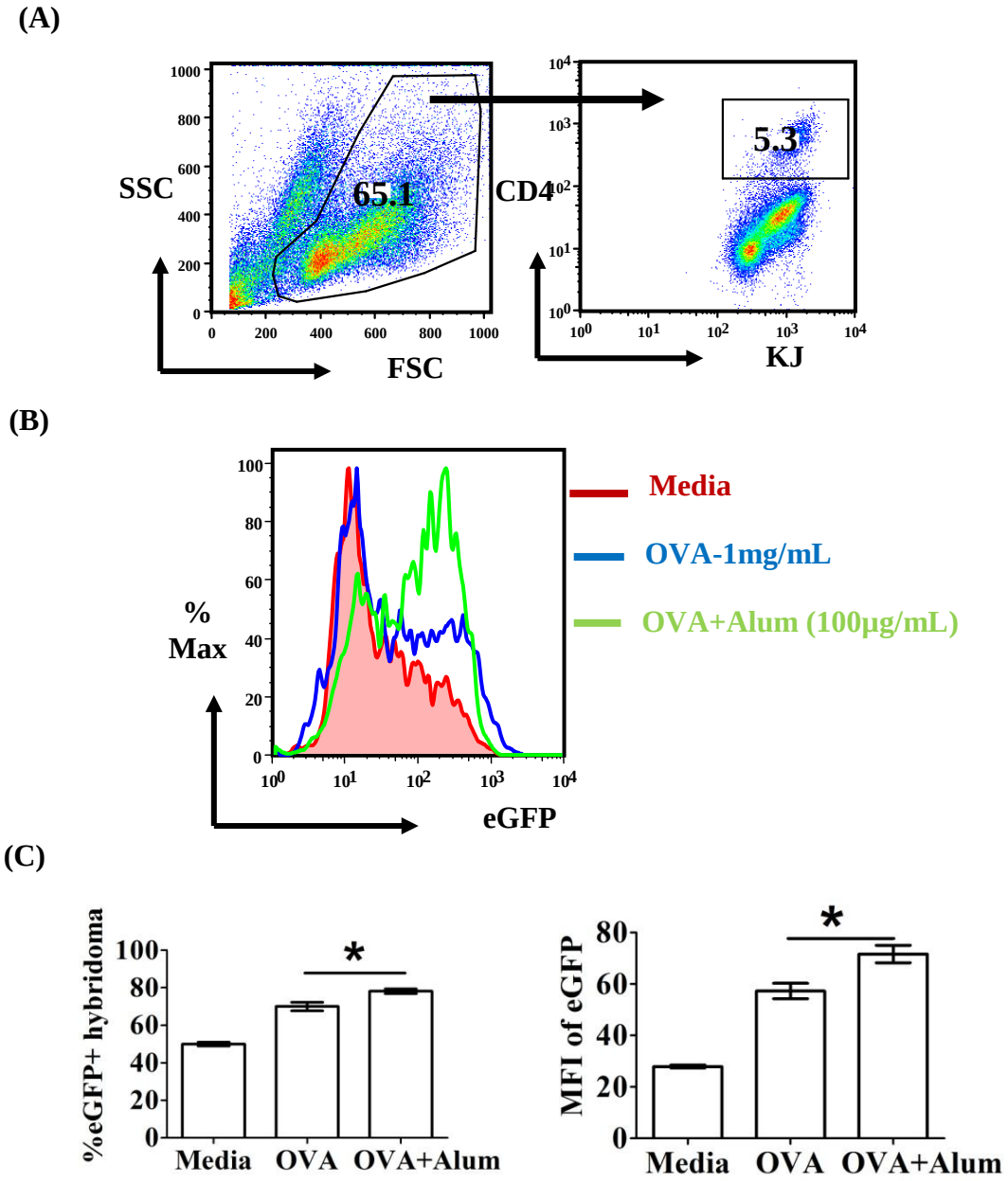

FIGURE 3.16: Detecting antigen presentation using the DO11.GFP hybridoma.

DCs (1x10^6/mL) obtained from BALB/c were treated with OVA (1mg/mL) or OVA adsorbed to Alum (100µg/mL) and incubated with hybridoma (1x10^6/mL) overnight. Hybridoma were stained with anti-CD4 and KJ1.26 antibody and analysed by flow cytometry. **(A)** Forward and side scatter characteristics of DO11.GFP (left) and characteristics of dot plots of hybridoma (CD4+KJ+) (right). **(B)** Overlay histograms showing % of maximum of eGFP expressing cell line incubated in different groups. **(C)** The bar graphs showing proportion of eGFP-expressing hybridoma (left) and MFI of eGFP (right) in different treatment groups. *:P<0.05 after comparing mean±S.E.M. (n=3–6) between OVA- and OVA+Alum-treated groups by unpaired 't' test.

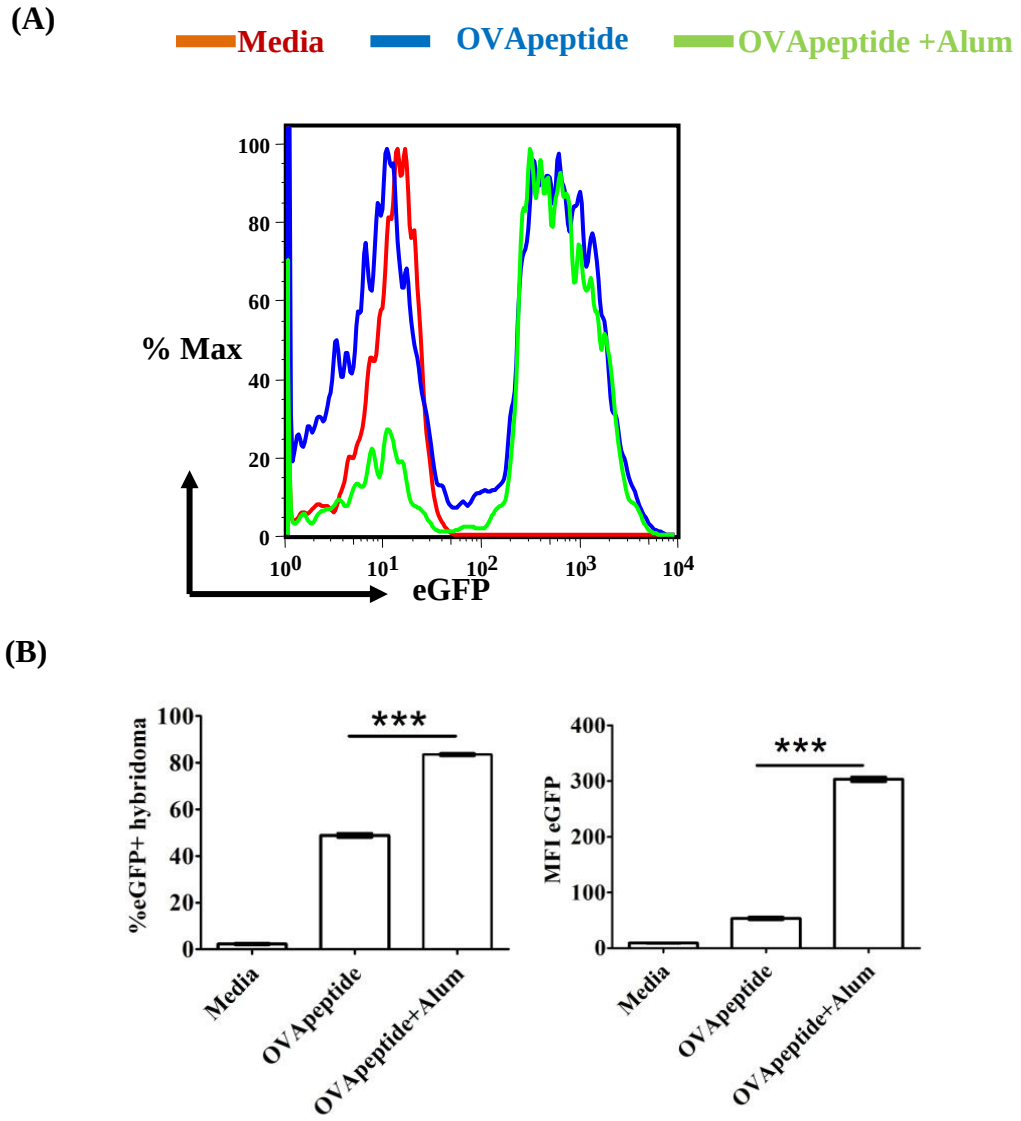

FIGURE 3.17: Detecting antigen presentation using the DO11.GFP hybridoma.

DCs ($1x10^6$/mL) obtained from BALB/c were treated with OVApeptide323–339 (1µg/mL) or OVApeptide323–339 adsorbed to Alum (100µg/mL) and incubated with hybridoma ($1x10^6$/mL) overnight. Hybridoma were stained with anti-CD4 and KJ1.26 and analysed by flow cytometry. **(A)** Overlay histograms showing % of maximum of eGFP expressing cell line incubated in different groups. **(B)** The bar graphs showing proportion of eGFP+ve hybridoma (left) and MFI of eGFP in different treatment groups. ***:P<0.0001 after comparing mean±S.E.M. (n=3) between OVApeptide- and OVApeptide+Alum- groups by Tukey post test.

3.11 Discussion

In this chapter, the enhancing role of Alum in antigen uptake and presentation by BMDCs has been elucidated. The previously described EαGFP/YAe system [183,407] was applied to directly track antigen internalisation, degradation and presentation in BMDCs and the impact that Alum adjuvants have on the magnitude and kinetics of these processes. The fluorescent protein moiety in the chimaeric EαGFP antigen allowed tracking of antigen uptake and degradation. This approach confirmed previous *in vitro* studies demonstrating the ability of Alum to enhance internalisation of antigens by APCs [194,381].

In the current experiment, antigen internalisation by DCs started within 15minutes with its sustained accumulation till 96hours indicating Alum increases the rate and magnitude of antigen internalisation by DCs *in vitro*. The data confirm that Alum acts a delivery vehicle enhancing the the magnitude and duration of antigen accumulation by the cells. It has been observed that even a low dose of Alum such as 100ng/mL is sufficient for the enhancement of antigen presentation by DCs, with higher doses of Alum further increasing this response *in vitro*.

In this study, Alum-mediated internalisation of antigen was highly dependent on actin polymerisation; in contrast to previous studies [53], addition of Cytochalasin D significantly reduced antigen uptake. This drug hampers actin-dependent endocytosis such as phagocytosis, macropinocytosis and caveolae-mediated endocytosis [414,415,424]. Therefore, it may be possible that antigens are predominantly engulfed in F-actin-dependent manner, although other several routes of entry may contribute to Alum-mediated antigen internalisation. In this context, DCs were pretreated with EIPA that reduces Na^+/H^+-dependent macropinocytosis. Interestingly, following EαGFP adsorbed to Alum treatment, this drug had a minor impact on antigen accumulating efficiency of DCs indicating most of the antigens are taken up by DCs in Na^+/H^+-exchange-independent manner, most probably via phagocytosis.

The increased antigen internalisation may be the outcome of several factors such as the size of antigens [194,195,433]. This is because antigens of smaller sizes such as antigens that elute from the adjuvant surface are usually pinocytosed. In contrast, antigens of large sizes such as antigens adsorbed to adjuvants are phagocytosed [194]. Interestingly, the shorter proteins or peptides are known to adsorb to Alum (Aluminium hydroxide) by electrostatic interactions between proteins and the positively charged Aluminium hydroxide resulting in the modification of soluble antigens into particulate form [60]. These particulate forms, similar to liposomes and microparticles, have large surfaces with charged, hydrophobic and receptor-interacting properties [434]. Therefore, compared with soluble antigens, particulates efficiently interact with APCs resulting in enhanced phagocytosis as observed in the current experiment. As well as going through the internalisation process, the soluble antigens may be trapped inside the irregular aggregates of large sized (1–10μm) Aluminium hydroxide particles formed by fibrous primary particles [49,57,58,431]. These primary particles in the aggregates are loosely associated and are readily broken [194] with the subsequent release of antigens in tissue culture media. As release of antigens in media is a time-dependent phenomenon, initial antigen uptake may consist of trapped antigens in Alum particles via phagocytosis. Subsequently, low amounts of soluble protein released from Alum may be taken up by DCs via macropinocytosis [431]. More recently, Alum has been suggested to drive a process called ‘abortive phagocytosis’ [53]. In this situation, Alum causes lipid-sorting in the DC plasma membrane which facilitates soluble antigen entry into DCs. In this event, the Alum crystal is not internalised by the DC [53]. However in the same study Alum particles were identified inside DCs [53] indicating that DCs are efficient in phagocytic uptake of particulates similar to the present study.

By using the EαGFP/YAe system, it was possible to demonstrate that Alum has a significant impact on the rate of degradation of antigen within DCs. While the GFP signal was completely extinguished within 24hours of administration of soluble antigen, formulation in Alum allowed intact antigen to persist for up to 72hours. Degradation of antigens by lysosomal proteases is an essential step in liberating

peptide antigens from proteins, and agents that interfere with this process, such as protease inhibitors or inhibitors of lysosomal acidificaiton have been shown to reduce antigen presentation [207,435]. This would suggest that slowing of antigen degradation by Alum may result in poorer peptide loading and antigen presentation on MHC class II molecules. However, by virtue of the ability of the YAe antibody to directly recognise Eα:MHCII complexes, it was possible to show that Alum actually enhances the magnitude and duration of antigen presentation by BMDC from less than 24hours observed with soluble antigen, to at least 72hours. In agreement with our data, previous work has demonstrated that limiting the susceptibility of antigens to lysosomal proteolysis actually acts to increase antigen presentation and immunogenicity [436]. In terms of adjuvant activity *in vivo*, slowing down antigen degradation and increasing antigen persistence makes physiological sense. It takes hours for peripheral DCs to migrate to DLNs where naïve cognate T cells are resident. Furthermore, functional interactions between DCs and T cells are thought to occur over the following 48hours or more [183] and blockade or interruption of this interaction is known to block the development of effective T cell responses [437,438]. The reduction in the rate of antigen degradation as observed could therefore lead to a temporal increase in availability of peptide for binding to MHCII in peptide loading compartments resulting in increased duration and magnitude of antigen presentation, as it was also observed. However, it remains unclear at this point, exactly how this mechanism works.

In the current study, it was also demonstrated that exposure to Alum/EαGFP induces increased cell surface MHCII expression on BMDC. Similarly, previous studies have shown the high expression of MHCII molecules following Alum treatment in human PBMCs *in vitro* [337,339,439]. Interestingly, in the current study the dose response of Alum induced MHCII expression was similar to that observed when detecting Eα:MHCII complexes using the YAe antibody. Previous studies have demonstrated that inhibition of lysosomal proteases enhances the stability of p:MHCII complexes and lead to increased accumulation MHCII complexes on the DC surface [440]. Therefore, if Alum was to block lysosomal proteolysis, as suggested by the antigen persistence described above, this would

explain the increased cell surface MHCII expression, although further studies would be required to validate this hypothesis.

The positive impact of Alum on antigen presentation by DCs by using DO11.GFP hybridoma has also been elucidated. By using this hybridoma, it was possible to show an enhancing role of presentation of protein antigens by DCs as measured by costimulator-independent CD4 T cell activation. Thus, as well as YAe system, DO11.GFP hybridoma system suggested that Alum enhances antigen presentation. When the OVApeptide323–339 was used in the experiment, there was significantly enhanced antigen presentation by hybridoma indicating that Alum can enhance antigen presentation with or without requirement for processing of antigens *in vitro* [432]. In the context of enhanced antigen presentation without effect on processing, increasing surface expression of MHC class II molecules by Alum may be the default mechanisms of enhanced antigen presentation *in vitro*. The hybridoma experiment here suggests that Alum can affect loading of peptides that does not require further processing. Interestingly, these events may take place on the plasma membrane of BMDC [441]. In addition, it can affect processing of peptide antigens derived from proteins and loading of these antigens on MHCII molecules as described in the EαGFP/YAe assay. In summary, the current study shows that Alum might be a crucial adjuvant to enhance the efficacy of both protein and peptide based vaccines.

This is first report in which it has been found that preadsorption of antigens is not necessary to enhance antigen presenting efficiency of BMDC by Alum *in vitro*. The current study challenges the notion that antigen must be adsorbed to an Aluminium-containing adjuvant to enhance immune response [442]. This clearly supports the previous *in vivo* reports [431] in which the authors have found an enhanced antibody titer by non-adsorbed antigens formulated in Alum [431]. In another study by Flach and colleagues (2011) [53], they pretreated DCs with CsAl for 2 hours and transferred these DCs in mice. Subsequently they found similar amounts of serum IgG1 in mice immunised by these techniques and in mice immunised by standard *in vivo* protocols of subcutaneous injection of OVA and CsAl

indicating an initial effect of Alum on DC. Current studies were performed by changing the sequence of incubation of antigen and Alum with washing of DC in between; the sequence of incubation had no impact on antigen uptake or presentation either. They further suggest that Alum either directly affects the function of APC that allows increased uptake and presentation of antigen, for example by binding to the surface of DC and mediating effects there or through changing the DC phenotype. In the first case, the previous studies by Flach and colleagues, with Alum inducing abortive phagocytosis is particularly relevant [53]. However, their studies are based on scanning electron microscope (SEM) rather than transmission electron microscope (TEM) that could detect the presence of Aluminium inside cell. The phagocytosis of Alum particles has been clearly shown by Hornung and colleagues (2008) [328] who have even shown the rupture of phagosome probably due to overload. This proof also comes from the current study in which most of the antigens are phagocytosed in an actin-dependent manner as Cytochalasin D inhibition greatly inhibited antigen uptake by BMDC in the presence of Alum. In addition, it is difficult to imagine that this effect could occur when incubating DC with antigen followed by Alum. If a kinetic study coupled with EαGFP/YAe had been done, it would be easy to compare the magnitude and duration of internalisation, degradation and presentation of antigens by Alum. Even cellular studies on TEM would allow understanding the mechanisms of Alum engulfment. At least, from the current study, it can be summarised that Alum may also have direct effects on DC phenotype, for example increasing Class II MHC expression on the surface of antigen as shown here. Currently a limited range of effects of Alum on the phenotype of DC have been understood, therefore in the subsequent chapter the aim is to further characterise these effects.

CHAPTER-4: IMPACT OF ALUM ON THE ACTIVATION STATE OF BMDCs

4.1 Introduction

In the above experiments, the positive role of Alum in the induction of antigen uptake and antigen presentation was addressed. While these data suggest that Alum may play a crucial role in antigen-specific T cell activation, antigen presentation alone is not sufficient to induce T cell activation. This is because in the absence of costimulatory signals (signal 2), the encounter of TcR with p:MHCII complexes may lead to a state of tolerance called anergy [257,261,443]. Therefore, the activation or maturation state of DC characterised by expression of costimulatory molecules plays a determining role in the induction of T cell clonal expansion because only activated or mature DCs are able to perform this function [243]. Thus, costimulation is the key determining factor of whether a naive T cell becomes activated or becomes tolerised [261]. In addition to costimulatory molecules, activated or matured DCs are characterised by the capacity to produce cytokines, which also play a crucial role in T cell expansion [191]. Importantly, understanding which costimulatory molecules and cytokines are, or are not, affected by Alum will be helpful in rationally modifying Alum to improve its adjuvant potential in vaccine design. Therefore in this chapter, the impact of Alum was analysed on the expression of costimulatory molecules and the production of cytokines by DCs *in vitro*.

4.2 Impact of Alum on the expression of costimulatory molecules by DCs

As already described, DCs must express costimulatory ligands which bind costimulatory receptors expressed on T cells for effective T cell activation. Therefore, the impact of Alum on the expression of major costimulatory molecules by DCs was analysed. CD86 and CD80 are the primary costimulatory molecules that take part in T cell responses [444]. Both of these molecules share about 25% sequence homology and bind the same receptors, CD28 and CTLA-4 expressed on T cells [445]. Both of them provide the most important costimulatory signals to T cells [446] resulting in IL-2 production, T cell activation, T cell expansion and survival [447] and T cell-dependent B cell help for the class switching [448]. It has been suggested that CD86 and CD80 molecules can substitute for each other during antigen-specific CD4 T cell activation and expansion [449]. However, studies using CD80 and CD86 gene deficient mice have shown that these molecules do not have any overlapping functions [450]. Alternative costimulatory molecules include members of the TNFR superfamily such as CD40 [451] and OX-40L [452]. CD40 is particularly important in B cell activation [264]. However, stimulation via CD40 has also been shown to enhance the efficiency of DCs in expanding T cells [453] and in T cell survival [454]. In addition, CD40 triggering by Th cells has been shown to modulate efficiency of DCs in activating cytotoxic T cells [455,456]. OX-40L (CD252) has been shown to be an important target for adjuvant action because signalling via this molecule is necessary in priming T cells [457] as well as in generating sufficient additional signals to maintain a sustained primary CD4 T cell response [452]. This molecule provides an additional event in optimal clonal expansion during primary CD4 T cell response especially in the late phase response following initial interactions of B7-CD28, Intercellular Adhesion molecule (ICAM)-Lymphocyte Function-Associated Antigen (LFA) and CD40-CD40L [452].

In this section it has been addressed whether Alum adjuvant affects costimulatory molecule expression on DC. This is clearly a significant question that could facilitate the rational modification of this adjuvant; however previous studies have only partially addressed this issue.

4.2.1 Impact of Alum on CD86 costimulatory molecule expression by BMDCs

Across a range of doses, Alum induced an increase in CD86 molecule expression, although these values were lower than in the cells treated with LPS ($P<0.0001$) (**FIGURE 4.1A,B)**. The expression of CD86 molecules was dependent on the dose of Alum used, with both the highest proportion of the cells positive for CD86 molecules and the highest expression of CD86 molecules on the cells treated with 100.0µg/mL of Alum. BMDCs treated with 1000.0µg/mL had lower CD86 expression than the cells treated with 100.0µg/mL Alum, but higher than other doses used in the experiment. Similar results were obtained when analysing the proportion of BMDCs expressing CD86 molecules *in vitro* **(TABLE 4.1)**. While the data suggest that Alum can induce CD86 expression on BMDC and therefore may provide signal 2 during CD4 T cell activation, these levels were significantly lower than those induced using LPS ($P<0.0001$).

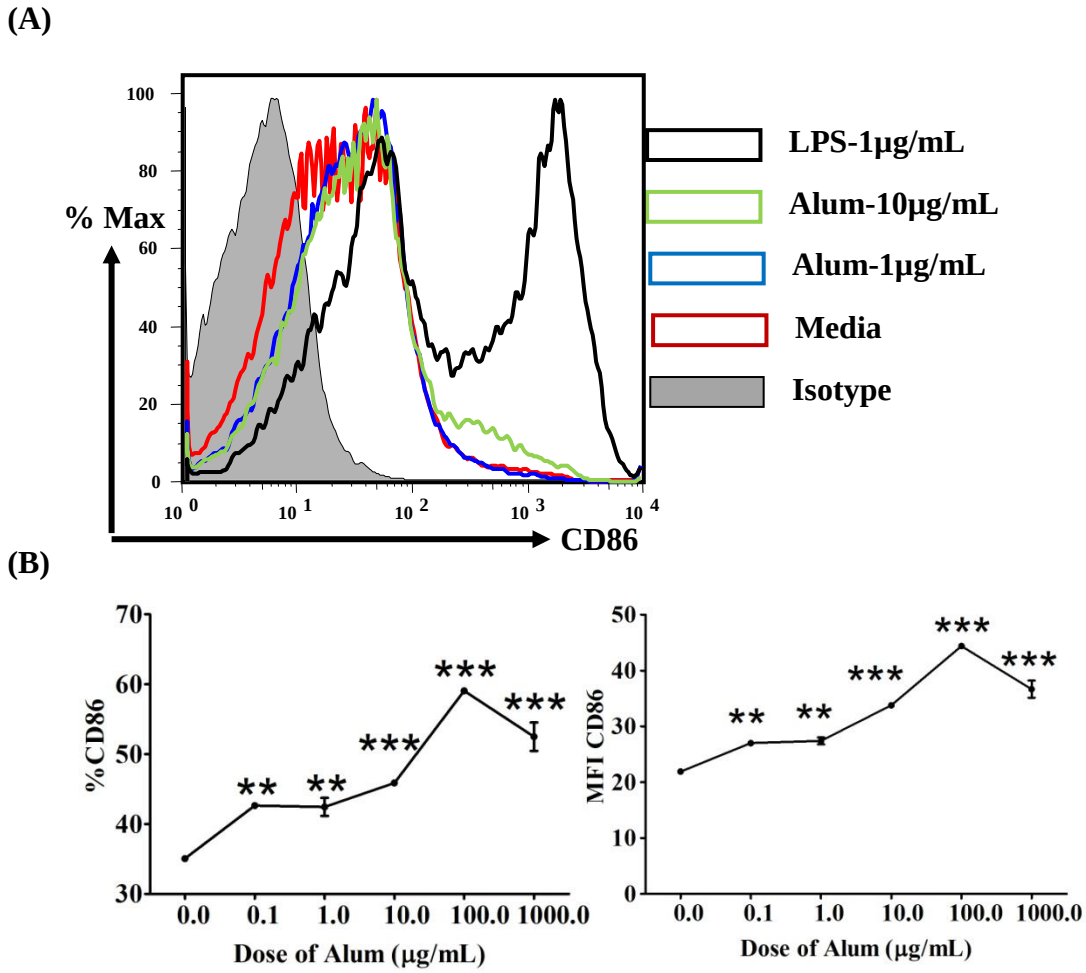

FIGURE 4.1: Alum increases the expression of CD86 molecules on the surface of DCs

BMDCs ($2x10^6$/5mL) obtained from C57BL/6 mice were incubated with 0.1, 1.0, 10.0, 100.0, 1000.0µg/mL Alum, LPS (1.0µg/mL) or media for 24hours. Cells were stained with anti-CD11c and anti-CD86 antibody and analysed by flow cytometry. (A) Overlay histograms showing the % of maximum of cells positive for CD86, within the CD11c+ population. (B) Line graphs showing the proportion of CD86 positive cells (left) and the MFI of CD86 (right) on CD11c+ DCs. Tukey Post Test was used to compare values (mean±S.E.M., n=3) between control (Alum; 0.0µg/mL) and increasing concentration of Alum. ***: P<0.0001, **: P<0.001.

4.2.2 Impact of Alum on CD80 costimulatory molecule expression by BMDCs

Alum induced an increase in the proportion of CD80 molecule-expressing BMDCs at low doses such as at 0.1µg/mL **(FIGURE 4.2A,B)** ($P<0.001$) and at 1.0µg/mL ($P<0.01$). Similar results were obtained when analysing the level of CD80 expression using MFI values. In contrast, at higher doses (100.0µg/mL) of Alum, the level of CD80 expression on BMDC was reduced ($P<0.001$) althought there was no significant effect on the proportion of cells expressing CD80 ($P>0.05$). The data indicate that low doses of Alum may be sufficient to enhance the expression of CD80 costimulatory molecules on BMDCs *in vitro*. However, even at these optimum doses, Alum was relatively poor at inducing CD80 expression on BMDC in comparison with LPS ($P<0.0001$) **(TABLE 4.1)**.

(A)

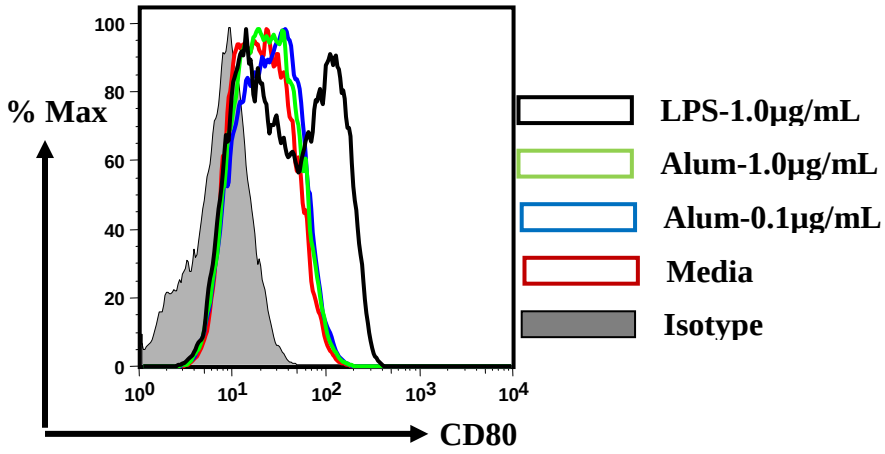

(B)

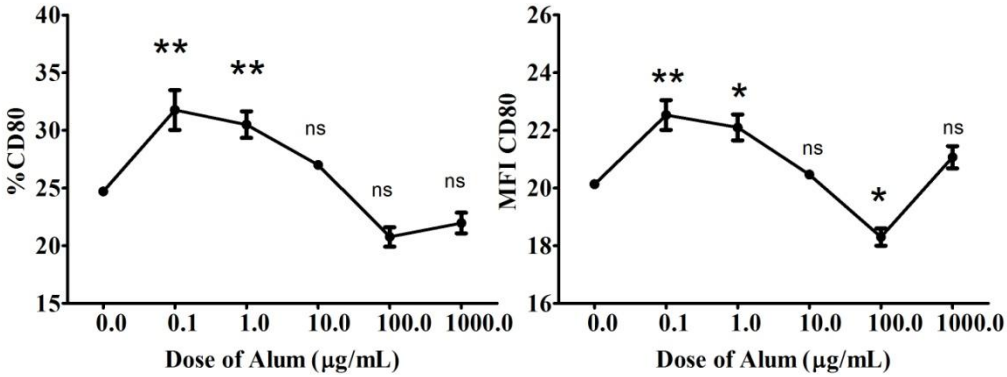

FIGURE 4.2: Low dose of Alum increases the expression of CD80 molecules on the surface of DCs.

BMDCs ($2x10^6$/5mL) obtained from C57BL/6 mice were incubated with 0.1, 1.0, 10.0, 100.0, 1000.0µg/mL Alum, LPS (1.0µg/mL) or media for 24hours. Cells were stained with anti-CD11c and anti-CD80 antibody and analysed by flow cytometry. (A) Overlay histograms showing the % of maximum of cells positive for CD80, within the CD11c+ population. (B) Line graphs showing the proportion of CD80 positive cells (left) and the MFI of CD80 (right) on CD11c+ DCs. Tukey Post Test was used to compare values (mean±S.E.M., n=3) between control (Alum; 0.0µg/mL) and increasing concentration of Alum. **: P<0.001, *: P<0.01, ns: not significant.

4.2.3 Impact of Alum on CD40 costimulatory molecule expression by BMDCs

The data show that the level of CD40 expression as well as proportion of CD40-expressing cells decreased significantly following treatment with Alum at low doses such as 0.1µg/mL ($P<0.001$), 1.0 µg/mL ($P<0.01$) and 10.0 µg/mL ($P<0.01$) **(FIGURE 4.3A,B)**. Higher doses of Alum (100.0 – 1000.0µg/mL), did not affect expression of these molecules. Overall, the data suggest that Alum has a broadly negative effect on CD40 expression by BMDC. In contrast, LPS induced a significant increase in both proportion of CD40 positive cells as well as MFI of these molecules ($P<0.0001$) **(TABLE 4.1)**.

(A)

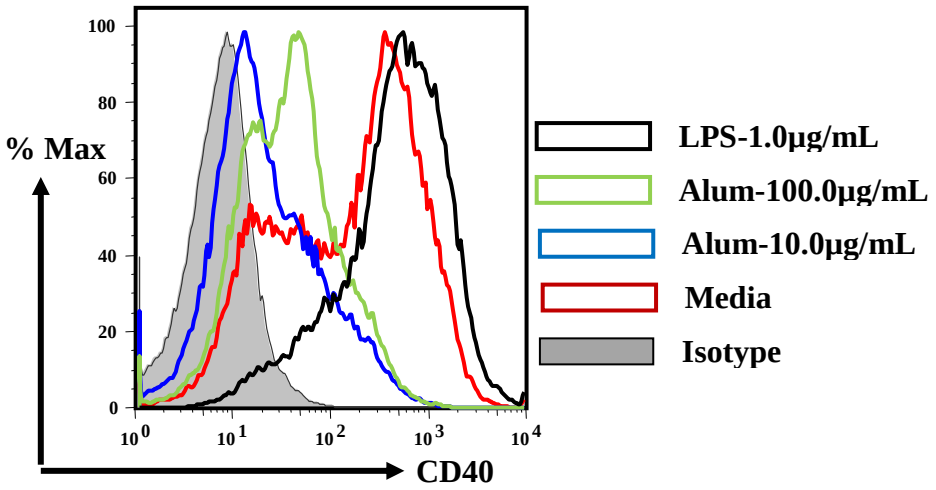

(B)

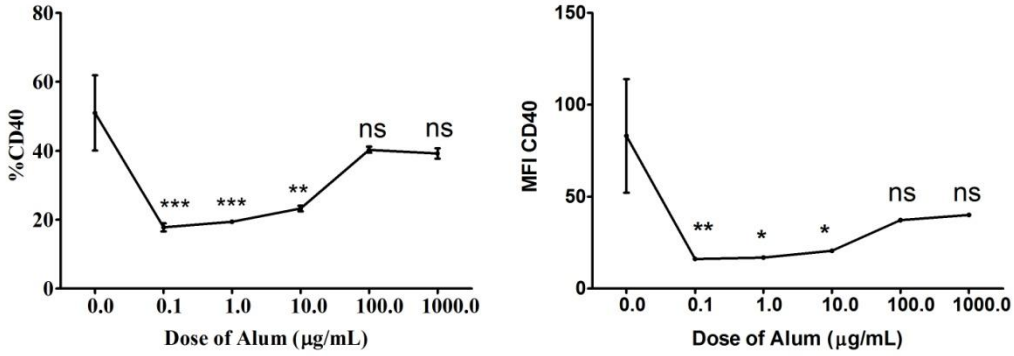

FIGURE 4.3: Alum has a broadly negative effect on CD40 expression by BMDC *in vitro*.

BMDCs ($2x10^6$/5mL) obtained from C57BL/6 mice were incubated with 0.1, 1.0, 10.0, 100.0, 1000.0µg/mL Alum, LPS (1.0µg/mL) or media for 24hours. Cells were stained with anti-CD11c and anti-CD40 antibody and analysed by flow cytometry. (A) Overlay histograms showing the % of maximum of cells positive for CD40, within the CD11c+ population. (B) Line graphs showing the proportion of CD40 positive cells (left) and the MFI of CD40 (right) on CD11c+ DCs. Tukey Post Test was used to compare values (mean±S.E.M., n=4) between control (Alum; 0.0µg/mL) and increasing concentration of Alum. ***: P<0.0001, **: P<0.001, *: P<0.01, ns: not significant.

4.2.4 Impact of Alum on OX-40L (CD252) costimulatory molecule expression by BMDCs

Interestingly, Alum had a biphasic effect on the expression levels of OX-40L by BMDCs, with low doses significantly decreasing expression (0.1µg/mL; $P<0.0001$, 1.0µg/mL; $P<0.0001$ and 10.0µg/mL; $P<0.001$) and higher doses significantly increasing expression (100.0 µg/mL; $P<0.0001$ and 1000.0µg/mL; $P<0.00001$) **(FIGURE 4.4A,B)**. Similarly, Alum significantly decreased the proportion of OX-40L-expressing cells following incubation with Alum at low dose (0.1–10.0µg/mL). However, at higher doses (100.0–1000.0µg/mL), Alum did not increase the proportion of OX-40L-expressing BMDCs *in vitro*, indicating that Alum caused an increase in OX-40L expression by the whole BMDC population, rather than in a subset of cells. LPS significantly enhanced both the proportion of OX-40L-expressing BMDCs compared with Alum at all doses ($P<0.001$) and the level of OX-40L expression compared with low doses of Alum (0.1–10.0 µg/mL, $P<0.001$) only. The level of expression (MFI) of this molecule was not significantly different between Alum (100.0–1000.0 µg/mL)-treated BMDCs and LPS-treated BMDCs ($P>0.05$). The data suggest that high doses of Alum seems to be as effective as LPS in the induction of OX-40L molecules on BMDCs *in vitro* **(TABLE 4.1)**.

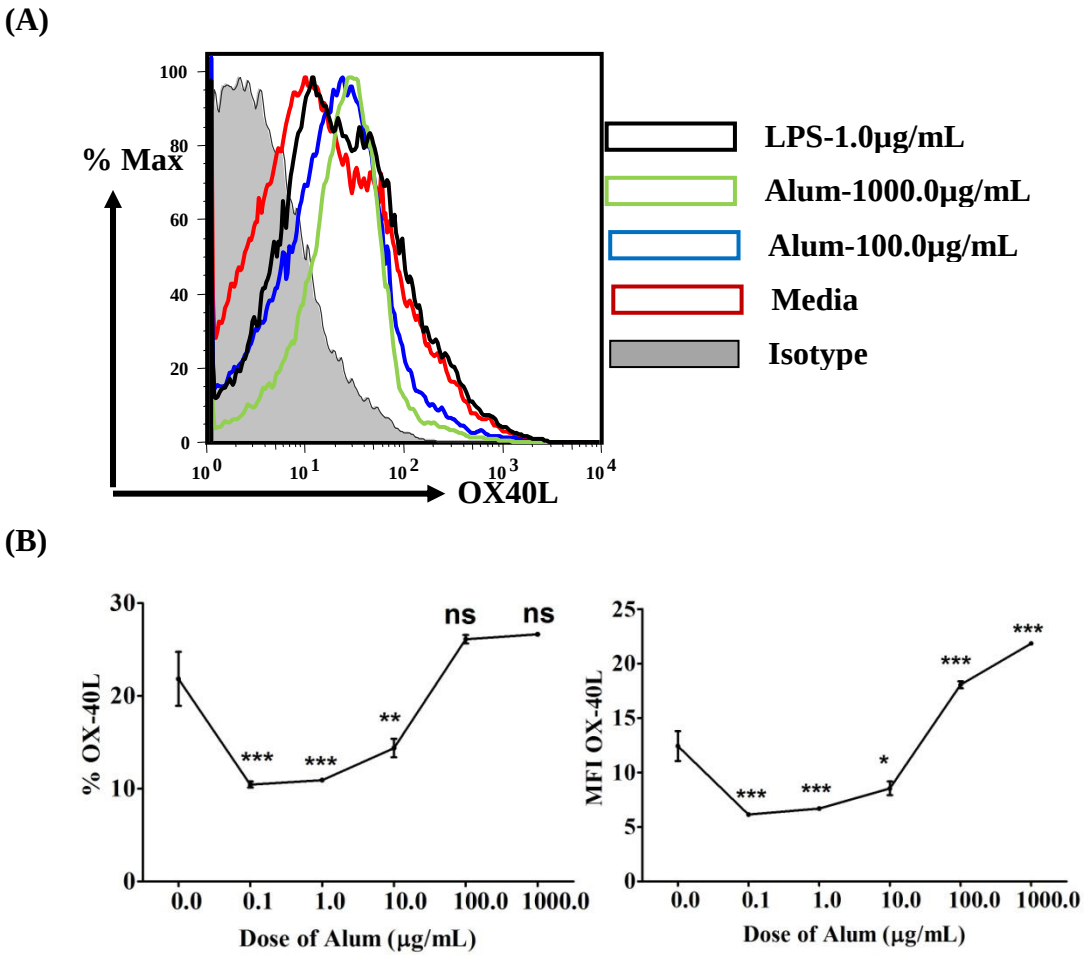

FIGURE 4.4: Alum has a biphasic effect on the expression of OX-40L by BMDCs *in vitro*.

BMDCs ($2x10^6$/5mL) obtained from C57BL/6 mice were incubated with 0.1, 1.0, 10.0, 100.0, 1000.0µg/mL Alum, LPS (1.0µg/mL) or media for 24hours. Cells were stained with anti-CD11c and anti-OX40L antibody and analysed by flow cytometry. (A) Overlay histograms showing the % of maximum of cells positive for OX-40L, within the CD11c+ population. (B) Line graphs showing the proportion of OX-40L positive cells (left) and the MFI of OX-40L (right) on CD11c+ DCs. Tukey Post Test was used to compare values (mean±S.E.M. n=4) between control (Alum; 0.0µg/mL) and increasing concentration of Alum. ***: P<0.0001, **: P<0.001, *: P<0.01, ns: not significant.

4.3 Summary of the impact of Alum on the expression of costimulatory molecules by BMDC

In summary, the impact of Alum has been addressed on the activation or maturation state in the context of influence on the expression of selected costimulatory molecule expression by BMDCs. The results demonstrate that Alum treatment has an enhancing role on CD86 expression at all doses tested, on CD80 expression at 0.1–1.0µg/mL, on OX-40L at 100.0–1000.0µg/mL and an inhibitory role on CD40 and OX-40L expression at 0.1–10.0µg/mL and no effect on CD80 expression at 10.0–1000.0µg/mL and on CD40 expression at 100.0–1000.0µg/mL **(TABLE 4.1)**. The results reveal a complex effect of Alum on BMDCs that is dependent on both dose and the costimulatory molecule being examined.

TABLE 4.1: Summary table of effects of Alum on DC costimulatory molecule expression.

These values were calculated by using Tukey Post Test and by comparing the MFI (mean±S.E.M.) of costimulatory molecules between DCs incubated in media and DCs incubated in various concentrations of Alum (0.1–1000.0 µg/mL). Symbol: +=P<0.01; ++=P<0.001; +++=P<0.0001 (For enhanced values). -=P<0.01;--=P<0.001; ---=P<0.0001 (For reduced values) and 0=P means not significant.

Costimulatory molecules	Dose of Alum (µg/mL)				
	0.1	**1.0**	**10.0**	**100.0**	**1000.0**
CD86	++	++	+++	+++	+++
CD80	++	+	0	-	0
CD40	--	-	-	0	0
OX-40L	---	---	-	+++	+++

4.4 Impact of Alum on the production of cytokines by BMDCs

In the previous section, the diverse (both positive and negative) effect of Alum was expressed on the expression of costimulatory molecules. The data suggest that Alum plays a complex role in activating BMDCs and this may impact on subsequent T cell activation. However, the role of soluble cytokines (signal 3) on T cell activation and differentiation is essential, though redundant, with the same activity of different cytokines depending on situation [188,458,459]. Signaling via cytokines has various effects on DC, such as increasing antigen presenting function [306], inducing their migration to the DLNs [460-463], direct effects on T cell activation [458] and consequently the polarisation of various CD4 T cells into Th1, Th2, Th17, Tfh and Treg cells [266,270,271]. Therefore, signaling via these soluble factors released by APCs is important in determining the outcome of immune responses and their duration and magnitude *in vitro* and *in vivo*.

In this section, the effect of Alum was observed on the production of cytokines such as IL-1β, IL-6, IL-10, IL-12p70, IL-13, IL-15, TNF-α, and IL-33 that are known to be produced by BMDCs. Among these molecules, IL-1β, IL-6, IL-12p70, TNF and IL-33 are proinflammatory and have previously been associated with potent adjuvant activity mediated though pleiotropic biological effects [397,464-468]. Inflammatory cytokines such as IL-1β, TNF-α and IL-12 play an important role in antigen presentation and T cell responses. IL-1β is translated as pro-IL-1β that undergoes caspase-1-dependent maturation resulting in the secretion of the mature form of IL-1β [334,335]. This cytokine has been traditionally proposed to act as a signal 3 for the full activation of T cells [458]. Similar to IL-1β, TNF-α is a potent proinflammatory cytokine. This cytokine is involved in cell proliferation and apoptosis and necrosis [469]. In addition, it has been reported to act as a signal for DC maturation [155]. Several *in vitro* studies have described the direct effect of Alum on DCs to enhance production of cytokines such as IL-1β, IL-18 [338,470]. Both TNFα and IL-1β play a significant role in DC migration because both of these cytokines can induce trafficking of DCs to DLNs following s.c. administration [460-463]. These cytokines decrease epithelial (E)-cadherin messanger RNA (mRNA) and

protein expression in DCs resulting in the detachment of cells from neighbouring cells and matrix components [471] thereby increasing the efficiency of DC mobilisation. Both cytokines have been shown to regulate lysosomal protease activity in DCs and affect p:MHCII presentation [306]. These activities may be associated with the increased activity of cathepsin S and cathepsin B by these cytokines [306]. IL-33, a newly discovered proinflammatory cytokine, shares structural and functional characteristics with the IL-1 cytokine family [472]. This cytokine signals via a heterodimer receptor complex with an IL-33-specific ST2L (IL-1 receptor-like 1 molecule or IL-1R1) accompanied by another subunit, IL-1R1 accessory protein [473]. IL-33 has been shown to trigger the activation and maturation of DCs [474]. In addition, IL-33-activated DC has been shown to promote T cell expansion and Th2 polarisation [475]. IL-12p70 is a heterodimer that consists of covalently linked p35 and p40 subunits encoded by two different genes [476]. This cytokine has been classified as an excellent adjuvant that targets adaptive immunity [97]. This is because it has been reported to drive cytotoxic T cell induction and Th1 polarisation via IFN-γ production [476-479]. Therefore, IL-12 has been considered in clinical scenarios such as in cancer therapy where CMI is critical [97].

IL-6 is a pleiotropic cytokine that regulates immune and inflammatory responses via the heterodimeric receptors subunits (gp130 and IL-6R) [480,481]. This cytokine has been suggested to be important in Tfh cell generation and in B cell activation and differentiation and antibody production [469]. It has been shown that on IL-6 exposure, DCs enhanced presentation of cryptic T cell epitopes derived from native HEL [482]. This may be attributed to the influence of IL-6 on modulation of peripheral or early endosomal pH [482] and on enhancement of lysosomal enzymes such as cathepsin S [483].

IL-10 is an anti-inflammatory cytokine that inhibits expansion of T cells and IL-2 production [484] and induces antigen-specific nonresponsiveness [485]. Although IL-10 does not have any impact on MHC class II formation or antigen loading [484,486], it has been shown to prevent newly synthesized MHC class II

molecules from reaching the plasma membrane of monocytes with a subsequent reduction in p:MHCII presentation [306,486].

IL-13 potently suppresses IFN-γ production by Th2 cells via regulatory effects on DCs [487]. IL-13 is produced by Th2 cells [267] and by immature monocyte-derived human DCs after incubation with allergen [488] or by human DCs after incubation in PMA/ionomycin [489]. IL-13 derived from human DCs has been reported to enhance a strong Th2 response via secretion of IL-4 from Th2 cells [488]. IL-15 is a survival factor for murine DCs [490] where both mRNA of IL-15 as well as IL-15Rα are expressed and the levels of both IL-15 and the IL-15R are enhanced by LPS [491]. IL-15 enhances expression of CD86, CD40 and MHC class II, MHC class I-related chains α and β on DC surface accompanied by the release of IFN-γ and enhances CD8 T cell expansion and activate NK cells [491,492].

Although many of the cytokines identified above have associated adjuvant activity, their induction and consequently role in the activity of Alum adjuvants have not been comprehensively characterised. Therefore understanding the impact of Alum on the production of these cytokines would be crucial to know the antigen presenting functions of DCs, their mobilisation in DLNs with the consequent effects on T cell activation. Therefore in this section, the cytokine production by DCs has been investigated at different times and at different concentrations of Alum.

4.4.1 Impact of Alum on IL-1β production by DCs

In the current study, DCs incubated with a range of doses of Alum (0.1–1000.0µg/ml) for 24hours did not produce any IL-1β cytokine **(FIGURE 4.5A)** in contrast to other studies [338,470]. Similar to previous studies [338,470], LPS significantly induced the production of IL-1β by DCs within this period (**FIGURE 4.5A)**. Notably, the time dependent production of IL-1β was observed in response to a fixed dose of Alum (100µg/mL), corresponding to the highest level of GFP and highest level of YAe staining on the antigen presenting assay described in **CHAPTER-3**. Alum was able to induce cytokine induction following longer incubations with DC, with IL-1β production increasing by 8 fold from day 2 to day 3

and by 7 fold from day 3 to day 4 **(FIGURE 4.5B)**. LPS treatment produced a very distinct time dependent pattern of IL-1β production, with significant production occurring from day 1 to day 2, then, sharply decreased after incubation for 4days. At day 4, compared with LPS-treated cells, the level of IL-1β was more than 2-fold higher in Alum-treated cells ($P<0.001$) **(APPENDIX-III)**.

(A)

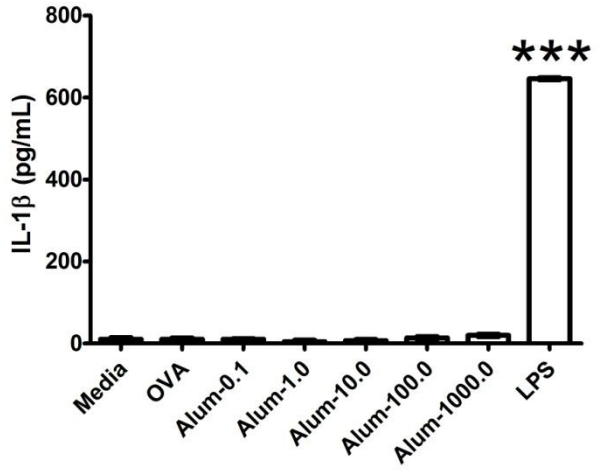

(B)

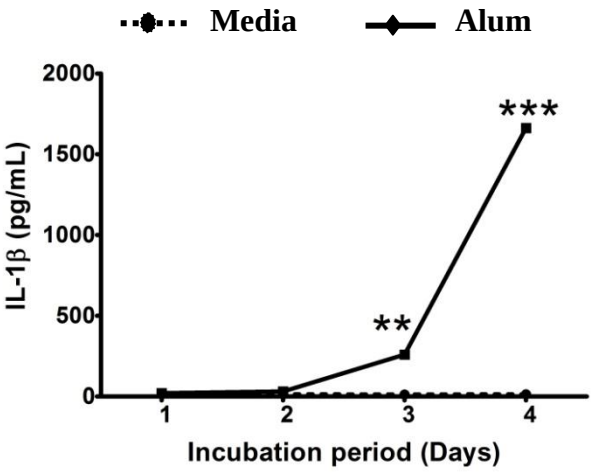

FIGURE 4.5: Alum induces the production of IL-1β by DCs in time-dependent manner *in vitro*.

BMDCs ($2x10^6$/5mL) produced from C57BL/6 mice were incubated in media, OVA (100µg/mL), LPS (1µg/mL) and different concentration of Alum (0.1–1000µg/mL) for different days. DC supernatants were analysed by Multiplex ELISA to assess the level of IL-1β. **(A)** Upper bar charts show the concentration of IL-1β in supernatants obtained in DCs following incubation for 24hours in different treatment groups (mean±S.E.M., n=3). Tukey post test was used to assess the P values by comparing the concentration of IL-1β between individual group and LPS-treated group. **(B)** Lower line graphs show the concentration (mean±S.E.M., n=3) of IL-1β in cells incubated in media or Alum (100µg/mL) at different days of incubation. Bonferronni post test was used to assess the P values by comparing the concentration of IL-1β between media or Alum-incubated DCs at specific time. ***: P<0.001, **: P<0.01.

4.4.2 Impact of Alum on TNF-α production by DCs

In contrast to LPS-treated cells, DCs incubated with different doses of Alum for 24hours did not produce any TNF-α (**FIGURE 4.6A)**. The time dependent production of this cytokine in response to 100µg/mL Alum was however, noted at day 2 and day 3 and consequently, at day 4, the level of this cytokine following Alum treatment was significantly higher compared with DCs incubated in media ($P<0.001$) **(FIGURE 4.6B)**. The data obtained with DCs incubated with LPS or LPS adsorbed to Alum was inconsistent because of the large standard errors **(APPENDIX-III)**.

(A)

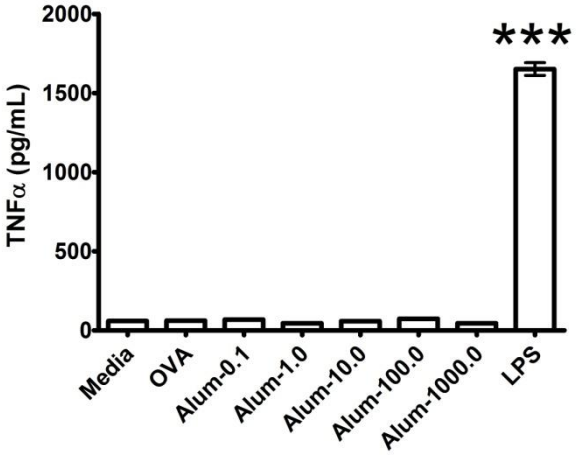

(B)

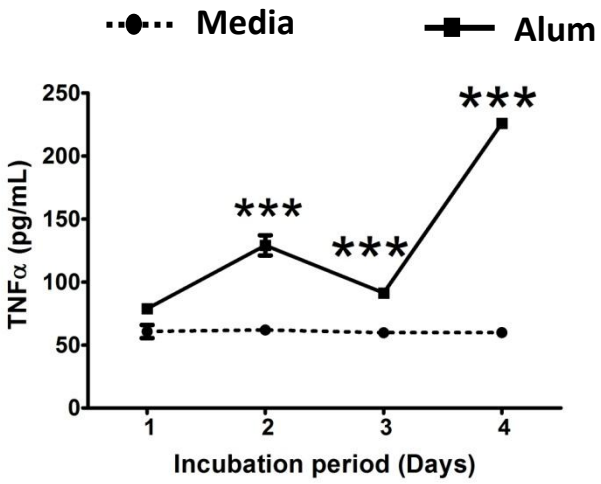

FIGURE 4.6: Alum induces the production of TNF-α by DCs in time-dependent manner *in vitro*.

BMDCs ($2x10^6$/5mL) produced from C57BL/6 mice were incubated in media, OVA (100.0µg/mL), LPS (1.0µg/mL) and different concentrations of Alum (0.1–1000.0µg/mL) for different days. DC supernatants were analysed by Multiplex ELISA to assess the level of TNF-α. **(A)** Upper bar charts show the concentration of TNF-α in supernatants obtained in DCs following incubation for 24hours in different treatment groups (mean±S.E.M., n=3). Tukey post test was used to assess the P values by comparing the concentration of TNF-α between individual group and LPS-treated group **(B)** Lower line graphs show the concentration (mean±S.E.M., n=3) of TNF-α in cells incubated in media or Alum (100µg/mL) at different days of incubation. Bonferronni post test was used to compare the concentration of TNF-α between media or Alum-incubated DCs at specific time. ***: P<0.001.

4.4.3 Impact of Alum on IL-6 production by DCs

Similar to a previous study [338], BMDC did not produce IL-6 in response to different concentrations of Alum at 24hours **(FIGURE 4.7A)**. In contrast, LPS significantly induced the production of high concentrations of IL-6 within this period. The production of this cytokine in response to incubation with 100µg/mL Alum was increased by 2 fold from 2 to 3days of incubation periods and by 8 fold from 3 to 4days of incubation periods **(FIGURE 4.7B)**. The concentration of IL-6 in Alum-treated DCs was significantly higher ($P<0.001$) compared with that of DCs incubated in media **(FIGURE 4.7B)**. The data obtained in LPS or LPS adsorbed to Alum-treated groups were very variable **(APPENDIX-III)**.

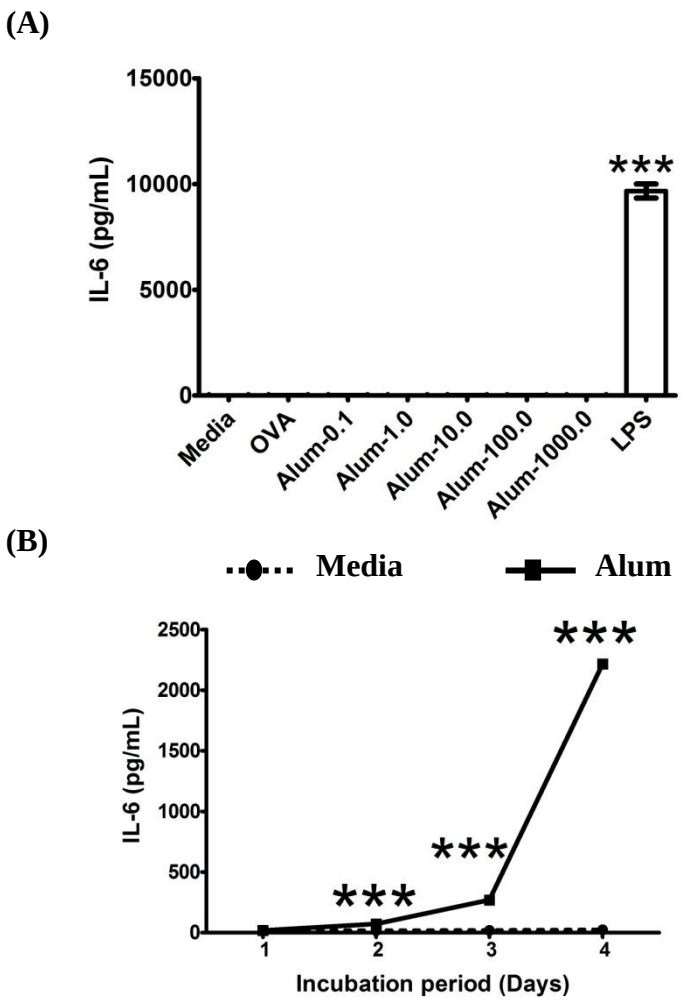

FIGURE 4.7: Alum induces the production of IL-6 by DCs in time-dependent manner *in vitro*.

BMDCs ($2x10^6$/5mL) produced from C57BL/6 mice were incubated in media, OVA (100.0µg/mL), LPS (1µg/mL) and different concentration of Alum (0.1–1000.0µg/mL) for different days. DC supernatants were analysed by Multiplex ELISA to assess the level of IL-6. **(A)** Upper bar charts show the concentration of IL-6 in supernatants obtained in DCs following incubation for 24hours in different treatment groups (mean±S.E.M., n=3). Tukey post test was used to assess the P value by comparing the concentration of IL-6 between individual group and LPS-treated groups to calculate P values **(B)** Lower line graphs show the concentration (mean±S.E.M., n=3) of IL-6 in cells incubated in media or Alum (100.0µg/mL) at different days of incubation. Bonferronni post test was used to calculate P value by comparing the concentration of IL-6 between media or Alum-incubated DCs at specific time. ***: P<0.001.

4.4.4 Impact of Alum on IL-10 production by DCs

Similar to the results obtained previously [338], in the current study, DCs produced very low amounts of IL-10, with this level becoming undetectable following 1 to 4days of incubation with different doses of Alum **(FIGURE 4.8A,B)**. In contrast to these previous results [338], LPS significantly induced the production of high concentration of IL-10 in each incubation period. Compared with LPS-treated cells, LPS adsorbed to Alum treatment showed decreased IL-10 production by DCs at day 1, though no significant effect was observed with increasing incubation periods **(FIGURE 4.8B, APPENDIX-III)**.

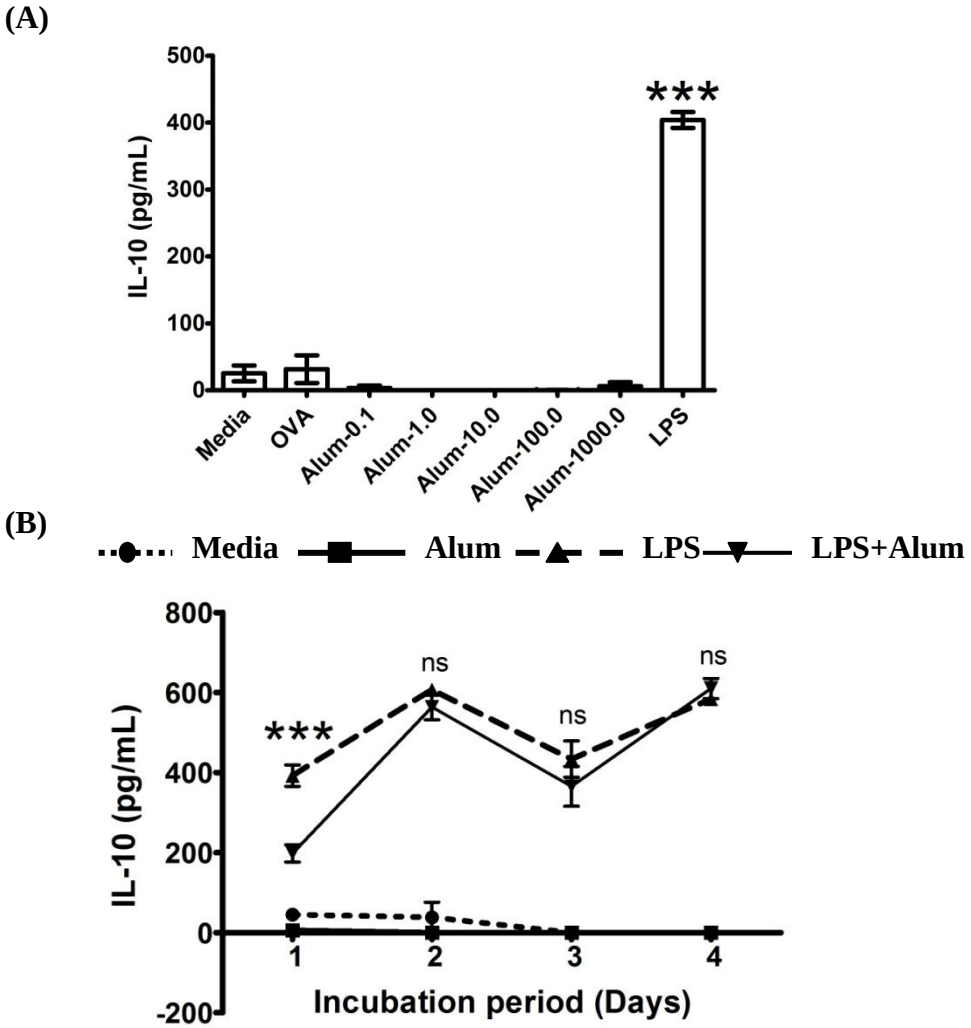

FIGURE 4.8: Alum reduces LPS-mediated IL-10 production by DCs *in vitro*.

BMDCs ($2x10^6$/5mL) produced from C57BL/6 mice were incubated in media, OVA (100.0µg/mL), LPS (1.0µg/mL) and different concentration of Alum (0.1–1000.0µg/mL) for different days. DC supernatants were analysed by sandwich ELISA to assess the level of IL-10. **(A)** Upper bar charts show the concentration (mean±S.E.M., n=3) of IL-10 in supernatants obtained in DCs following incubation for 24hours in different treatment groups. Tukey post test was used to assess P values by comparing the concentration of IL-10 between individual group and LPS-treated groups **(B)** Lower line graphs show the concentration (mean±S.E.M., n=3) of IL-10 in cells incubated in media or Alum (100.0µg/mL) at different days of incubation. Bonferronni post test was used to assess P values by comparing the concentration of IL-10 between LPS and LPS+Alum-incubated DCs at specific time. ***: P<0.001, ns=not significant.

4.4.5 Impact of Alum on IL-12p70 production by DCs

DCs incubated at different concentrations of Alum for 24hours did not produce any cytokines, similar to a previous study [338] **(FIGURE 4.9A)**. Unlike the cytokine responses noted above (IL-1, TNF, IL-6), this cytokine was not induced by Alum following incubation for longer periods **(FIGURE 4.9B)**. In contrast, LPS significantly induced the production of IL-12p70 at all incubation periods. Interestingly, the level of IL-12p70 enhanced by LPS was significantly decreased by LPS adsorbed to Alum treatment at each incubation period **(FIGURE 4.9B)**.

(A)

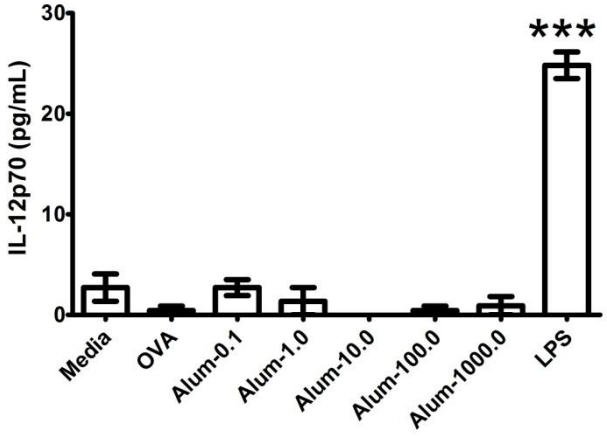

(B)

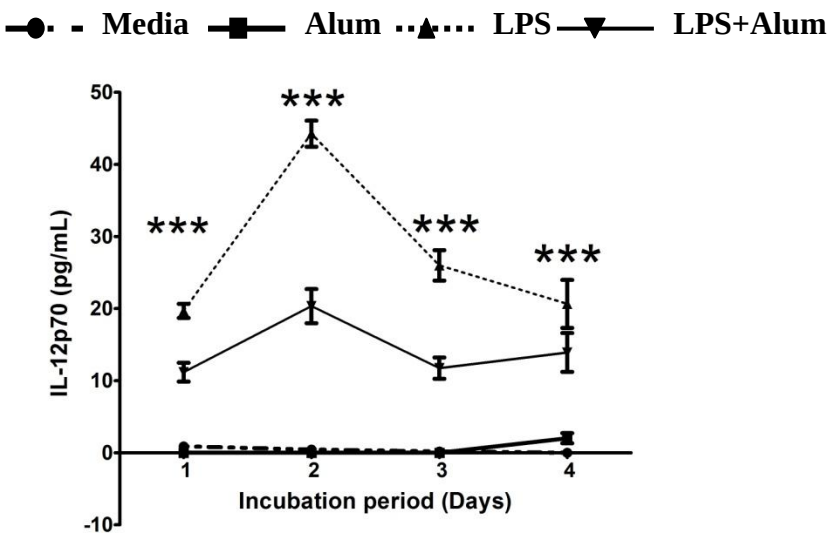

FIGURE 4.9: Alum reduces the LPS-mediated IL-12p70 production by DCs *in vitro*.

BMDCs ($2x10^6$/5mL) produced from C57BL/6 mice were incubated in media, OVA (100.0µg/mL), LPS (1.0µg/mL) and different concentration of Alum (0.1–1000µg/mL) for different days. DC supernatants were analysed by Multiplex ELISA to assess the level of IL-12. **(A)** Upper bar charts show the concentration (mean±S.E.M., n=3) of IL-12 in supernatants obtained in DCs following incubation for 24hours in different treatment groups. Tukey post test was used to assess the P values by comparing the concentration of IL-12 between individual group and LPS-treated groups **(B)** Lower line graphs show the concentration of IL-12 (mean±S.E.M., n=3) in different treatment groups at different days of incubation. Bonferronni post test was used to assess the P values by comparing the concentration of IL-12 between LPS and LPS+Alum-incubated DCs at specific time. ***: P<0.001.

4.4.6 Impact of Alum on IL-13 production by DCs

DCs incubated at different concentrations of Alum for 24hours did not produce IL-13 **(FIGURE 4.10A)**. Similarly, increasing the duration of incubation did not affect the production of IL-13 by DCs at 100.0µg/mL Alum **(FIGURE 4.10B)**. In contrast, LPS significantly induced the production of IL-13 cytokine by DCs at the first and second days of incubation periods **(FIGURE 4.10B)**. Interestingly, the level of IL-13 in LPS-incubated DCs was significantly higher than DCs incubated with LPS adsorbed to Alum for 1 or 2days of incubation ($P<0.01–0.001$) **(FIGURE 4.10B, APPENDIX-III)**.

(A)

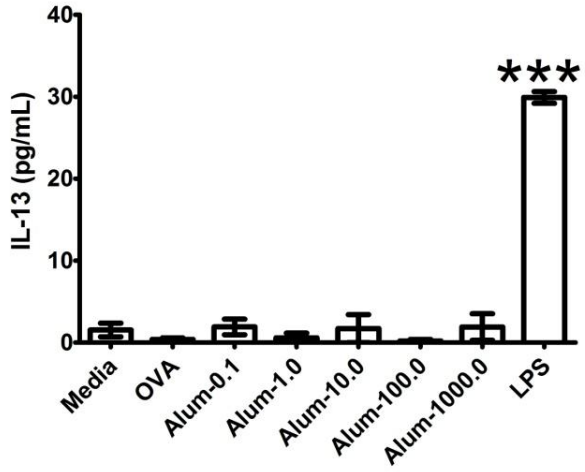

(B)

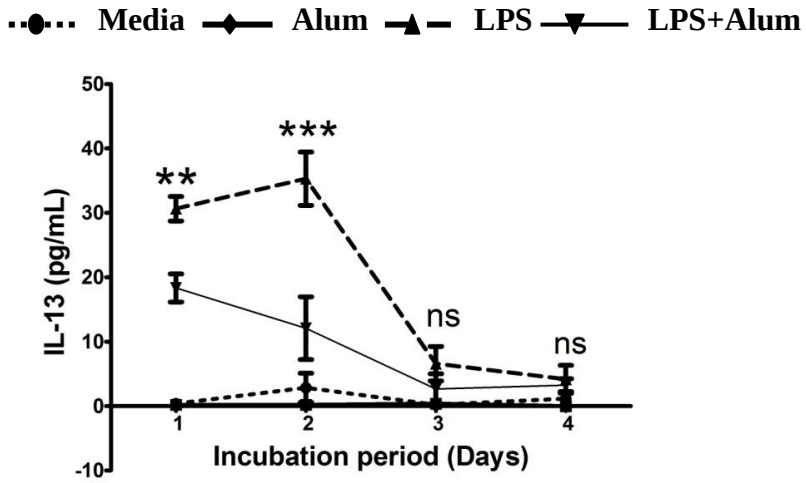

FIGURE 4.10: Alum reduces the LPS-mediated IL-13 production by DCs *in vitro*.

BMDCs ($2x10^6$/5mL) produced from C57BL/6 mice were incubated in media, OVA (100.0µg/mL), LPS (1µg/mL) and different concentration of Alum (0.1–1000.0µg/mL) for different days. DC supernatants were analysed by Multiplex ELISA to assess the level of IL-13. **(A)** Upper bar charts show the concentration (mean±S.E.M., n=3) of IL-13 in supernatants obtained in DCs following incubation for 24hours in different treatment groups. Tukey post test was used to assess the P values by comparing the concentration of IL-13 between individual group and LPS-treated groups **(B)** Lower line graphs show the concentration (mean±S.E.M., n=3) of IL-13 in different treatment groups at different days of incubation. Bonferronni post test was used to assess the P values by comparing the concentration of IL-13 between LPS and LPS+Alum-incubated DCs at specific time. ***: P<0.001, **: P<0.01, ns=not significant.

4.4.7 Impact of Alum on IL-15 production by DCs

In this study, the production of IL-15 by DCs was not observed even after cells were incubated with either various concentrations of Alum, or in LPS, or in LPS adsorbed to Alum.

4.4.8 Impact of Alum on IL-33 production by DCs

IL-33 production was not observed in DC supernatants in response to incubation of BMDC with Alum, LPS or LPS adsorbed to Alum.

4.5 Summary of influence of Alum on the production of cytokines by BMDCs

From the above data, several points were observed regarding cytokine production by DCs *in vitro*. Firstly, Alum at any dose used in this study does not induce the production of IL-1β, TNF-α, IL-6, IL-10, IL-p70, IL-13, IL-15, and IL-33 by DCs within 24hours. Secondly, Alum induced the production of IL-1β and IL-6 on DCs robustly after 3days of incubation; whereas the production of TNF-α was observed following 4days of incubation. Thirdly, Alum does not have any effect on the production of IL-10, IL-12p70, and IL-13 by DCs at any incubation periods. Fourthly, Alum reduces the LPS-mediated production of IL-10, IL-12p70 and IL-13 by DCs. Finally, DCs do not produce IL-15 and IL-13 cytokines *in vitro*. Even, LPS or different doses of Alum do not impact on the production of these cytokines by DCs **(TABLE 4.2, APPENDIX-III)**.

TABLE 4.2: Summary table of effects of Alum on cytokine production by DCs.

These values were calculated by comparing the concentration (mean±S.E.M.) of cytokine level (pg/mL) in between DCs incubated in Alum (0µg/mL) and in Alum (100µg/mL) at different incubation periods. Symbol: ++=P<0.01; +++=P<0.001 (For enhanced values), and 0=P means not significant.

Cytokines	**Incubation period (Days)**			
	1	**2**	**3**	**4**
IL-1β	**0**	**0**	++	+++
TNF-α	**0**	+++	+++	+++
IL-6	**0**	+++	+++	+++
IL-12p70	**0**	**0**	**0**	**0**
IL-10	**0**	**0**	**0**	**0**
IL-13	**0**	**0**	**0**	**0**

4.6 Impact of Alum on death of DCs

In the above experiments, the positive impact of Alum was observed on the expression of costimulatory molecules and the production of cytokines by DCs. The production of inflammatory cytokines such as IL-1β, TNF-α and IL-6 by DCs was observed in time-dependent manner, requiring incubation for more than 24hours. This suggested that these cytokines were not being produced directly in response to Alum, but could be produced indirectly, perhaps due to apoptotic or necrotic cell debris induced by incubation with Alum. It has been described that necrosis is one of the signals that trigger the maturation state of DCs [242] with the consequent release of DNA as well as other DAMPs that are able to induce DC activation and act as adjuvants [55]. Therefore, to analyse the impact of Alum on apoptotis and necrosis of DCs, Annexin- V and 7-AAD were used. These chemicals can label apoptotic cells and necrotic cells respectively **(FIGURE 4.11)**.

In the present study, Alum at different concentrations caused significant increase in apoptosis of DCs *in vitro* (10µg/mL; $P<0.01$, 100µg/mL; $P<0.0001$) **(FIGURE 4.12A)**. Compared with apoptosis observed in media, Alum at 1000µg/mL did not induce any apoptosis ($P>0.05$). The reason behind this was associated with the lack of many cells in the group treated with Alum (1000µg/mL), because the decreased proportion, numbers and the level (MFI) of CD11c positive cells were detected in this group **(Results Not Shown)**. Notably, Alum at any dose used in this study did not cause necrosis of DCs. This was evaluated by comparing the proportion of 7-AAD positive DCs between each treatment group **(FIGURE 4.12B)**. Interestingly, these results indicate that Alum might affect the viability of cells via apoptosis pathway.

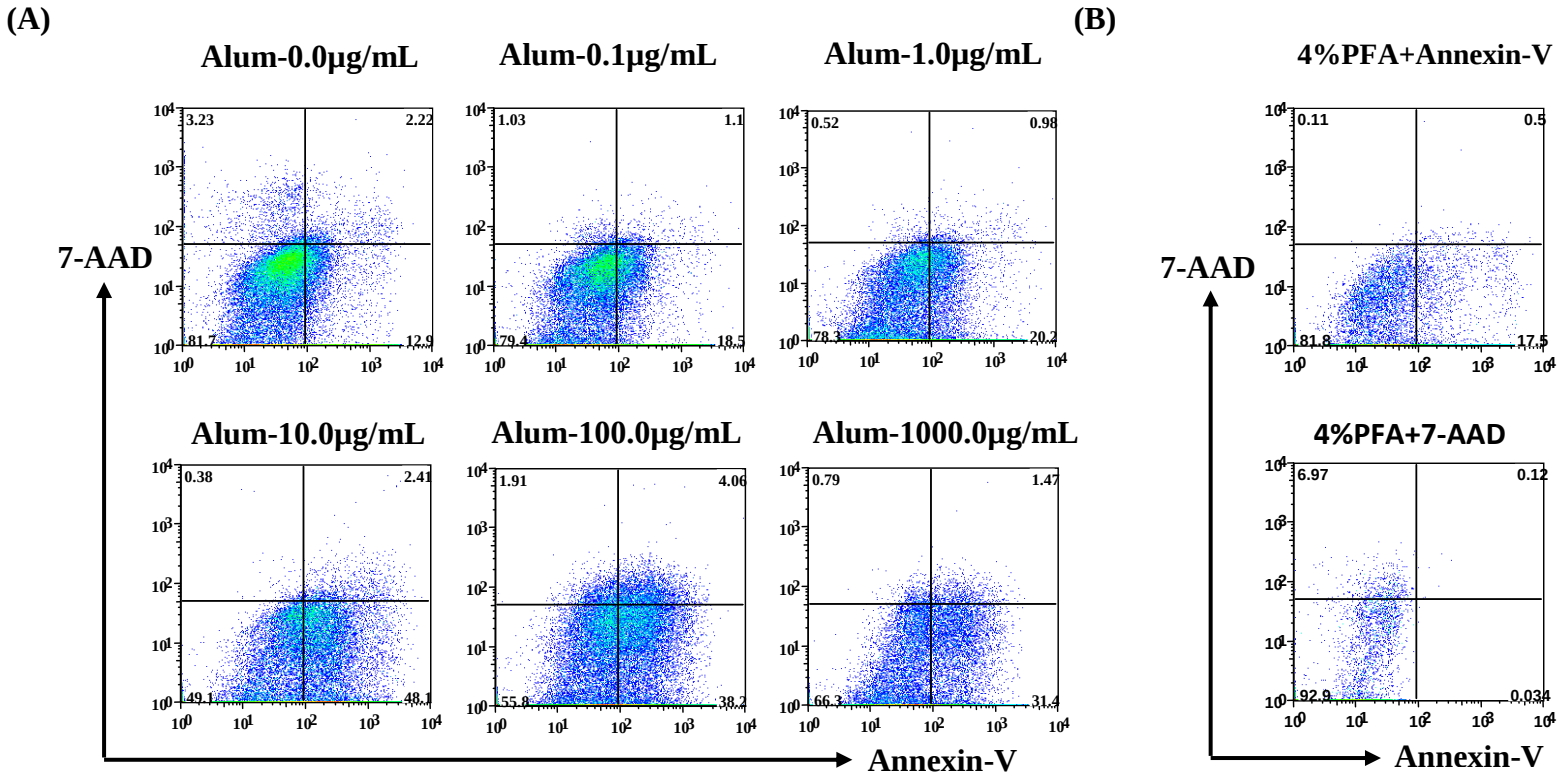

FIGURE 4.11: Gating strategy of apoptotic and necrotic bodies observed in BMDCs following incubation in 4% PFA.

BMDCs ($2x10^6$/5mL) produced from C57BL/6 mice were incubated for 24hours and stained with CD11c antibody and then labelled with Annexin- V and or 7-AAD before analysing by flow cytometry. A total of 50,000 cells were collected on the basis of forward and side scatter characteristics. **(A)** Histograms showing 7-AAD vs Annexin-V in various treatment groups. **(B)** Positive controls prepared by the addition of 4% PFA and staining with either Annexin-V or 7-AAD.

(A)

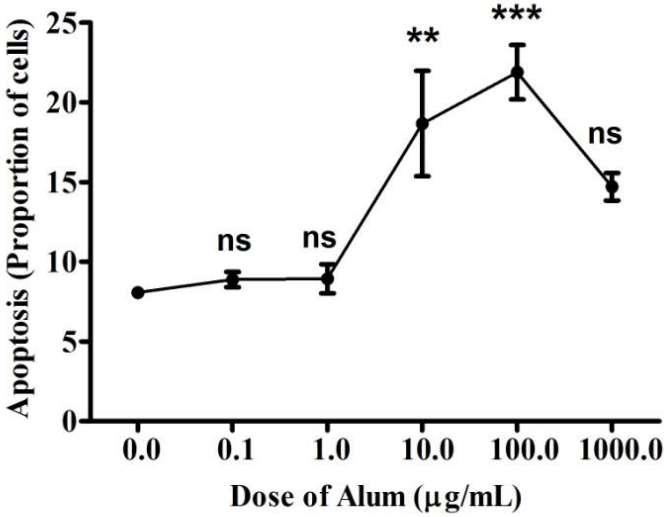

(B)

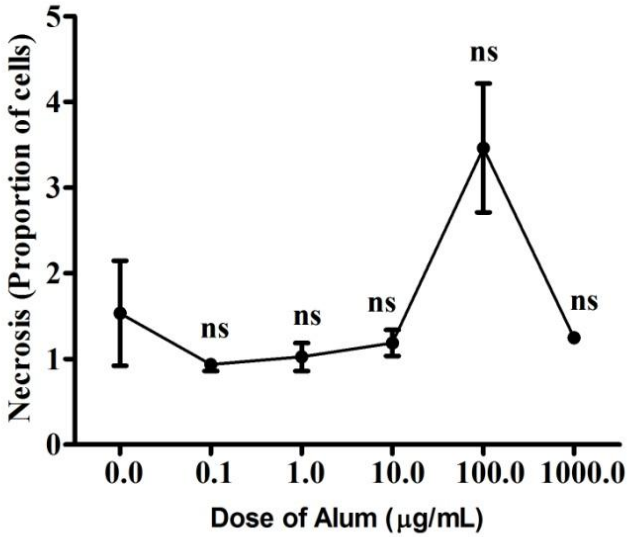

FIGURE 4.12: Alum causes apoptosis of DCs *in vitro*.

The flow cytometry data obtained in the above experiments **(FIGURE 4.11)** were analysed by line graphs **(A)** and **(B)**. Above line graphs show the proportion (mean±S.E.M., n=3) of apoptotic **(A)** or necrotic **(B)** DCs following incubation in various concentrations of Alum (0.0 – 1000.0µg/mL). Tukey post tests were used to evaluate probability values by comparing the mean proportion (mean±S.E.M.) of apoptosis or necrosis between the cells incubated in media (Alum=0.0µg/mL) and successive concentrations of Alum.

4.7 Discussion

The data in this chapter clearly demonstrated that Alum differentially affected expression of DC activation markers such as CD86, CD80, OX-40L and CD40 *in vitro* and, that this was dose dependent. Furthermore, Alum had an impact on cytokine production including IL-1β, IL-6 and TNF-α that was time-dependent and also affected cell viability, inducing apoptosis of DCs in a dose-dependent manner.

Firstly, it was observed that Alum enhanced the expression of the costimulatory molecule CD86, had some postive impact on CD80, while reducing the expression of CD40. A previous study by Sun and colleagues did not observe any effect of Alum on these three costimulatory molecules on CD11c positive BMDCs derived from BALB/c mice after 24hours incubation with Alum adjuvants [384]. As these studies were performed with a single dose of Alum, the current study extends these findings demonstrating dose dependent effects of Alum, particularly in the context of CD86 expression. This agrees with previous *in vitro* studies conducted by Sokolovska and colleagues [338]. However, this group also observed that Alum had no impact on CD40 and induced CD80, whereas in this chapter it has been seen that Alum inhibited CD40 and both inhibited as well as increased CD80 expression depending on dose of Alum. These results are difficult to resolve as similar concentrations and similar incubation periods of Alum were used. Recent studies by Flach and colleagues did not find any effect of Cesium Alum (CsAl at 5mg/mL concentration) on CD86, CD80 and CD40 expression on BMDCs derived from C57BL/6 mice following 24hours incubation [53]. The different patterns of induction of different costimulatory molecules by Alum in these *in vitro* studies conducted by Sokolovska and colleagues [338], Sun and colleagues [384] and Flach and colleagues [53] and in the current *in vitro* study could be due to differences in host strains. For example, the expression of maturation markers such as CD86, CD40 and Stat4, an IL-12-inducing gene, are quantitatively higher in spleen-derived DCs of C57BL/6 compared with BALB/c mice [493]. Similarly, another study conducted by Ulanova and colleagues showed a dose-response effect of Alum in the induction of CD86 and CD40 molecules on monocytes derived from human PBMCs after 48hours [339].

Similar to the current experiment, the dose-dependence has been further shown by decreased CD80 and increased CD86 costimulatory molecule expression on human macrophages derived from PBMCs after 48hours [439]. Furthermore, the time-dependent manner of expression of costimulatory molecules in various cell subsets has been proved by Seubert and colleagues who showed a time-dependent increase in CD86 with the decrease in CD80 molecules on monocytes derived from human PBMCs [337]. The different results from these studies emphasise the importance of comprehensive analysis of variables such as incubation period, concentration and structural form of Alum and phenotypic markers analysed.

Following Alum treatment, the expression of both CD86 and CD80 molecules were influenced differentially with a clear dose-response of Alum on CD86 and with a small but significant effect of low dose of Alum on CD80. It may be possible that signaling via CD86 molecule is enough for the priming of naïve CD4 T cell by Alum. While it has been suggested that CD80 and CD86 can substitute for each other during priming of naïve CD4 T cells [449], this finding is controversial [450]. In this context, CD80 has been suggested to act as an initial ligand that binds CD152 and maintains immune tolerance. These resulting inhibitory effects are over-ridden by the enhanced expression of CD86 molecules on DCs due to inflammatory stimuli that results in the immune response [450]. Further evidence of discrete functions of these costimulatory molecules came from their potentiality to polarise T cell responses into either Th1 or Th2. Studies show that CD86 costimulation appeared to direct the immune response toward Th2 development, whereas CD80 costimulation biased toward a Th1 response in murine model [494]. These results are consistent with the default role of Alum in Th2 response perhaps acting via induction of CD86 on DC.

In addition to these molecules, OX-40L seems to be an important target of Alum adjuvant *in vitro.* Alum showed a biphasic dose response on OX-40 ligand expression by DCs, with induction at higher doses. As results obtained using the EαGFP/YAe system revealed high doses of Alum also sustained antigen presentation, this would suggest that high doses of Alum may induce optimal signal

1 and signal 2 in responding CD4 T cells. Therefore, in addition to CD86, Alum may provide additional costimulatory signals via OX-40L to optimise the initiation and generation of long-lived CD4 T cell responses [452].

While signaling via CD40 is significant in B cell activation [264] that is also important in Alum-mediated antibody responses, the current *in vitro* experiment showed inhibition of expression of this costimulatory molecule. It is difficult to analyse this result of CD40 inhibition by Alum because this experiment system is artificial and even a single cell may behave differently *in vivo*. Further studies involving kinetics of expression of these molecules allow understanding the magnitude and duration of CD40 costimulation.

Alum also significantly induced the production of proinflammatory cytokines such as IL-1β, TNF-α and IL-6 by DCs in a time-dependent manner. Interestingly, all of these inflammatory cytokines have several functions on DCs such as modulation of antigen presentation [306,482,483], mobilisation of DCs to the DLNs [460-463,471], direct activation of antigen-specific T cells [294,396] and importantly inflammation. While these inflammatory cytokines have important roles in DC function and adjuvant activity, TNF-α and IL-6 have previously been shown to be dispensable for Alum action *in vivo* [495]. It is therefore proposed that IL-1β may be a default cytokine to play a role in immune response mediated by Alum *in vitro*.

IL-1β and IL-33 are translated as pro-forms that undergo caspase-1-dependent maturation resulting in the secretion of the mature form of the cytokine [334,335]. Interestingly, Alum has been shown to activate caspase-1 (encoded by Casp1) via the NLRP3-inflammasome [328,388-390,496]. Caspase-1 is also involved in programmed cell death, apoptosis or pyroptosis [497]. In the current study, apoptosis of Alum treated DCs could be observed within 24hours, without any clear impact on necrosis. Interestingly, it required longer incubation periods (3 – 4days) for significant levels of IL-1β to be detected following Alum treatment, suggesting that the induction of this, and other inflammatory cytokines, TNF-α and IL-6, though not IL-33 could be secondary to cell death. As mentioned above, previous studies

have suggested that Alum adjuvant induces the breakdown of the phagosomal membrane, reduction in intracellular potassium level, and consequently NALP3-inflammasome activation [328]. The NALP3 signaling results in the activation of caspase-1, which is required for the production of mature IL-1β from pro-IL-1β [464-467,498]. However, while some studies implicate NALP3-mediated signaling in adjuvant activity [328,388-390], more recently this has become contentious [53,55,383,496]. The studies in which the authors [53,55,383,496] have concluded the indispensibility of this inflammasome in Alum adjuvanticity came from the experiment conducted on mice deficient in NLRP3 or Caspase 1. Therefore, the variations may be associated with the different formulations of vaccine adjuvants such as Alum, contamination with TLR agonists or incomplete characterisation of the Alum induced immune response [398].

It has alternatively been suggested that the release of host-DNA from dying cells may act as an endogenous danger signal or alarmin, that could indirectly mediate the Alum adjuvant signal [55,400]. The released DNA from necrotic bodies has been shown to enhance Th2 responses via TLR9-IRF3-dependent pathway by activating inflammatory DC or via IRF3-independent pathway by activating Tfh responses or Tfh responses that affect the B cell responses accompanied by IgE isotype switching and IgG1 production [55]. In addition to these effects, signals derived from necrotic cells induce the release of biologically functional IL-33 [403,404] that is thought to act similarly [400,499], though its production was not detected in the present studies. However, the timing of the current studies suggests that inflammatory cytokine production by DC could be the result of bystander cell death during the culture. To investigate this question directly, further studies using agents (Caspase inhibitors) that block programmed cell death *in vitro* or mice lacking molecule (Caspase $1^{-/-}$) that controls programmed cell death *in vivo* will be informative.

In addition to these effects, death of cells may have several consequences in the immune responses. Firstly, before a cell undergoes apoptosis, the breakage of lysosomal membrane also underlies the modulation of antigen processing pathway.

Following the lysosomal membrane breakdown, lysosomal antigens are released into the cytosol where they are processed via MHCI pathway. This may be one of the causes why Alum enhances the CD8 T cell activation *in vivo* [383]. Secondly, both necrotic and apoptotic bodies are phagocytosed by APCs such as DCs [191]. When necrotic cells are engulfed by DCs, they are processed and presented on both MHCII as well as MHCI to both CD4T cells as well as CD8T cells respectively in the first antigen encounter. Following the second encounter, CD4 T cells lead to a delayed-hypersensitivity response and CD8 cells lead to cytotoxic responses. In contrast, apoptotic cells engulfed by DCs are processed via MHCI pathway which provides activation of CD8 T cells in the first encounter and consequently provides cytotoxic responses under the help generated by activated Th1 cells or provides tolerance responses under no help signals by these cells [500]. Therefore, understanding these mechanisms will be important in rational design of vaccine adjuvants that lead to death of cells.

While Alum influenced proinflammatory cytokine-producing efficiency of DCs, it did not affect the production of IL-10, IL-12p70 or IL-13 at any dose used in the experiment and at any incubation period. However, Alum significantly decreased the LPS-mediated IL-10, IL-12p70 and IL-13 production by DCs in time-dependent manner. Previous studies have suggested that Alum could neutralise LPS via a ligand-exchange mechanism as well as decreasing LPS induced signaling *in vivo* [501]. At pH more than 2 (for example, pH: 7.4), strong attraction occurs between positively charged Aluminium hydroxide and negatively charged LPS that contains 2 easter-bound phosphate groups within lipid A portion [501,502]. Because IL-10 downregulates MHC class II expression by DCs [306,486], its regulatory effects on antigen presentation by Alum has been shown to have an adjuvant effect [503]. Inhibition of LPS induced IL-10 by Alum could similarly act to enhance the adjuvant effect of LPS or other immunostimulatory adjvuants associated with IL-10 production, for example MPL A as part of the AS04 vaccine formulation [202].

In conclusion, Alum can enhance the DC activation characterised by the enhanced expression of CD86, CD80 and OX-40L expression in a dose-dependent

manner and enhanced the production of IL-1β, IL-6 and TNF-α by DCs in a time-dependent manner *in vitro*. Alum also affected the cell viability in the context of apoptosis that may be related to the production of above inflammatory cytokines *in vitro*. These molecules are crucial in changing DC phenotype from antigen sampling to antigen-presenting cell and in determining the functional outcome of T cell responses.

CHAPTER-5: IMPACT OF ALUM ON CD4 T CELL RESPONSES *IN VIVO*

5.1 Introduction

Despite our current knowledge and understanding of immunology, the study of vaccine adjuvants remains largely empirical. Reductionist approaches, such as analysing adjuvant effects on key immune system cells *in vitro* as described in previous chapters, will help define the features of adjuvants that are critical for their function. However, adjuvants ultimately interact with a complex physiological, anatomical and immunological system within the vertebrate body. Even a single cell may behave differently *in vitro* under different experimental situations, therefore understanding how cells behave *in vivo* and what interactions with their environment and with adjuvants underlie these functions are important immunological questions. Importantly, these can only currently be fully understood *in vivo*.

In the previous chapters, the increased uptake and presentation of antigens (signal 1) and dose response of Alum of the expression of costimulatory molecules (signal 2) and kinetic response of Alum of cytokine production (signal 3) by DCs have been well-presented *in vitro*. As already described, the former two signals, signal 1 and signal 2, are required for T cell activation [257], the latter signal (signal 3) is essential to boost T cell responses [188,459]. Though it has been suggested that an antigen pulse of a few hours is sufficient to support subsequent T cell division [504], the continued engagement of the peptide:MHCII-T cell receptor (p:MHCII-TcR) complex is required for enhanced T cell expansion [438,505,506]. Therefore, if Alum adjuvants work by influencing duration and magnitude of the antigen presentation *in vitro*, it may have significant contributions in T cell responses *in vivo*. Interestingly, Alum adjuvant has previously been reported to act as a depot, allowing for slow release of antigen, and consequently enhancing the duration and magnitude of the antibody response [45]. In this context, the duration and magnitude of T cell responses is crucial to understand adjuvant-derived responses *in vivo*.

5.2 Impact of Alum on magnitude and duration of the immune response

It is widely believed that duration and magnitude of immune response in the context of T cell immune response is crucial to understand vaccine as well as adjuvant-derived responses *in vivo*. To address this issue, an adoptive transfer system was used [507]. Adoptive transfer of TcR transgenic cells into a naïve recipient with the same genetic background allows the detection of precursor T cells in sufficient numbers to study their characteristics and functionality during an immune response [507]. To investigate the effect of Alum on the magnitude and duration of the adaptive immune response, antigen-specific DO11.10 CD4 T cells were transferred to BALB/c mice followed by PBS, OVA and OVA adsorbed to Alum immunisation after 1 day. Then, DLNs were extracted from these mice at days 1, 5 and 11 post-immunisation. Using flow cytometry, total numbers of viable accumulated cells, antigen-nonspecific and antigen-specific CD4 T cells in DLNs and the divided antigen-specific CD4 T cells *in vivo* were analysed **(FIGURE 5.1)**.

Higher numbers of viable LN cells were observed in mice immunised with OVA adsorbed to Alum at days 1, 5 and 11 compared to the mice exposed to OVA or PBS alone ($P<0.001$) **(FIGURE 5.2A)**. Interestingly, Immunisation with OVA adsorbed to Alum caused a significant increase in total CD4+ T cell numbers at all days post-immunisation compared with mice immunised with OVA ($P<0.001$) **(FIGURE 5.2B)**. Subsequently, the magnitude and duration of the antigen-specific T cell responses enhanced by Alum were analysed on the basis of proportion **(FIGURE 5.2C)** and numbers **(FIGURE 5.2D)** of antigen-specific T cells as recognised by CD4+KJ+ cells. Immunisation of mice with OVA adsorbed to Alum caused a significant increase in antigen-specific T cell numbers at day 5 post-immunisation compared with mice immunised with OVA ($P<0.001$) **(FIGURE 5.2D)**. Similar data were observed when they were analysed on the basis of the proportion of cells positive for CD4+KJ+ **(FIGURE 5.2C)**. These data indicate that Alum induces an increase in antigen-specific CD4 T cells only at day 5 post-immunisation, while it induces accumulation of total CD4 T cells in DLNs at all days post-immunisation. In conclusion, these data demonstrate that Alum induces an

increase in the total cellularity, as well as an increase in the total number of antigen-specific T cells in DLN.

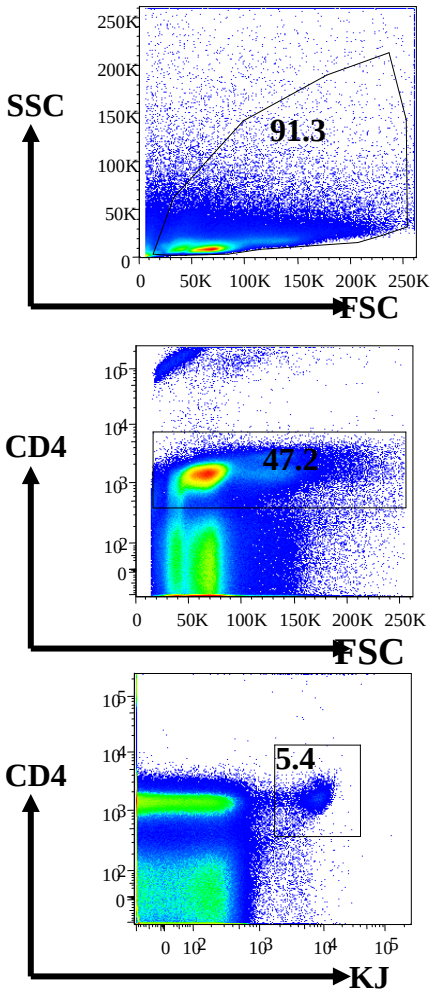

FIUGRE 5.1: Dot plots showing staining of total CD4 + and antigen-specific CD4+ T cells.

Antigen-specific CD4+KJ+ T cells from DO.11.10 mice were transferred into the BALB/c mice at day (-1). The next day, OVA or OVA adsorbed to Alum were administered via s.c. injection. After 5days, mice were culled and brachial and axillary DLNs were used to prepare single cell suspensions. DLN cells were stained with anti-CD4 and DO11.10 TCR KJ1.26 antibody and analysed by flow cytometry. The above histograms represent the characteristics of cells derived from DLNs following day 5 post-immunisation with Alum. The cells were gated based on light scatter characteristics (FSC vs SSC) of the cells (upper) from which either CD4+ (middle) or CD4+KJ+ cells (DO11.10 Tg, lower) were distinguished.

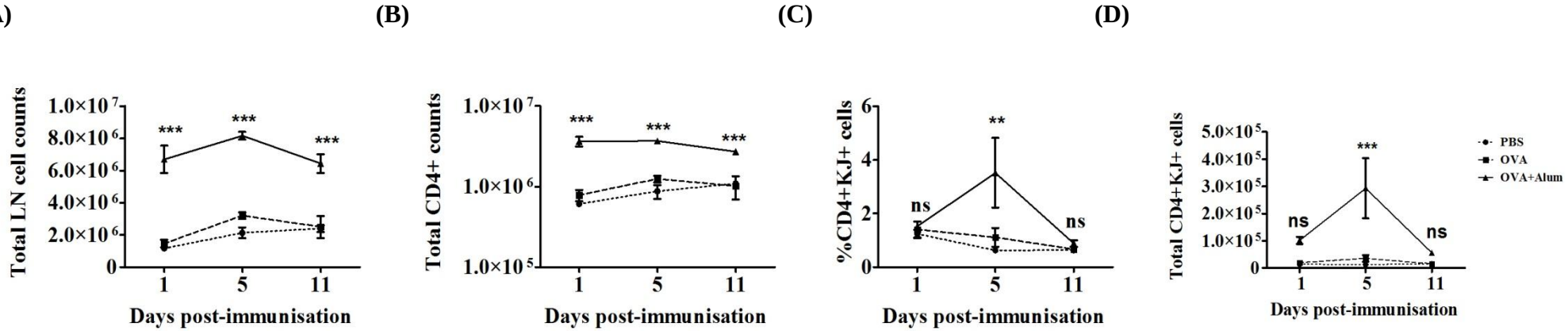

FIGURE 5.2: Alum enhances the recruitment of both total cells as well as total CD4+ and antigen-specific CD4+ T cells in DLNs.

OVA-specific CD4+KJ+ T cells from DO.11.10 mice were transferred into the BALB/c mice at day (-1). The next day, OVA or OVA+Alum were administered via s.c. injection. After days 1, 5 and 11, mice were culled and brachial and axillary DLNs were used to prepare single cell suspensions. DLN cells were stained with anti-CD4 and DO11.10 TCR KJ1.26 antibody and analysed by flow cytometry. The line graphs show the total cell count collected in DLNs **(A)**, the total numbers of CD4+ cells in DLNS **(B)**, the % of CD4+KJ+ cells in DLNS **(C)** and the total numbers of CD4+KJ+ cells in DLNS **(D)** at different days post-immunisation. Data have been presented as the mean±S.E.M. (n=3 mice per group). Bonferronni post tests (Two Way ANOVA) were used to assess the P values by comparing the number of cells (mean±S.E.M.) between OVA and OVA adsorbed to Alum immunised mice at specific day post-immunisation. ns: not significant, ***:P<0.001, **: P<0.01, ns: not significant.

5.3 Impact of Alum on duration and magnitude of antigen-specific CD4 T cell expansion

The increase in antigen-specific T cell numbers observed noted above could be attributed to increased cell accumulation and/or increased cell proliferation. To investigate the impact of Alum on antigen-specific CD4 T cell proliferation, CFSE dilution [508,509] was measured within CD4+KJ+ cells **(FIGURE 5.3)**. In the current study, the fraction of antigen-specific CD4 T cells that had divided in groups immunised with OVA plus Alum was not significantly different compared with soluble OVA-immunised groups at day 1 or day 11 post-immunisation ($P>0.05$). However, at day 5 post-immunisation, a significantly higher proportion of cells had undergone division in the OVA plus Alum- versus OVA-immunised groups **(FIGURE 5.4A)**. The numbers of undivided cells were significantly higher in OVA plus Alum-immunised groups compared with soluble OVA-immunised groups ($P<0.01$) at day 1 and day 5 post-immunisation **(FIGURE 5.4A)**. These undivided cells presumably reflect the ability of Alum to induce T cell recruitment that occurs at day 1 and day 5 post-immunisation. In contrast, increased number of divided cells at day 5 post immunisation demonstrates the ability of Alum to induce antigen-specific CD4 T cell proliferation. In addition, the numbers of divided and undivided T cells **(FIGURE 5.4A)** were very low compared with the total numbers of cells accumulated in DLNs **(FIGURE 5.2A)** at all days post-immunisation. These data suggest that Alum can induce recruitment of T cells to the DLNs and induce activation and division of antigen-specific cells.

In the same way, the numbers of cells in each generation was also considered as a parameter reflecting antigen-specific CD4 T cell expansion following Alum immunisation **(FIGURE 5.4B)**. At 0 generation, the numbers of CD4+ T cells were statistically higher at 1 day post-immunisation with OVA adsorbed to Alum compared with OVA-immunised groups. At this period, cell division after the 0 generation was not observed indicating all cells do not undergo further division in mice immunised with OVA adsorbed to Alum by this stage. Notably, the pattern of division of CD4+ T cells was almost similar in mice immunised with Alum at day 5 and 11 post-immunisation as assessed by the significant increased numbers of

divided cells from the second to fifth generation and from the 0 to sixth generation respectively **(FIGURE 5.4B)**. However, the numbers of cells undergoing division were higher in mice immunised with Alum at day 5 post-immunisation compared to mice immunised with Alum at day 11 post-immunisation indicating that most of the cells divide by day 5 post-immunisation. These results suggest that Alum has a major impact on CD4+ T cell expansion only at day 5 post-immunisation *in vivo*.

In summary, the current *in vivo* experiments show that following s.c. immunisation, Alum produces an increase in cellularity of the DLN, including an enhanced accumulation of CD4+ T cells and this is accompanied by an increase in the numbers and expansion of antigen-specific T cells.

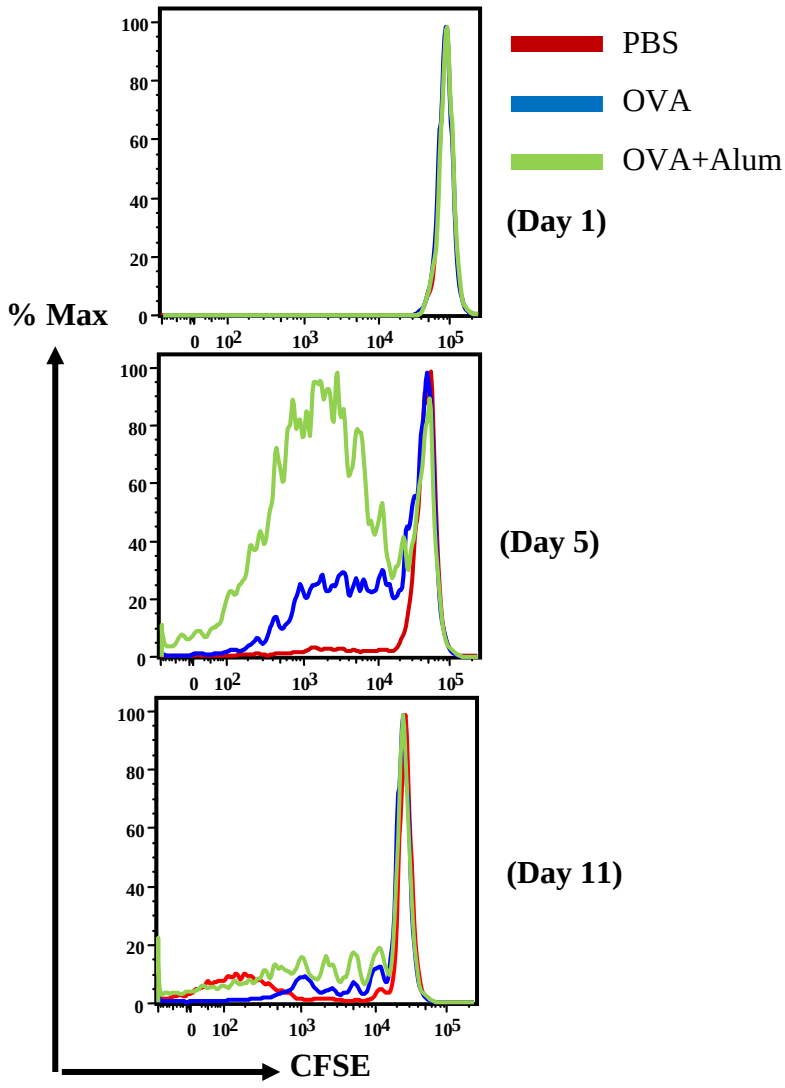

FIUGRE 5.3: Alum immunisation enhances antigen-specific CD4+ T cell division *in vivo*.

The data obtained for antigen-specific transgenic DO11.10 cells in the experiment described in **FIGURE 5.1** was analysed. The above overlay histograms show the % maximum of cells with CFSE dilution for different groups of mice immunised with PBS, OVA and OVA adsorbed to Alum at day 1, 5 and 11 post-immunisation.

(A)

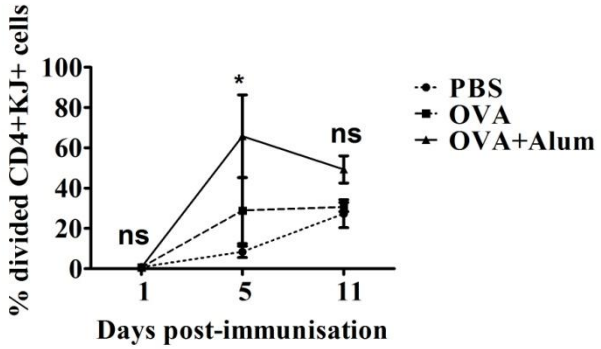

(B)

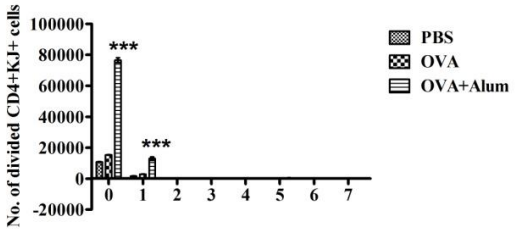

(Day 1)

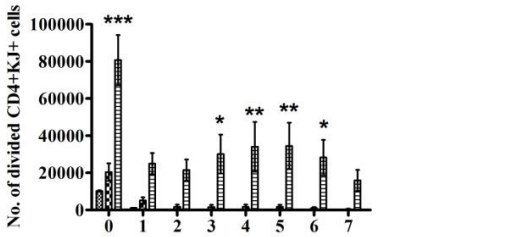

(Day 5)

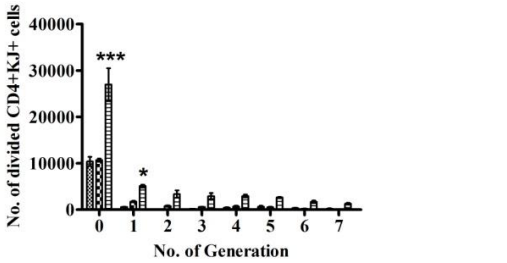

(Day 11)

FIGURE 5.4: Alum immunisation does not sustain antigen-specific CD4+ T cells expansion *in vivo*.

(A) Line graphs showing the % of divided antigen-specific T cells (CD4+KJ+) on different days post-immunisation. **(B)** Bar graphs showing numbers of divided CD4+KJ+ cells in each generation (0 to 7) in different mice at day 1 (upper), day 5 (middle) and day 11 (lower) post-immunisation with PBS, OVA and OVA adsorbed to Alum. Data have been presented as the mean±S.E.M. of triplicate reading in each group.*: P<0.05, **: P<0.01, ***: P<0.001, ns=not significant, calculated using Bonferronni post test after comparing values (mean±S.E.M.) between OVA- and OVA+Alum-immunised groups.

5.4 Discussion

The previous chapters investigated how Alum affects antigen uptake and presentation, costimulatory molecule expression and cytokine production by DCs *in vitro*. These processes lead to the initiation of activating signals in naïve T cells leading to induction of the adaptive immune response. To investigate the impact of Alum on T cell responses *in vivo* requires the ability to track naive, antigen-specific T cell development. As the precursor frequency of antigen-specific T cells in the resting host is vanishingly small [255], an adoptive transfer of low numbers of OVA-TcR transgenic T cells in to naïve recipients was employed. The kinetics and magnitude of accumulated antigen-specific CD4 T cells could then be assessed through the use of the clonotypic antibody, KJ1.26.

It was noted that Alum substantially increased the total number of viable cells and the total number of CD4+ T cells per LN at all time points analysed post-immunisation compared with soluble antigen. These results suggest that Alum enhances the duration and magnitude of immune responses in the context of accumulation of CD4 T cells, as well as other LN cell populations such as B cells, DCs, macrophages, monocytes. This phenomenon has been described as LN 'shutdown'. LN shutdown is primarily associated with the increased rate of entry of lymphocytes from the blood and decreased output of these cells via the efferent vessels [510]. Interestingly, TNF, IL-1β and IL-6, studied in the previous chapter **(CHAPTER-4)**, are among the different adhesion molecules, chemokines and cytokines that are involved in increasing lymphocyte trafficking and retention of lymphocytes within LNs during antigen stimulation [510-513]. Although these cytokines play a crucial role in lymphocyte trafficking into DLNs, Alum adjuvanticity in the context of antibody responses was not affected by a targeted mutation in TNFR-1, the major receptor for TNF-α or IL-6, indicating the lack of these cytokines on Alum adjuvanticity [495]. However, IL-1β performs a similar role, increasing cellular traffic into DLNs as described previously [460-463]. In the previous chapter **(CHAPTER-4)**, the production of this cytokine by DC was demonstrated in response to incubation with Alum. IL-1β has also been shown to enhance the detachment of cells from neighbouring cells and matrix components

[471] and increase the migration of antigen-laden monocytes to DLN [54]. The enhanced cellular trafficking of APC to the LN and the effects of LN shutdown can therefore increase the probability of antigen-specific T cells encountering their cognate p:MHC complexes during an immune response. This can be observed in the increased total number of cells, including CD4+ T cells recruited in DLNs at all days post-immunisation. The total number of antigen-specific T cells was enhanced only 5 days post-immunisation of OVA adsorbed to Alum which corresponded to maximum proliferation of these cells.

By day 11 after Alum/OVA immunisation, levels of antigen-specific CD4 T cells were reduced and there were few proliferating cells remaining in the LN. This suggests firstly that the activated and proliferated cells detectable at day 5 have left the LN. In this context, expression of CD69, an activation marker of T cells and expression of sphingosine 1-phosphate receptor type ($S1P_1$) plays a crucial role. Following T cell activation, interaction with CD69 leads to internalisation and degradation of $S1P_1$ which results in the exit of lymphocytes into efferent vesicles and into circulation [511,514]. However, there remained undivided, antigen-specific T cell in the DLN, suggesting that the signals for T cell activation and proliferation are no longer present at this time point. Therefore, even if slow elimination of antigen occurs following immunisation with antigen adsorbed to Alum as described by Glenny and colleagues [45], this antigen is incapable of stimulating antigen-specific T cells. This is supported by the currently published article by Hutchison and colleagues [379] who failed to observe activation of antigen-specific T cells transferred into recipient mice later than 5 days post-immunisation with OVA formulated in Alum. These studies further demonstrated a lack of antigen persistence and presentation in APC populations in the DLN [379]. Remarkably, B cells were the first APCs to present Eα:MHCII complexes within 6–12hours after immunisation, then, cDCs presented these complexes within 12–24hours following Alum+EαGFP immunisation, and pDCs presented antigens within 48–72hours after Alum administration in DLNs *in vivo*. The consequent study did not find any difference in antigen uptake and presentation by B cells, cDCs and pDCs due to injection site

ablation 2 hours after EαGFP administration suggesting the lack of depot in Alum adjuvanticity [379].

Another strong support against the depot have been discussed by Noe and colleagues (2010) who conducted a study to show the relation between antigen retention at the site of injection and antibody titers in rat sera following 5 weeks after primary immunisation and 2 weeks after boost [515]. The authors injected rats with ^{111}In-labelled alpha casein (IDCAS) antigen adsorbed to AH or IDCAS adsorbed to AP or non-adsorbed IDCAS antigen formulated in phosphate-treated AP (PTAP) or IDCAS solution subcutaneously. They observed antigen retention in the following order IDCAS+AH>IDCAS+AP>PTAP=IDCAS and the antibody titers in the order: PTAP=IDCAS+AP>IDCAS+AH>>IDCAS suggesting indispensible of antigen retention in Alum-mediated immune responses [515]. This is in contrast to report published by de Veer and colleagues (2010) [376]. They found that Aluminium adjuvants reduce slow release of the antigen from the site of immunisation into afferent lymph though Alum adjuvanticity depends on retention of antigen at the site of injection and the consequent trafficking of cells [376]. Interestingly, antigen retention has not been observed in the experiment involving immunisation of mice with radioactively labelled with ^{14}C TT adsorbed to Aluminium phosphate adjuvant [374] indicating no relation of Alum on retention.

In summary, Alum enhanced the magnitude and duration of accumulation and retention of CD4+ lymphocytes in DLNs. However Alum only induced increased antigen-specific T cell numbers in the DLN at day 5 and did not alter the duration of antigen-specific T cell activation beyond this time point. The current data may probably challenge the previously hypothesised depot effect [45,367,378] indicating that there are other mechanism(s) involved in Alum adjuvanticity *in vivo*.

CHAPTER-6: CONCLUSIONS AND FUTURE STUDIES

6.1 Conclusions

In conclusion, it has been identified how Alum modulates several key steps in DC functions that lead to T cell activation which could therefore underpin adjuvant function. These can be summarised in the following steps:

A. Influence of Alum on Signal 1

In the current thesis, the influence of Alum on the detailed mechanisms of uptake and presentation of antigens **(Signal 1)** by BMDC has been studied. Firstly, formulation of antigen in Alum results in an increased rate and magnitude of antigen internalisation in an actin-dependent manner by BMDC *in vitro*, consistent with the hypothesis that Alum acts as an antigen delivery system **(FIGURE 6.1A1, A2)**. Subsequently, it has been demonstrated that Alum slows protein degradation, thereby increasing the duration of peptide availability intracellularly **(FIGURE 6.1B)**. Then, it has been shown that Alum enhances the rate, magnitude and duration of expression of p:MHCII complexes on the DC surface, with an accompanying increase in MHCII expression **(FIGURE 6.1C1)**. In addition, by using the DO11.GFP hybridoma system, it has been found that Alum increases the presentation of antigens derived from both OVA protein and OVApeptide323–339, indicating that Alum can enhance antigen presentation with or without the requirement for processing of antigens *in vitro*. These studies also prove that increasing surface expression of MHC class II molecules by Alum may be the default mechanism of enhanced antigen presentation *in vitro*.

While Alum enhanced antigen uptake and presentation in a way similar to a delivery vehicle, it has also been observed that this adjuvant works by mechanism(s) other than simply antigen delivery as adsorption to Alum has been dispensable for boosting antigen presenting efficiency of DCs *in vitro.* The result also challenges the concept that antigen must be adsorbed to an Aluminium-containing adjuvant to enhance immune responses [442].

B. Influence of Alum on Signal 2

As well as having a direct impact on antigen presentation by BMDC, Alum has impact on the activation or maturation state in the context of expression of selected costimulatory molecules **(Signal 2) (FIGURE 6.1C2)**. Alum selectively increases the expression of CD86, CD80 and OX-40L and decreases the expression of CD40 on the surface of these cells in a dose-dependent manner *in vitro*. These results suggest that Alum is able to induce the activation of CD4 T cells via the former three costimulatory molecules and is efficient to bias Th2 response perhaps acting via induction of CD86 [494] and to initiate and generate long-lived CD4 T cells via induction of OX-40L [452] on DC.

C. Influence of Alum on Signal 3

Alum not only affects the antigen presenting and costimulating efficiency of BMDCs but also affects the cytokine production **(Signal 3)** by these cells. Alum increases the production of IL-1β, TNF-α and IL-6 by BMDC in a time-dependent manner suggesting that this adjuvant plays a role in modulation of antigen presentation, mobilisation of APCs to the DLNs, direct activation of antigen-specific T cells and inflammation **(FIGURE 6.1D)**. These inflammatory roles of Alum in the context of production of cytokines may be linked to the apoptosis or necrosis.

D. Influence of Alum on T cell responses

While the current study does not directly address whether the 'depot effect' would be the usual mode of mechanism of action of Alum adjuvant, it shows an increased accumulation of cells into DLNs, known as 'LN shutdown' by Alum adjuvant. The significant point of the thesis is that Alum did not prolong antigen-specific T cell expansion *in vivo* questioning the 'depot effect' of Alum. Therefore, LN shutdown seems to be a default mechanism of action of this adjuvant and this be possibly due to the increased production of inflammatory cytokines such as IL-6, TNF-α and IL-1β by DC following treatment with this adjuvant.

In summary, these findings suggest that Alum plays a role in increasing the uptake and presentation of antigens, the expression of costimulatory molecules and the production of inflammatory cytokines by BMDC leading CD4 T cell responses. However, there are no evidences to support a role for a depot effect in the function of Alum in other studies [375,376,379,515] similar to the present experiments have been unable to find any evidence.

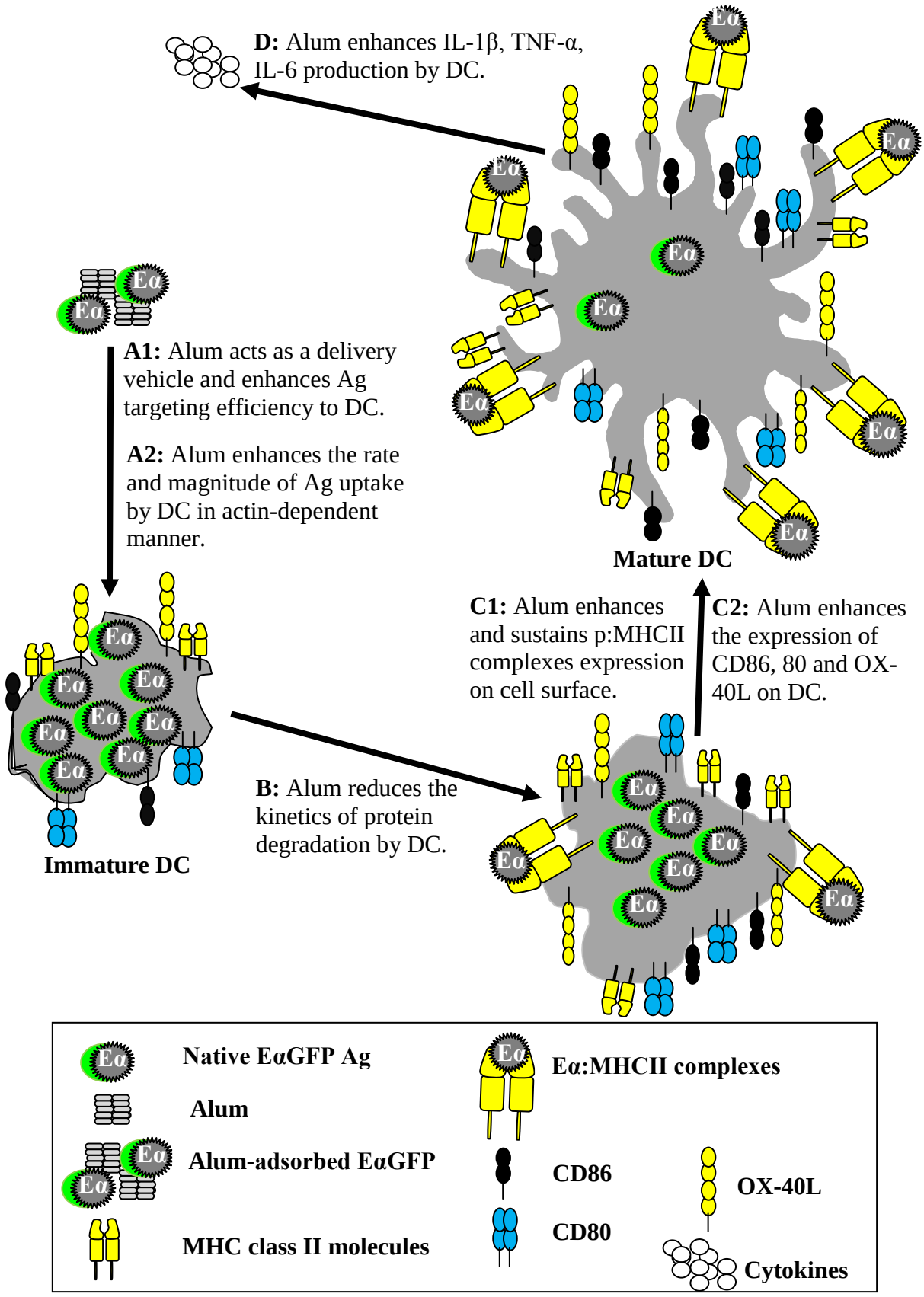

FIGURE 6.1: Illustrative conclusion of mechanisms of Alum adjuvants *in vitro*.

6.2 Future studies

In the studies presented in this thesis, the impact of Alum on the cell biology of BMDC has been characterised *in vitro*. However, several remaining questions have to be addressed in future. They are described below:

A. Remaining questions related to antigen presentation (Signal 1)

The first issue is how Alum influences antigen processing. This is important as recent studies suggest that adjuvants can influence the breadth of peptide recognition in a vaccine, in addition to well characterised effects on magnitude and quality of T cell response [348,516]. To fully understand the processing of antigen in the context of p:MHC complexes, four issues are important.

Firstly, how Alum slows down processing of antigen inside endosomes is not completely understood. This can be studied, for example by a time-dependent experiment using protease inhibitors that block antigen processing in late endosomes [348] or use of chloroquine that raises endosomal pH and inhibits antigen processing in late endosomes [517].

The second issue to be addressed is where does Alum induce a peptide loading step in DCs, i.e., in early endosomes or in late endosomes or on plasma membrane [441]. This can be studied by using cycloheximide that inhibits MHC class II synthesis by blocking translation elongation [518] or Brefeldin A that blocks the transport of MHC class II molecules from ER to the Golgi bodies [519] or using fluorescently tagged antigens and/or antibodies followed by confocal imaging.

Thirdly, it is an important question whether Alum allows cross presentation of externally treated protein antigens. This question is important because of the influence of Alum on phagocytic activity of DCs in the current *in vitro* experiment **(CHAPTER-3)** and cytotoxic responses generated by Alum in the previous *in vivo* experiments [382,383]. This question can be addressed by using the same kind of approach as EαGFP/YAe. For example, a monoclonal antibody (T cell AntiGen

monoclonal antibody) specific for MHC class I (H-2K^b)-SIINFEKL (OVApeptide257–264) can be used to detect the p:MHCI complexes [520]. In addition, an anti-peptide antibody that binds cognate peptide (SIINFEKL) and blocks MHC class I pathway [521] can be used as a negative control in the study of the impact of Alum in the presentation of p:MHCI complexes.

Finally, it is not clear why preadsorption of antigen in Alum is not necessary to boost antigen presenting efficiency of DCs *in vitro*. Therefore, if Alum does not work as an antigen delivery vehicle, an alternative mechanism of action remains to be elucidated. In this context, Flach and colleagues (2011) have found that initial interaction of Alum with DC membrane leads to lipid sorting and consequently enhances antigen uptake by DC without Alum being internalised [53]. Though their results are based on SEM, TEM would be the best tool to observe Alum particles inside cells which would prove the hypothesis that Alum enhances adsorbed antigens via phagocytosis in an actin-dependent manner [53]. This would also prove Hornung's idea (2008) that Alum induces breakage of phagosome following antigen uptake in actin-dependent manner and consequently enhances production of IL-1β [328]. Therefore, further studies should be conducted to confirm the presence or absence of Alum particles inside BMDC by TEM.

B. Remaining questions related to costimulation (Signal 2)

While the current experiments have descrbed the role of Alum in the expression of costimulatory molecules on DC, analysis of only 4 costimulatory molecules did not give us complete understanding of costimulation. For example, costimulatory molecules such as CD70 and CD83, other than those studied in this thesis are gaining significant interest for vaccinologists because both molecules play roles in adaptive immune responses. For example, CD70-CD27 ligation has been suggested to control the priming, expansion and memory function of CD8+ T cells [522]. This ligation seems to be more important than CD80/86-CD28 in survival of antigen-activated CD8 T cells in non-lymphoid tissues [265]. The study of this costimulatory molecule will therefore be important to further understand the

mechanisms of Alum adjuvant in MHC class I-mediated activation of naive CD8 T cells.

In the same way, the membrane-bound CD83 molecule drives activation and proliferation of naive CD8 T cells *in vitro* [523] and peripheral CD4 T cells *in vivo* [524]. Though wild type DCs and $CD83^{-/-}$ DCs are equally able to induce proliferation in mixed lymphocyte reaction (MLR) assays, several studies have shown the significance of this molecule in antigen presentation. MHC class II and cell surface CD86 levels are significantly decreased on the surface of APCs from $CD83^{-/-}$ mice [525,526]. In contrast, the transgenic overexpression of CD83 leads to enhanced cell surface MHC class II and CD86 expression by mouse B cells [527] indicating the possible role of this molecule in antigen presentation and T cell activation. In the context of vaccine adjuvant, the impact of Alum on CD83 has been previously studied in human PBMCs [339,439]. For example, Ulanova et al., 2001 reported that a 2-day exposure of whole PMBCs to Aluminium hydroxide (5µg/mL) induces monocytes to acquire CD83 expression, a typical DC morphology, and an increased expression of MHCII molecules and CD86 [339]. Rimaniol et al. 2007 has reported the increased CD83 expression from macrophages after cells were incubated with 3µg/mL for 3days [528]. Their study in 2004 found the positive impact of Alum adjuvant (from 1–10µg/mL) in dose-dependent manner in CD83 expression from macrophages after they were incubated for 2days [439]. They also reported that incubation at 2µg/mL initially increased CD83 positive cells at 15hours, and then increased at 36hours with its reduction after 120hours indicating the phenotypic change of macrophages into a mature DCs-like structure [439]. These studies also conclude that the waay Alum modulates the function of DCs by influencing CD83 molecules will be crucial in rational vaccine design. In addition, the comprehensive analysis of variables such as incubation period, concentration and structural form of Alum and the types of costimulatory molecules will furnish the answers related to costimulation on BMDC influenced by this adjuvant.

C. Remaining questions related to cytokine production (Signal 3)

In the current thesis, the influence of Alum has been addressed on selective cytokine production. However, how this adjuvant affects the production of other key pro-inflammatory cytokines such as IL-1α, IL-8, and IL-18 by BMDCs is not known. Therefore, further studies would be critical to understand the cumulative production of these cytokines by BMDCs. In addition, detailed studies should be conducted to assess the level of IL-33 cytokines by different ways such as flow cytometry other than by ELISA.

D. Remaining questions related to death of cells

In this thesis, the influence of Alum has been addressed in death of cells especially via apoptosis and necrosis pathway. While Alum induced apoptosis of DCs, necrosis has not been found within 24hours incubation. Therefore, further studies involving the kinetics of apoptosis and necrosis of DCs following Alum treatment would tell us its effect on proinflammatory cytokines. In addition, studies involving mice lacking NALP3 inflammasomes ($NALP3^{-/-}$ mice), agents that block programmed cell death and cell culture involving using of necrotic bodies produced by Alum will be helpful to understand the mechanism of inflammation, apoptosis and bystander effects of Alum via the necrosis pathway.

E. Remaining questions related to depot effects of Alum

The current *in vivo* studies have limitations regarding the hypothesis that Alum enhances LN shutdown. This study clearly show that Alum does not enhance magnitude and duration of the antigen-specific CD4 T cell expansion, but it does not show whether it affects CD8 T cell expansion *in vivo*. Therefore, tracking antigen-specific CD8 T cells will give us understanding how these adjuvants affect the magnitude and duration of immune responses in the context of cytotoxic T cell induction.

Another issue of Alum-mediated response is inflammation at the injection site. To understand the slowly released antigens from the injection sites into the DLNs, EαGFP/YAe system can be used [407]. Performing an experiment which involves injection of animals with EαGFP adsorbed to Alum following preparation of single cell suspension of excised portion of immunised sites and finally analysing the magnitude and duration of the GFP and YAe staining will clearly demonstrate the depot effect of Alum. Though similar type of study has been conducted recently [379], a different kinetic study and transfer of APCs that engulf Alum particles will allow us to know the lifecycle of adsorbed antigens in the injection site.

While the current study directly shows LN shutdown to be due to the recruitment of antigen-nonspecific CD4 positive cells, it does not show which subsets of lymphocytes other than CD4 positive population are affected by this process. LN shutdown increases the probability that an antigen-specific T cell will encounter its cognate antigen presented by APC in the inflamed LN draining the site of vaccine administration [510,511,513]. Therefore, targeting those cells responsible for LN shutdown is important in designing vaccines. In addition, studies involving the detailed information about chemokines (for example, CCR7), cytokines (for example, inflammatory cytokines) and $S1P_1$ molecules involved in Alum-mediated LN shutdown and antigen-specific T cell expansion will provide answers *in vivo*. Understanding the mechanism(s) of Alum adjuvant in controlling the expression and production of these proteins and consequently in determining the magnitude and duration of these responses will make a significant contribution to the rational design of effective, safe and new adjuvants in future.

REFERENCES

[1] Bonanni P, Santos, J.I. Vaccine evolution: Elsevier, 2011.

[2] WHO. WHO vaccine-preventable diseases: monitoring system, 2010 global summary. In: The Department of Immunisation VaB, editor: World Health Organisation, 2010: 1-31.

[3] WHO. Polio vaccines and polio immunization in the pre-eradication era: WHO position paper. *Wkly Epidemiol Rec* 2010; **85:** 213-228.

[4] Rappuoli R, Miller HI, Falkow S. The intangible value of vaccination. *Science* 2002; **297:** 937-939.

[5] Ebensen T, Link, C, Guzman, CA. Classical bacterial vaccines: WILEY- VCH Verlag GmbH & Co. KGaA, Weinheim, 2004.

[6] Wilson-Welder JH, Torres MP, Kipper MJ, Mallapragada SK, Wannemuehler MJ, Narasimhan B. Vaccine adjuvants: current challenges and future approaches. *J Pharm Sci* 2009; **98:**1278-1316.

[7] Melnick JL. Advantages and inconveniences of inactive and live antipoliomyelitis vaccines. *Bull World Health Organ* 1978; **56:** 677-698.

[8] Melnick JL. Viral vaccines: new problems and prospects. *Hosp Pract* 1978; **13:** 104-112.

[9] Baxter D. Active and passive immunity, vaccine types, excipients and licensing. *Occup Med (Lond)* 2007; **57:** 552-556.

[10] CDC. Epidemiology and prevention of vaccine-preventable diseases. Washington DC: Public Health Foundation, 2011.

[11] Anonymous. Diphtheria and tetanus toxoids and acellular pertussis vaccine adsorbed tripedia. AHFS Category: **80:** 08. Accessed from, http://www.fda.gov/downloads/biologicsbloodvaccines/vaccines/approvedproducts/ucm101580.pdf, Accessed on 14 March 2012.

[12] Kwok R. Vaccines: The real issues in vaccine safety. *Nature* 2011; **473:** 436-438.

[13] Lattanzi M, Giudice G.D., Rappuoli, R. Subunit vaccines and toxoids: WILEY-VCH Verlag GmbH &Co. KGaA, Weinheim, 2004.

[14] Relyveld EH. A History of Toxoids. In: Plotkin SA, editor. History of Vaccine Development: Springer New York Dordrecht Heidelberg London, 2011: 57-64.

[15] Rappuoli R. Bridging the knowledge gaps in vaccine design. *Nat Biotechnol* 2007; **25:** 1361-1366.

[16] Coenen F, Tolboom JT, Frijlink HW. Stability of influenza sub-unit vaccine. Does a couple of days outside the refrigerator matter? *Vaccine* 2006; **24:** 525-531.

[17] Plotkin SA. Vaccines, vaccination, and vaccinology. *J Infect Dis* 2003; **187:** 1349-1359.

[18] Schiller JT, Lowy, D.R. Developmental history of HPV prophylactic vaccines: Springer Science+Business Media, LLC, 2011.

[19] Hilleman MR. Three Decades of Hepatitis Vaccinology in Historic Perspective. A Paradigm of Successful Pursuits: Springer Science, 2011.

[20] Wiktor TJ, Macfarlan RI, Reagan KJ, Dietzschold B, Curtis PJ, Wunner WH, et al. Protection from rabies by a vaccinia virus recombinant containing the rabies virus glycoprotein gene. *Proc Natl Acad Sci USA* 1984; **81:** 7194-7198.

[21] Rupprecht CE, Wiktor TJ, Johnston DH, Hamir AN, Dietzschold B, Wunner WH, et al. Oral immunization and protection of raccoons (*Procyon lotor*) with a vaccinia-rabies glycoprotein recombinant virus vaccine. *Proc Natl Acad Sci USA* 1986; **83:** 7947-7950.

[22] Van Regenmortel MH. Reductionism and complexity in molecular biology. Scientists now have the tools to unravel biological and overcome the limitations of reductionism. *EMBO Rep* 2004; **5:** 1016-1020.

[23] Germain RN. Vaccines and the future of human immunology. *Immunity* 2010; **33:** 441-450.

[24] Levine MM, Sztein MB. Vaccine development strategies for improving immunization: the role of modern immunology. *Nat Immunol* 2004; **5:** 460-464.

[25] Beverley PC. Immunology of vaccination. *Br Med Bull* 2004; **62:** 15-28.

[26] Siegrist C-A. Vaccine Immunology: Elsevier Inc., 2008.

[27] Edelman R. The development and use of vaccine adjuvants. *Mol Biotechnol* 2002; **21:** 129-148.

[28] Edelman R, Tacket CO. Adjuvants. *Int Rev Immunol* 1990; **7:** 51-66.

[29] Janeway CA, Jr. Approaching the asymptote? Evolution and revolution in immunology. *Cold Spring Harb Symp Quant Biol* 1989; **54 Pt 1:** 1-13.

[30] Schijns VE, Lavelle EC. Trends in vaccine adjuvants. *Expert Rev Vaccines*

2011; **10:** 539-550.

[31] Schijns VE. Immunological concepts of vaccine adjuvant activity. *Curr Opin Immunol* 2000; **12:** 456-463.

[32] Schijns VE. Mechanisms of vaccine adjuvant activity: initiation and regulation of immune responses by vaccine adjuvants. *Vaccine* 2003; **21:** 829-831.

[33] Mosca F, Tritto E, Muzzi A, Monaci E, Bagnoli F, Iavarone C, et al. Molecular and cellular signatures of human vaccine adjuvants. *Proc Natl Acad Sci USA* 2008; **105:** 10501-10506.

[34] O'Hagan DT, De Gregorio E. The path to a successful vaccine adjuvant--'the long and winding road'. *Drug Discov Today* 2009; **14:** 541-551.

[35] Leroux-Roels G. Unmet needs in modern vaccinology: adjuvants to improve the immune response. *Vaccine* 2010; **28 (Suppl 3):** C25-36.

[36] Leroux-Roels I, Roman F, Forgus S, Maes C, De Boever F, Drame M, et al. Priming with AS03 A-adjuvanted H5N1 influenza vaccine improves the kinetics, magnitude and durability of the immune response after a heterologous booster vaccination: an open non-randomised extension of a double-blind randomised primary study. *Vaccine* 2010; **28:** 849-857.

[37] Aimanianda V, Haensler J, Lacroix-Desmazes S, Kaveri SV, Bayry J. Novel cellular and molecular mechanisms of induction of immune responses by Aluminum adjuvants. *Trends Pharmacol Sci* 2009; **30:** 287-295.

[38] Clements CJ, Griffiths E. The global impact of vaccines containing Aluminium adjuvants. *Vaccine* 2002; **20 (Suppl 3):** S24-33.

[39] Duthie MS, Windish HP, Fox CB, Reed SG. Use of defined TLR ligands as adjuvants within human vaccines. *Immunol Rev* 2011; **239:** 178-196.

[40] Einstein MH, Baron M, Levin MJ, Chatterjee A, Edwards RP, Zepp F, et al. Comparison of the immunogenicity and safety of Cervarix and Gardasil human papillomavirus (HPV) cervical cancer vaccines in healthy women aged 18-45 years. *Hum Vaccin* 2009; **5:** 705-719.

[41] Einstein MH, Schiller JT, Viscidi RP, Strickler HD, Coursaget P, Tan T, et al. Clinician's guide to human papillomavirus immunology: knowns and unknowns. *Lancet Infect Dis* 2009; **9:** 347-356.

[42] Tritto E, Mosca F, De Gregorio E. Mechanism of action of licensed vaccine adjuvants. *Vaccine* 2009; **27:** 3331-3334.

[43] Mbow ML, De Gregorio E, Valiante NM, Rappuoli R. New adjuvants for human vaccines. *Curr Opin Immunol* 2010; **22:** 411-416.

[44] Glenny AT, Pope, C.G., Waddington, H., Wallace, U. Immunological notes. XXIII. The antigenic value of toxoid precipitated by potassium Alum. *Journal of Pathology* 1926; **29:** 38-49.

[45] Glenny AT, Buttle, G.A.H., Stevens, M.F. Rate of disappearance of diphtheria toxoid injected into rabbits and guinea pigs: toxoid precipitated with Alum. *Journal of Pathology and Bacteriology* 1931; **34:** 267-275.

[46] Glenny AT, Sudmersen HJ. Notes on the Production of Immunity to Diphtheria Toxin. *J Hyg (Lond)* 1921; **20:** 176-220.

[47] Marrack P, McKee AS, Munks MW. Towards an understanding of the adjuvant action of Aluminium. *Nat Rev Immunol* 2009; **9:** 287-293.

[48] Baylor NW, Egan W, Richman P. Aluminum salts in vaccines—US perspective. *Vaccine* 2002; **20 (Suppl 3):** S18-23.

[49] Shirodkar S, Hutchinson RL, Perry DL, White JL, Hem SL. Aluminum compounds used as adjuvants in vaccines. *Pharm Res* 1990; **7:** 1282-1288.

[50] Lindblad EB. Aluminium adjuvants--in retrospect and prospect. *Vaccine* 2004; **22:** 3658-3668.

[51] Fujimaki H, Ozawa M, Imai T, Kubota K, Watanabe N. Adjuvant effects of Aluminum silicate on IgE and IgG1 antibody production in mice. *Int Arch Allergy Appl Immunol* 1984; **75:** 351-356.

[52] Cooper PD, Steele EJ. Algammulin, a new vaccine adjuvant comprising gamma inulin particles containing Alum: preparation and *in vitro* properties. *Vaccine* 1991; **9:** 351-357.

[53] Flach TL, Ng G, Hari A, Desrosiers MD, Zhang P, Ward SM, et al. Alum interaction with dendritic cell membrane lipids is essential for its adjuvanticity. *Nat Med* 2011; **17:** 479-487.

[54] Kool M, Soullie T, van Nimwegen M, Willart MA, Muskens F, Jung S, et al. Alum adjuvant boosts adaptive immunity by inducing uric acid and activating inflammatory dendritic cells. *J Exp Med* 2008; **205:** 869-882.

[55] Marichal T, Ohata K, Bedoret D, Mesnil C, Sabatel C, Kobiyama K, et al. DNA released from dying host cells mediates Aluminum adjuvant activity. *Nat Med* 2011; **17:** 996-1002.

[56] Hem SL, Johnston CT, HogenEsch H. Imject Alum is not Aluminum hydroxide adjuvant or Aluminum phosphate adjuvant. *Vaccine* 2007; **25:** 4985-4986.

[57] Hem SL, HogenEsch H. Aluminum-containing adjuvants: Properties,

Formulations and Use. New Jersey: John Wiley & Sons, Inc., 2007.

[58] Johnston CT, Wang SL, Hem SL. Measuring the surface area of Aluminum hydroxide adjuvant. *J Pharm Sci* 2002; **91:** 1702-1706.

[59] Iyer S, HogenEsch H, Hem SL. Effect of the degree of phosphate substitution in Aluminum hydroxide adjuvant on the adsorption of phosphorylated proteins. *Pharm Dev Technol* 2003; **8:** 81-86.

[60] Lindblad EB. Aluminium compounds for use in vaccines. *Immunol Cell Biol* 2004; **82:** 497-505.

[61] Yau KP, Schulze DG, Johnston CT, Hem SL. Aluminum hydroxide adjuvant produced under constant reactant concentration. *J Pharm Sci* 2006; **95:** 1822-1833.

[62] Seeber SJ, White JL, Hem SL. Predicting the adsorption of proteins by Aluminium-containing adjuvants. *Vaccine* 1991; **9:** 201-203.

[63] Lindblad EB, Schonberg NE. Aluminum adjuvants: preparation, application, dosage, and formulation with antigen. *Methods Mol Biol* 2010; **626:** 41-58.

[64] Morefield GL, Jiang D, Romero-Mendez IZ, Geahlen RL, Hogenesch H, Hem SL. Effect of phosphorylation of ovalbumin on adsorption by Aluminum-containing adjuvants and elution upon exposure to interstitial fluid.*Vaccine* 2005; **23:** 1502-1506.

[65] Rinella Jr JV, White JL, Hem SL. Effect of Anions on Model Aluminum-Adjuvant-Containing Vaccines. *Journal of Colloid and Interface Science* 1995; **172:**121.

[66] Burrell LS, Lindblad EB, White JL, Hem SL. Stability of Aluminium-containing adjuvants to autoclaving. *Vaccine* 1999; **17:** 2599-2603.

[67] Vecchi S, Bufali S, Skibinski DA, O'Hagan DT, Singh M. Aluminum adjuvant dose guidelines in vaccine formulation for preclinical evaluations. *J Pharm Sci* 2012; **101:** 17-20.

[68] Gherardi RK. Lessons from macrophagic myofasciitis: towards definition of a vaccine adjuvant-related syndrome. *Rev Neurol (Paris)* 2003; **159:** 162-164.

[69] Gherardi RK, Coquet M, Cherin P, Authier FJ, Laforet P, Belec L, et al. Macrophagic myofasciitis: an emerging entity. Groupe d'Etudes et Recherche sur les Maladies Musculaires Acquises et Dysimmunitaires (GERMMAD) de l'Association Francaise contre les Myopathies (AFM). *Lancet* 1998; **352:** 347-352.

[70] Brenner A. Macrophagic Myofasciitis: a summary of Dr. Gherardi’s

presentations. *Vaccine* 2002; **20 (Supplement 3):** S5-S6.

[71] Mrak RE. Muscle granulomas following intramuscular injection. *Muscle Nerve* 1982; **5:** 637-639.

[72] Erdohazi M, Newman RL. Aluminium hydroxide granuloma. *Br Med J* 1971; **3:** 621-623.

[73] Savage J. Proceedings: Aluminium hydroxide granuloma. *Proc R Soc Med* 1973; **66:** 984-985.

[74] Lacson AG, D'Cruz CA, Gilbert-Barness E, Sharer L, Jacinto S, Cuenca R. Aluminum phagocytosis in quadriceps muscle following vaccination in children: relationship to macrophagic myofasciitis. *Pediatr Dev Pathol* 2002; **5:** 151-158.

[75] Gupta RK, Relyveld EH, Lindblad EB, Bizzini B, Ben-Efraim S, Gupta CK. Adjuvants--a balance between toxicity and adjuvanticity. *Vaccine* 1993; **11:** 293-306.

[76] Frost L, Johansen P, Pedersen S, Veien N, Ostergaard PA, Nielsen MH. Persistent subcutaneous nodules in children hyposensitized with Aluminium-containing allergen extracts. *Allergy* 1985; **40:** 368-372.

[77] Tomljenovic L, Shaw CA. Aluminum vaccine adjuvants: are they safe? *Curr Med Chem* 2011; **18:** 2630-2637.

[78] Gupta RK, Griffin P, Jr., Chang AC, Rivera R, Anderson R, Rost B, et al. The role of adjuvants and delivery systems in modulation of immune response to vaccines. *Adv Exp Med Biol* 1996; **397:** 105-113.

[79] Gupta RK, Rost BE, Relyveld E, Siber GR. Adjuvant properties of Aluminum and calcium compounds. *Pharm Biotechnol* 1995; **6:** 229-248.

[80] Plotkin SA. Correlates of protection induced by vaccination. *Clin Vaccine Immunol* 2010; **17:** 1055-1065.

[81] Mascola JR, Frankel SS, Broliden K. HIV-1 entry at the mucosal surface: role of antibodies in protection. *Aids* 2000; **14 (Suppl 3):** S167-174.

[82] Mascola JR, Stiegler G, VanCott TC, Katinger H, Carpenter CB, Hanson CE, et al. Protection of macaques against vaginal transmission of a pathogenic HIV-1/SIV chimeric virus by passive infusion of neutralizing antibodies. *Nat Med* 2000; **6:** 207-210.

[83] Moorthy VS, Ballou WR. Immunological mechanisms underlying protection mediated by RTS,S: a review of the available data. *Malar J* 2009; **8:** 312.

[84] Seder RA, Hill AV. Vaccines against intracellular infections requiring cellular immunity. *Nature* 2000; **406:** 793-798.

[85] Brewer JM, Conacher M, Satoskar A, Bluethmann H, Alexander J. In interleukin-4-deficient mice, Alum not only generates T helper 1 responses equivalent to freund's complete adjuvant, but continues to induce T helper 2 cytokine production. *Eur J Immunol* 1996; **26:** 2062-2066.

[86] Grun JL, Maurer PH. Different T helper cell subsets elicited in mice utilizing two different adjuvant vehicles: the role of endogenous interleukin 1 in proliferative responses. *Cell Immunol* 1989; **121:** 134-145.

[87] Bomford R. The comparative selectivity of adjuvants for humoral and cell-mediated immunity. II. Effect on delayed-type hypersensitivity in the mouse and guinea pig, and cell-mediated immunity to tumour antigens in the mouse of Freund's incomplete and complete adjuvants, alhydrogel, *Corynebacterium parvum, Bordetella pertussis,* muramyl dipeptide and saponin. *Clin Exp Immunol* 1980; **39:** 435-441.

[88] Serre K, Mohr E, Toellner KM, Cunningham AF, Granjeaud S, Bird R, et al. Molecular differences between the divergent responses of ovalbumin-specific CD4 T cells to Alum-precipitated ovalbumin compared to ovalbumin expressed by *Salmonella*. *Mol Immunol* 2008; **45:** 3558-3566.

[89] Zurbriggen R, Novak-Hofer I, Seelig A, Gluck R. IRIV-adjuvanted hepatitis A vaccine: *in vivo* absorption and biophysical characterization. *Prog Lipid Res* 2000; **39:** 3-18.

[90] Ott G, Barchfeld GL, Chernoff D, Radhakrishnan R, van Hoogevest P, Van Nest G. MF59. Design and evaluation of a safe and potent adjuvant for human vaccines. *Pharm Biotechnol* 1995; **6:** 277-296.

[91] Ott G, Barchfeld GL, Van Nest G. Enhancement of humoral response against human influenza vaccine with the simple submicron oil/water emulsion adjuvant MF59. *Vaccine* 1995; **13:** 1557-1562.

[92] Morel S, Didierlaurent A, Bourguignon P, Delhaye S, Baras B, Jacob V, et al. Adjuvant System AS03 containing alpha-tocopherol modulates innate immune response and leads to improved adaptive immunity. *Vaccine* 2011; **29:** 2461-2473.

[93] Singh M, Ugozzoli M, Kazzaz J, Chesko J, Soenawan E, Mannucci D, et al. A preliminary evaluation of alternative adjuvants to Alum using a range of established and new generation vaccine antigens. *Vaccine* 2006; **24:** 1680-1686.

[94] Giannini SL, Hanon E, Moris P, Van Mechelen M, Morel S, Dessy F, et al. Enhanced humoral and memory B cellular immunity using HPV16/18 L1 VLP vaccine formulated with the MPL/Aluminium salt combination (AS04)

compared to Aluminium salt only. *Vaccine* 2006; **24:** 5937-5949.

[95] Steinhagen F, Kinjo T, Bode C, Klinman DM. TLR-based immune adjuvants. *Vaccine* 2011; **29:** 3341-3355.

[96] Cox JC, Coulter AR. Adjuvants--a classification and review of their modes of action. *Vaccine* 1997; **15:** 248-256.

[97] Chiarella P, Massi E, De Robertis M, Signori E, Fazio VM. Adjuvants in vaccines and for immunisation: current trends. *Expert Opin Biol Ther* 2007; **7:** 1551-1562.

[98] Reed SG, Bertholet S, Coler RN, Friede M. New horizons in adjuvants for vaccine development. *Trends Immunol* 2009; **30:** 23-32.

[99] van Duin D, Medzhitov R, Shaw AC. Triggering TLR signaling in vaccination. *Trends Immunol* 2006; **27:** 49-55.

[100] Kawai T, Akira S. The role of pattern-recognition receptors in innate immunity: update on Toll-like receptors. *Nat Immunol* 2010; **11:** 373-384.

[101] Sieling PA, Chung W, Duong BT, Godowski PJ, Modlin RL. Toll-like receptor 2 ligands as adjuvants for human Th1 responses. *J Immunol* 2003; **170:** 194-200.

[102] Rharbaoui F, Drabner B, Borsutzky S, Winckler U, Morr M, Ensoli B, et al. The Mycoplasma-derived lipopeptide MALP-2 is a potent mucosal adjuvant. *Eur J Immunol* 2002; **32:** 2857-2865.

[103] Takeuchi O, Kaufmann A, Grote K, Kawai T, Hoshino K, Morr M, et al. Cutting edge: preferentially the R-stereoisomer of the mycoplasmal lipopeptide macrophage-activating lipopeptide-2 activates immune cells through a toll-like receptor 2- and MyD88-dependent signaling pathway. *J Immunol* 2000; **164:** 554-557.

[104] Jackson DC, Lau YF, Le T, Suhrbier A, Deliyannis G, Cheers C, et al. A totally synthetic vaccine of generic structure that targets Toll-like receptor 2 on dendritic cells and promotes antibody or cytotoxic T cell responses. *Proc Natl Acad Sci USA* 2004; **101:** 15440-15445.

[105] Underhill DM, Ozinsky A, Hajjar AM, Stevens A, Wilson CB, Bassetti M, et al. The Toll-like receptor 2 is recruited to macrophage phagosomes and discriminates between pathogens. *Nature* 1999; 401: 811-815.

[106] Underhill DM, Ozinsky A, Smith KD, Aderem A. Toll-like receptor-2 mediates mycobacteria-induced proinflammatory signaling in macrophages. *Proc Natl Acad Sci USA* 1999; **96:** 14459-14463.

[107] Schnare M, Barton GM, Holt AC, Takeda K, Akira S, Medzhitov R. Toll-like receptors control activation of adaptive immune responses. *Nat Immunol* 2001; **2:** 947-950.

[108] Schulz O, Diebold SS, Chen M, Naslund TI, Nolte MA, Alexopoulou L, et al. Toll-like receptor 3 promotes cross-priming to virus-infected cells. *Nature* 2005; **433:** 887-892.

[109] Alexopoulou L, Holt AC, Medzhitov R, Flavell RA. Recognition of double-stranded RNA and activation of NF-kappaB by Toll-like receptor 3. *Nature* 2001; **413:** 732-738.

[110] Gitlin L, Barchet W, Gilfillan S, Cella M, Beutler B, Flavell RA, et al. Essential role of mda-5 in type I IFN responses to polyriboinosinic:polyribocytidylic acid and encephalomyocarditis picornavirus. *Proc Natl Acad Sci USA* 2006; **103:** 8459-8464.

[111] McSorley SJ, Ehst BD, Yu Y, Gewirtz AT. Bacterial flagellin is an effective adjuvant for CD4+ T cells *in vivo*. *J Immunol* 2002; **169:** 3914-3919.

[112] Franchi L, Park JH, Shaw MH, Marina-Garcia N, Chen G, Kim YG, et al. Intracellular NOD-like receptors in innate immunity, infection and disease. *Cell Microbiol* 2008; **10:** 1-8.

[113] Zamboni DS, Kobayashi KS, Kohlsdorf T, Ogura Y, Long EM, Vance RE, et al. The Birc1e cytosolic pattern-recognition receptor contributes to the detection and control of *Legionella pneumophila* infection. *Nat Immunol* 2006; **7:** 318-325.

[114] Hemmi H, Kaisho T, Takeuchi O, Sato S, Sanjo H, Hoshino K, et al. Small anti-viral compounds activate immune cells via the TLR7 MyD88-dependent signaling pathway. *Nat Immunol* 2002; **3:** 196-200.

[115] Klinman DM, Currie D, Gursel I, Verthelyi D. Use of CpG oligodeoxynucleotides as immune adjuvants. *Immunol Rev* 2004; **199:** 201-216.

[116] Coban C, Ishii KJ, Kawai T, Hemmi H, Sato S, Uematsu S, et al. Toll-like receptor 9 mediates innate immune activation by the malaria pigment hemozoin. *J Exp Med* 2005; **201:** 19-25.

[117] Willart MA, Lambrecht BN. The danger within: endogenous danger signals, atopy and asthma. *Clin Exp Allergy* 2009; **39:** 12-19.

[118] Takemoto S, Nishikawa M, Takakura Y. Pharmacokinetic and tissue distribution mechanism of mouse recombinant heat shock protein 70 in mice. *Pharm Res* 2005; **22:** 419-426.

[119] Stebbing J, Savage P, Patterson S, Gazzard B. All for CD91 and CD91 for all. *J*

Antimicrob Chemother 2004; **53:** 1-3.

[120] Aalamian M, Fuchs E, Gupta R, Levey DL. Autologous renal cell cancer vaccines using heat shock protein-peptide complexes. *Urol Oncol* 2006; **24:** 425-433.

[121] Basu S, Binder RJ, Ramalingam T, Srivastava PK. CD91 is a common receptor for heat shock proteins gp96, hsp90, hsp70, and calreticulin. *Immunity* 2001; **14:** 303-313.

[122] Udono H, Yamano T, Kawabata Y, Ueda M, Yui K. Generation of cytotoxic T lymphocytes by MHC class I ligands fused to heat shock cognate protein 70. *Int Immunol* 2001; **13:** 1233-1242.

[123] Osterloh A, Breloer M. Heat shock proteins: linking danger and pathogen recognition. *Med Microbiol Immunol* 2008; **197:** 1-8.

[124] Osterloh A, Veit A, Gessner A, Fleischer B, Breloer M. Hsp60-mediated T cell stimulation is independent of TLR4 and IL-12. *Int Immunol* 2008; **20:** 433-443.

[125] Blachere NE, Li Z, Chandawarkar RY, Suto R, Jaikaria NS, Basu S, et al. Heat shock protein-peptide complexes, reconstituted *in vitro*, elicit peptide- specific cytotoxic T lymphocyte response and tumor immunity. *J Exp Med* 1997; **186:** 1315-1322.

[126] Schaefer L. Extracellular matrix molecules: endogenous danger signals as new drug targets in kidney diseases. *Curr Opin Pharmacol* 2010; **10:** 185-190.

[127] Wagner H, Bauer S. All is not Toll: new pathways in DNA recognition. *J Exp Med* 2006; **203:** 265-268.

[128] Takaoka A, Wang Z, Choi MK, Yanai H, Negishi H, Ban T, et al. DAI (DLM-1/ZBP1) is a cytosolic DNA sensor and an activator of innate immune response. *Nature* 2007; **448:** 501-505.

[129] Idzko M, Panther E, Sorichter S, Herouy Y, Berod L, Geissler M, et al. Characterization of the biological activities of uridine diphosphate in human dendritic cells: Influence on chemotaxis and CXCL8 release. *J Cell Physiol* 2004; **201:** 286-293.

[130] Warny M, Aboudola S, Robson SC, Sevigny J, Communi D, Soltoff SP, et al. P2Y(6) nucleotide receptor mediates monocyte interleukin-8 production in response to UDP or lipopolysaccharide. *J Biol Chem* 2001; **276:** 26051-26056.

[131] Yang Z, Tao T, Raftery MJ, Youssef P, Di Girolamo N, Geczy CL. Proinflammatory properties of the human S100 protein S100A12. *J Leukoc Biol* 2001; **69:** 986-994.

[132] Messmer D, Yang H, Telusma G, Knoll F, Li J, Messmer B, et al. High mobility group box protein 1: an endogenous signal for dendritic cell maturation and Th1 polarization. *J Immunol* 2004; **173:** 307-313.

[133] Sundberg E, Fasth AE, Palmblad K, Harris HE, Andersson U. High mobility group box chromosomal protein 1 acts as a proliferation signal for activated T lymphocytes. *Immunobiology* 2009; **214:** 303-309.

[134] Yang D, Tewary P, de la Rosa G, Wei F, Oppenheim JJ. The alarmin functions of high-mobility group proteins. *Biochim Biophys Acta* 2010; **1799:** 157-163.

[135] Coutinho-Silva R, Correa G, Sater AA, Ojcius DM. The P2X(7) receptor and intracellular pathogens: a continuing struggle. *Purinergic Signal* 2009; **5:** 197-204.

[136] Coutinho-Silva R, Monteiro da Cruz C, Persechini PM, Ojcius DM. The role of P2 receptors in controlling infections by intracellular pathogens. *Purinergic Signal* 2007; **3:** 83-90.

[137] Schaefer L, Schaefer RM. Proteoglycans: from structural compounds to signaling molecules. *Cell Tissue Res* 2010; **339:** 237-246.

[138] Bosch FX. Broad-spectrum human papillomavirus vaccines: new horizons but one step at a time. *J Natl Cancer Inst* 2009; **101:** 771-773.

[139] Guy B. The perfect mix: recent progress in adjuvant research. *Nat Rev Microbiol* 2007; **5:** 505-517.

[140] Harandi AM, Medaglini D, Shattock RJ. Vaccine adjuvants: a priority for vaccine research. *Vaccine* 2010; **28:** 2363-2366.

[141] Stanberry LR, Strugnell R. Vaccines of the future. *Perspectives in Vaccinology* 2011; **1:** 151-199.

[142] Akira S, Uematsu S, Takeuchi O. Pathogen recognition and innate immunity. *Cell* 2006; **124:** 783-801.

[143] Janeway CA, Jr., Medzhitov R. Innate immune recognition. *Annu Rev Immunol* 2002; **20:** 197-216.

[144] Gray D. A role for antigen in the maintenance of immunological memory. *Nat Rev Immunol* 2002; **2:** 60-65.

[145] Fazilleau N, Eisenbraun MD, Malherbe L, Ebright JN, Pogue-Caley RR, McHeyzer-Williams LJ, et al. Lymphoid reservoirs of antigen-specific memory T helper cells. *Nat Immunol* 2007; **8:** 753-761.

[146] Banchereau J, Steinman RM. Dendritic cells and the control of immunity.

Nature 1998; **392:** 245-252.

[147] Rossi M, Young JW. Human dendritic cells: potent antigen-presenting cells at the crossroads of innate and adaptive immunity. *J Immunol* 2005; **175:** 1373-1381.

[148] Steinman RM. Dendritic cells *in vivo*: a key target for a new vaccine science. *Immunity* 2008; **29:** 319-324.

[149] Steinman RM, Banchereau J. Taking dendritic cells into medicine. *Nature* 2007; **449:** 419-426.

[150] Steinman RM. Dendritic cells and vaccines. *Proc (Bayl Univ Med Cent)* 2008; **21:** 3-8.

[151] Randolph GJ, Sanchez-Schmitz G, Liebman RM, Schakel K. The CD16(+) (FcgammaRIII(+)) subset of human monocytes preferentially becomes migratory dendritic cells in a model tissue setting. *J Exp Med* 2002; **196:** 517-527.

[152] Lutz MB, Kukutsch N, Ogilvie AL, Rossner S, Koch F, Romani N, et al. An advanced culture method for generating large quantities of highly pure dendritic cells from mouse bone marrow. *J Immunol Methods* 1999; **223:** 77-92.

[153] Inaba K, Inaba M, Deguchi M, Hagi K, Yasumizu R, Ikehara S, et al. Granulocytes, macrophages, and dendritic cells arise from a common major histocompatibility complex class II-negative progenitor in mouse bone marrow. *Proc Natl Acad Sci USA* 1993; **90:** 3038-3042.

[154] Wu L, Liu YJ. Development of dendritic-cell lineages. *Immunity* 2007; **26:** 741-750.

[155] Sallusto F, Lanzavecchia A. Efficient presentation of soluble antigen by cultured human dendritic cells is maintained by granulocyte/macrophage colony-stimulating factor plus interleukin 4 and downregulated by tumor necrosis factor alpha. *J Exp Med* 1994; **179:** 1109-1118.

[156] Shortman K, Lahoud MH, Caminschi I. Improving vaccines by targeting antigens to dendritic cells. *Exp Mol Med* 2009; **41:** 61-66.

[157] Shortman K, Naik SH. Steady-state and inflammatory dendritic-cell development. *Nat Rev Immunol* 2007; **7:** 19-30.

[158] Sato K, Fujita S. Dendritic cells: nature and classification. *Allergol Int* 2007; **56:** 183-191.

[159] Bjorck P. Isolation and characterization of plasmacytoid dendritic cells from

Flt3 ligand and granulocyte-macrophage colony-stimulating factor-treated mice. *Blood* 2001; **98:** 3520-3526.

[160] Nakano H, Yanagita M, Gunn MD. CD11c(+)B220(+)Gr-1(+) cells in mouse lymph nodes and spleen display characteristics of plasmacytoid dendritic cells. *J Exp Med* 2001; **194:** 1171-1178.

[161] Villadangos JA, Young L. Antigen-presentation properties of plasmacytoid dendritic cells. *Immunity* 2008; **29:** 352-361.

[162] Liu YJ. IPC: professional type 1 interferon-producing cells and plasmacytoid dendritic cell precursors. *Annu Rev Immunol* 2005; **23:** 275-306.

[163] Colonna M, Trinchieri G, Liu YJ. Plasmacytoid dendritic cells in immunity. *Nat Immunol* 2004; **5:** 1219-1226.

[164] Banchereau J, Pascual V, Palucka AK. Autoimmunity through cytokine-induced dendritic cell activation. *Immunity* 2004; **20:** 539-550.

[165] Banchereau J, Pulendran B, Steinman R, Palucka K. Will the making of plasmacytoid dendritic cells *in vitro* help unravel their mysteries? *J Exp Med* 2000; **192:** F39-44.

[166] den Haan JM, Lehar SM, Bevan MJ. CD8(+) but not CD8(-) dendritic cells cross-prime cytotoxic T cells *in vivo*. *J Exp Med* 2000; **192:** 1685-1696.

[167] Grohmann U, Fallarino F, Silla S, Bianchi R, Belladonna ML, Vacca C, et al. CD40 ligation ablates the tolerogenic potential of lymphoid dendritic cells. *J Immunol* 2001; **166:** 277-283.

[168] Yarovinsky F, Kanzler H, Hieny S, Coffman RL, Sher A. Toll-like receptor recognition regulates immunodominance in an antimicrobial CD4+ T cell response. *Immunity* 2006; **25:** 655-664.

[169] Maroof A, Kaye PM. Temporal regulation of interleukin-12p70 (IL-12p70) and IL-12-related cytokines in splenic dendritic cell subsets during Leishmania donovani infection. *Infect Immun* 2008; **76:** 239-249.

[170] Belz GT, Shortman K, Bevan MJ, Heath WR. CD8alpha+ dendritic cells selectively present MHC class I-restricted noncytolytic viral and intracellular bacterial antigens *in vivo*. *J Immunol* 2005; **175:** 196-200.

[171] Dudziak D, Kamphorst AO, Heidkamp GF, Buchholz VR, Trumpfheller C, Yamazaki S, et al. Differential antigen processing by dendritic cell subsets *in vivo*. *Science* 2007; **315:** 107-111.

[172] Pulendran B, Smith JL, Caspary G, Brasel K, Pettit D, Maraskovsky E, et al.

Distinct dendritic cell subsets differentially regulate the class of immune response *in vivo*. *Proc Natl Acad Sci USA* 1999; **96:** 1036-1041.

[173] Reis e Sousa C, Hieny S, Scharton-Kersten T, Jankovic D, Charest H, Germain RN, et al. *In vivo* microbial stimulation induces rapid CD40 ligand-independent production of interleukin 12 by dendritic cells and their redistribution to T cell areas. *J Exp Med* 1997; **186:** 1819-1829.

[174] Soares H, Waechter H, Glaichenhaus N, Mougneau E, Yagita H, Mizenina O, et al. A subset of dendritic cells induces CD4+ T cells to produce IFN-gamma by an IL-12-independent but CD70-dependent mechanism *in vivo*. *J Exp Med* 2007; **204:** 1095-1106.

[175] Vremec D, Pooley J, Hochrein H, Wu L, Shortman K. CD4 and CD8 expression by dendritic cell subtypes in mouse thymus and spleen. *J Immunol* 2000; **164:** 2978-2986.

[176] Ingulli E, Ulman DR, Lucido MM, Jenkins MK. In situ analysis reveals physical interactions between CD11b+ dendritic cells and antigen-specific CD4 T cells after subcutaneous injection of antigen. *J Immunol* 2002; **169:** 2247-2252.

[177] Lopez-Bravo M, Ardavin C. *In vivo* induction of immune responses to pathogens by conventional dendritic cells. *Immunity* 2008; **29:** 343-351.

[178] Yasumi T, Katamura K, Yoshioka T, Meguro TA, Nishikomori R, Heike T, et al. Differential requirement for the CD40-CD154 costimulatory pathway during Th cell priming by CD8 alpha+ and CD8 alpha- murine dendritic cell subsets. *J Immunol* 2004; **172:** 4826-4833.

[179] Valladeau J, Ravel O, Dezutter-Dambuyant C, Moore K, Kleijmeer M, Liu Y, et al. Langerin, a novel C-type lectin specific to Langerhans cells, is an endocytic receptor that induces the formation of Birbeck granules. *Immunity* 2000; **12:** 71-81.

[180] Valladeau J, Saeland S. Cutaneous dendritic cells. *Semin Immunol* 2005; **17:** 273-283.

[181] Kissenpfennig A, Ait-Yahia S, Clair-Moninot V, Stossel H, Badell E, Bordat Y, et al. Disruption of the langerin/CD207 gene abolishes Birbeck granules without a marked loss of Langerhans cell function. *Mol Cell Biol* 2005; **25:** 88-99.

[182] Kissenpfennig A, Henri S, Dubois B, Laplace-Builhe C, Perrin P, Romani N, et al. Dynamics and function of Langerhans cells *in vivo*: dermal dendritic cells colonize lymph node areas distinct from slower migrating Langerhans cells. *Immunity* 2005; **22:** 643-654.

[183] Itano AA, McSorley SJ, Reinhardt RL, Ehst BD, Ingulli E, Rudensky AY, et al. Distinct dendritic cell populations sequentially present antigen to CD4 T cells and stimulate different aspects of cell-mediated immunity. *Immunity* 2003; **19:** 47-57.

[184] Bursch LS, Wang L, Igyarto B, Kissenpfennig A, Malissen B, Kaplan DH, et al. Identification of a novel population of Langerin+ dendritic cells. *J Exp Med* 2007; **204:** 3147-3156.

[185] Ginhoux F, Collin MP, Bogunovic M, Abel M, Leboeuf M, Helft J, et al. Blood-derived dermal langerin+ dendritic cells survey the skin in the steady state. *J Exp Med* 2007; **204:** 3133-3146.

[186] Poulin LF, Henri S, de Bovis B, Devilard E, Kissenpfennig A, Malissen B. The dermis contains langerin+ dendritic cells that develop and function independently of epidermal Langerhans cells. *J Exp Med* 2007; **204:** 3119-3131.

[187] Stutte S, Jux B, Esser C, Forster I. CD24a expression levels discriminate Langerhans cells from dermal dendritic cells in murine skin and lymph nodes. *J Invest Dermatol* 2008; **128:** 1470-1475.

[188] Janeway C. Immunogenicity signals 1,2,3. and 0. *Immunol Today* 1989; **10:** 283-286.

[189] Watts C. Capture and processing of exogenous antigens for presentation on MHC molecules. *Annu Rev Immunol* 1997; **15:** 821-850.

[190] Nelson CA, Vidavsky I, Viner NJ, Gross ML, Unanue ER. Amino-terminal trimming of peptides for presentation on major histocompatibility complex class II molecules. *Proc Natl Acad Sci USA* 1997; **94:** 628-633.

[191] Trombetta ES, Mellman I. Cell biology of antigen processing *in vitro* and *in vivo*. *Annu Rev Immunol* 2005; **23:** 975-1028.

[192] Platt CD, Ma JK, Chalouni C, Ebersold M, Bou-Reslan H, Carano RA, et al. Mature dendritic cells use endocytic receptors to capture and present antigens. *Proc Natl Acad Sci USA* 2010; **107:** 4287-4292.

[193] Swanson JA, Watts C. Macropinocytosis. *Trends Cell Biol* 1995; **5:** 424-428.

[194] Morefield GL, Sokolovska A, Jiang D, HogenEsch H, Robinson JP, Hem SL. Role of Aluminum-containing adjuvants in antigen internalization by dendritic cells *in vitro*. *Vaccine* 2005; **23:** 1588-1595.

[195] Xiang SD, Scholzen A, Minigo G, David C, Apostolopoulos V, Mottram PL, et al. Pathogen recognition and development of particulate vaccines: does size matter? *Methods* 2006; 40: 1-9.

[196] Travaglione S, Falzano L, Fabbri A, Stringaro A, Fais S, Fiorentini C. Epithelial cells and expression of the phagocytic marker CD68: scavenging of apoptotic bodies following Rho activation. *Toxicol In vitro* 2002; **16:** 405-411.

[197] Kumari S, Mg S, Mayor S. Endocytosis unplugged: multiple ways to enter the cell. *Cell Res* 2010; **20:** 256-275.

[198] van Kooyk Y. C-type lectins on dendritic cells: key modulators for the induction of immune responses. *Biochem Soc Trans* 2008; **36:** 1478-1481.

[199] van Vliet SJ, Garcia-Vallejo JJ, van Kooyk Y. Dendritic cells and C-type lectin receptors: coupling innate to adaptive immune responses. *Immunol Cell Biol* 2008; **86:** 580-587.

[200] Schjetne KW, Thompson KM, Nilsen N, Flo TH, Fleckenstein B, Iversen JG, et al. Cutting edge: link between innate and adaptive immunity: Toll-like receptor 2 internalizes antigen for presentation to CD4+ T cells and could be an efficient vaccine target. *J Immunol* 2003; **171:** 32-36.

[201] West MA, Wallin RP, Matthews SP, Svensson HG, Zaru R, Ljunggren HG, et al. Enhanced dendritic cell antigen capture via toll-like receptor-induced actin remodeling. *Science* 2004; **305:** 1153-1157.

[202] Garcon N, Morel S, Didierlaurent A, Descamps D, Wettendorff M, Van Mechelen M. Development of an AS04-adjuvanted HPV vaccine with the adjuvant system approach. *BioDrugs* 2011; **25:** 217-226.

[203] Watts C. Antigen processing in the endocytic compartment. *Curr Opin Immunol* 2001; **13:** 26-31.

[204] Villadangos JA, Ploegh HL. Proteolysis in MHC class II antigen presentation: who's in charge? *Immunity* 2000; **12:** 233-239.

[205] Nakagawa TY, Rudensky AY. The role of lysosomal proteinases in MHC class II-mediated antigen processing and presentation. *Immunol Rev* 1999; **172:** 121-129.

[206] Landsverk OJ, Bakke O, Gregers TF. MHC II and the endocytic pathway: regulation by invariant chain. *Scand J Immunol* 2009; **70:** 184-193.

[207] Watts C, Moss CX, Mazzeo D, West MA, Matthews SP, Li DN, et al. Creation versus destruction of T cell epitopes in the class II MHC pathway. *Ann N Y Acad Sci* 2003; **987:** 9-14.

[208] Kaufman JF, Auffray C, Korman AJ, Shackelford DA, Strominger J. The class II molecules of the human and murine major histocompatibility complex. *Cell* 1984; **36:** 1-13.

[209] Romagnoli P, Germain RN. The CLIP region of invariant chain plays a critical role in regulating major histocompatibility complex class II folding, transport, and peptide occupancy. *J Exp Med* 1994; **180:** 1107-1113.

[210] Benaroch P, Yilla M, Raposo G, Ito K, Miwa K, Geuze HJ, et al. How MHC class II molecules reach the endocytic pathway. *Embo J* 1995; **14:** 37-49.

[211] Warmerdam PA, Long EO, Roche PA. Isoforms of the invariant chain regulate transport of MHC class II molecules to antigen processing compartments. *J Cell Biol* 1996; **133:** 281-291.

[212] Ong GL, Goldenberg DM, Hansen HJ, Mattes MJ. Cell surface expression and metabolism of major histocompatibility complex class II invariant chain (CD74) by diverse cell lines. *Immunology* 1999; **98:** 296-302.

[213] Wang K, Peterson PA, Karlsson L. Decreased endosomal delivery of major histocompatibility complex class II-invariant chain complexes in dynamin-deficient cells. *J Biol Chem* 1997; **272:** 17055-17060.

[214] Bonifacino JS, Traub LM. Signals for sorting of transmembrane proteins to endosomes and lysosomes. *Annu Rev Biochem* 2003; **72:** 395-447.

[215] Roche PA, Cresswell P. Invariant chain association with HLA-DR molecules inhibits immunogenic peptide binding. *Nature* 1990; **345:** 615-618.

[216] Rudensky A, Preston-Hurlburt P, Hong SC, Barlow A, Janeway CA, Jr. Sequence analysis of peptides bound to MHC class II molecules. *Nature* 1991; **353:** 622-627.

[217] Lotteau V, Teyton L, Peleraux A, Nilsson T, Karlsson L, Schmid SL, et al. Intracellular transport of class II MHC molecules directed by invariant chain. *Nature* 1990; **348:** 600-605.

[218] Riese RJ, Wolf PR, Bromme D, Natkin LR, Villadangos JA, Ploegh HL, et al. Essential role for cathepsin S in MHC class II-associated invariant chain processing and peptide loading. *Immunity* 1996; **4:** 357-366.

[219] Mellman I. Antigen processing and presentation by dendritic cells: cell biological mechanisms. *Adv Exp Med Biol* 2005; **560:** 63-67.

[220] Mosyak L, Zaller DM, Wiley DC. The structure of HLA-DM, the peptide exchange catalyst that loads antigen onto class II MHC molecules during antigen presentation. *Immunity* 1998; **9:** 377-383.

[221] Busch R, Reich Z, Zaller DM, Sloan V, Mellins ED. Secondary structure composition and pH-dependent conformational changes of soluble recombinant HLA-DM. *J Biol Chem* 1998; **273:** 27557-27564.

[222] Kelly AP, Monaco JJ, Cho SG, Trowsdale J. A new human HLA class II-related locus, DM. *Nature* 1991; **353:** 571-573.

[223] Cho SG, Attaya M, Monaco JJ. New class II-like genes in the murine MHC. *Nature* 1991; **353:** 573-576.

[224] Vyas JM, Kim YM, Artavanis-Tsakonas K, Love JC, Van der Veen AG, Ploegh HL. Tubulation of class II MHC compartments is microtubule dependent and involves multiple endolysosomal membrane proteins in primary dendritic cells. *J Immunol* 2007; **178:** 7199-7210.

[225] Pamer E, Cresswell P. Mechanisms of MHC class I--restricted antigen processing. *Annu Rev Immunol* 1998; **16:** 323-358.

[226] Yewdell JW, Nicchitta CV. The DRiP hypothesis decennial: support, controversy, refinement and extension. *Trends Immunol* 2006; **27:** 368-373.

[227] Jung T, Catalgol B, Grune T. The proteasomal system. *Mol Aspects Med* 2009; **30:** 191-296.

[228] Rock KL, Goldberg AL. Degradation of cell proteins and the generation of MHC class I-presented peptides. *Annu Rev Immunol* 1999; **17:** 739-779.

[229] Cresswell P, Arunachalam B, Bangia N, Dick T, Diedrich G, Hughes E, et al. Thiol oxidation and reduction in MHC-restricted antigen processing and presentation. *Immunol Res* 1999; **19:** 191-200.

[230] Cresswell P, Bangia N, Dick T, Diedrich G. The nature of the MHC class I peptide loading complex. *Immunol Rev* 1999; **172:** 21-28.

[231] Dick TP, Bangia N, Peaper DR, Cresswell P. Disulfide bond isomerization and the assembly of MHC class I-peptide complexes. *Immunity* 2002; **16:** 87-98.

[232] Koch J, Guntrum R, Heintke S, Kyritsis C, Tampe R. Functional dissection of the transmembrane domains of the transporter associated with antigen processing (TAP). *J Biol Chem* 2004; **279:** 10142-10147.

[233] Cresswell P. Intracellular surveillance: controlling the assembly of MHC class I-peptide complexes. *Traffic* 2000; **1:** 301-305.

[234] Bevan MJ. Cross-priming. *Nat Immunol* 2006; **7:** 363-365.

[235] Bevan MJ. Minor H antigens introduced on H-2 different stimulating cells cross-react at the cytotoxic T cell level during *in vivo* priming. *J Immunol* 1976; **117:** 2233-2238.

[236] Bevan MJ. Cross-priming for a secondary cytotoxic response to minor H antigens with H-2 congenic cells which do not cross-react in the cytotoxic assay. *J Exp Med* 1976; **143:** 1283-1288.

[237] Kurts C, Cannarile M, Klebba I, Brocker T. Dendritic cells are sufficient to cross-present self-antigens to CD8 T cells *in vivo*. *J Immunol* 2001; **166:** 1439-1442.

[238] Amigorena S, Savina A. Intracellular mechanisms of antigen cross presentation in dendritic cells. *Curr Opin Immunol* 2010; **22:** 109-117.

[239] Heath WR, Carbone FR. Cytotoxic T lymphocyte activation by cross- priming. *Curr Opin Immunol* 1999; **11:** 314-318.

[240] Villadangos JA, Heath WR, Carbone FR. Outside looking in: the inner workings of the cross-presentation pathway within dendritic cells. *Trends Immunol* 2007; **28:** 45-47.

[241] Heath WR, Belz GT, Behrens GM, Smith CM, Forehan SP, Parish IA, et al. Cross-presentation, dendritic cell subsets, and the generation of immunity to cellular antigens. *Immunol Rev* 2004; **199:** 9-26.

[242] Sauter B, Albert ML, Francisco L, Larsson M, Somersan S, Bhardwaj N. Consequences of cell death: exposure to necrotic tumor cells, but not primary tissue cells or apoptotic cells, induces the maturation of immunostimulatory dendritic cells. *J Exp Med* 2000; **191:** 423-434.

[243] Reis e Sousa C. Dendritic cells in a mature age. *Nat Rev Immunol* 2006; **6:** 476-483.

[244] Sallusto F, Palermo B, Lenig D, Miettinen M, Matikainen S, Julkunen I, et al. Distinct patterns and kinetics of chemokine production regulate dendritic cell function. *Eur J Immunol* 1999; **29:** 1617-1625.

[245] Yanagihara S, Komura E, Nagafune J, Watarai H, Yamaguchi Y. EBI1/CCR7 is a new member of dendritic cell chemokine receptor that is up-regulated upon maturation. *J Immunol* 1998; **161:** 3096-3102.

[246] Huang FP, Platt N, Wykes M, Major JR, Powell TJ, Jenkins CD, et al. A discrete subpopulation of dendritic cells transports apoptotic intestinal epithelial cells to T cell areas of mesenteric lymph nodes. *J Exp Med* 2000; **191:** 435-444.

[247] Steinman RM, Turley S, Mellman I, Inaba K. The induction of tolerance by dendritic cells that have captured apoptotic cells. *J Exp Med* 2000; **191:** 411-416.

[248] Forster R, Schubel A, Breitfeld D, Kremmer E, Renner-Muller I, Wolf E, et al. CCR7 coordinates the primary immune response by establishing functional microenvironments in secondary lymphoid organs. *Cell* 1999; **99:** 23-33.

[249] Jenkins MK, Khoruts A, Ingulli E, Mueller DL, McSorley SJ, Reinhardt RL, et

al. *In vivo* activation of antigen-specific CD4 T cells. *Annu Rev Immunol* 2001; **19:** 23-45.

[250] Mempel TR, Henrickson SE, Von Andrian UH. T-cell priming by dendritic cells in lymph nodes occurs in three distinct phases. *Nature* 2004; **427:** 154-159.

[251] Gretz JE, Anderson AO, Shaw S. Cords, channels, corridors and conduits: critical architectural elements facilitating cell interactions in the lymph node cortex. *Immunol Rev* 1997; **156:** 11-24.

[252] Gretz JE, Norbury CC, Anderson AO, Proudfoot AE, Shaw S. Lymph-borne chemokines and other low molecular weight molecules reach high endothelial venules via specialized conduits while a functional barrier limits access to the lymphocyte microenvironments in lymph node cortex. *J Exp Med* 2000; **192:** 1425-1440.

[253] Gretz JE, Kaldjian EP, Anderson AO, Shaw S. Sophisticated strategies for information encounter in the lymph node: the reticular network as a conduit of soluble information and a highway for cell traffic. *J Immunol* 1996; **157:** 495-499.

[254] Heimlich JM, Regnier FE, White JL, Hem SL. The *in vitro* displacement of adsorbed model antigens from Aluminium-containing adjuvants by interstitial proteins. *Vaccine* 1999; **17:** 2873-2881.

[255] Catron DM, Itano AA, Pape KA, Mueller DL, Jenkins MK. Visualizing the first 50 hr of the primary immune response to a soluble antigen. *Immunity* 2004; **21:** 341-347.

[256] Manickasingham S, Reis e Sousa C. Microbial and T cell-derived stimuli regulate antigen presentation by dendritic cells *in vivo*. *J Immunol* 2000; **165:** 5027-5034.

[257] Mueller DL, Jenkins MK, Schwartz RH. Clonal expansion versus functional clonal inactivation: a costimulatory signalling pathway determines the outcome of T cell antigen receptor occupancy. *Annu Rev Immunol* 1989; **7:** 445-480.

[258] Jenkins MK, Schwartz RH. Antigen presentation by chemically modified splenocytes induces antigen-specific T cell unresponsiveness *in vitro* and *in vivo*. *J Exp Med* 1987; **165:** 302-319.

[259] Jenkins MK, Pardoll DM, Mizuguchi J, Quill H, Schwartz RH. T-cell unresponsiveness *in vivo* and *in vitro*: fine specificity of induction and molecular characterization of the unresponsive state. *Immunol Rev* 1987; **95:** 113-135.

[260] Jenkins MK, Pardoll DM, Mizuguchi J, Chused TM, Schwartz RH. Molecular

events in the induction of a nonresponsive state in interleukin 2- producing helper T-lymphocyte clones. *Proc Natl Acad Sci USA* 1987; **84:** 5409-5413.

[261] Mueller DL, Jenkins MK, Schwartz RH. An accessory cell-derived costimulatory signal acts independently of protein kinase C activation to allow T cell proliferation and prevent the induction of unresponsiveness. *J Immunol* 1989; **142:** 2617-2628.

[262] Sharpe AH. Analysis of lymphocyte costimulation *in vivo* using transgenic and 'knockout' mice. *Curr Opin Immunol* 1995; **7:** 389-395.

[263] Grewal IS, Flavell RA. CD40 and CD154 in cell-mediated immunity. *Annu Rev Immunol* 1998; **16:** 111-135.

[264] van Kooten C, Banchereau J. CD40-CD40 ligand. *J Leukoc Biol* 2000; **67:** 2-17.

[265] Hendriks J, Xiao Y, Borst J. CD27 promotes survival of activated T cells and complements CD28 in generation and establishment of the effector T cell pool. *J Exp Med* 2003; **198:** 1369-1380.

[266] Wan YY, Flavell RA. How diverse--CD4 effector T cells and their functions. *J Mol Cell Biol* 2009; **1:** 20-36.

[267] Mosmann TR, Cherwinski H, Bond MW, Giedlin MA, Coffman RL. Two types of murine helper T cell clone. I. Definition according to profiles of lymphokine activities and secreted proteins. *J Immunol* 1986; **136:** 2348-2357.

[268] Mosmann TR, Cherwinski H, Bond MW, Giedlin MA, Coffman RL. Two types of murine helper T cell clone. I. Definition according to profiles of lymphokine activities and secreted proteins. *J Immunol* 1986; **175:** 5-14.

[269] Mosmann TR, Sad S. The expanding universe of T-cell subsets: Th1, Th2 and more. *Immunol Today* 1996; **17:** 138-146.

[270] Fazilleau N, Mark L, McHeyzer-Williams LJ, McHeyzer-Williams MG. Follicular helper T cells: lineage and location. *Immunity* 2009; **30:** 324-335.

[271] Amsen D, Spilianakis CG, Flavell RA. How are T(H)1 and T(H)2 effector cells made? Curr Opin Immunol 2009; **21:** 153-160.

[272] Bluestone JA, Abbas AK. Natural versus adaptive regulatory T cells. *Nat Rev Immunol* 2003; **3:** 253-257.

[273] Sadick MD, Heinzel FP, Shigekane VM, Fisher WL, Locksley RM. Cellular and humoral immunity to Leishmania major in genetically susceptible mice after *in vivo* depletion of L3T4+ T cells. *J Immunol* 1987; **139:** 1303-1309.

[274] Heinzel FP, Sadick MD, Holaday BJ, Coffman RL, Locksley RM. Reciprocal expression of interferon gamma or interleukin 4 during the resolution or progression of murine leishmaniasis. Evidence for expansion of distinct helper T cell subsets. *J Exp Med* 1989; **169:** 59-72.

[275] Buchmeier NA, Schreiber RD. Requirement of endogenous interferon- gamma production for resolution of Listeria monocytogenes infection. *Proc Natl Acad Sci USA* 1985; **82:** 7404-7408.

[276] Kobayashi K, Nakata N, Kai M, Kasama T, Hanyuda Y, Hatano Y. Decreased expression of cytokines that induce type 1 helper T cell/interferon- gamma responses in genetically susceptible mice infected with *Mycobacterium avium*. *Clin Immunol Immunopathol* 1997; **85:** 112-116.

[277] Micallef MJ, Tanimoto T, Kohno K, Ikeda M, Kurimoto M. Interleukin 18 induces the sequential activation of natural killer cells and cytotoxic T lymphocytes to protect syngeneic mice from transplantation with Meth A sarcoma. *Cancer Res* 1997; **57:** 4557-4563.

[278] Nagarkatti M, Clary SR, Nagarkatti PS. Characterization of tumor-infiltrating CD4+ T cells as Th1 cells based on lymphokine secretion and functional properties. *J Immunol* 1990; **144:** 4898-4905.

[279] Davidson NJ, Leach MW, Fort MM, Thompson-Snipes L, Kuhn R, Muller W, et al. T helper cell 1-type CD4+ T cells, but not B cells, mediate colitis in interleukin 10-deficient mice. *J Exp Med* 1996; **184:** 241-251.

[280] Leung BP, McInnes IB, Esfandiari E, Wei XQ, Liew FY. Combined effects of IL-12 and IL-18 on the induction of collagen-induced arthritis. *J Immunol* 2000; **164:** 6495-6502.

[281] Sher A, Gazzinelli RT, Oswald IP, Clerici M, Kullberg M, Pearce EJ, et al. Role of T-cell derived cytokines in the downregulation of immune responses in parasitic and retroviral infection. *Immunol Rev* 1992; **127:** 183-204.

[282] Maizels RM, Bundy DA, Selkirk ME, Smith DF, Anderson RM. Immunological modulation and evasion by helminth parasites in human populations. *Nature* 1993; **365:** 797-805.

[283] Coffman RL, Carty J. A T cell activity that enhances polyclonal IgE production and its inhibition by interferon-gamma. *J Immunol* 1986; **136:** 949-954.

[284] Maizels RM, Holland MJ. Parasite immunology: pathways for expelling intestinal helminths. *Curr Biol* 1998; **8:** R711-714.

[285] Urban JF, Jr., Noben-Trauth N, Donaldson DD, Madden KB, Morris SC, Collins M, et al. IL-13, IL-4Ralpha, and Stat6 are required for the expulsion of the gastrointestinal nematode parasite *Nippostrongylus brasiliensis*. *Immunity*

1998; **8:** 255-264.

[286] Happel KI, Dubin PJ, Zheng M, Ghilardi N, Lockhart C, Quinton LJ, et al. Divergent roles of IL-23 and IL-12 in host defense against *Klebsiella pneumoniae*. *J Exp Med* 2005; **202:** 761-769.

[287] Langrish CL, Chen Y, Blumenschein WM, Mattson J, Basham B, Sedgwick JD, et al. IL-23 drives a pathogenic T cell population that induces autoimmune inflammation. *J Exp Med* 2005; **201:** 233-240.

[288] Yen D, Cheung J, Scheerens H, Poulet F, McClanahan T, McKenzie B, et al. IL-23 is essential for T cell-mediated colitis and promotes inflammation via IL-17 and IL-6. *J Clin Invest* 2006; **116:** 1310-1316.

[289] Jordan MS, Boesteanu A, Reed AJ, Petrone AL, Holenbeck AE, Lerman MA, et al. Thymic selection of CD4+CD25+ regulatory T cells induced by an agonist self-peptide. *Nat Immunol* 2001; **2:** 301-306.

[290] Weiner HL. Induction and mechanism of action of transforming growth factor-beta-secreting Th3 regulatory cells. *Immunol Rev* 2001; **182:** 207-214.

[291] Stassen M, Fondel S, Bopp T, Richter C, Muller C, Kubach J, et al. Human CD25+ regulatory T cells: two subsets defined by the integrins alpha 4 beta 7 or alpha 4 beta 1 confer distinct suppressive properties upon CD4+ T helper cells. *Eur J Immunol* 2004; **34:** 1303-1311.

[292] Smith KM, Brewer JM, Rush CM, Riley J, Garside P. *In vivo* generated Th1 cells can migrate to B cell follicles to support B cell responses. *J Immunol* 2004; **173:** 1640-1646.

[293] Breitfeld D, Ohl L, Kremmer E, Ellwart J, Sallusto F, Lipp M, et al. Follicular B helper T cells express CXC chemokine receptor 5, localize to B cell follicles, and support immunoglobulin production. *J Exp Med* 2000; **192:** 1545-1552.

[294] Nurieva RI, Chung Y, Hwang D, Yang XO, Kang HS, Ma L, et al. Generation of T follicular helper cells is mediated by interleukin-21 but independent of T helper 1, 2, or 17 cell lineages. *Immunity* 2008; **29:** 138-149.

[295] Schaerli P, Willimann K, Lang AB, Lipp M, Loetscher P, Moser B. CXC chemokine receptor 5 expression defines follicular homing T cells with B cell helper function. *J Exp Med* 2000; **192:** 1553-1562.

[296] Hardtke S, Ohl L, Forster R. Balanced expression of CXCR5 and CCR7 on follicular T helper cells determines their transient positioning to lymph node follicles and is essential for efficient B-cell help. *Blood* 2005; **106:** 1924-1931.

[297] Deenick EK, Chan A, Ma CS, Gatto D, Schwartzberg PL, Brink R, et al.

Follicular helper T cell differentiation requires continuous antigen presentation that is independent of unique B cell signaling. *Immunity* 2010; **33:** 241-253.

[298] Deenick EK, Ma CS, Brink R, Tangye SG. Regulation of T follicular helper cell formation and function by antigen presenting cells. *Curr Opin Immunol* 2010; **23:** 111-118.

[299] Crotty S. Follicular helper CD4 T cells (TFH). *Annu Rev Immunol* 2011; **29:** 621-663.

[300] Patakas A, Platt AM, Butcher JP, Maffia P, McInnes IB, Brewer JM, et al. Putative existence of reciprocal dialogue between Tfh and B cells and its impact on infectious and autoimmune disease. *Immunol Lett* 2011; **138:** 38-46.

[301] Brewer JM. (How) do Aluminium adjuvants work? *Immunol Lett* 2006; **102:** 10-15.

[302] Pulendran B, Dillon S, Joseph C, Curiel T, Banchereau J, Mohamadzadeh M. Dendritic cells generated in the presence of GM-CSF plus IL-15 prime potent CD8+ Tc1 responses *in vivo*. *Eur J Immunol* 2004; **34:** 66-73.

[303] Ishii KJ, Coban C, Akira S. Manifold mechanisms of Toll-like receptor- ligand recognition. *J Clin Immunol* 2005; **25:** 511-521.

[304] Ishii KJ, Akira S. Toll or toll-free adjuvant path toward the optimal vaccine development. *J Clin Immunol* 2007; **27:** 363-371.

[305] Ishii KJ, Akira S. Innate immune recognition of nucleic acids: beyond toll- like receptors. *Int J Cancer* 2005; **117:** 517-523.

[306] Fiebiger E, Meraner P, Weber E, Fang IF, Stingl G, Ploegh H, et al. Cytokines regulate proteolysis in major histocompatibility complex class II- dependent antigen presentation by dendritic cells. *J Exp Med* 2001; **193:** 881-892.

[307] MartIn-Fontecha A, Sebastiani S, Hopken UE, Uguccioni M, Lipp M, Lanzavecchia A, et al. Regulation of dendritic cell migration to the draining lymph node: impact on T lymphocyte traffic and priming. *J Exp Med* 2003; **198:** 615-621.

[308] Kawai T, Akira S. The roles of TLRs, RLRs and NLRs in pathogen recognition. *Int Immunol* 2009; **21:** 317-337.

[309] Samuelsson P, Hang L, Wullt B, Irjala H, Svanborg C. Toll-like receptor 4 expression and cytokine responses in the human urinary tract mucosa. Infect Immun 2004; **72:** 3179-3186.

[310] Gribar SC, Anand RJ, Sodhi CP, Hackam DJ. The role of epithelial Toll-like receptor signaling in the pathogenesis of intestinal inflammation. *J Leukoc Biol*

2008; **83:** 493-498.

[311] Chalifour A, Jeannin P, Gauchat JF, Blaecke A, Malissard M, N'Guyen T, et al. Direct bacterial protein PAMP recognition by human NK cells involves TLRs and triggers alpha-defensin production. *Blood* 2004; **104:** 1778-1783.

[312] Caron G, Duluc D, Fremaux I, Jeannin P, David C, Gascan H, et al. Direct stimulation of human T cells via TLR5 and TLR7/8: flagellin and R-848 up-regulate proliferation and IFN-gamma production by memory CD4+ T cells. *J Immunol* 2005; **175:** 1551-1557.

[313] Peiser M, Wanner R, Kolde G. Human epidermal Langerhans cells differ from monocyte-derived Langerhans cells in CD80 expression and in secretion of IL-12 after CD40 cross-linking. *J Leukoc Biol* 2004; **76:** 616-622.

[314] Hornung V, Rothenfusser S, Britsch S, Krug A, Jahrsdorfer B, Giese T, et al. Quantitative expression of toll-like receptor 1-10 mRNA in cellular subsets of human peripheral blood mononuclear cells and sensitivity to CpG oligodeoxynucleotides. *J Immunol* 2002; **168:** 4531-4537.

[315] Farina C, Theil D, Semlinger B, Hohlfeld R, Meinl E. Distinct responses of monocytes to Toll-like receptor ligands and inflammatory cytokines. *Int Immunol* 2004; **16:** 799-809.

[316] Spohn R, Buwitt-Beckmann U, Brock R, Jung G, Ulmer AJ, Wiesmuller KH. Synthetic lipopeptide adjuvants and Toll-like receptor 2--structure-activity relationships. *Vaccine* 2004; **22:** 2494-2499.

[317] Becker PD, Bertot GM, Souss D, Ebensen T, Guzman CA, Grinstein S. Intranasal vaccination with recombinant outer membrane protein CD and adamantylamide dipeptide as the mucosal adjuvant enhances pulmonary clearance of *Moraxella catarrhalis* in an experimental murine model. *Infect Immun* 2007; **75:** 1778-1784.

[318] Yoder A, Wang X, Ma Y, Philipp MT, Heilbrun M, Weis JH, et al. Tripalmitoyl-S-glyceryl-cysteine-dependent OspA vaccination of toll-like receptor 2-deficient mice results in effective protection from Borrelia burgdorferi challenge. *Infect Immun* 2003; **71:** 3894-3900.

[319] Latz E, Franko J, Golenbock DT, Schreiber JR. Haemophilus influenzae type b-outer membrane protein complex glycoconjugate vaccine induces cytokine production by engaging human toll-like receptor 2 (TLR2) and requires the presence of TLR2 for optimal immunogenicity. *J Immunol* 2004; **172:** 2431-2438.

[320] Honko AN, Sriranganathan N, Lees CJ, Mizel SB. Flagellin is an effective adjuvant for immunization against lethal respiratory challenge with Yersinia pestis. *Infect Immun* 2006; **74:** 1113-1120.

[321] Franchini M, Schweizer M, Matzener P, Magkouras I, Sauter KS, Mirkovitch J, et al. Evidence for dissociation of TLR mRNA expression and TLR agonist-mediated functions in bovine macrophages. *Vet Immunol Immunopathol* 2006; **110:** 37-49.

[322] Kumar H, Kawai T, Akira S. Toll-like receptors and innate immunity. *Biochem Biophys Res Commun* 2009; **388:** 621-625.

[323] Beutler BA. TLRs and innate immunity. *Blood* 2009; **113:** 1399-1407.

[324] Kawai T, Akira S. Toll-like receptor and RIG-I-like receptor signaling. *Ann N Y Acad Sci* 2008; **1143:** 1-20.

[325] Gorden KB, Gorski KS, Gibson SJ, Kedl RM, Kieper WC, Qiu X, et al. Synthetic TLR agonists reveal functional differences between human TLR7 and TLR8. *J Immunol* 2005; **174:** 1259-1268.

[326] Zarember KA, Godowski PJ. Tissue expression of human Toll-like receptors and differential regulation of Toll-like receptor mRNAs in leukocytes in response to microbes, their products, and cytokines. *J Immunol* 2002; **168:** 554-561.

[327] Zaks K, Jordan M, Guth A, Sellins K, Kedl R, Izzo A, et al. Efficient immunization and cross-priming by vaccine adjuvants containing TLR3 or TLR9 agonists complexed to cationic liposomes. *J Immunol* 2006; **176:** 7335-7345.

[328] Hornung V, Bauernfeind F, Halle A, Samstad EO, Kono H, Rock KL, et al. Silica crystals and Aluminum salts activate the NALP3 inflammasome through phagosomal destabilization. *Nat Immunol* 2008; **9:** 847-856.

[329] Coban C, Ishii KJ, Uematsu S, Arisue N, Sato S, Yamamoto M, et al. Pathological role of Toll-like receptor signaling in cerebral malaria. *Int Immunol* 2007; **19:** 67-79.

[330] Kato H, Takeuchi O, Sato S, Yoneyama M, Yamamoto M, Matsui K, et al. Differential roles of MDA5 and RIG-I helicases in the recognition of RNA viruses. *Nature* 2006; **441:** 101-105.

[331] Venkataraman T, Valdes M, Elsby R, Kakuta S, Caceres G, Saijo S, et al. Loss of DExD/H box RNA helicase LGP2 manifests disparate antiviral responses. *J Immunol* 2007; **178:** 6444-6455.

[332] Proell M, Riedl SJ, Fritz JH, Rojas AM, Schwarzenbacher R. The Nod-like receptor (NLR) family: a tale of similarities and differences. *PLoS One* 2008; **3:** e2119.

[333] Kanneganti TD, Lamkanfi M, Nunez G. Intracellular NOD-like receptors in host defense and disease. *Immunity* 2007; **27:** 549-559.

[334] Martinon F, Mayor A, Tschopp J. The inflammasomes: guardians of the body. *Annu Rev Immunol* 2009; **27:** 229-265.

[335] Martinon F, Gaide O, Petrilli V, Mayor A, Tschopp J. NALP inflammasomes: a central role in innate immunity. *Semin Immunopathol* 2007; **29:** 213-229.

[336] Fitzgerald KA. NLR-containing inflammasomes: central mediators of host defense and inflammation. *Eur J Immunol* 2010; **40:** 595-598.

[337] Seubert A, Monaci E, Pizza M, O'Hagan DT, Wack A. The adjuvants Aluminum hydroxide and MF59 induce monocyte and granulocyte chemoattractants and enhance monocyte differentiation toward dendritic cells. *J Immunol* 2008; **180:** 5402-5412.

[338] Sokolovska A, Hem SL, HogenEsch H. Activation of dendritic cells and induction of CD4(+) T cell differentiation by Aluminum-containing adjuvants. *Vaccine* 2007; **25:** 4575-4585.

[339] Ulanova M, Tarkowski A, Hahn-Zoric M, Hanson LA. The Common vaccine adjuvant Aluminum hydroxide up-regulates accessory properties of human monocytes via an interleukin-4-dependent mechanism. *Infect Immun* 2001; **69:** 1151-1159.

[340] Qin H, Cha SC, Neelapu SS, Lou Y, Wei J, Liu YJ, et al. Vaccine site inflammation potentiates idiotype DNA vaccine-induced therapeutic T cell-, and not B cell-, dependent antilymphoma immunity. *Blood* 2009; 114: 4142-4149.

[341] Matzinger P. Tolerance, danger, and the extended family. *Annu Rev Immunol* 1994; **12:** 991-1045.

[342] Gallucci S, Lolkema M, Matzinger P. Natural adjuvants: endogenous activators of dendritic cells. *Nat Med* 1999; **5:** 1249-1255.

[343] Gallucci S, Matzinger P. Danger signals: SOS to the immune system. *Curr Opin Immunol* 2001; **13:** 114-119.

[344] Spisek R, Charalambous A, Mazumder A, Vesole DH, Jagannath S, Dhodapkar MV. Bortezomib enhances dendritic cell (DC)-mediated induction of immunity to human myeloma via exposure of cell surface heat shock protein 90 on dying tumor cells: therapeutic implications. *Blood* 2007; **109:** 4839-4845.

[345] Spisek R, Dhodapkar MV. Towards a better way to die with chemotherapy: role of heat shock protein exposure on dying tumor cells. *Cell Cycle* 2007; **6:** 1962-1965.

[346] Coutinho-Silva R, Robson T, Beales PE, Burnstock G. Changes in expression of P2X7 receptors in NOD mouse pancreas during the development of diabetes. *Autoimmunity* 2007; **40:** 108-116.

[347] Pashine A, Valiante NM, Ulmer JB. Targeting the innate immune response with improved vaccine adjuvants. *Nat Med* 2005; **11:** S63-68.

[348] Bonifaz LC, Bonnyay DP, Charalambous A, Darguste DI, Fujii S, Soares H, et al. *In vivo* targeting of antigens to maturing dendritic cells via the DEC-205 receptor improves T cell vaccination. *J Exp Med* 2004; **199:** 815-824.

[349] Birkholz K, Schwenkert M, Kellner C, Gross S, Fey G, Schuler-Thurner B, et al. Targeting of DEC-205 on human dendritic cells results in efficient MHC class II-restricted antigen presentation. *Blood* 2010; **116:** 2277-2285.

[350] Brewer JM, Pollock KG, Tetley L, Russell DG. Vesicle size influences the trafficking, processing, and presentation of antigens in lipid vesicles. *J Immunol* 2004; **173:** 6143-6150.

[351] Wang C, Ge Q, Ting D, Nguyen D, Shen HR, Chen J, et al. Molecularly engineered poly(ortho ester) microspheres for enhanced delivery of DNA vaccines. *Nat Mater* 2004; **3:** 190-196.

[352] Langer R, Cleland JL, Hanes J. New advances in microsphere-based single-dose vaccines. *Adv Drug Deliv Rev* 1997; **28:** 97-119.

[353] Ambrosch F, Wiedermann G, Jonas S, Althaus B, Finkel B, Gluck R, et al. Immunogenicity and protectivity of a new liposomal hepatitis A vaccine. *Vaccine* 1997; **15:** 1209-1213.

[354] Riedl P, Stober D, Oehninger C, Melber K, Reimann J, Schirmbeck R. Priming Th1 immunity to viral core particles is facilitated by trace amounts of RNA bound to its arginine-rich domain. *J Immunol* 2002; **168:** 4951-4959.

[355] de Witte L, Nabatov A, Pion M, Fluitsma D, de Jong MA, de Gruijl T, et al. Langerin is a natural barrier to HIV-1 transmission by Langerhans cells. *Nat Med* 2007; **13:** 367-371.

[356] Turville SG, Cameron PU, Handley A, Lin G, Pohlmann S, Doms RW, et al. Diversity of receptors binding HIV on dendritic cell subsets. *Nat Immunol* 2002; **3:** 975-983.

[357] Geijtenbeek TB, Kwon DS, Torensma R, van Vliet SJ, van Duijnhoven GC, Middel J, et al. DC-SIGN, a dendritic cell-specific HIV-1-binding protein that enhances trans-infection of T cells. *Cell* 2000; **100:** 587-597.

[358] Bozzacco L, Trumpfheller C, Huang Y, Longhi MP, Shimeliovich I, Schauer

JD, et al. HIV gag protein is efficiently cross-presented when targeted with an antibody towards the DEC-205 receptor in Flt3 ligand-mobilized murine DC. *Eur J Immunol* 2010; **40:** 36-46.

[359] Trumpfheller C, Finke JS, Lopez CB, Moran TM, Moltedo B, Soares H, et al. Intensified and protective CD4+ T cell immunity in mice with anti-dendritic cell HIV gag fusion antibody vaccine. *J Exp Med* 2006; **203:** 607-617.

[360] Reis e Sousa C, Germain RN. Major histocompatibility complex class I presentation of peptides derived from soluble exogenous antigen by a subset of cells engaged in phagocytosis. *J Exp Med* 1995; **182:** 841-851.

[361] Carbone FR, Bevan MJ. Class I-restricted processing and presentation of exogenous cell-associated antigen *in vivo*. *J Exp Med* 1990; **171:** 377-387.

[362] Bramwell VW, Perrie Y. Particulate delivery systems for vaccines. *Crit Rev Ther Drug Carrier Syst* 2005; **22:** 151-214.

[363] Hattori Y, Kawakami S, Suzuki S, Yamashita F, Hashida M. Enhancement of immune responses by DNA vaccination through targeted gene delivery using mannosylated cationic liposome formulations following intravenous administration in mice. *Biochem Biophys Res Commun* 2004; **317:** 992-999.

[364] Arigita C, Bevaart L, Everse LA, Koning GA, Hennink WE, Crommelin DJ, et al. Liposomal meningococcal B vaccination: role of dendritic cell targeting in the development of a protective immune response. *Infect Immun* 2003; **71:** 5210-5218.

[365] van Broekhoven CL, Parish CR, Demangel C, Britton WJ, Altin JG. Targeting dendritic cells with antigen-containing liposomes: a highly effective procedure for induction of antitumor immunity and for tumor immunotherapy. Cancer Res 2004; **64:** 4357-4365.

[366] Fukasawa M, Shimizu Y, Shikata K, Nakata M, Sakakibara R, Yamamoto N, et al. Liposome oligomannose-coated with neoglycolipid, a new candidate for a safe adjuvant for induction of CD8+ cytotoxic T lymphocytes. *FEBS Lett* 1998; **441:** 353-356.

[367] Harrison WT. Some Observations on the Use of Alum Precipitated Diphtheria Toxoid. *Am J Public Health Nations Health* 1935; **25:** 298-300.

[368] Farago FC. Alum-Precipitated Toxoid in Diphtheria. Duration of immunity after one-shot method. *The Lancet* 1940: 68-40.

[369] White RG, Coons AH, Connolly JM. Studies on antibody production. III. The Alum granuloma. *J Exp Med* 1955; **102:** 73-82.

[370] HogenEsch H. Mechanisms of stimulation of the immune response by Aluminum adjuvants. *Vaccine* 2002; **20 (Suppl 3):** S34-39.

[371] Herbert WJ. The mode of action of mineral-oil emulsion adjuvants on antibody production in mice. *Immunology* 1968; **14:** 301-318.

[372] Herbert WJ. Antigenicity of soluble protein in the presence of high levels of antibody: a possible mode of action of the antigen adjuvants. *Nature* 1966; **210:** 747-748.

[373] Flarend RE, Hem SL, White JL, Elmore D, Suckow MA, Rudy AC, et al. *In vivo* absorption of Aluminium-containing vaccine adjuvants using 26Al. *Vaccine* 1997; **15:** 1314-1318.

[374] Gupta RK, Chang AC, Griffin P, Rivera R, Siber GR. *In vivo* distribution of radioactivity in mice after injection of biodegradable polymer microspheres containing 14C-labeled tetanus toxoid. *Vaccine* 1996; **14:** 1412-1416.

[375] Holt LB. Developments in diphtheria prophylaxis. London, United Kingdom: Heinemann, 1950.

[376] de Veer M, Kemp J, Chatelier J, Elhay MJ, Meeusen EN. The kinetics of soluble and particulate antigen trafficking in the afferent lymph, and its modulation by Aluminum-based adjuvant. *Vaccine* 2010; **28:** 6597-6602.

[377] Beh KJ, Lascelles AK. The effect of adjuvants and prior immunization on the rate and mode of uptake of antigen into afferent popliteal lymph from sheep. *Immunology* 1985; **54:** 487-495.

[378] Verdier F, Burnett R, Michelet-Habchi C, Moretto P, Fievet-Groyne F, Sauzeat E. Aluminium assay and evaluation of the local reaction at several time points after intramuscular administration of Aluminium containing vaccines in the Cynomolgus monkey. *Vaccine* 2005; **23:** 1359-1367.

[379] Hutchison S, Benson RA, Gibson VB, Pollock AH, Garside P, Brewer JM. Antigen depot is not required for Alum adjuvanticity. *FASEB J* 2012; **26(3):** 1272-1279.

[380] Oussoren C, Zuidema J, Crommelin DJ, Storm G. Lymphatic uptake and biodistribution of liposomes after subcutaneous injection. II. Influence of liposomal size, lipid compostion and lipid dose. *Biochim Biophys Acta* 1997; **1328:** 261-272.

[381] Mannhalter JW, Neychev HO, Zlabinger GJ, Ahmad R, Eibl MM. Modulation of the human immune response by the non-toxic and non-pyrogenic adjuvant Aluminium hydroxide: effect on antigen uptake and antigen presentation. *Clin Exp Immunol* 1985; **61:** 143-151.

[382] Dillon SB, Demuth SG, Schneider MA, Weston CB, Jones CS, Young JF, et al. Induction of protective class I MHC-restricted CTL in mice by a recombinant influenza vaccine in Aluminium hydroxide adjuvant. *Vaccine* 1992; **10:** 309-318.

[383] McKee AS, Munks MW, MacLeod MK, Fleenor CJ, Van Rooijen N, Kappler JW, et al. Alum induces innate immune responses through macrophage and mast cell sensors, but these sensors are not required for Alum to act as an adjuvant for specific immunity. *J Immunol* 2009; **183:** 4403-4414.

[384] Sun H, Pollock KG, Brewer JM. Analysis of the role of vaccine adjuvants in modulating dendritic cell activation and antigen presentation *in vitro*. *Vaccine* 2003; **21:** 849-855.

[385] Turk JL, Parker D. Granuloma formation in normal guinea pigs injected intradermally with Aluminum and zirconium compounds. *J Invest Dermatol* 1977; **68:** 336-340.

[386] Munks MW, McKee AS, Macleod MK, Powell RL, Degen JL, Reisdorph NA, et al. Aluminum adjuvants elicit fibrin-dependent extracellular traps *in vivo*. *Blood* 2010; **116:** 5191-5199.

[387] Calabro S, Tortoli M, Baudner BC, Pacitto A, Cortese M, O'Hagan DT, et al. Vaccine adjuvants Alum and MF59 induce rapid recruitment of neutrophils and monocytes that participate in antigen transport to draining lymph nodes. *Vaccine* 2011; **29:** 1812-1823.

[388] Kool M, Petrilli V, De Smedt T, Rolaz A, Hammad H, van Nimwegen M, et al. Cutting edge: Alum adjuvant stimulates inflammatory dendritic cells through activation of the NALP3 inflammasome. *J Immunol* 2008; **181:** 3755-3759.

[389] Li H, Willingham SB, Ting JP, Re F. Cutting edge: inflammasome activation by Alum and Alum's adjuvant effect are mediated by NLRP3. *J Immunol* 2008; **181:** 17-21.

[390] Eisenbarth SC, Colegio OR, O'Connor W, Sutterwala FS, Flavell RA. Crucial role for the Nalp3 inflammasome in the immunostimulatory properties of Aluminium adjuvants. *Nature* 2008; **453:** 1122-1126.

[391] Okamura H, Kashiwamura S, Tsutsui H, Yoshimoto T, Nakanishi K. Regulation of interferon-gamma production by IL-12 and IL-18. *Curr Opin Immunol* 1998; **10:** 259-264.

[392] Okamura H, Tsutsi H, Komatsu T, Yutsudo M, Hakura A, Tanimoto T, et al. Cloning of a new cytokine that induces IFN-gamma production by T cells. *Nature* 1995; **378:** 88-91.

[393] Okamura H, Tsutsui H, Kashiwamura S, Yoshimoto T, Nakanishi K. Interleukin-18: a novel cytokine that augments both innate and acquired immunity. *Adv Immunol* 1998; **70:** 281-312.

[394] Wild JS, Sur S. Interleukin-18 and allergic asthma. *Isr Med Assoc J* 2000; **2:** 16-18.

[395] Brewer JM, Conacher M, Hunter CA, Mohrs M, Brombacher F, Alexander J. Aluminium hydroxide adjuvant initiates strong antigen-specific Th2 responses in the absence of IL-4- or IL-13-mediated signaling. *J Immunol* 1999; **163:** 6448-6454.

[396] Ben-Sasson SZ, Hu-Li J, Quiel J, Cauchetaux S, Ratner M, Shapira I, et al. IL-1 acts directly on CD4 T cells to enhance their antigen-driven expansion and differentiation. *Proc Natl Acad Sci USA* 2009; **106:** 7119-7124.

[397] Pape KA, Khoruts A, Mondino A, Jenkins MK. Inflammatory cytokines enhance the *in vivo* clonal expansion and differentiation of antigen-activated CD4+ T cells. *J Immunol* 1997; **159:** 591-598.

[398] Lambrecht BN, Kool M, Willart MA, Hammad H. Mechanism of action of clinically approved adjuvants. *Curr Opin Immunol* 2009; **21:** 23-29.

[399] Hentze H, Lin XY, Choi MS, Porter AG. Critical role for cathepsin B in mediating caspase-1-dependent interleukin-18 maturation and caspase-1-independent necrosis triggered by the microbial toxin nigericin. *Cell Death Differ* 2003; **10:** 956-968.

[400] Oboki K, Nakae S, Matsumoto K, Saito H. IL-33 and Airway Inflammation. *Allergy Asthma Immunol Res* 2011; **3:** 81-88.

[401] Cayrol C, Girard JP. The IL-1-like cytokine IL-33 is inactivated after maturation by caspase-1. *Proc Natl Acad Sci USA* 2009; **106:** 9021-9026.

[402] Luthi AU, Cullen SP, McNeela EA, Duriez PJ, Afonina IS, Sheridan C, et al. Suppression of interleukin-33 bioactivity through proteolysis by apoptotic caspases. *Immunity* 2009; **31:** 84-98.

[403] Ohno T, Oboki K, Kajiwara N, Morii E, Aozasa K, Flavell RA, et al. Caspase-1, caspase-8, and calpain are dispensable for IL-33 release by macrophages. *J Immunol* 2009; **183:** 7890-7897.

[404] Talabot-Ayer D, Lamacchia C, Gabay C, Palmer G. Interleukin-33 is biologically active independently of caspase-1 cleavage. *J Biol Chem* 2009; **284:** 19420-19426.

[405] Robertson JM, Jensen PE, Evavold BD. DO11.10 and OT-II T cells recognize a C-terminal ovalbumin 323-339 epitope. *J Immunol* 2000; **164:** 4706-4712.

[406] Murphy KM, Heimberger AB, Loh DY. Induction by antigen of intrathymic apoptosis of CD4+CD8+TCRlo thymocytes *in vivo*. *Science* 1990; **250:** 1720-1723.

[407] Rush CM, Brewer JM. Tracking dendritic cells *in vivo*. *Methods Mol Biol* 2010; **626:** 169-185.

[408] Tsien RY. The green fluorescent protein. *Annu Rev Biochem* 1998; **67:** 509-544.

[409] Rudensky A, Preston-Hurlburt P, al-Ramadi BK, Rothbard J, Janeway CA, Jr. Truncation variants of peptides isolated from MHC class II molecules suggest sequence motifs. *Nature* 1992; **359:** 429-431.

[410] Rudensky A, Rath S, Preston-Hurlburt P, Murphy DB, Janeway CA, Jr. On the complexity of self. *Nature* 1991; **353:** 660-662.

[411] Studier FW, Moffatt BA. Use of bacteriophage T7 RNA polymerase to direct selective high-level expression of cloned genes. *J Mol Biol* 1986; **189:** 113-130.

[412] Hansen B, Malyala P, Singh M, Sun Y, Srivastava I, Hogenesch H, et al. Effect of the strength of adsorption of HIV 1 SF162dV2gp140 to Aluminum-containing adjuvants on the immune response. *J Pharm Sci* 2011; **100:** 3245-3250.

[413] Hansen B, Sokolovska A, HogenEsch H, Hem SL. Relationship between the strength of antigen adsorption to an Aluminum-containing adjuvant and the immune response. *Vaccine* 2007; **25:** 6618-6624.

[414] Korsholm KS, Agger EM, Foged C, Christensen D, Dietrich J, Andersen CS, et al. The adjuvant mechanism of cationic dimethyldioctadecylammonium liposomes. *Immunology* 2007; **121:** 216-226.

[415] Nakase I, Niwa M, Takeuchi T, Sonomura K, Kawabata N, Koike Y, et al. Cellular uptake of arginine-rich peptides: roles for macropinocytosis and actin rearrangement. *Mol Ther* 2004; **10:** 1011-1022.

[416] Meier O, Boucke K, Hammer SV, Keller S, Stidwill RP, Hemmi S, et al. Adenovirus triggers macropinocytosis and endosomal leakage together with its clathrin-mediated uptake. *J Cell Biol* 2002; **158:** 1119-1131.

[417] Koivusalo M, Welch C, Hayashi H, Scott CC, Kim M, Alexander T, et al. Amiloride inhibits macropinocytosis by lowering submembranous pH and preventing Rac1 and Cdc42 signaling. *J Cell Biol* 2010; **188:** 547-563.

[418] Underhill DM, Bassetti M, Rudensky A, Aderem A. Dynamic interactions of macrophages with T cells during antigen presentation. *J Exp Med* 1999; **190:**

1909-1914.

[419] von Delwig A, Bailey E, Gibbs DM, Robinson JH. The route of bacterial uptake by macrophages influences the repertoire of epitopes presented to CD4 T cells. *Eur J Immunol* 2002; **32:** 3714-3719.

[420] Schliwa M. Action of cytochalasin D on cytoskeletal networks. *J Cell Biol* 1982; **92:** 79-91.

[421] Flanagan MD, Lin S. Cytochalasins block actin filament elongation by binding to high affinity sites associated with F-actin. *J Biol Chem* 1980; **255:** 835-838.

[422] Friederich E, Kreis TE, Louvard D. Villin-induced growth of microvilli is reversibly inhibited by cytochalasin D. *J Cell Sci* 1993; **105 (Pt 3):** 765-775.

[423] Lin DC, Tobin KD, Grumet M, Lin S. Cytochalasins inhibit nuclei-induced actin polymerization by blocking filament elongation. *J Cell Biol* 1980; **84:** 455-460.

[424] Thomsen P, Roepstorff K, Stahlhut M, van Deurs B. Caveolae are highly immobile plasma membrane microdomains, which are not involved in constitutive endocytic trafficking. *Mol Biol Cell* 2002; **13:** 238-250.

[425] Amyere M, Mettlen M, Van Der Smissen P, Platek A, Payrastre B, Veithen A, et al. Origin, originality, functions, subversions and molecular signalling of macropinocytosis. *Int J Med Microbiol* 2002; **291:** 487-494.

[426] Allison AC, Davies P, De Petris S. Role of contractile microfilaments in macrophage movement and endocytosis. *Nat New Biol* 1971; **232:** 153-155.

[427] Fretz M, Jin J, Conibere R, Penning NA, Al-Taei S, Storm G, et al. Effects of Na+/H+ exchanger inhibitors on subcellular localisation of endocytic organelles and intracellular dynamics of protein transduction domains HIV- TAT peptide and octaarginine. *J Control Release* 2006; **116:** 247-254.

[428] Grinstein S, Cohen S, Goetz JD, Rothstein A, Gelfand EW. Characterization of the activation of Na+/H+ exchange in lymphocytes by phorbol esters: change in cytoplasmic pH dependence of the antiport. *Proc Natl Acad Sci USA* 1985; **82:** 1429-1433.

[429] Liaw YS, Yang PC, Yu CJ, Kuo SH, Luh KT, Lin YJ, et al. PKC activation is required by EGF-stimulated Na(+)-H+ exchanger in human pleural mesothelial cells. *Am J Physiol* 1998; **274:** L665-672.

[430] Guermonprez P, Valladeau J, Zitvogel L, Thery C, Amigorena S. Antigen presentation and T cell stimulation by dendritic cells. *Annu Rev Immunol* 2002; **20:** 621-667.

[431] Romero Mendez IZ, Shi Y, HogenEsch H, Hem SL. Potentiation of the immune response to non-adsorbed antigens by Aluminum-containing adjuvants. *Vaccine* 2007; **25:** 825-833.

[432] Kakiuchi T, Watanabe M, Hozumi N, Nariuchi H. Differential sensitivity of specific and nonspecific antigen-presentation by B cells to a protein synthesis inhibitor. *J Immunol* 1990; **145:** 1653-1658.

[433] Bachmann MF, Jennings GT. Vaccine delivery: a matter of size, geometry, kinetics and molecular patterns. *Nat Rev Immunol* 2010; **10:** 787-796.

[434] Ahsan F, Rivas IP, Khan MA, Torres Suarez AI. Targeting to macrophages: role of physicochemical properties of particulate carriers--liposomes and microspheres--on the phagocytosis by macrophages. *J Control Release* 2002; **79:** 29-40.

[435] Vidard L, Rock KL, Benacerraf B. The generation of immunogenic peptides can be selectively increased or decreased by proteolytic enzyme inhibitors. *J Immunol* 1991; **147:** 1786-1791.

[436] Delamarre L, Couture R, Mellman I, Trombetta ES. Enhancing immunogenicity by limiting susceptibility to lysosomal proteolysis. *J Exp Med* 2006; **203:** 2049-2055.

[437] Celli S, Lemaitre F, Bousso P. Real-time manipulation of T cell-dendritic cell interactions *in vivo* reveals the importance of prolonged contacts for CD4+ T cell activation. *Immunity* 2007; **27:** 625-634.

[438] Obst R, van Santen HM, Mathis D, Benoist C. Antigen persistence is required throughout the expansion phase of a CD4(+) T cell response. *J Exp Med* 2005; **201:** 1555-1565.

[439] Rimaniol AC, Gras G, Verdier F, Capel F, Grigoriev VB, Porcheray F, et al. Aluminum hydroxide adjuvant induces macrophage differentiation towards a specialized antigen-presenting cell type. *Vaccine* 2004; **22:** 3127-3135.

[440] Shin JS, Ebersold M, Pypaert M, Delamarre L, Hartley A, Mellman I. Surface expression of MHC class II in dendritic cells is controlled by regulated ubiquitination. *Nature* 2006; **444:** 115-118.

[441] Robinson JH, Delvig AA. Diversity in MHC class II antigen presentation. *Immunology* 2002; **105:** 252-262.

[442] WHO. Immunological adjuvants. Report of a WHO scientific group. World Health Organ Tech Rep Ser:1-40, 1976.

[443] Mueller DL, Jenkins MK. Autoimmunity: when self-tolerance breaks down.

Curr Biol 1997; **7:** R255-257.

[444] Freeman GJ, Boussiotis VA, Anumanthan A, Bernstein GM, Ke XY, Rennert PD, et al. B7-1 and B7-2 do not deliver identical costimulatory signals, since B7-2 but not B7-1 preferentially costimulates the initial production of IL-4. *Immunity* 1995; **2:** 523-532.

[445] Bhatia S, Edidin M, Almo SC, Nathenson SG. B7-1 and B7-2: similar costimulatory ligands with different biochemical, oligomeric and signaling properties. *Immunol Lett* 2006; **104:** 70-75.

[446] Linsley PS, Ledbetter JA. The role of the CD28 receptor during T cell responses to antigen. *Annu Rev Immunol* 1993; **11:** 191-212.

[447] Levine BL, Ueda Y, Craighead N, Huang ML, June CH. CD28 ligands CD80 (B7-1) and CD86 (B7-2) induce long-term autocrine growth of CD4+ T cells and induce similar patterns of cytokine secretion *in vitro*. *Int Immunol* 1995; **7:** 891-904.

[448] Paterson AM, Vanguri VK, Sharpe AH. SnapShot: B7/CD28 costimulation. *Cell* 2009; **137:** 974-974 e971.

[449] Vasilevko V, Ghochikyan A, Holterman MJ, Agadjanyan MG. CD80 (B7-1) and CD86 (B7-2) are functionally equivalent in the initiation and maintenance of CD4+ T-cell proliferation after activation with suboptimal doses of PHA. *DNA Cell Biol* 2002; **21:** 137-149.

[450] Sansom DM, Manzotti CN, Zheng Y. What's the difference between CD80 and CD86? *Trends Immunol* 2003; **24:** 314-319.

[451] Foy TM, Aruffo A, Bajorath J, Buhlmann JE, Noelle RJ. Immune regulation by CD40 and its ligand GP39. *Annu Rev Immunol* 1996; **14:** 591-617.

[452] Gramaglia I, Weinberg AD, Lemon M, Croft M. Ox-40 ligand: a potent costimulatory molecule for sustaining primary CD4 T cell responses. *J Immunol* 1998; **161:** 6510-6517.

[453] Cella M, Scheidegger D, Palmer-Lehmann K, Lane P, Lanzavecchia A, Alber G. Ligation of CD40 on dendritic cells triggers production of high levels of interleukin-12 and enhances T cell stimulatory capacity: T-T help via APC activation. *J Exp Med* 1996; **184:** 747-752.

[454] Bjorck P, Banchereau J, Flores-Romo L. CD40 ligation counteracts Fas-induced apoptosis of human dendritic cells. *Int Immunol* 1997; **9:** 365-372.

[455] Bennett SR, Carbone FR, Karamalis F, Flavell RA, Miller JF, Heath WR. Help for cytotoxic-T-cell responses is mediated by CD40 signalling. *Nature* 1998; **393:** 478-480.

[456] Schoenberger SP, Toes RE, van der Voort EI, Offringa R, Melief CJ. T-cell help for cytotoxic T lymphocytes is mediated by CD40-CD40L interactions. *Nature* 1998; **393:** 480-483.

[457] Ohshima Y, Tanaka Y, Tozawa H, Takahashi Y, Maliszewski C, Delespesse G. Expression and function of OX40 ligand on human dendritic cells. *J Immunol* 1997; **159:** 3838-3848.

[458] Curtsinger JM, Schmidt CS, Mondino A, Lins DC, Kedl RM, Jenkins MK, et al. Inflammatory cytokines provide a third signal for activation of naive CD4+ and CD8+ T cells. *J Immunol* 1999; 162: 3256-3262.

[459] Janeway CA, Jr. The role of CD4 in T-cell activation: accessory molecule or co-receptor? *Immunol Today* 1989; **10:** 234-238.

[460] Cumberbatch M, Dearman RJ, Kimber I. Langerhans cells require signals from both tumour necrosis factor alpha and interleukin 1 beta for migration. *Adv Exp Med Biol* 1997; **417:** 125-128.

[461] Cumberbatch M, Dearman RJ, Kimber I. Stimulation of Langerhans cell migration in mice by tumour necrosis factor alpha and interleukin 1 beta. *Adv Exp Med Biol* 1997; **417:** 121-124.

[462] Cumberbatch M, Dearman RJ, Kimber I. Interleukin 1 beta and the stimulation of Langerhans cell migration: comparisons with tumour necrosis factor alpha. *Arch Dermatol Res* 1997; **289:** 277-284.

[463] Cumberbatch M, Dearman RJ, Kimber I. Langerhans cells require signals from both tumour necrosis factor-alpha and interleukin-1 beta for migration. *Immunology* 1997; **92:** 388-395.

[464] Dinarello CA. Interleukin-1beta. *Crit Care Med* 2005; **33:** S460-462.

[465] Dinarello CA. IL-1: discoveries, controversies and future directions. *Eur J Immunol* 2010; **40:** 599-606.

[466] Dinarello CA. A clinical perspective of IL-1beta as the gatekeeper of inflammation. *Eur J Immunol* 2011; **41:** 1203-1217.

[467] Dinarello CA. The IL-1 family and inflammatory diseases. *Clin Exp Rheumatol* 2002; **20:** S1-13.

[468] Khoruts A, Osness RE, Jenkins MK. IL-1 acts on antigen-presenting cells to enhance the *in vivo* proliferation of antigen-stimulated naive CD4 T cells via a CD28-dependent mechanism that does not involve increased expression of CD28 ligands. *Eur J Immunol* 2004; **34:** 1085-1090.

[469] Tayal V, Kalra BS. Cytokines and anti-cytokines as therapeutics--an update. *Eur J Pharmacol* 2008; **579:** 1-12.

[470] Li H, Nookala S, Re F. Aluminum hydroxide adjuvants activate caspase-1 and induce IL-1beta and IL-18 release. *J Immunol* 2007; **178:** 5271-5276.

[471] Jakob T, Udey MC. Regulation of E-cadherin-mediated adhesion in Langerhans cell-like dendritic cells by inflammatory mediators that mobilize Langerhans cells *in vivo*. *J Immunol* 1998; **160:** 4067-4073.

[472] Schmitz J, Owyang A, Oldham E, Song Y, Murphy E, McClanahan TK, et al. IL-33, an interleukin-1-like cytokine that signals via the IL-1 receptor-related protein ST2 and induces T helper type 2-associated cytokines. *Immunity* 2005; **23:** 479-490.

[473] Kurowska-Stolarska M, Hueber A, Stolarski B, McInnes IB. Interleukin-33: a novel mediator with a role in distinct disease pathologies. *J Intern Med* 2011; **269:** 29-35.

[474] Rank MA, Kobayashi T, Kozaki H, Bartemes KR, Squillace DL, Kita H. IL-33-activated dendritic cells induce an atypical TH2-type response. *J Allergy Clin Immunol* 2009; **123:** 1047-1054.

[475] Besnard AG, Togbe D, Guillou N, Erard F, Quesniaux V, Ryffel B. IL-33-activated dendritic cells are critical for allergic airway inflammation. *Eur J Immunol* 2011; **41:** 1675-1686.

[476] Ma X, Sun J, Papasavvas E, Riemann H, Robertson S, Marshall J, et al. Inhibition of IL-12 production in human monocyte-derived macrophages by TNF. *J Immunol* 2000; 164: 1722-1729.

[477] Gollob JA, Mier JW, Veenstra K, McDermott DF, Clancy D, Clancy M, et al. Phase I trial of twice-weekly intravenous interleukin 12 in patients with metastatic renal cell cancer or malignant melanoma: ability to maintain IFN-gamma induction is associated with clinical response. *Clin Cancer Res* 2000; **6:** 1678-1692.

[478] Atkins MB, Robertson MJ, Gordon M, Lotze MT, DeCoste M, DuBois JS, et al. Phase I evaluation of intravenous recombinant human interleukin 12 in patients with advanced malignancies. *Clin Cancer Res* 1997; **3:** 409-417.

[479] Magram J, Connaughton SE, Warrier RR, Carvajal DM, Wu CY, Ferrante J, et al. IL-12-deficient mice are defective in IFN gamma production and type 1 cytokine responses. *Immunity* 1996; **4:** 471-481.

[480] Connell L, McInnes IB. New cytokine targets in inflammatory rheumatic diseases. *Best Pract Res Clin Rheumatol* 2006; **20:** 865-878.

[481] Kishimoto T. Interleukin-6: discovery of a pleiotropic cytokine. *Arthritis Res*

Ther 2006; **8 (Suppl 2):** S2.

[482] Drakesmith H, O'Neil D, Schneider SC, Binks M, Medd P, Sercarz E, et al. *In vivo* priming of T cells against cryptic determinants by dendritic cells exposed to interleukin 6 and native antigen. *Proc Natl Acad Sci USA* 1998; **95:** 14903-14908.

[483] Kitamura H, Kamon H, Sawa S, Park SJ, Katunuma N, Ishihara K, et al. IL-6-STAT3 controls intracellular MHC class II alphabeta dimer level through cathepsin S activity in dendritic cells. *Immunity* 2005; **23:** 491-502.

[484] de Waal Malefyt R, Abrams J, Bennett B, Figdor CG, de Vries JE. Interleukin 10(IL-10) inhibits cytokine synthesis by human monocytes: an autoregulatory role of IL-10 produced by monocytes. *J Exp Med* 1991; **174:** 1209-1220.

[485] Groux H, Bigler M, de Vries JE, Roncarolo MG. Interleukin-10 induces a *long-term antigen-specific anergic state in human CD4+ T cells. J Exp Med* 1996; **184:** 19-29.

[486] Koppelman B, Neefjes JJ, de Vries JE, de Waal Malefyt R. Interleukin-10 down-regulates MHC class II alphabeta peptide complexes at the plasma membrane of monocytes by affecting arrival and recycling. *Immunity* 1997; **7:** 861-871.

[487] Webb DC, Cai Y, Matthaei KI, Foster PS. Comparative roles of IL-4, IL-13, and IL-4Ralpha in dendritic cell maturation and CD4+ Th2 cell function. *J Immunol* 2007; **178:** 219-227.

[488] Bellinghausen I, Brand P, Bottcher I, Klostermann B, Knop J, Saloga J. Production of interleukin-13 by human dendritic cells after stimulation with protein allergens is a key factor for induction of T helper 2 cytokines and is associated with activation of signal transducer and activator of transcription- 6. *Immunology* 2003; **108:** 167-176.

[489] de Saint-Vis B, Fugier-Vivier I, Massacrier C, Gaillard C, Vanbervliet B, Ait-Yahia S, et al. The cytokine profile expressed by human dendritic cells is dependent on cell subtype and mode of activation. *J Immunol* 1998; **160:** 1666-1676.

[490] Dubois SP, Waldmann TA, Muller JR. Survival adjustment of mature dendritic cells by IL-15. *Proc Natl Acad Sci USA* 2005; **102:** 8662-8667.

[491] Mattei F, Schiavoni G, Belardelli F, Tough DF. IL-15 is expressed by dendritic cells in response to type I IFN, double-stranded RNA, or lipopolysaccharide and promotes dendritic cell activation. *J Immunol* 2001; **167:** 1179-1187.

[492] Jinushi M, Takehara T, Tatsumi T, Kanto T, Groh V, Spies T, et al. Autocrine/paracrine IL-15 that is required for type I IFN-mediated dendritic cell

expression of MHC class I-related chain A and B is impaired in hepatitis C virus infection. *J Immunol* 2003; **171:** 5423-5429.

[493] Liu T, Matsuguchi T, Tsuboi N, Yajima T, Yoshikai Y. Differences in expression of toll-like receptors and their reactivities in dendritic cells in BALB/c and C57BL/6 mice. *Infect Immun* 2002; **70:** 6638-6645.

[494] Kuchroo VK, Das MP, Brown JA, Ranger AM, Zamvil SS, Sobel RA, et al. B7-1 and B7-2 costimulatory molecules activate differentially the Th1/Th2 developmental pathways: application to autoimmune disease therapy. *Cell* 1995; **80:** 707-718.

[495] Brewer JM, Conacher M, Gaffney M, Douglas M, Bluethmann H, Alexander J. Neither interleukin-6 nor signalling via tumour necrosis factor receptor-1 contribute to the adjuvant activity of Alum and Freund's adjuvant. *Immunology* 1998; **93:** 41-48.

[496] Franchi L, Nunez G. The Nlrp3 inflammasome is critical for Aluminium hydroxide-mediated IL-1beta secretion but dispensable for adjuvant activity. *Eur J Immunol* 2008; **38:** 2085-2089.

[497] Miao EA, Rajan JV, Aderem A. Caspase-1-induced pyroptotic cell death. *Immunol Rev* 2011; **243:** 206-214.

[498] Agostini L, Martinon F, Burns K, McDermott MF, Hawkins PN, Tschopp J. NALP3 forms an IL-1beta-processing inflammasome with increased activity in Muckle-Wells autoinflammatory disorder. *Immunity* 2004; **20:** 319-325.

[499] Dumitriu IE, Bianchi ME, Bacci M, Manfredi AA, Rovere-Querini P. The secretion of HMGB1 is required for the migration of maturing dendritic cells. *J Leukoc Biol* 2007; **81:** 84-91.

[500] Ferguson TA, Choi J, Green DR. Armed response: how dying cells influence T-cell functions. *Immunol Rev* 2011; **241:** 77-88.

[501] Shi Y, HogenEsch H, Regnier FE, Hem SL. Detoxification of endotoxin by Aluminum hydroxide adjuvant. *Vaccine* 2001; **19:** 1747-1752.

[502] Burton AJ, Carter HE. Purification and characterization of The Lipid A component of The Lipopolysaccharides from *Escherichia coli*. *Biochemistry* 1964; **3:** 411-418.

[503] O'Garra A, Murphy KM. From IL-10 to IL-12: how pathogens and their products stimulate APCs to induce T(H)1 development. *Nat Immunol* 2009; **10:** 929-932.

[504] Lee WT, Pasos G, Cecchini L, Mittler JN. Continued antigen stimulation is not required during CD4(+) T cell clonal expansion. *J Immunol* 2002; **168:** 1682-

1689.

[505] Bajenoff M, Granjeaud S, Guerder S. The strategy of T cell antigen- presenting cell encounter in antigen-draining lymph nodes revealed by imaging of initial T cell activation. *J Exp Med* 2003; **198:** 715-724.

[506] Schrum AG, Turka LA. The proliferative capacity of individual naïve CD4(+) T cells is amplified by prolonged T cell antigen receptor triggering. *J Exp Med* 2002; **196:** 793-803.

[507] Kearney ER, Pape KA, Loh DY, Jenkins MK. Visualization of peptide- specific T cell immunity and peripheral tolerance induction *in vivo*. *Immunity* 1994; **1:** 327-339.

[508] Parish CR, Glidden MH, Quah BJ, Warren HS. Use of the intracellular fluorescent dye CFSE to monitor lymphocyte migration and proliferation. *Curr Protoc Immunol* 2009; Chapter 4:Unit4 9.

[509] Quah BJ, Warren HS, Parish CR. Monitoring lymphocyte proliferation *in vitro* and *in vivo* with the intracellular fluorescent dye carboxyfluorescein diacetate succinimidyl ester. *Nat Protoc* 2007; **2:** 2049-2056.

[510] Seabrook TJ, Borron PJ, Dudler L, Hay JB, Young AJ. A novel mechanism of immune regulation: interferon-gamma regulates retention of CD4 T cells during delayed type hypersensitivity. *Immunology* 2005; **116:** 184-192.

[511] Schwab SR, Cyster JG. Finding a way out: lymphocyte egress from lymphoid organs. *Nat Immunol* 2007; **8:** 1295-1301.

[512] Cyster JG. Chemokines, sphingosine-1-phosphate, and cell migration in secondary lymphoid organs. *Annu Rev Immunol* 2005; **23:** 127-159.

[513] Cyster JG. Chemokines and cell migration in secondary lymphoid organs. *Science* 1999; **286:** 2098-2102.

[514] Bankovich AJ, Shiow LR, Cyster JG. CD69 suppresses sphingosine 1-phosophate receptor-1 (S1P1) function through interaction with membrane helix 4. *J Biol Chem* 2010; **285:** 22328-22337.

[515] Noe SM, Green MA, HogenEsch H, Hem SL. Mechanism of immunopotentiation by Aluminum-containing adjuvants elucidated by the relationship between antigen retention at the inoculation site and the immune response. *Vaccine* 2010; **28:** 3588-3594.

[516] Malherbe L, Mark L, Fazilleau N, McHeyzer-Williams LJ, McHeyzer-Williams MG. Vaccine adjuvants alter TCR-based selection thresholds. Immunity 2008; **28:** 698-709.

[517] Wu Y, Wu W, Wong WM, Ward E, Thrasher AJ, Goldblatt D, et al. Human gamma delta T cells: a lymphoid lineage cell capable of professional phagocytosis. *J Immunol* 2009; **183:** 5622-5629.

[518] Lin WW, Hsu YW. Cycloheximide-induced cPLA(2) activation is via the MKP-1 down-regulation and ERK activation. *Cell Signal* 2000; **12:** 457-461.

[519] Ramachandra L, Harding CV. Phagosomes acquire nascent and recycling class II MHC molecules but primarily use nascent molecules in phagocytic antigen processing. *J Immunol* 2000; **164:** 5103-5112.

[520] Porgador A, Yewdell JW, Deng Y, Bennink JR, Germain RN. Localization, quantitation, and in situ detection of specific peptide-MHC class I complexes using a monoclonal antibody. *Immunity* 1997; **6:** 715-726.

[521] Hilton CJ, Dahl AM, Rock KL. Anti-peptide antibody blocks peptide binding to MHC class I molecules in the endoplasmic reticulum. *J Immunol* 2001; **166:** 3952-3956.

[522] Xiao Y, Peperzak V, Keller AM, Borst J. CD27 instructs CD4+ T cells to provide help for the memory CD8+ T cell response after protein immunization. *J Immunol* 2008; **181:** 1071-1082.

[523] Hirano N, Butler MO, Xia Z, Ansen S, von Bergwelt-Baildon MS, Neuberg D, et al. Engagement of CD83 ligand induces prolonged expansion of CD8+ T cells and preferential enrichment for antigen specificity. *Blood* 2006; **107:** 1528-1536.

[524] Prazma CM, Yazawa N, Fujimoto Y, Fujimoto M, Tedder TF. CD83 expression is a sensitive marker of activation required for B cell and CD4+ T cell longevity *in vivo*. *J Immunol* 2007; **179:** 4550-4562.

[525] Fujimoto Y, Tu L, Miller AS, Bock C, Fujimoto M, Doyle C, et al. CD83 expression influences CD4+ T cell development in the thymus. *Cell* 2002; **108:** 755-767.

[526] Kuwano Y, Prazma CM, Yazawa N, Watanabe R, Ishiura N, Kumanogoh A, et al. CD83 influences cell-surface MHC class II expression on B cells and other antigen-presenting cells. *Int Immunol* 2007; **19:** 977-992.

[527] Kretschmer B, Luthje K, Schneider S, Fleischer B, Breloer M. Engagement of CD83 on B cells modulates B cell function *in vivo*. *J Immunol* 2009; **182:** 2827-2834.

[528] Rimaniol AC, Gras G, Clayette P. *In vitro* interactions between macrophages and Aluminum-containing adjuvants. *Vaccine* 2007; **25:** 6784-6792.

APPENDIX-I

Kinetics of antigen uptake and presentation

DCs= 2x10^6/5mL media

EaGFP=100 µg/mL

Alum=100 µg/mL

Incubation period=96 hours

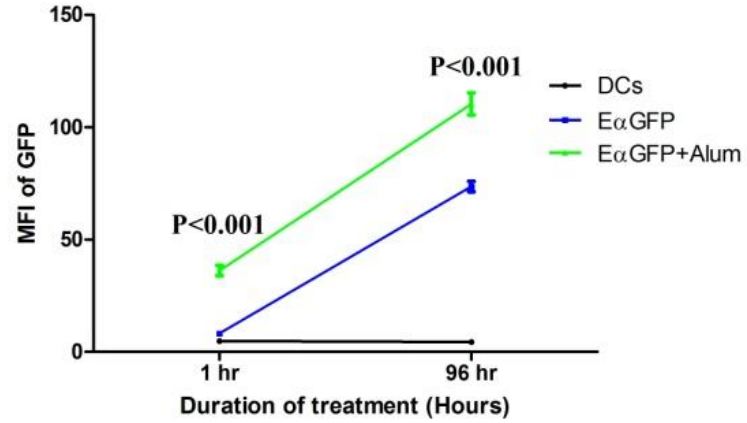

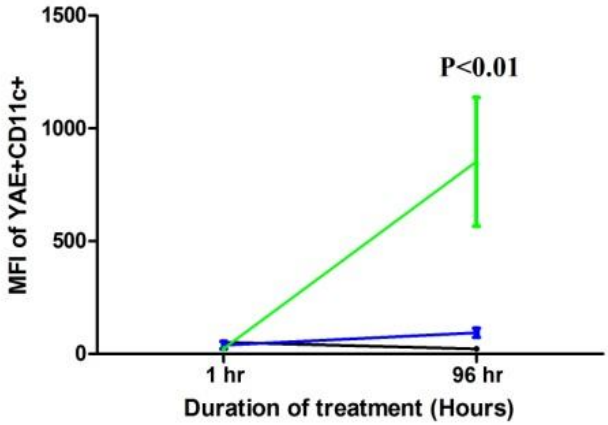

APPENDIX-II

Curve-fitting data of Multiplex ELISA

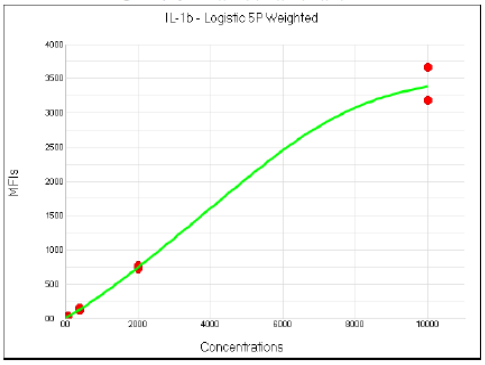

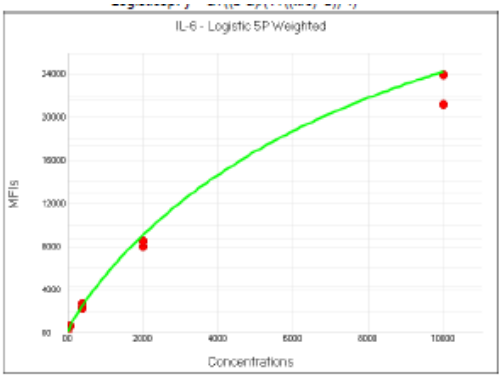

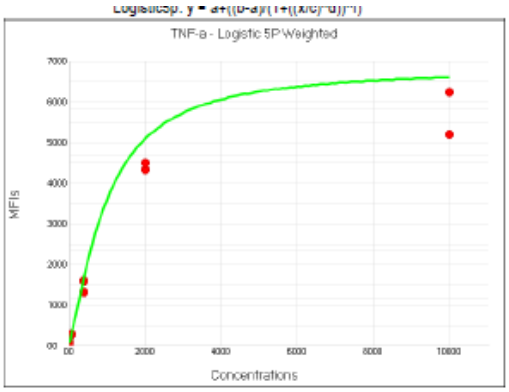

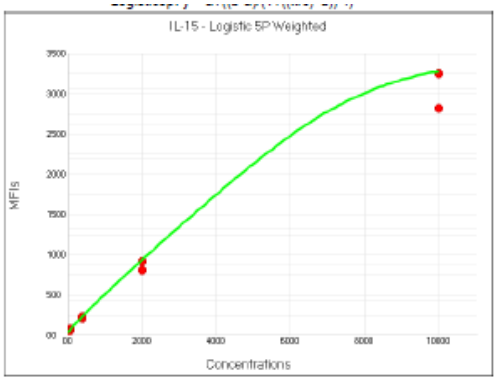

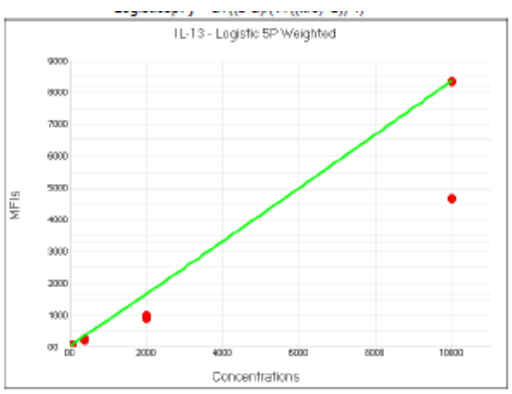

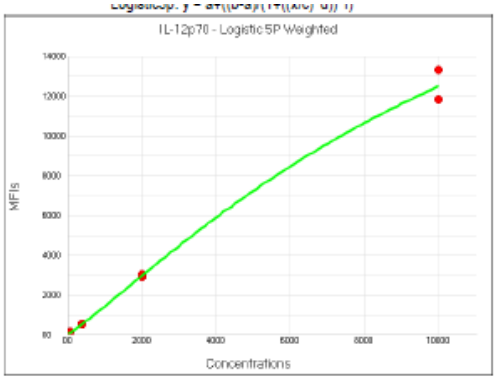

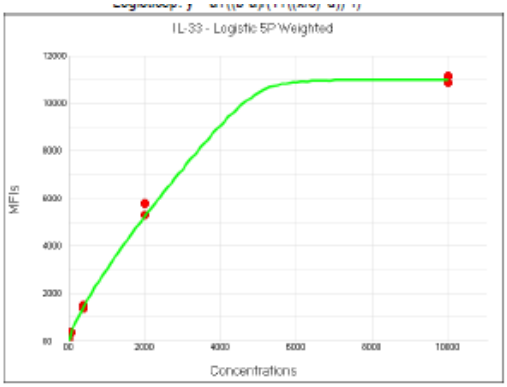

APPENDIX-III

Mean concentration (mean+S.E.M.) of cytokine level (pg/mL) in DCs (C57BL/6 mice) incubated with Alum (100µg/mL) or LPS (1µg/mL) or LPS+Alum (100µg/mL) *in vitro*.

Cytokines	Incubation period (Days)	Media	Alum	LPS (1µg/mL)	LPS (1µg/mL)+Alum (100µg/mL)
IL-1β	**1**	13.16±5.78	20.40±1.96	577.23±20.42	4290.92±197.84
	2	13.48±3.19	31.19±1.39	1599.39±131.03	10000.00±0.00
	3	12.02±0.00	259.82±13.91	1103.49±86.01	4677.35±158.78
	4	13.57±1.55	1662.96±4.47	708.87±57.67	2203.40±33.29
TNF-α	**1**	60.70±5.22	78.88±1.40	2302.24±64.26	1625.23±109.34
	2	61.96±1.87	129.07±8.03	4452.29±1276.68	3768.60±557.13
	3	59.77±2.88	91.36±0.34	1761.30±265.78	1676.93±182.69
	4	59.94±2.50	226.05±0.86	1426.53±136.02	1046.18±36.63
IL-6	**1**	19.02±1.67	18.37±0.39	317505.40±174027.60	21312.01±1028.82
	2	16.29±0.93	72.40±50.38	10000.00±0.00	10000.00±0.00
	3	18.18±1.89	269.99±6.02	173765.20±163765.20	61807.87±9956.48
	4	23.76±0.42	2215.93±15.41	317349.30±146050.00	24317.86±732.23
IL-12p70	**1**	0.89±0.44	0.00±0.00	19.68±0.97	11.19±1.30
	2	0.44±0.44	0.00±0.00	44.27±1.81	20.34±2.37
	3	0.18±0.18	0.00±0.00	25.99±2.10	11.75±1.48
	4	0.00±0.00	2.026±0.70	20.66±3.33	13.92±2.70
IL-10	**1**	45.00±16.46	5.67±5.67	392.33±26.87	198.00±21.39
	2	38.00±38.00	0.00±0.00	607.00±8.54	563.67±32.00
	3	0.00±0.00	0.00±0.00	433.67±45.32	365.67±49.72
	4	0.00±0.00	0.00±0.00	583.67±16.76	610.00±25.17
IL-13	**1**	0.38±0.19	0.19±0.19	30.63±1.90	18.33±2.18
	2	2.83±2.26	0.19±0.19	35.29±4.13	12.08±4.87
	3	0.19±0.19	0.38±0.19	6.58±2.67	2.64±2.36
	4	1.14±0.88	0.00±0.00	4.15±2.17	3.23±0.99